# Understanding the Role of OmpV, an Outer Membrane Protein of *Salmonella* Typhimurium Towards Bacterial Pathogenesis and Host Immune Activation

**Deepinder Kaur**

*A thesis submitted for the partial fulfillment of*
*the degree of Doctor of Philosophy*


Department of Biological Sciences
Indian Institute of Science Education and Research Mohali
Knowledge city, Sector 81, SAS Nagar, Manauli PO, Mohali 140306, Punjab, India.

January, 2021

I dedicate this thesis to my mother Sdn. Amarjeet Kaur and father S. Mohinder Pal Singh for their endless love, support and encouragement

# Declaration

The work presented in this thesis has been carried out by me under the guidance of Dr. Arunika Mukhopadhaya at the Indian Institute of Science Education and Research Mohali. This work has not been submitted in part or in full for a degree, a diploma, or a fellowship to any other university or institute. Whenever contributions of others are involved, every effort is made to indicate this clearly, with due acknowledgment of collaborative research and discussions. This thesis is a bonafide record of original work done by me and all sources listed within have been detailed in the bibliography.

Deepinder Kaur

In my capacity as the supervisor of the candidate's thesis work, I certify that the above statements by the candidate are true to the best of my knowledge.

Dr. Arunika Mukhopadhaya

# Acknowledgements

**“Gratitude is when memory is stored in the heart and not in the mind.”**

**~~Lionel Hampton**

I want to express my deepest and sincere gratitude to my supervisor Dr. Arunika Mukhopadhaya for giving me the opportunity to work in her lab and for her continuous guidance throughout my research. Her valuable advice, encouragement and motivation helped me during my research work as well as in writing this thesis. I faced several ups and downs during the long journey of my Ph.D. but having such a wonderful person as a guide kept me enthusiastic and passionate about research. A great deal of credit goes to her for improving my presentation and writing skills, as she always encouraged me to present my work in seminars.

I would also like to extend my sincere thanks to my doctoral thesis committee members Dr. Kausik Chattopadhyay and Dr. Samarjit Bhattacharyya for their valuable suggestions, encouragement and insightful questions. Their comments always helped me to gain knowledge and rectify my experimental designs. I am incredibly grateful to Dr. Kausik for helping me with biophysical experiments and allowing me to use his lab facilities. I very much appreciate Dr. Samarjit for giving access to the confocal microscope facility and providing us with reagents for knockdown studies. I also want to thank Dr. Francis Ramos Morale for providing us with the deletion mutant used for this study.

Many thanks to my seniors Dr. Junaid, Dr. Sanica, Dr. Shelly, Dr. Krishna, Dr. Aakanksha and former postdocs Dr. Ranjai and Dr. Ritam for teaching me various experimental techniques. Their critical questions and discussions during lab meetings helped me immensely to grow as a researcher. I thank my lab mates Vinica, Shraddha, Arpita, Shashi, Yogesh, Sanjeev, Dwipjyoti and MS thesis students Alok, Raminder, Rhythm, Mohit, Shivansh, Celina and Manisha for their love, support and encouragement.

I also wish to thank past and present lab members of Dr. Kausik's lab; Dr. Karan, Dr. Kusum, Dr. Anand, Dr. Barkha, Dr. Nidhi, Reema, Anish, Pratima, Mahendra, Kusum and Shamaita for

sharing their lab space. I take this opportunity to specially thanks Anish Mondal for assisting me with biophysical experiments.

Thanks should also go to my friends Anuj Shukla and Dr. Bhupinder Singh for their motivation and support throughout this journey. I will always remember the wonderful times we shared, especially the adventurous trips to Himachal and Uttarakhand. I am grateful to all my colleagues for making this journey memorable and joyful.

I would like to extend my sincere thanks to IISER Mohali for providing us with a beautiful campus and ideal infrastructure for research work. I would also like to acknowledge Small Animal Facility For Experimentation (SAFE) at IISER Mohali and the mice community for their contribution to this study. I must thank all members of the department of biology for their timely help and suggestions during department presentations. I gratefully acknowledge the funding assistance I got from UGC, DBT and DST.

Finally, I want to thank my parents, brother and sister in law for their continuous and unparalleled love and support. I am deeply indebted to my parents for giving me all the freedom and support one can wish for. Their trust and encouragement always inspired me throughout this journey. I can never thank them enough for the beautiful life they have given me. Their selfless encouragement always helped me to explore new directions and made me who I am. Their presence always made me feel strong and comfortable. This journey would not have been possible if it was not for them and hence I dedicate this milestone to them.

Last but not least, I want to thank God for its heavenly blessings and for giving me strength, happiness and good health.

**ਸਤਿਗੁਰ ਅਪੁਨੇ ਸੁਨੀ ਅਰਦਾਸਿ**

The true Guru has listened to my prayer

**ਕਾਰਜੁ ਆਇਆ ਸਗਲਾ ਰਾਸਿ॥**

All my affairs have been resolved.

# Table of Contents

# List of Tables

# List of Illustrations

# List of Figures

# List of Abbreviations

ACK lysis buffer: Ammonium-chloride-potassium lysis buffer

ANS: 1-anilinonaphthalene-8-sulfonic acid

APC: Antigen presenting cell

ATR: Acid tolerance response

BMDC: Bone marrow derived dendritic cell

BMDM: Bone marrow derived macrophages

BSA: Bovine serum albumin

CD: Circular Dichroism

CFU: Colony forming unit

DAMP: Danger associated molecular patterns

DC: Dendritic cell

DTT: Dithiothreitol

ELISA: Enzyme linked immunosorbent assay

FAK: Focal adhesion kinase

GM-CSF: Granulocyte macrophage colony stimulating factor

HRP: Horse radish peroxidase

IEC: Intestinal epithelial cells

IFN-γ: Interferon gamma

IL: Interleukin

IRAK: Interleukin-1 receptor associated kinase

LDAO: N,N-Dimethyldodecylamine N-oxide

LD: Lethal dose

LPS: Lipopolysaccharide

M cell: Microfold cell

MAPK: Mitogen activate protein kinase

MAPKK: Mitogen activate protein kinase kinase

MAPKKK: Mitogen activate protein kinase kinase kinase

M-CSF: Macrophage colony stimulating factor

MipA: MltA interacting protein

MOI: Multiplicity of infection

MTT: 3-(4,5-dimethylthiazol-2-yl)-2,5-diphenyltetrazolium bromide

MyD88: Myeloid differentiation factor 88

MyD88-/- mice: MyD88 knockout mice

NFκB: Nuclear factor kappa B

NO: Nitric oxide

Omp: Outer membrane protein

PAGE: Polyacrylamide gel electrophoresis

PAMP: Pathogen Associated Molecular Patterns

PBS: Phosphate buffer saline

PCR: Polymerase chain reaction

PEI: Polyethylenimine

PL: Proteoliposome

PmB: Polymyxin B sulphate

PRR: Pattern Recognition Receptors

SCV: *Salmonella* containing vacuole

SDS: Sodium dodecyl sulphate

shRNA: Short hairpin RNA

siRNA: Small interfering RNA

SPI: *Salmonella* pathogenicity island

TLR2-/-: TLR2 knockout mice

TBST: Tris buffer saline with Tween

TLR: Toll like receptor

TNFα: Tumor necrosis factor α

# I.
# Introduction

**"The most powerful therapeutic in the world is our own immune system."**

**-Francis deSouza**

The human body is a complex ecosystem containing more microbes than the human cells itself (1). Several parts of our body, such as the gut, are populated with microbes. These microbes, generally known as "normal microflora" are harmless and often favorable for the host (2). On the other hand, pathogens like such as *Shigella, Salmonella, Vibrio* etc., are microbes that can cause disease in the gut, and they are collectively known as enteric pathogens.

### 1.1 Enteric pathogens

Enteric pathogens are a large group of gram-negative bacteria that enter the human body through contaminated food and water. Most food and water bodies get contaminated due to diffusion of bacteria from sources such as wastewater treatment plants into agricultural land (3,4). These pathogens colonize the intestine and lead to disease if not cleared by the immune system (5). Enteric pathogens are responsible for gastro-enteric diseases such as diarrhea, dysentery, and enteric fever and cause more than 3 million deaths each year (6).

Enteric bacteria could be invasive or non-invasive, i.e., they can cause disease by invading the host cells or by secreting toxins without invasion. *Vibrio cholerae* and some *Escherichia coli* produce enterotoxins causing the small intestine to secrete fluid and electrolytes, leading to diarrhea (7). The invasive pathogens such as *Yersinia enterocolitica*, *Salmonella enterica,* and *Campylobacter jejuni* follow a traditional infectious cycle that includes adhesion and establishment of pathogens followed by its invasion and multiplication (6,8). Initial adhesion and establishment of bacteria is generally mediated by flagella, pili, adhesins, and fimbriae. Besides, virulence factors secreted by bacteria help in its invasion and multiplication inside host cells (9).

### 1.2 *Salmonella enterica* – an enteric pathogen

*Salmonella* is a genus belonging to the Enterobacteriaceae family containing gram-negative, rod-shaped bacteria. It majorly infects humans through contaminated food and water. The nomenclature of *Salmonella* is complex as various systems are used for its classification across the globe (10). Kauffmann, in 1966 proposed the first nomenclature based on somatic (O) and flagellar (H) antigens (11). In this concept, each serotype was considered as separate species. Later, in 1973, Crosa *et al*. modified this nomenclature based on DNA-DNA hybridization (12). Le Minor and Popoff (1987) referred to seven subgenera of *Salmonella* as subspecies based on genomic relatedness and biochemical reactions (13). Presently, CDC has divided genus *Salmonella* into two species *S. enterica* and *S. bongori*. *S. enterica* is further divided into six subspecies based on genomic relatedness and biochemical reactions. There are currently about 2,600 serovars of *Salmonella* (14). Out of these, 59 % belong to *S. enterica* subsp *enterica*. These strains cause about 99 % of *Salmonella* infections in warm-blooded animals and humans (10). Further, *S. enterica* subsp *enterica* is divided into typhoidal and non-typhoidal serovars Typhi, Paratyphi, Typhimurium and Enteritidis (**Illustration 1**).

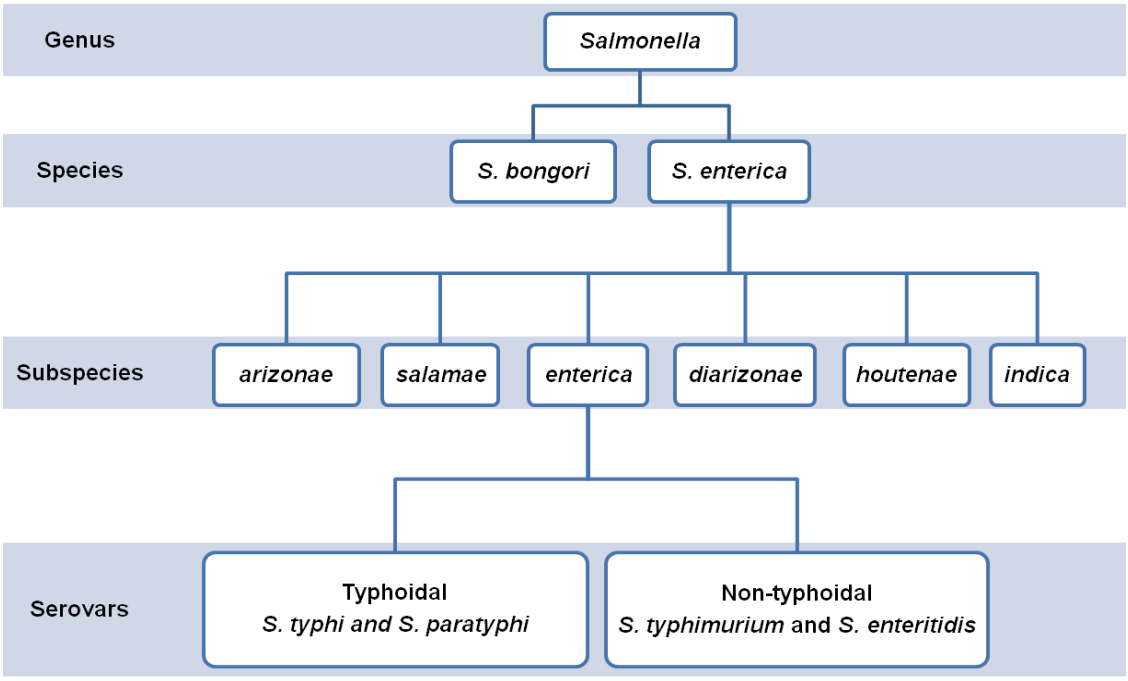


**Illustration 1:** Classification table of *Salmonella*
(modified from Hurley *et al.* 2014 (15))

### 1.2.1 *Salmonella enterica* pathogenesis

*Salmonella enterica* is predominantly transmitted through contaminated water, poultry, eggs, dairy products, fresh fruits, and vegetables (16). The health status of individuals and the serotype of *Salmonella* majorly determine the severity of the infection. People with a weakened immune system, older people, and younger children are more prone to disease than healthy individuals. *Salmonella* tends to adhere to and invade intestinal epithelial cells. Invasion in these non-phagocytic cells is one of the remarkable characters of *Salmonella* to protect itself from the host immune system (17).

*S. enterica* upon entering human body travels to gut (18). To protect itself from the acidic environment of the stomach, *Salmonella* activates acid tolerance response (ATR) to maintain the intracellular pH higher than the extracellular environment (19,20).

On reaching the intestine, the bacterium adheres itself to intestinal epithelial cells and colonizes in the gut. Then it invades epithelial cells from the apical side with the help of a type 3 secretion system (trigger mechanism) (21) or moves to the basolateral side through microfold cells (M cells) (22-25). On reaching the basolateral surface, the bacterium can further invade intestinal epithelial cells by modulating actin filaments through integrin signaling (zipper mechanism) (21). Apart from this, upon crossing M cells, the bacterium comes in contact with immune cells such as macrophages present in Peyer's patches (26). *Salmonella* can also invade and replicate inside macrophages (27-30). SPI-1 plays a role in invasion, whereas SPI-2 plays a role in the replication of bacteria inside the host cell (31). Briefly, upon invasion inside macrophages or intestinal epithelial cells, *Salmonella* resides in the host cell in a membrane compartment composed of a host cell membrane called SCV (*Salmonella* containing vacuole) (32). These SCVs are initially integrated with the endocytic pathway, but later with the help of SPI-2 effector proteins, it avoids fusion with secondary lysosomes by modulating endocytic trafficking. On maturation, these SCV further move towards Golgi to obtain nutrients essential for replication of bacteria (33). Moreover, the intracellular *Salmonella* can lead to the formation of SIFs (*Salmonella*-induced filaments) which further increases availability of nutrients inside SCV (34). After replicating, *Salmonella* disseminates from these cells and further infects organs such as spleen and liver (35).

### 1.2.2 Virulence factors of *Salmonella enterica*

The complexity of the pathogenesis mechanism of *Salmonella enterica* correlates with the presence of various defensive and offensive virulence factors (36). Virulence genes can be encoded by both chromosomes (mainly *Salmonella* pathogenicity islands or SPIs) and virulence plasmid (like Spv operon) of *Salmonella* (37). To date, 17 SPIs (SPI-1 to SPI-17) have been identified in *Salmonella*, out of which SPI-1 and SPI-2 play a significant role in invasion and replication of bacteria, respectively (31).

Major virulence factors of *Salmonella* include:

a. **Endotoxin:** It is a pyrogen. It is the Lipid A part of the outer membrane of gram-negative bacteria. It is majorly responsible for systemic disease caused by *Salmonella enterica*.

b. **Fimbriae and adhesins:** These are responsible for adhesion, which is the first step in pathogenesis of *Salmonella*. It helps in the binding of bacteria to M cells and the apical surface of intestinal epithelial cells. It also helps in adhesion to extracellular matrix components present on basolateral surface after translocation of bacteria through M cells.

c. **Acid tolerance response (ATR) gene:** The proteins encoded by these genes help bacteria survive in the stomach by protecting it from the acidic pH of the stomach.

d. **Catalase and Superoxide dismutase:** These are the enzymes that protect *Salmonella* from intracellular killing by macrophages.

e. **Type III secretion systems:** These are the molecular syringes that help in translocation of effector proteins into host cells (38). Over 30 effector proteins regulated by SPI-1 or SPI-2 are reported to be translocated by these systems (39,40). However, there are still many virulence phenotypes that could not be linked to any of the reported effectors (41-43).

Some of the effector proteins of SPI-1 and SPI-2 and their significant roles are indicated in **Table1 and Table 2**.

| Effectors | Functions |
|---|---|
| SipA | Rearrangement of cytoskeleton and neutrophil recruitment |
| SipB | Actin nucleation/translocation of other effectors |
| SipC | Translocation of other effectors |
| SopA | Immune cell recruitment, fluid secretion |
| SopB | Cytoskeleton rearrangement, neutrophil recruitment, fluid secretion |
| SopC | Neutrophil recruitment, fluid secretion |
| SopD | Neutrophil recruitment, fluid secretion |
| SopE | Rearrangement of cytoskeleton |
| SptP | Rearrangement of cytoskeleton |

**Table 1:** Salmonella Pathogenicity Island 1 associated effector proteins (modified from Lostroh and Lee, 2001(44)).

| Effectors | Functions |
|---|---|
| SpiC | Disruption of vesicular transport |
| SseF | Aid in Salmonella-induced filament formation |
| SseG | Aid in Salmonella-induced filament formation |
| SifA | Salmonella-containing vacuole membrane integrity |
| SifB | Targeting to Salmonella induced filaments |
| SspH2 | Cytoskeleton rearrangement |
| SrfT | Apoptosis |
| SseI | Cytoskeleton rearrangement |
| SseJ | Salmonella-containing vacuole membrane dynamics/acyl transferase |
| PipB | Targeting to Salmonella induced filaments |
| SopD2 | Targeting to Salmonella induced filaments/late endosomes |

**Table 2:** Salmonella Pathogenicity Island 2 associated effector proteins (modified from Waterman and Holden, 2003 (45)).

### 1.2.3 Difference in the genome of typhoidal and non-typhoidal *Salmonella*

The pathogenesis of different serovars of *Salmonella* varies according to the host. The serovars infecting humans are mainly divided into two categories – typhoidal and non-typhoidal. Typhoidal serovars such as *S.* Typhi causes a fatal enteric fever called typhoid, whereas non-typhoidal serovars such as *S.* Typhimurium causes a self-limiting gastroenteritis disorder, salmonellosis in humans. While typhoidal serovars primarily infect humans, non-typhoidal serovars can infect a wide range of animals. One such example is *S.* Typhimurium that causes typhoid-like systemic disease in mice.

The reason behind the difference in the pathogenesis of these serovars that have more than 96 % similarity between shared genes is still not wholly answered (46). During *in vitro* studies, it was observed that contrary to *S.* Typhimurium, *S.* Typhi is not recognized by TLR5 to trigger an innate immune response. Also, when T84 (intestinal epithelial cell line) was infected with *S.* Typhi, it produces significantly lower levels of IL-8 (neutrophil chemoattractant) compared to *S.* Typhimurium. In *S.* Typhi, one of the polysaccharide capsular antigen Vi is reported to help in hiding the bacterial PAMPs from the innate immune system (47) and thereby induces a lesser neutrophil influx and reduced intestinal inflammation (48,49). Moreover, Vi is also reported to help the bacteria resist phagocytosis and complement killing (50). But as Vi-deletion mutant of *S.* Typhi can still cause typhoid in humans (51), and the Vi antigen is limited to *S.* Typhi and not present in other enteric fever causing serovars such as *S.* Paratyphi. This questions the role of Vi in creating a difference in the pathogenesis of these serovars (52).

Many of the homologs of *S.* Typhimurium genes present in *S.* Typhi are inactivated or functionally disrupted. These genes mostly encode for virulence factors such as effector proteins, fimbrial proteins, or adhesins (53). Apart from this, the pathogenicity islands such as SPI-7, SPI-15, SPI-17, and SPI-18 are present only in *S.* Typhi and not in *S.* Typhimurium, whereas SPI-14 is present only in *S.* Typhimurium and not in *S.* Typhi (54). Furthermore, it was found that a group of 469 genes involved in metabolic pathways were degraded in *S.* Typhi (55). These genes may lead to the survival of *S.* Typhimurium during the inflammation and help it to compete with the gut microbiota. The degradation of these genes in *S.* Typhi makes it sensitive to the inflammatory gut (56,57). The above fact might be the reason that *S.* Typhi causes systemic disease rather than causing inflammation. The degradation of various genes in *S.* Typhi thus explains the difference between the pathogenicity of two serovars to some extent.

Some of the significant differences between *S.* Typhimurium and *S.* Typhi are shown in **Illustration 2**.

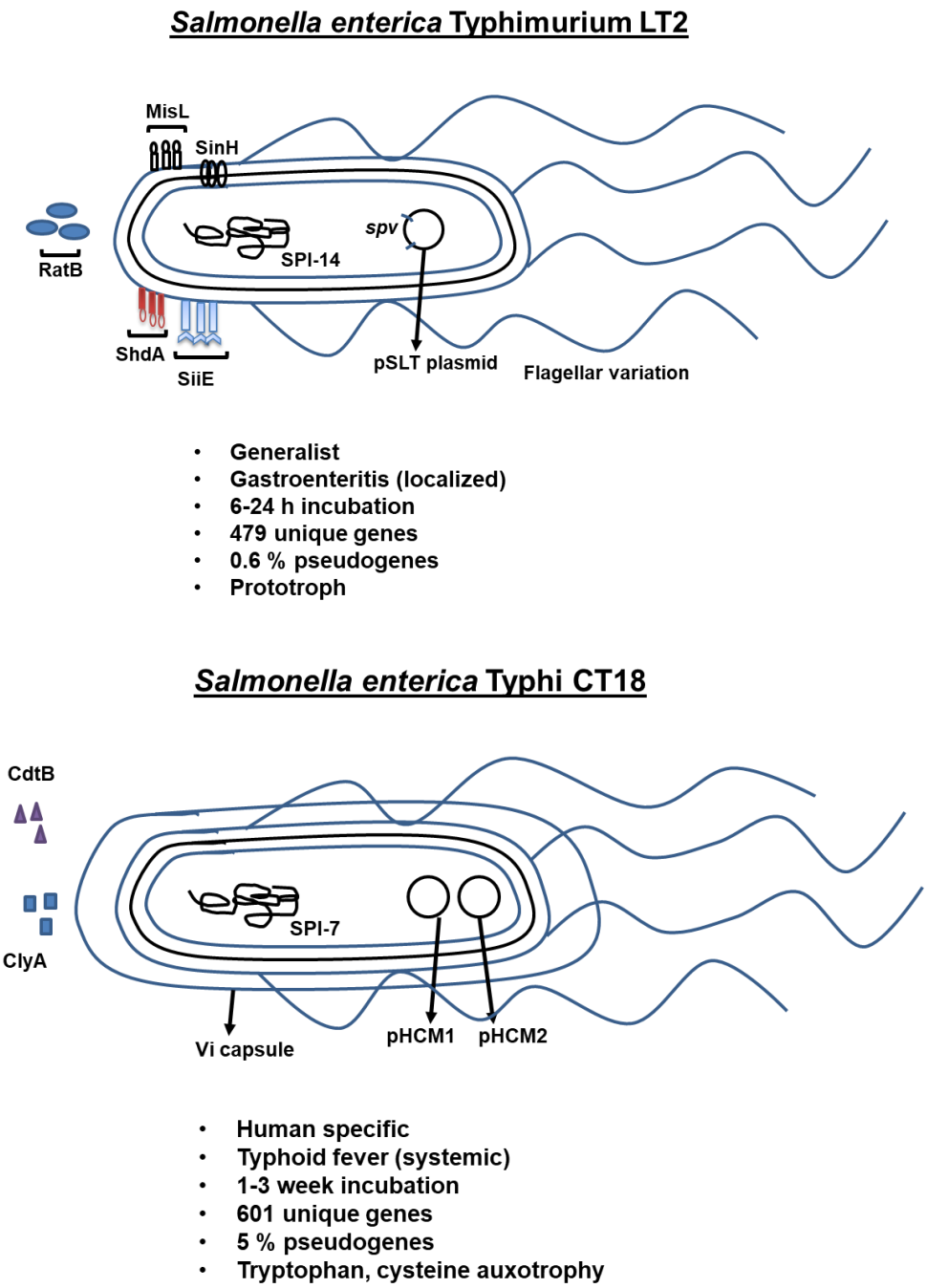


**Illustration 2:** Difference between non-typhoidal *S.* Typhimurium and typhoidal *S.* Typhi

### 1.3 History of *Salmonella* outbreaks

*Salmonella* was first visualized by Karl Eberth in 1880 in the abdominal lymph nodes and spleen of a typhoid patient (58). In 1885, Daniel Elmer Salmon and Smith first isolated this

bacteria during their search for the cause of common hog cholera (35). *S.* Typhi and *S.* Paratyphi causing typhoid and paratyphoid fevers are common in tropical regions, including South and Southeast Asia. However, travellers from these regions caused outbreaks in the non-tropical areas such as U.S and Japan. One such outbreak was reported in Japan in 1998 (59). Although typhoidal serovars are restricted to humans, non-typhoidal serovars can cause disease in a wide range of hosts. Different serotypes of non-typhoidal *Salmonella* were found in poultry in Britain and North America since 1930. *S.* Pullorum caused "bacillary white diarrhea" which was considered a major threat to the poultry industry (60). This disease was eliminated in Britain and the United States by the mid-1970s. Later in 1968, there was an increase in *S. enteritidis* infections in humans. In a 5-year report, the U.S. stated that *S. enteritidis* was 6$^{th}$ most common causative serotype for salmonellosis in 1963 and shifted to 3$^{rd}$ most common in 1967 (61). Also, a six-fold rise in *S.* Enteritidis infections was found in the U.S. during 1976-1986. Later, during 1998-2017, *S.* Typhimurium was the most common cause of salmonellosis in Shanghai (62). Moreover, about 84 % of salmonellosis cases in Australia during 2001-2016 were due to *S.* Typhimurium (63). The geographical distribution of typhoidal and non-typhoidal *Salmonella* is shown in **Illustration 3**.

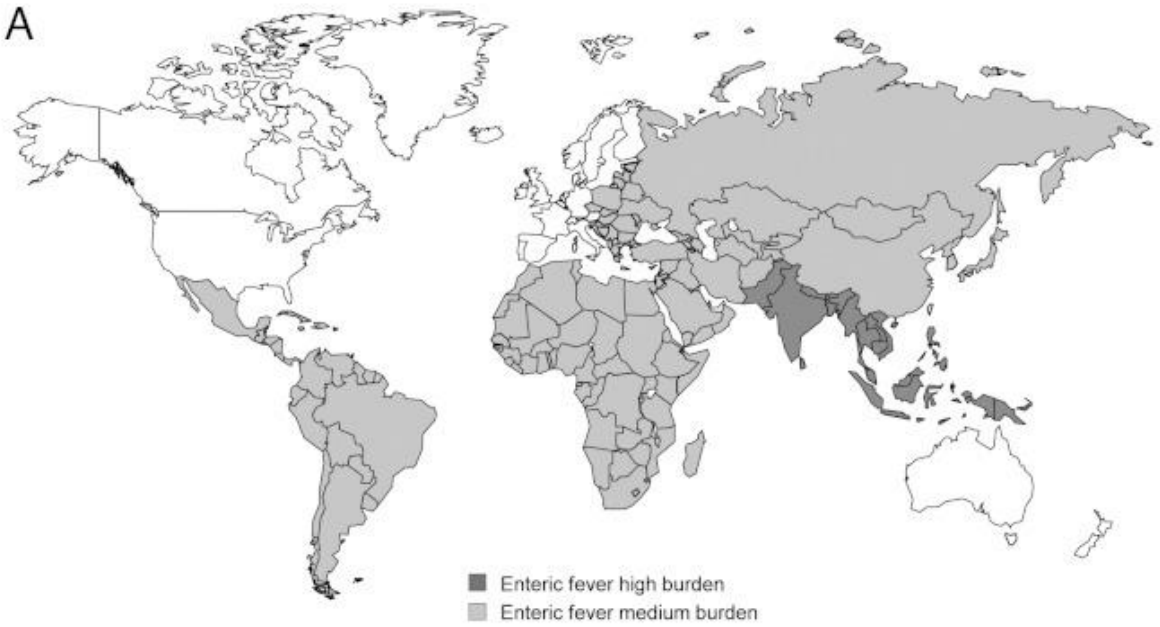

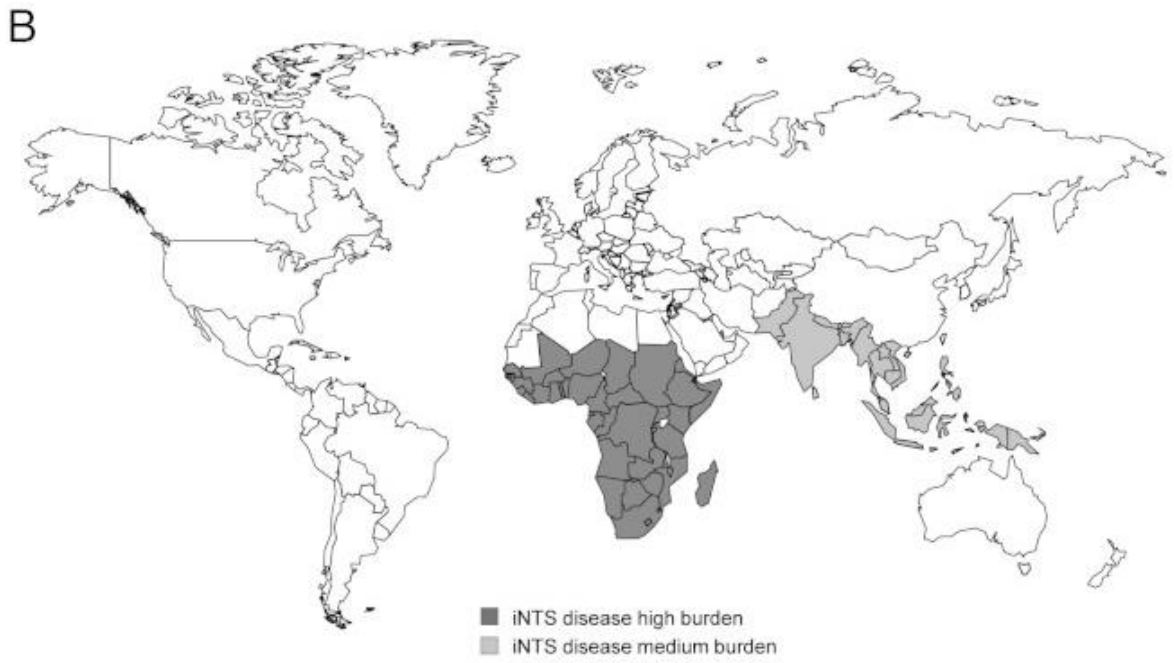


**Illustration 3:** Geographical distribution of typhoidal (A) and non-typhoidal (B) *Salmonella* (Calman A MacLennan, June 2014 (64))

### 1.4 Salmonellosis – a form of gastroenteritis

Non-typhoidal *Salmonella* is one of the four principal causes of diarrheal disease worldwide (**Illustration 4**). *Salmonella enterica* Typhimurium and *Salmonella enterica* Enteritidis are two major non-typhoidal serovars of *Salmonella* that cause a foodborne gastroenteritis disorder called salmonellosis. Foodborne diseases are a serious concern all over the world. According to WHO, 33 million lives are lost every year due to foodborne diseases. There are about 550 million people affected each year by foodborne diarrhea. Salmonellosis is one of the major player in causing foodborne diarrheal diseases in developing countries (65). It severely affects older adults, younger children, and immunocompromised individuals like HIV-patients (64).

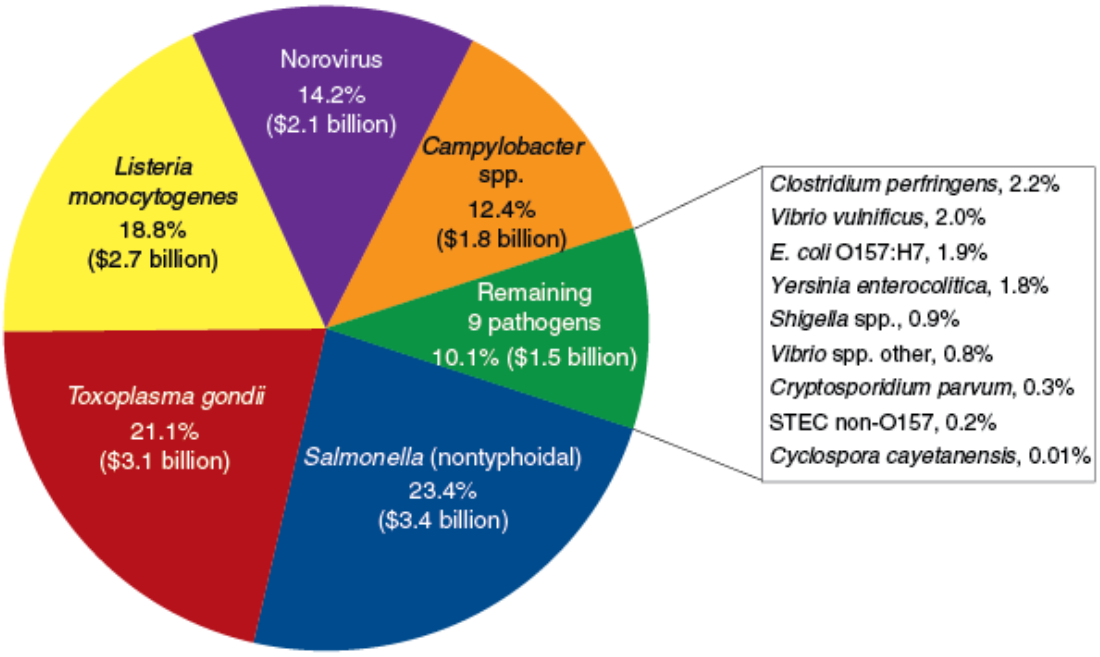


**Illustration 4:** Salmonellosis is major contributor of diarrheal diseases (Source: USDA, Economic Research Service)

It is reported that *S.* Typhimurium contributes to 50 % of cases of salmonellosis in humans (66). The Global Burden of Diseases, Injuries, and Risk Factors Study (GBD) 2017 reported 95.1 million cases and 50771 deaths worldwide due to salmonellosis in 2017 (67,68).

Significant symptoms of salmonellosis include fever, nausea, vomiting, diarrhea and abdominal pain. These symptoms generally occur 12-36 h after *Salmonella* ingestion. However, the symptoms are mild in healthy individuals; people with a weakened immune system are at high risk of infection.

### 1.5 *S.* Typhimurium – major serotype of *Salmonella* causing salmonellosis

*S.* Typhimurium causes salmonellosis in humans and typhoid-like fever in mice. In humans, typhoid is caused by other serotypes of *Salmonella*, i.e., *S.* Typhi (69,70). To date, many outbreaks of salmonellosis have been reported worldwide due to *S.* Typhimurium.

**Scientific classification of *S.* Typhimurium**

| | |
|---|---|
| Domain: Bacteria | Family: Enterobacteriaceae |
| Phylum: Proteobacteria | Genus: *Salmonella* |
| Class: Gammaproteobacteria | Species: *enterica* |
| Order: Enterobacteriales | Serotype: Typhimurium |

Most of the studies on *S.* Typhimurium to date come from research on majorly three laboratory strains: LT2, ATCC 14028 and SL1344. The other two strains which are rarely used include SR11 and UK1. SR11 is closely related to SL1344 and UK1 is related to ATCC 14028 (71). *S.* Typhimurium LT2 has defective RpoS due to which it shows attenuated virulence in mice. Due to this reason, this strain is not used for *in vivo* studies (72). Thus, SL1344 and ATCC 14028 are the most commonly used strains in the laboratory to study pathogenesis (73,74). The genomes of all three above strains differ mostly in prophage sequences and plasmids. All strains contain a virulence plasmid pSLT (90 kb), whereas SL1344 carries 112 additional genes on plasmids pRSF1010 and pCol1b9 (74).

### 1.6 Outer membrane

Gram-negative bacteria have an outer membrane in addition to the cytoplasmic cell membrane **(Illustration 5)**. The inner leaflet of this membrane contains phospholipids, and the outer leaflet contains lipopolysaccharides and outer membrane proteins. The outer membrane is essential for the viability of the cell. It plays a role in the interaction of bacteria to the host cells. It also acts as a barrier to toxic compounds (75-77). The structure of the outer membrane is conserved among different gram-negative bacteria (78).

### 1.6.1 Lipopolysaccharide (LPS)

LPS is composed of three parts: (a) Lipid A is the hydrophobic lipid component that anchors LPS to the outer membrane. It is highly conserved. (ii) a core oligosaccharide (iii) O-antigen (O polysaccharide), which acts as a hydrophilic surface. It is highly flexible (76,79). The anionic phosphate groups present in the inner region of the core oligosaccharide of LPS form cross-bridges by interacting with neighboring LPS molecules. These cross-bridges confer resistance against hydrophobic antimicrobial agents by limiting their diffusion (78). It also plays a role in the integrity of the outer membrane (77). LPS, in particular, the core-OS plays an essential factor in providing selectivity to hydrophobic molecules.

### 1.6.2 Outer membrane proteins

Outer membrane proteins can be classified majorly into β-barrel proteins and lipoproteins. Out of these, lipoproteins are embedded in the inner leaflet of the outer membrane due to the presence of lipid moieties (80). Most of the transmembrane proteins belong to the category of β-barrel proteins. Some of these β-barrel proteins can help in passive diffusion of small molecules and thus called porins. LamB, OmpA and PhoE are examples of *E. coli* porins. Apart from porins, outer membrane proteins can act as specific receptors (FhuA and FepA from *E. coli*), enzymes (phospholipase A and OmpT protease from *E. coli*) and adhesins (OmpX from *Yersinia enterocolitica*) (81). Outer membrane proteins play a significant role in the adaptation of bacteria to fluctuating habitat conditions. The expression of these proteins may vary based on the external environment (82). Apart from adaptation, these proteins also play a role in the pathogenesis of bacteria as they are the first candidates to come in contact with host cells (PagC and Rck from *S.* Typhimurium) (81). So far, 69 outer membrane proteins of *S.* Typhimurium are known. Among these, few proteins such as Lpp1, Lpp2, PagN, ShdA and OmpX are implicated in *S.* Typhimurium pathogenesis (83).

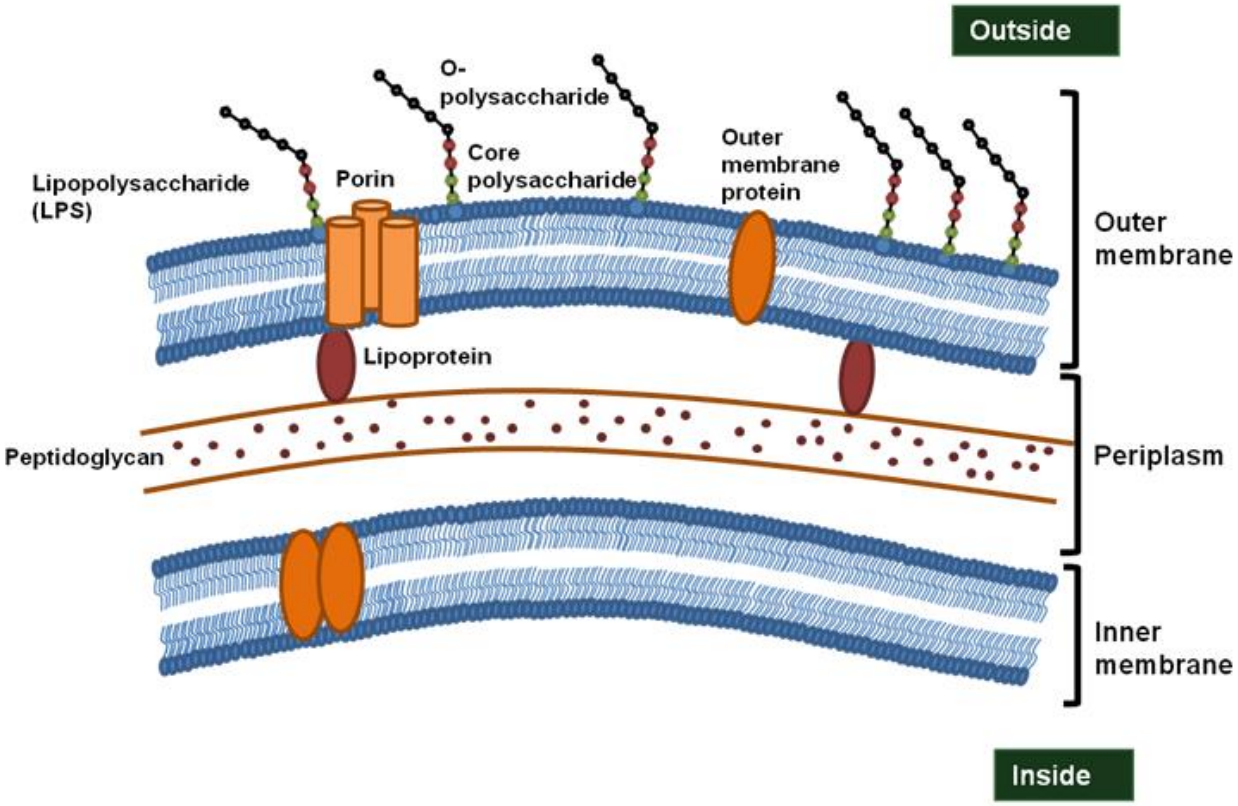


**Illustration 5:** Outer membrane structure of gram-negative bacteria

### 1.6.3 Outer membrane protein V (OmpV)

OmpV is an immunogenic low molecular weight protein of *S.* Typhimurium (84). The *ompV* gene is located at 1364089-1365035 on chromosome of *S.* Typhimurium LT2 [accession no. NC_003197.1 (1364189-1364935)]. The molecular weight of OmpV with the signal sequence is 28.052 kDa (747 bp), and without signal sequence is 25.767 kDa (681 bp). It has a homolog with 99.46 % similarity in *S.* Typhi as well as *S.* Paratyphi. Moreover, it has 88 % similarity with *E. coli* MltA- interacting protein. OmpV is a member of the MltA-interacting protein (mipA) family, which are earlier reported to be involved in the septation of the murein sacculus (85). These proteins are known to form adhesion sites for transglycosylase enzymes, and one such protein has also been reported to give protection during *S.* Paratyphi infection (86).

### 1.7 Adhesins of *S.* Typhimurium

Adhesion is the first step in the pathogenesis of *S.* Typhimurium and is majorly mediated by fimbriae or outer membrane proteins. There are 13 fimbrial and 7 nonfimbrial adhesins in *S.* Typhimurium infection known to date (87). The fimbrial adhesins participate in the initial adhesion of *S.* Typhimurium to the mucus layer, and they mostly bind to the glycoproteins and probably help in crossing the mucosal barrier (88). Non-fimbrial adhesins reported so far include BapA, SadA, SiiE, Rck, PagN, MisL and ShdA (87). Among these, BapA and SadA are known to mediate biofilm formation and probably increase colonization of bacteria in the host (89,90). SiiE binds to host cell apical membranes in a lectin-like manner and probably mediates the first contact to the host cells and initiate SPI-1-T3SS-mediated translocation of the effector proteins. The ligands for SiiE are the glycoconjugates such as GlcNAc and α2–3 linked sialic acid-containing structures (91). Rck and PagN majorly play a role in invasion (87,92). MisL and ShdA are expressed only when *S.* Typhimurium is present in the caecum, suggesting their role in adherence and colonization of the bacteria in the caecum (93,94).

### 1.8 Vaccines for *Salmonell*a infection

The vaccine induces immunological responses against specific antigens of the pathogen. The role of many virulence factors crucial for the pathogenesis of *Salmonella* is still not completely understood. Thus, broad-spectrum antibiotics are the first line of treatment in the case of *Salmonella*. The consequent use of these antibiotics leads to the emergence of multi-drug resistant (MDR) strains, which is a major concern for public health (95). One of the most potent ways to reduce multi-drug resistance is vaccination.

To date, only three vaccines are approved by the world health organization (WHO) for typhoid fever caused by *S.* Typhi, but these vaccines do not give long-lasting protection, and also the absence of any vaccine against salmonellosis underscores the need for understanding the mechanism of pathogenesis in greater detail and characterization of all the virulence factors.

**The approved vaccines against *Salmonella* so far:**

- an injectable unconjugated polysaccharide vaccine based on the purified Vi antigen (known as Vi-PS vaccine)
- an injectable typhoid conjugate vaccine (TCV), consisting of Vi polysaccharide antigen linked to tetanus toxoid protein
- an oral live-attenuated Ty21a vaccine in the capsule formulation

But the efficiency of these available vaccines is lesser than 80 % in the case of typhoid. Moreover, typhoid vaccines have not proved to be useful against salmonellosis caused by *S.* Typhimurium.

Currently, no vaccine is available for salmonellosis, and antibiotics are the only mode of treatment available. Thus new vaccine targets are being studied to find a suitable vaccine. Various vaccine candidates are being studied for non-typhoidal *Salmonella* in recent times. Some of them are listed below in **Table 3** (64).

| Name | Description | Stage of development | References |
|---|---|---|---|
| O:4,5/O:9-flagellin | O:4,5/O:9 Conjugate | Preclinical | (96,97) |
| O:4,12-TT | O:4-TT Conjugate | Preclinical | (98) |
| Os-po | O:4-porin Conjugate | Preclinical | (99) |
| O:4,5/O:9-$CRM_{197}$ | O:4,5/O:9 Conjugate | Preclinical | (100) |
| WT05 | Live attenuated | Phase 1 | (101) |
| CVD 1921 and CVD 1941 | Live attenuated | Preclinical | (102) |
| *S.* Typhimuirum ruvB mutant | Live attenuated | Preclinical | (103) |
| *Salmonella* hfq deletion mutant | Live attenuated | Preclinical | (104) |

| | | | |
|---|---|---|---|
| SA186 | Live attenuated | Preclinical | (105) |
| Porins | *S.* Typhimurium porins | Preclinical | (99) |
| *S.* Typhimurium and *S.* Enteritidis GMMA | Generalized Modules for Membrane Antigens | Preclinical | (106,107) |
| OmpD | Outer membrane protein | Preclinical | (108) |
| OmpL | Outer membrane protein | Preclinical | (109) |
| OmpF | Outer membrane protein | Preclinical | (110) |
| OmpC | Outer membrane protein | Preclinical | |

**Table 3:** Vaccine candidates against salmonellosis

Apart from above-studied proteins, an outer membrane protein OmpA from *S.* Typhimurium is known to activate dendritic cells (DCs) and induces Th1 polarization (111).

### 1.9 Properties of an ideal vaccine (Beverley, 2002 (112))

- Should give life-long immunity
- Should be broadly protective against all variants of an organism
- Should prevent disease transmission, e.g., by avoiding shedding
- Should induce effective immunity rapidly
- Should be useful in all vaccinated subjects, including infants and the elderly
- Should transmit maternal protection to the fetus
- Requires few (ideally one) immunizations to induce protection
- Would not need to be administered by injection
- Should be cheap, stable (no requirement for cold chain), and safe

## 1.10 Adjuvants are important for vaccine development

An adjuvant is a pharmacological agent that helps in boosting the immune response of a vaccine. It can increase antibody titers, immunologic memory and prolong the protective response. Thus it can help in reducing the number or amount of doses of antigen. Despite being used for almost a century, very few adjuvants are approved for use in humans due to limited understanding of their signaling pathways. An ideal adjuvant should increase immune response without imposing any side effects. Mostly aluminum salt-based adjuvants are used on a commercial scale (113). But there are some other adjuvants, including lipids, emulsions, saponins, cytokines, and nucleotides under clinical trials (114). Apart from this, outer membrane proteins are also being considered for adjuvants recently as they can evoke a significant immune response (115).

### 1.10.1. Liposome as an adjuvant

Liposome was discovered in the mid-1960s and used as a delivery vehicle since then. In 1974, it was first reported to be useful for vaccine delivery (116). Liposomes can enhance the solubility and stability of antigens. Also, they can help in the controlled release of antigen. Moreover, liposomes act as suitable adjuvants as they stimulate the humoral and cell-mediated immune response (117). Proteoliposomes are liposomes in which proteins are incorporated. It has been widely used in vaccine research since the 1980s, when adjuvant properties of proteoliposome were first discovered.

### 1.11 Objectives of the study

Based on this above background we wanted to characterize the role of OmpV in pathogenesis and immune activation of host. Towards this the broad aims of our study were:

**Aim I:** Does OmpV have a role in the pathogenesis of *S.* Typhimurium
**Aim II:** Whether OmpV has the potential to act as a vaccine candidate

# II.
# Materials and Methods

## 2.1 Bacterial strains

### 2.1.1 Culture conditions

Bacterial strains (*E. coli* and *Salmonella*) were grown at 37 °C in liquid cultures in Luria broth (LB) medium (#M1245-2.5KG, HiMedia, Mumbai, India) and maintained in Luria agar (LA) plates prepared by adding 15 g/litre agar-agar (#RM026, HiMedia, Mumbai, India) to the liquid medium. Ampicillin sodium salt (#MB504-1G, HiMedia, Mumbai, India), Chloramphenicol (#CMS218-5G, HiMedia, Mumbai, India) and Streptomycin sulphate (#S6501, Sigma, Missouri, USA) were added at a concentration of 50 μg/ml. Kanamycin sulphate (#TC136-5G, HiMedia, Mumbai, India) was added at a concentration of 30 μg/ml. All plasmids and strains used in the study are mentioned in **Table 4**.

$Amp^r$ – Ampicillin resistance; $Kan^r$ – Kanamycin resistance; $Cm^r$ – Chloramphenicol resistance; $Strep^r$ – Streptomycin resistance

| **Strains** | **Characteristics** | **Source** |
|---|---|---|
| ***S.* Typhimurium** | | |
| SL1344 | Wild type; $Strep^r$; mice virulent | Kind gift from Dr. Mahak Sharma |
| LT2 | Wild type | MTCC |
| LT2-GFP | *S.* Typhimurium LT2 strain transformed with GFP expressing plasmid pFU95; $Amp^r$ | This study |
| SL1344Δ*ompV* | *S.* Typhimurium SL1344 with chromosomal deletion of *ompV* and insertion of Kanamycin cassette; $Strep^r$; $Kan^r$ | This study |
| SL1344–comp | *S.* Typhimurium SL1344 with chromosomal deletion of *ompV* complemented with *ompV* in pACYC177 vector; $Strep^r$; $Kan^r$; $Amp^r$ | This study |
| LT2Δ*ompV* | *S.* Typhimurium LT2 with chromosomal deletion of *ompV* and insertion of chloramphenicol cassette; $Cm^r$ | This study |
| LT2- comp | *S.* Typhimurium LT2 with chromosomal deletion of *ompV* complemented with *ompV* in pACYC177 vector; $Cm^r$; $Amp^r$ | This study |

| | | |
|---|---|---|
| SL14028Δ*spi1* | *S.* Typhimurium SL14028 with chromosomal deletion of Δ*spi-1* and insertion of Kanamycin cassette; Kan$^r$ | Dr. Francisco Ramos-Morales |
| LT2Δ*spi1* | *S.* Typhimurium LT2 strain prepared with phage transduction of SL14028Δ*spi-1* strain ;Kan$^r$ | This study |
| LT2Δ*spi1*Δ*ompV* | *S.* Typhimurium LT2 with chromosomal deletion of *ompV* in LT2Δ*spi1*background; Kan$^r$; Cm$^r$ | This study |
| ***E. coli*** | | |
| *E. coli* BL21(DE3) | Wild type | MTCC |
| *E. coli*-OmpV | *E. coli* BL21(DE3) expressing *S.* Typhimurium OmpV in outer membrane; Amp$^r$ | This study |
| *E. coli* Top10 | Wild type; for plasmid storage | MTCC |
| | | |
| **Plasmids** | | |
| pKD3 | Plasmid containing chloramphenicol cassette; Cm$^r$ | Kind gift from Dr. Rachna Chaba |
| pKD13 | Plasmid containing kanamycin cassette; Kan$^r$ | |
| pACYC177 | Low copy number cloning vector; Kan$^r$; Amp$^r$ | |
| pKD46 | Temperature sensitive; encodes lambda Red genes; arabinose inducible; Amp$^r$ | |
| pFU95 | gapA-rbs-gfpmut3.1; ColE1;Amp$^r$ | Kind gift from Dr. Mahak Sharma |
| pGEX-4T3 | Glutathione S-transferase (GST) fused protein expression vector, Amp$^r$ | |
| pGEX-4T3-*ompV* | Expression contruct of GST fused with OmpV in pGEX-4T3, Amp$^r$ | This study |
| pET-14b | Protein expression vector; 6X His-tag, Amp$^r$ | Laboratory stock |
| pET-14b-*ompV* | Expression contruct of His-tagged OmpV in pET-14b, Amp$^r$ | This study |
| pET-14b-*ompV* with signal sequence | Expression contruct of His-tagged OmpV with signal peptide in pET-14b, Amp$^r$ | This study |

**Table 4:** Strains and plasmids used in the study

### 2.1.2 Cloning and primers

The list of primers used for construction of bacterial strains is given in **Table 5**.

| Primer | Sequence |
|---|---|
| OmpV-forward | AATAATCATATGGAAAGCAACCTGACGTTGG |
| OmpV-reverse | GAATAAGGATCCTCAGAATCTATAGGTCACG |
| OmpV-forward with signal | CCAGGCATATGGTGACCAAACTTAAACTTCT |
| OmpV deletion (kanamycin)-forward | GCGGTTACACTTTTGCCGCAGAACATTTGAATAAGGA ATTATGGATTGTGTAGGCTGGAGCTGCTTCG |
| OmpV deletion (kanamycin)-reverse | AGCCCGCATAACGCAGGCTTTGTCGTGGTTTTTCCGG CAAATTCAATCAATCAATTCCGGGGATCCGTCGACC |
| OmpV deletion (chloramphenicol)- forward | GCGGTTACACTTTTGCCGCAGAACATTTGAATAAGGA ATTATGGATTGTGTAGGCTGGAGCTGCTTCG |
| OmpV deletion (chloramphenicol)-reverse | TCAACAGCGCATTTATGCAAGCCGTCATGTTCGCGTT TCACATATGAATATCCTCCTTAGTTCC |
| OmpV complement-forward | ATAAGGATCCAGTGGATTTCGATGACATAT |
| OmpV complement-reverse | GATGCTGACGTCTCAGAATCTATAGGTCAC |
| GST OmpV-forward | AATAATGGATCCGAAAGCAACCTGACGTTGG |
| GST OmpV-reverse | GAATAACTCGAGTCAGAATCTATAGGTCACG |
| K1 (Kan cassette) | GAGGCTATTCGGCTATGACTG |
| K2 (Kan cassette) | TTCCATCCGAGTACGTGCTC |
| C1 (Chlor cassette) | AGAAGTTGTCCATATTGGCC |
| C2 (Chlor cassette) | CCTACCTGTGACGGAAGATC |

**Table 5:** Primer sequences used in the study

### 2.1.3 Construction of *S.* Typhimurium-Δ*ompV* mutant and complementation strain

Deletion of the *ompV* gene (located at 1364089-1365035) from the chromosome of *S.* Typhimurium LT2 (accession No. NC_003197.1) was performed using the lambda Red recombinase system using pKD46 plasmid. pKD3 was used as the template plasmid (118). Firstly, the chloramphenicol resistance cassette having 50 upstream bases of *ompV* was amplified from pKD3 and the *ompV* gene was then replaced by the chloramphenicol cassette

to obtain LT2Δ*ompV* construct. Further, the deletion of *ompV* in SL1344 strain was done using a similar method by inserting a kanamycin cassette amplified from pKD13 to obtain SL1344Δ*ompV* construct. The deletion was further confirmed by PCR and western blot at both gene and protein levels respectively. The sequence of primers is mentioned in **Table 5**. To complement the mutant, we created a complementation plasmid of pACYC177-*ompV* using restriction enzymes BamHI (#R0136S, New England Biolabs, Massachusetts, USA) and AatII (#R0117, New England Biolabs, Massachusetts, USA). This recombinant plasmid was then transformed into the mutant strain LT2Δ*ompV* and SL1344Δ*ompV* and thus, the complemented strain LT2-comp and SL1344-comp were obtained.

#### 2.1.3.1 Preparation of electro-competent cells and electroporation

**Super Optimal Broth (SOB):** 2 % tryptone, 0.5 % yeast extract, 8.56 mM NaCl, 2.5 mM KCl, 10 mM $MgCl_2$)
**SOC:** SOB containing 20 mM glucose (#15896-8, Sigma, Missouri, USA)

Overnight grown culture of *Salmonella* was used as an inoculum for 50 ml SOB. On reaching $O.D._{600}$ to 0.1, 10 mM arabinose (#A3256, Sigma, Missouri, USA) was added. Further cells were pelleted using centrifugation for 15 min at 3300 x g when $O.D._{600}$ reached 0.4-0.6. The pellet was then washed four times with 50 ml, 25 ml, 12.5 ml and 10 ml of 10 % sterile glycerol (#MB060, HiMedia, Mumbai, India) respectively. After the last washing, the supernatant was discarded and the pellet was dissolved in 250 µl of residual glycerol. The cells were then divided into 50 µl aliquots and stored at -80 ºC.

Further, amplified kanamycin or chloramphenicol cassette (20-1000 ng) was added to these competent cells and incubated on ice for 10 min. This mixture was then added to the pre-cooled 1 mm electro-cuvette (#1652089, BioRad, California, USA). A 1 s pulse of 1.8V was passed through it with the help of an electroporator (BioRad, California, USA). Following electroporation, 900 µl of SOC media was added to cells. The cells were grown for 1 h and plated on selection media accordingly. The colonies were screened for the presence of kanamycin or chloramphenicol cassette using PCR (K1, K2 primers for kanamycin cassette and C1, C2 primers for chloramphenicol cassette indicated in **Table 5**).

### 2.1.3.2 Phage transduction

**Green plates composition:** 2 g Bacto-tryptone (#211705, BD, New Jersey, USA), 0.25 g yeast (#212750, BD, New Jersey, USA), 1.25 g NaCl (#MB023, HiMedia, Mumbai, India), 1.9 g dextrose, 3.75 g agar, 1.65 mg methyl blue (#GRM348, HiMedia, Mumbai, India), 0.16 g alizarin yellow (#RM896, HiMedia, Mumbai, India) in 222.5 ml distilled water

Overnight grown culture of donor strain (1 ml) was incubated with P22 phage broth (4 ml) for 9 h at 37 ºC. Cells were then centrifuged at 6500 x g for 5 min. 100 µl of chloroform was added per 1 ml of supernatant in an autoclaved glass tube and vortexed for 2 min. After settling of chloroform, the upper layer containing the phage lysate was transformed into a fresh tube and stored at 4 ºC by sealing with parafilm. For transduction, this phage lysate was diluted in LB (1:1000 to 1:10000) and mixed with overnight grown recipient strain in 1:1 ratio (i.e., 100 µl each). This mixture was incubated at 37 ºC for 30 min and plated on LA plates containing 10 mM EGTA (#MB130, HiMedia, Mumbai, India). The transductants were streaked on green plates and light green or white colonies were restreaked 4-5 times for clearing the phage. Further, a streak of phage broth was made in the middle of green plate and colonies were streaked perpendicularly across it and incubated at 37 ºC. After 16 h, white colonies that turn green after touching phage broth were taken as lysogen free transductants (**Illustration 6**).

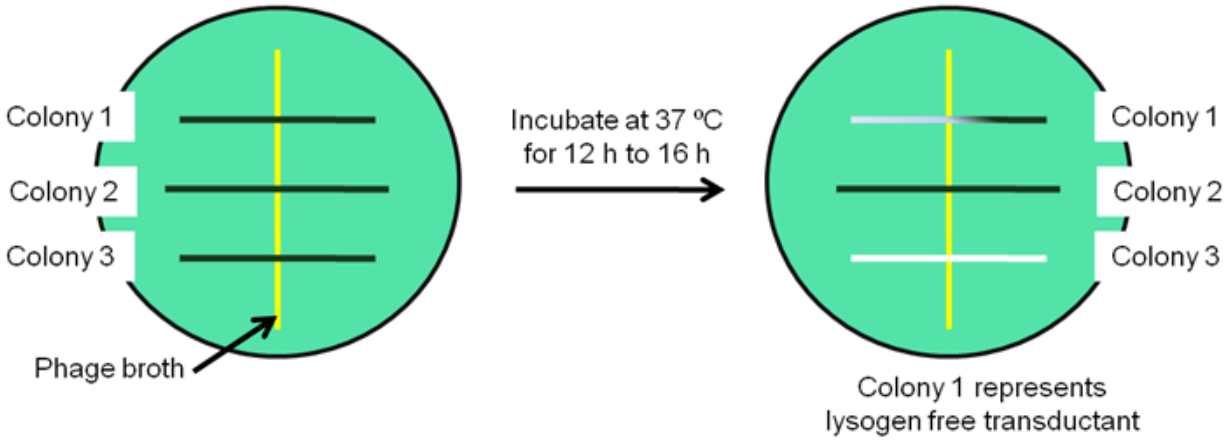


**Illustration 6:** Selection of lysogen free transductants

### 2.1.4 Construction of *E. coli* strain expressing *S.* Typhimurium OmpV (*E. coli*-OmpV strain)

The *ompV* gene with signal peptide was amplified from *S.* Typhimurium and cloned in pET-14b vector using BamHI and NdeI and transformed in *E. coli* BL21(DE3) by a similar protocol as done for the recombinant protein (as mentioned in section 2.2.1). Primers used were mentioned in **Table 2**. The expression of OmpV was then checked in the outer membrane fraction of *E. coli* after induction with 1 mM IPTG (#I6758, Sigma, Missouri, USA) for 4 h. Uninduced *E. coli* BL21(DE3) containing pET-14b-*ompV* plasmid and *E. coli* BL21(DE3) having empty pET-14b plasmid were used as a control for the experiments.

## 2.2 Protein purification and proteoliposome preparation

### 2.2.1 Purification and refolding of recombinant OmpV

*S.* Typhimurium OmpV (accession No. NC_003197.1) gene sequence was taken from NCBI online server- https://www.ncbi.nlm.nih.gov. Primers for amplification of *ompV* from *Salmonella* genome were designed with the help of this sequence by inserting the restriction sites for NdeI (#R0111S, New England Biolabs, Massachusetts, USA) and BamHI in forward and reverse primer respectively. Primer sequences are mentioned in **Table 2**. The signal peptide was removed from N-terminal region before designing of the forward primer with the help of Signal P software available online as Signal P 4.1 server (www.cbs.dtu.dk/services/SignalP/*)*. The amplified *ompV* gene was cloned into the digested pET-14b vector (Merck Millipore, Massachusetts, USA) using T4 DNA ligase (#M0202S, New England Biolabs, Massachusetts, USA). The ligated plasmid was then transformed into *E. coli* Top10 cells.

The colonies were screened using ampicillin resistance shown by pET-14b. Ampicillin sodium salt was added at a concentration of 50 μg/ml. *E. coli* Top10 cells positive for a vector having gene were checked using colony PCR and restriction digestion. The plasmid was isolated from a positive colony using mini prep kit (#27106, QIAGEN, Hilden, Germany) according to the manufacturer's protocol. The sequencing of this plasmid was done to verify the *ompV* sequence.

This plasmid was then transformed into chemically competent *E. coli* BL21(DE3) cells. Positive colonies were grown in LB medium (#M1245-2.5KG, HiMedia, Mumbai, India) in the presence of ampicillin. The bacterial cells were cultured till optical density $O.D._{600}$ reached 0.5–0.6 and then induced by 1mM IPTG at for 4 h. These cells were pelleted and dissolved in 1X PBS containing bacterial protease inhibitor (#P8465, Sigma, Missouri, USA). The cells were then lysed by sonication at 25 Å for 15 min with 30 s interval at 4 °C. The lysates were then centrifuged at 18,500 x g for 50 min at 4 °C to obtain inclusion bodies. These inclusion bodies were washed twice with PBS having 150 mM NaCl and then denatured using PBS containing 8 M urea (#MB032, HiMedia, Mumbai, India) for 2 h at room temperature.
The denatured protein was purified by Nickel-NTA affinity chromatography using the N-terminal 6X His-tag incorporated by pET-14b. For purification, 2 ml of Ni-NTA agarose resin (#30230, QIAGEN, Hilden, Germany) was used per 10 ml of urea dissolved denatured protein. Washing of resin was done using 10 ml of 20 mM imidazole (#RM1864, HiMedia, Mumbai, India) in PBS containing 8 M urea and elution of bound protein was performed using 300 mM imidazole in PBS containing 8 M urea.

The purified protein was then refolded by rapid dilution method with constant stirring using refolding buffer (10 % glycerol, 0.5 % LDAO (#40236, Sigma, Missouri, USA), 0.01 % Triton X-100 (#MB031, HiMedia, Mumbai, India) in PBS). Overnight refolding was done at 4 ºC and then insoluble aggregates were removed by centrifugation at 18,500 x g for 30 min at 4 ºC. Soluble protein was concentrated using Millipore Amicon centrifugal filter concentrator (3 kDa). Buffer was exchanged (0.5 % LDAO, 0.01 % Triton X-100 in 1X PBS) using size exclusion chromatography column Sephacryl S-200 (GE Life Sciences, California, USA). Fractions were collected and run on the SDS-PAGE gel which was then visualized using Coomassie brilliant blue staining.

### 2.2.2 Preparation of proteoliposome

Proteoliposome was prepared by dissolving cholesterol (#C3045-25G, Sigma, Missouri, USA) and asolectin (#11145-50G, Sigma, Missouri, USA) in 1:1 ratio in chloroform (#C2432-500ML, Sigma, Missouri, USA). This mixture was poured into a round bottom flask and a film was prepared on surface of the flask. The flask was then dried in a vacuum desiccator to remove the remaining chloroform content. After 3-4 h, 1 ml of recombinantly purified *Salmonella* OmpV (500 μg) dissolved in 1 X PBS was added to this flask. The film of lipids thus dissolved

and further washed three times by ultracentrifugation at 350,000 x g for 15 min at 4 ºC. Similarly, the control liposome was prepared by suspending the film made on surface of the flask in 1 X PBS.

## 2.3 Cells and mouse strains

### 2.3.1 Mouse strain

Balb/c mice (6-8 week old) were used for *in vivo* immunization experiments and isolation of BMDCs and splenic DCs. For isolation of BMDMs TLR2$^{-/-}$, MyD88$^{-/-}$ and wild type C57BL/6 mice (6-8 week old) were used.

### 2.3.2 Cell lines, primary cells and culture conditions

THP-1, a human monocytic cell line (NCCS Pune, India); RAW 264.7, a murine macrophage cell line (ATCC, VA, USA); T84, human carcinoma cell line (NCCS Pune, India); HT29, human colon cancer cell line (NCCS Pune, India) and Caco-2, a human epithelial colorectal adenocarcinoma cell line (ATCC, Virginia, USA) were used for this study. Roswell Park Memorial Institute (RPMI) (#31800, Life Technologies, CA, USA) media (for RAW 264.7 and THP-1 cells) and Dulbecco's modified eagle's medium (DMEM) (#12800-017, Life Technologies, CA, USA) media (for Caco-2, HT29 and T84 cells) having 10% FBS (#16000-044, Life Technologies, CA, USA), 100 units/ml of penicillin and 100 µg/ml of streptomycin (#15140-122, Invitrogen Life Technologies, CA, USA) was used to culture cells. Cells were maintained at 37 ºC in 5 % $CO_2$.

### 2.3.3 Preparation of bone marrow derived macrophages (BMDM) from WT, TLR2$^{-/-}$ and MyD88$^{-/-}$ mice

Femur and tibia bones were extracted from 6-8 week mice (C57BL/6 or TLR2$^{-/-}$ or MyD88$^{-/-}$) and then any muscle tissue was cleaned off and washed with ice-cold PBS. Further, the bones were dipped in 70 % alcohol for 2 min and were transferred to RPMI complete media. Further, with the help of sterile scissors, the epiphyses of the bones were cut and the bones were flushed with RPMI media, releasing the bone marrow cells into the media. Cells were washed with complete RPMI media and treated with 2-3 ml of ACK lysis buffer (#10492-01, Life

Technologies, CA, USA) for 5 min to remove erythrocytes. Further, these cells were resuspended in bone marrow differentiation media (RPMI 1640 supplemented with 10 % FBS, 100 units/ml of Penicillin and Streptomycin each, 1 mM sodium pyruvate (#11360070, (Life Technologies, CA, USA) 0.1 mM non-essential amino acids (NEAA) (#11140-050, Life Technologies, CA, USA), 1 % β-mercaptoethanol (#M6250, Sigma, Missouri, USA) and 20 ng/ml of M-CSF (#31502, Peprotech, NJ, USA)) and plated in 24-well plates. They were incubated at 37 °C with 5 % $CO_2$. The medium was changed every 2 days and fresh bone marrow differentiation medium was added. On day 7, cells were put in the medium without M-CSF and cells were treated with 10 µg/ml of polymyxin B followed by 2 µg/ml of OmpV and incubated for 24 h. The supernatants were collected and analyzed for cytokine using ELISA.

### 2.3.4 Preparation of bone marrow-derived dendritic cells (BMDC)

Bone marrow cells were isolated as mentioned above and treated with 2-3 ml of ACK lysis buffer for 5 min to remove erythrocytes. Further, these cells were resuspended in BMDC differentiation media (RPMI 1640 supplemented with 10 % FBS, 100 units/ml of Penicillin and Streptomycin each, 1 mM sodium pyruvate, 0.1 mM NEAA, 1 % β-mercaptoethanol and 10 ng/ml of GM-CSF (#31503, Peprotech, NJ, USA)) and seeded in 6-well plates. Cells were incubated at 37 °C with 5 % $CO_2$. The medium was changed every alternate day for 7 days and fresh BMDC differentiation medium was added. On day 7, cells were treated according to the experiment.

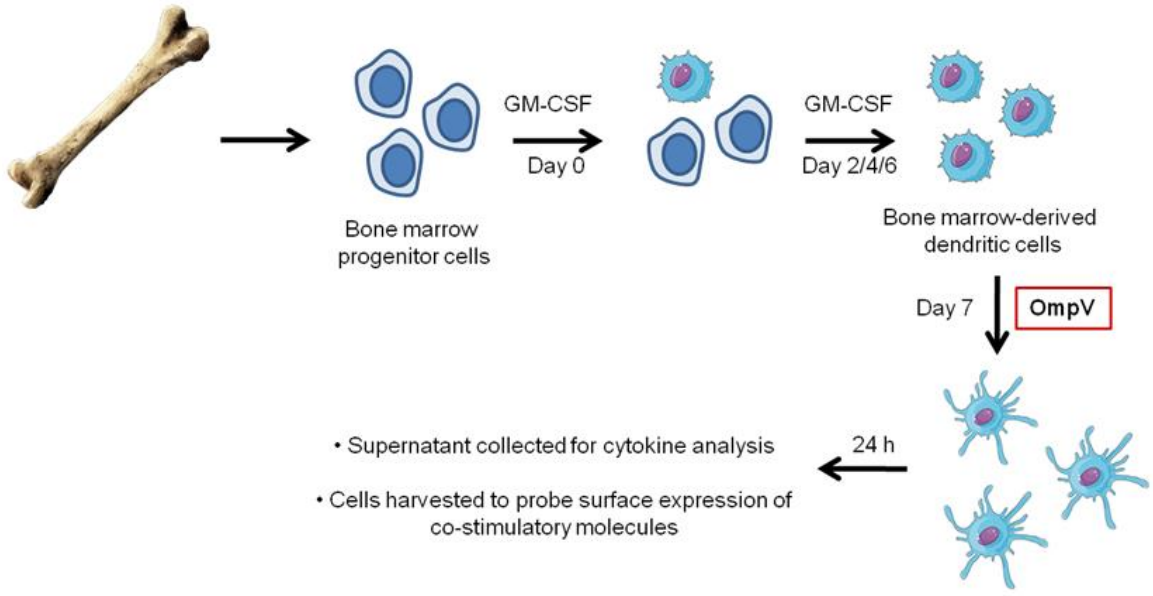


**Illustration 7:** Experimental design to assess effect of OmpV treatment of mouse BMDCs.

### 2.3.5 Isolation of splenic DCs

Mouse spleen was digested by ballooning the spleen with 5 ml calcium, magnesium-free HBSS (0.137 M NaCl, 5.4 mM KCl, 0.25mM $Na_2HPO_4$, 0.44 mM $KH_2PO_4$, 4.2 mM $NaHCO_3$, 0.1 % glucose (#G8270, Sigma, Missouri, USA) containing 400 U/ml Collagenase D (#11088866001, Roche, Basel, Switzerland) for 25 min at 37 ºC and 5 % $CO_2$. Further, 0.5 M EDTA was added for 5 min to stop the reaction. The cell suspension was then filtered through a 0.45 µm filter into RPMI complete media. Cells were washed with PBS and resuspended in 3 ml of 30 % BSA (#A9576, Sigma, MO, USA). Further 1 ml PBS was layered on top of BSA and centrifuged at 620 x g for 30 min at 12 ºC without acceleration and deceleration. Cells from interface were collected having a CD11c-enriched population. These cells were further used in the experiments.

### 2.3.6 Isolation of T cells

The mouse spleen was squashed and filtered through a 0.45 µm filter to obtain a single-cell suspension. Further, these cells were treated with ACK lysis buffer for 5 min to remove erythrocytes. Cells were washed and purified using mouse $CD4^+$ T-cell isolation kit II (Miltenyi Biotec, Bergisch Gladbach, Germany) by the negative selection method.

Briefly, $10^7$ cells were suspended in 40 µl of MACS buffer and 5 µl of biotin- antibody cocktail and incubated for 10 min at 4 ºC. Further 30 µl of MACS buffer and 10 µl of microbead cocktail was added for 15 min at 4 ºC. Cells were then washed with MACS buffer and resuspended in 500 µl MACS buffer. Cells were then loaded onto the pre-equilibrated MS MACS column and washed thrice with 3 ml MACS buffer. Flow-through containing T cells was collected and washed with MACS buffer and finally resuspended in complete RPMI media. These cells were further used for experiments.

### 2.3.7 Co-culture of splenic DCs and T cells

CFSE-labeled T cells were plated at a density of 0.5 x $10^6$ cells/ml. For CFSE labeling, 5 µM CellTrace™ CFSE **(#**C34554, Thermo Fisher, Massachusetts, USA) was added per 2 million T cells and incubated for 10 min at room temperature. CFSE was then quenched by adding an equal amount of FBS for 10 min. These cells were then washed with PBS and plated

accordingly. Further, OmpV (2 µg/ml for 24 h)-treated splenic DCs were diluted and added to these CFSE-labelled T cells in 1:20, 1:40, 1:80, 1:160 DC: T cell ratio/100 µl/well (Day 1). At Day 3, CFSE fluorescence was detected using BD FACS Accuri c6 (BD Biosciences, California, USA). CFSE-labelled T cells treated with buffer were taken as control.

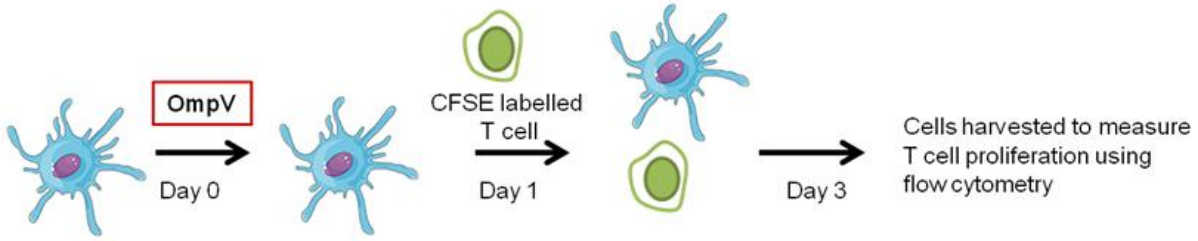


**Illustration 8:** Experimental design to determine T cell proliferation in response to OmpV treatment

## 2.4 Experimental procedures

### 2.4.1 CD (Circular dichroism) spectroscopy

Far–UV CD spectrum between a range of 200-260 nm was obtained with refolded purified recombinant OmpV protein, by taking 1 µM of the protein dissolved in 10 mM Tris-HCl (#MB030, HiMedia, Mumbai, India) buffer (pH 7.6), containing 10 mM NaCl, 0.01 % Triton X-100 and 0.5 % LDAO. Chirascan spectropolarimeter equipped with a Peltier-based temperature control system (Applied Photophysics Ltd., UK) was used to take scans using 5 mm quartz cuvette.

### 2.4.2 Tryptophan fluorescence

The intrinsic tryptophan fluorescence emission spectra of the OmpV (500 nM) were recorded using a Fluromax-4 (Horiba Scientific, New Jersey, USA) spectrofluorimeter, upon excitation at 295 nm as described in Rai et al. (119).

### 2.4.3 ANS (1-anilinonaphthalene-8-sulfonic acid) binding assay

ANS fluorescence measurements for OmpV (500 nM) were taken with a final ANS concentration of 10 µM, upon excitation at 350 nm as described by Lata *et al.* (120) using a Fluromax-4 (Horiba Scientific, New Jersey, USA) spectrofluorimeter.

### 2.4.4 Liposome swelling assay

Liposome was prepared by mixing 6.2 µmol of phosphatidylcholine (#P3556, Sigma, Missouri, USA) dissolved in chloroform and 0.2 µmol of dicetylphosphate (#D2631, Sigma, Missouri, USA) dissolved in 1:1 ratio of chloroform: methanol. This mixture was used to prepare a film on the inner surface of the round bottom flask. This film was further dried for 3-4 h and dissolved in 1 ml of recombinantly purified OmpV (final conc. 20 µg/ml diluted in 5 mM Tris–HCl buffer (pH 8.0)) to form proteoliposome. Control liposome was similarly prepared by dissolving the lipid film in 5 mM Tris–HCl buffer (pH 8.0). Both proteoliposome and liposome control were then washed with 5 mM Tris–HCl buffer by ultracentrifuging at 350,000 x g for 15 min at 4 ºC. The pellets obtained were then dried overnight in vacuum desiccators. Next day, the pellet was dissolved in 0.6 ml of 15 % dextran (#31392, Sigma, Missouri, USA) and incubated at room temperature for 2 h.

To perform liposome swelling assay, 40 µl of this liposome/ proteoliposome was mixed with 1.2 ml of 30 mM of glucose, arabinose (#A3131, Sigma, Missouri, USA), raffinose (R0250, Sigma, Missouri, USA) or sucrose (#84097, Sigma, Missouri, USA) solution and $OD_{400}$ was then monitored at an interval of 10 s for 10 min.

### 2.4.5 Outer membrane isolation

The outer membrane of *E. coli* and *Salmonella* was isolated using the following protocol. Briefly, the bacterial cells were harvested by centrifugation at 2,050 x g for 30 min at 4 °C and the cell pellet was suspended in 1 X PBS buffer (pH 7.6) containing bacterial protease inhibitor cocktail, followed by lysis using ultrasonic disruption. The cell lysate was subjected to centrifugation at 18,500 x g for 1 h, and the supernatant obtained was subjected to ultracentrifugation at 350,000 x g for 20 min at 4 °C to pellet down the membrane envelope fraction. The crude membrane fraction obtained was resuspended in PBS, ultracentrifuged

again at 350,000 x g for 20 min, and then the outer membrane fraction was extracted from the crude cell envelope by incubating with 1 % Triton X-100 at 37 °C, and the pellet was washed with 20 mM Tris–HCl (pH 7.6) by ultracentrifugation at 350,000 x g. The expression of OmpV in these outer membrane fractions was checked using western blot.

### 2.4.6 Protein estimation by Bradford assay

The protein concentration for recombinant protein, proteoliposome, mitochondrial fraction, nuclear fraction, cytoplasmic fraction and whole-cell fractions were measured using Bradford reagent (# B6916, Sigma, Missouri, USA) (121). BSA solution of different concentrations in the same buffer as that of the sample was used to make a standard curve (**Table 6**). For protein estimation, 95 µl of Bradford's reagent was added to 5 µl of protein. For nuclear, cytoplasmic or whole cell lysates, 99 µl of Bradford's reagent was added to 1 µl of sample. The samples were then mixed and kept in the dark for 15 min. The readings were taken in triplicates for each sample in a 96-well plate. The readings were taken at $OD_{595}$ using iMark Microplate Absorbance Reader (Bio-Rad Laboratories, CA, USA) and concentration of the proteins was estimated using a BSA standard curve plot.

| **Volume of BSA stock (1 mg/ml)** | **Volume of distilled water** | **Final volume** | **Concentration** |
|---|---|---|---|
| 0 µl | 100 µl | 100 µl | 0 mg/ml |
| 25 µl | 75 µl | 100 µl | 0.25 mg/ml |
| 50 µl | 50 µl | 100 µl | 0.5 mg/ml |
| 75 µl | 25 µl | 100 µl | 0.75 mg/ml |
| 100 µl | 0 µl | 100µ l | 1 mg/ml |

**Table 6:** Preparation of standards for Bradford's assay

### 2.4.7 SDS- PAGE and Western blotting

Solutions for SDS-PAGE and western blotting were prepared as follows

- **Solution A**: 29.2 g acrylamide (#MB068, HiMedia, Mumbai, India) and 0.8 g bis acrylamide (#MB005, HiMedia, Mumbai, India) in 100 ml distilled water
- **Solution B:** 1.5 M Tris-Cl, 0.4 % SDS (pH 8.8)
- **Solution C:** 0.5 M Tris-Cl, 0.4 % SDS (pH 6.8)
- **Running buffer:** 25 mM Tris (#MB029, HiMedia, Mumbai, India), 192 mM glycine (#MB013, HiMedia, Mumbai, India), 0.1 % SDS (#GRM205, HiMedia, Mumbai, India) (pH 8.3)
- **5x sample loading buffer:** 250 mM Tris-Cl (pH 6.8), 10 % SDS, 30 % Glycerol, 5 % β-mercaptoethanol (#MB041, HiMedia, Mumbai, India), 0.02 % bromophenol blue (#RM914, HiMedia, Mumbai, India)
- **Transfer buffer:** 25 mM Tris, 192 mM glycine, 20 % methanol (#1.94516, Merck, New Jersey, USA) (pH 8.3)
- **TBST buffer:** 20 mM Tris, 150 mM NaCl, 0.1 % Tween-20 (#MB067, HiMedia, Mumbai, India) (pH 7.6)

These solutions were mixed as shown in **Table 7** to form different percentage of gel

| | **Stacking** | **Resolving-10 %** | **Resolving-12.5 %** |
|---|---|---|---|
| **Solution A** | 0.45 | 3 | 3.75 |
| **Solution B** | - | 2.25 | 2.25 |
| **Solution C** | 0.75 | - | - |
| **Distilled water** | 1.8 | 3.75 | 3 |
| **10 % Ammonium persulphate** | 50 µl | 50 µl | 50 µl |
| **TEMED** | 5 µl | 5 µl | 5 µl |

**Table 7:** Buffer composition of SDS-PAGE gel

Resolving gel was cast by adding APS (#MB003, HiMedia, Mumbai, India) and TEMED (#MB026, HiMedia, Mumbai, India) just before use. Then water was layered above this to prevent oxidization. Then stacking gel was poured after resolving gel get solidified. Samples were boiled at 95 ºC for 10 min with sample loading buffer. These samples were then loaded onto gel and electrophoresis was done at 90 V at room temperature.

For western blotting, these samples were further transferred onto PVDF membrane (#162-0177, Millipore, Massachusetts, USA) at 70 V for 70 min in transfer buffer using the Mini Trans-Blot Module and Mini-PROTEAN Tetra Cell (BioRad, California, USA). The non-specific binding on these blots was blocked using 5 % BSA (#9048-468, HiMedia, Mumbai, India) prepared in TBST buffer for 1 h under rocking conditions. Following blocking, the membrane was incubated with the diluted primary antibody in 5 % BSA accordingly. Subsequently, blots were washed four times with TBST buffer for 15 min per wash and further incubated with diluted peroxidase-conjugated secondary antibody in TBST buffer for 1 h followed by four washings of 15 min each. These blots were then developed using Clarity™ Western ECL substrate (#170-5060, BioRad, California, USA) and visualized in ImageQuant LAS 4010 (GE Healthcare Bio-Sciences, Illinois, USA). The antibodies used are described in **Table 8.**

### 2.4.8 Dot Blot

ECM components such as fibronectin (#F1141, Sigma, Missouri, USA), RGD (#A8052, Sigma, Missouri, USA), laminin (#L4544, Sigma, Missouri, USA) collagen (#C7661, Sigma, Missouri, USA) and integrins such as β1 integrin (#ab219474, Abcam, Cambridge, UK) were immobilized on a nitrocellulose membrane by placing 5 µl of each of the proteins (1 mg/ml concentration) in designated circles on the membrane and dried in RT for 2-3 min. Further, the membrane containing immobilized proteins was washed and incubated with a blocking solution (5 % BSA in TBST) for 1 h. Following blocking, the membrane was incubated with recombinantly purified OmpV protein and detected with polyclonal anti-OmpV antibody (1:1000) and secondary rabbit HRP-conjugated antibody using ImageQuant LAS 4010 (GE Healthcare Bio-Sciences, Illinois, USA).

### 2.4.9 Whole-cell lysates and nuclear lysates preparation

**Buffers used:** Following buffers were prepared using HiMedia chemicals

- Lysis buffer: 50 mM Tris-Cl [pH-8], 150 mM NaCl, 0.1 % Triton-X 100, 0.1 % SDS
- Hypotonic buffer: 10 mM HEPES [pH-7.9], 1.5 mM $MgCl_2$ (#M8266, Sigma, Missouri, USA) 10 mM KCl (#MB043, HiMedia, Mumbai, India) and 0.5 M DTT (#MB070, HiMedia, Mumbai, India)

- Low salt buffer: 20 mM HEPES [pH=7.9], 25 % glycerol, 1.5 mM $MgCl_2$ , 0.02 M KCl and 0.2 mM EDTA (#MB011, HiMedia, Mumbai, India), 0.5 M DTT
- High salt buffer: Low salt buffer with 0.8 M KCl

To prepare whole-cell lysates, cells treated with OmpV or buffer following 10 µg/ml of polymyxin B (#P4932, Sigma, Missouri, USA) treatments. Following incubations, cells were washed twice with ice-cold 1 X PBS and finally the pellet was resuspended in 200 µl of lysis buffer and 1 % mammalian protease inhibitor cocktail (#P8340, Sigma, Missouri, USA). The cells were then sonicated thrice at 10 Å pulse for 3 s each time. The lysed cells were then centrifuged at 16000 x g for 30 min at 4 ºC. The supernatants were collected and estimated using Bradford reagent as mentioned in section 2.4.6 above. An equal amount of protein was loaded on SDS-PAGE and analyzed using western blots as specified in section 2.4.7 above.
For nuclear lysates, treated cells were washed once with 1 X PBS and then with hypotonic buffer. Cells were pelleted at 1850 x g for 5 min at 4 ºC. Pellet was resuspended in 150 µl of hypotonic buffer containing mammalian protease inhibitor cocktail. Cells were lysed using sonication twice at 10 Å for 3 s each. After centrifugation at 3300 x g for 15 min at 4 ºC supernatant was collected as a cytoplasmic fraction. The pellet was resuspended in 70 µl of low salt buffer along with mammalian protease inhibitor. Then 30 µl high salt buffer was added to the mixture and incubated for 10 min at 4 ºC. The mixture was then sonicated twice at 10 Å for 3 s each and incubated for 30 min on ice. The suspension was then centrifuged at 12000 x g for 30 min at 4 ºC. The supernatant was collected as nuclear lysate and analyzed using western blots as mentioned in section 2.4.7 above.

### 2.4.10 Co-immunoprecipitation and Immunoblots

For immunoprecipitation experiments, cells (RAW 264.7 or THP-1 or HT29 cells) were treated with buffer or OmpV (2 µg/ml) and whole-cell lysates were prepared as mentioned in section 2.4.9 above. To these lysates (for approximately 500 µg of protein), 0.5 µg of antibody was added and samples were incubated for 4 h at 4 ºC with constant agitation. Further, protein A/G PLUS-agarose beads (#sc-2003, Santa Cruz Biotechnology, Texas, USA) was added and incubated overnight at 4 ºC with constant agitation. The bead-protein complex was then washed thrice with lysis buffer (mentioned in section 2.4.9) and then protein was eluted from beads using 5 X sample loading buffer (mentioned in section 2.4.7) and heating for 10 min at 100 ºC.

Samples were loaded on SDS-PAGE and probed for different proteins using western blotting as specified in section 2.4.7. The antibodies used are described in **Table 8**.

### 2.4.11 GST-pull down

To express GST-tagged OmpV protein in *E. coli* BL21(DE3), the *ompV* gene without signal sequence was cloned into the pGEX vector (using primers mentioned in **Table 2**) and transformed into *E. coli*. The GST-OmpV expression was induced by incubation of transformed bacteria in the presence of 0.1 mM IPTG for 24 h at 25 ºC. Following incubation, the cells were harvested and checked for the presence of GST-OmpV in both supernatant and the pellet. A significant amount of GST-OmpV was found in the supernatant. This supernatant was then added to glutathione beads (#786-280, G Biosciences, Missouri, USA) to bind to the GST-OmpV. The unbound non-specific proteins were removed by washing with buffer (50 mM Tris (pH-8.0), 150 mM NaCl, 0.05 % NP-40 (#I8896, Sigma, Missouri, USA). The beads containing GST-OmpV were then incubated with cell lysates prepared from Caco-2 cells for overnight at 4 ºC. Following incubation, samples were washed with the above mentioned buffer and eluted from the beads with the help of heat and 5 X sample loading dye (mentioned in section 2.4.7). Further, the samples were analyzed by western blot as mentioned in section 2.4.7. The antibodies used are described in **Table 8**.

| **Western blotting** | | |
|---|---|---|
| **Antibody** | **Cat. No** | **Company** |
| β1 integrin | #ab7168 | Abcam, Cambridge, UK |
| Fibronectin | #ab6328 | |
| p-IκB | #SAB4504445 | Sigma, Missouri, USA |
| Anti-rabbit IgG HRP | #A0545 | |
| Anti-mouse IgG HRP | #A9044 | |
| GST | #16-209 | |
| *E. coli* RNA polymerase β | #663903 | BioLegend, California, USA |
| PCNA | #307902 | |
| O-antigen antibody | #225341 | BD Biosciences, New Jersey, USA |
| GAPDH | #sc-25778 | |

| | | |
|---|---|---|
| p65 | #sc-372 | Santa Cruz Biotechnology, Texas, USA |
| cRel | #sc-71 | |
| TLR2 | #sc-21760 | |
| TLR1 | #sc-514399 | |
| Lamin | #sc-20682 | |
| MyD88 | #sc-74532 | |
| JunD | #sc-74 | |
| β-actin | #sc-81178 | |
| IκB-α | #sc-847 | |
| TLR6 | #12717S | Cell Signaling Technology, Massachusetts, USA |
| cFos | #2250BC | |
| cJun | #9165BC | |
| JunB | #3753BC | |
| p-JNK | #9251BC | |
| Total JNK | #9252BC | |
| p-p38 | #4511BC | |
| Total p38 | #8690BC | |
| p-FAK | #3283S | |
| Total FAK | #44-624G | Invitrogen, California, USA |
| OmpV (polyclonal antibody) | generated | Bangalore Genei, Bengaluru, India |
| **Neutralizing antibodies** | | |
| Fibronectin | #ab6328 | Abcam, Cambridge, UK |
| α integrin | #ECM430 | Sigma, Missouri, USA |
| IgG isotype control | #400102 | BioLegend, California, USA |
| TLR2 (mouse and human) | #121802 | |
| TLR1 (human) | #mabg-htlr1 | Invivogen, California, USA |
| TLR6 (human) | #mabg-htlr6 | |
| **Flow cytometry** | | |
| PE tagged anti- mouse TLR1 | #12901180 | eBioscience, California, USA |
| FITC tagged anti- mouse/human TLR2 | #121805 | Biolegend, California, USA |
| APC tagged anti- mouse TLR6 | #FAB1533A | R&D, Minneapolis, USA |

| | | |
|---|---|---|
| FITC tagged anti-human TLR1 | #ab59702 | Abcam, Cambridge, UK |
| PE tagged anti-human TLR6 | #334707 | Biolegend, California, USA |
| FITC tagged anti- mouse CD80 | #553768 | BD Biosciences, New Jersey, USA |
| PE tagged anti mouse CD86 | #553692 | |
| FITC-mouse IgG1κ isotype control | #550616 | |
| PE-mouse IgG1κ isotype control | #550617 | |
| Fc block (anti-CD16/32) | #553142 | |
| **Microscopy** | | |
| Alexa 488 anti-rabbit | #A11034 | Invitrogen, California, USA |
| Alexa 568 anti-mouse | #A11004 | |

**Table 8:** List of antibodies used in the study

### 2.4.12 MTT-Cell Viability assay

Cell viability was determined using MTT (3- [4, 5dimethylthiazol-2-yl]-2, 5-diphenyl tetrazolium bromide) assay using MTT kit (#CCK003-2500, Sigma, Missouri, USA) as per manufacturer's protocol. Briefly, THP-1 cells were plated at a density of $1x10^5$ cells/100 µl using RPMI-1640 or DMEM complete medium. Cells were treated with 10 µg/ml polymyxin B for 30 min followed by treatments with different concentrations of OmpV and incubated at 37 ºC for 24 h. Buffer-treated cells were taken as control. Following incubations, 10 µl of MTT was added and incubated for 4 h. The precipitated MTT formazan crystals were formed (122), which was then dissolved in acidified propanol (0.1 M HCl in propan-2-ol). $O.D._{570}$ was taken on an iMark Microplate Absorbance Reader (Bio-Rad Laboratories, California, USA). Untreated cells represent 100 % cell viability.

### 2.4.13 Adhesion assay

Adhesion of bacteria to cells was quantified using CFU (colony forming unit) counting. Monolayer cultures of Caco-2 ($2 \times 10^5$ cells/500 µl/well) were grown in a 24 well plate and incubated overnight at 37 °C. Following incubation, media was removed and cells were infected with log-phase cultures of bacterial cells LT2 or SL1344 for 1 h and 15 min respectively. The multiplicity of infection (MOI) used for LT2 was 100 bacteria per Caco-2 cell and for SL1344, 20 bacteria per Caco-2 cell. The cells were washed and plated on a LA

plate without lysing, only the bacteria which remain extracellularly following washing i.e., only the adhered bacteria will grow in the LA plate. Number of adhered bacteria was enumerated by cfu counting. Adhesion of bacteria with ECM components was assessed by coating ECM components in 96-well plates followed by treatment with bacterial cells. For the competitive binding assay, cells or wells were pre-incubated with OmpV protein before addition of bacteria.

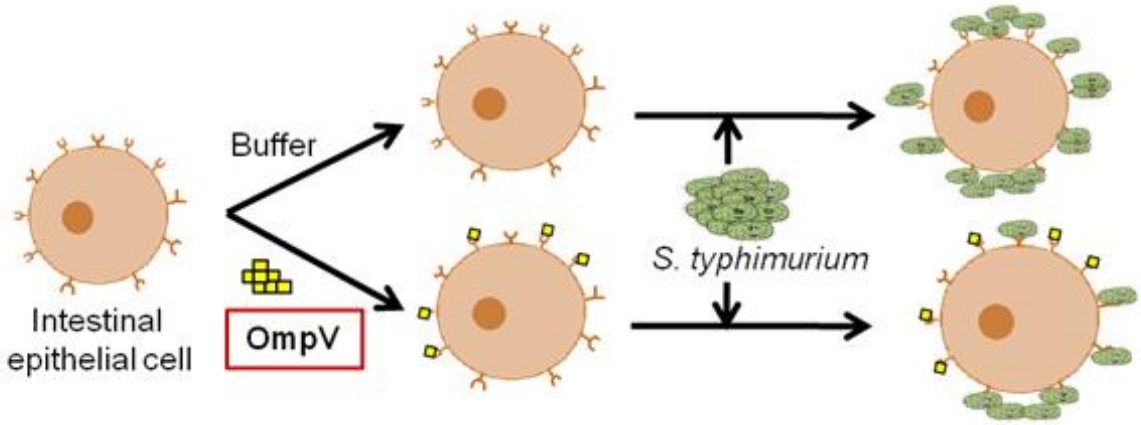


**Illustration 9:** Experimental design of competitive binding assay

### 2.4.14 Invasion assay (Gentamicin protection assay)

Monolayer cultures of Caco-2 (2 x $10^5$ cells/500 µl/well) were grown in a 24 well plate and overnight at 37 ºC. Following incubation, cells were infected with log-phase cultures of bacterial cells LT2 (MOI 100 bacteria per Caco-2 cell) or SL1344 (MOI 20 bacteria per Caco-2 cell) for 90 min and 30 min respectively. After infection, cells were incubated with gentamicin (100 µg/ml) (#TC026, HiMedia, Mumbai, India) for 60 min to kill the extracellular bacteria. Cells were then lysed with 0.1 % Triton X-100 for 30 min and the number of viable intracellular bacteria were determined by cfu count on LA plates.

### 2.4.15 Microscopy

To visualize the number of bacteria adhering to Caco-2 cells, Giemsa staining was done. Briefly, 5 x $10^4$ Caco-2 cells were plated per coverslip (VWR, Pennsylvania, USA) and incubated for 4 h. Following incubation, the cells were pre-treated with buffer or OmpV (10 µg/ml) for 1 h and then infected with *S.* Typhimurium (LT2 at MOI of 100 bacteria per Caco-2 cell) for 1 h. Following infection, the cells were washed with 1 X PBS for five times. After washing, 300 µl of 100 % ice-cold methanol was added and incubated for 20 min to fix the

cells. The fixed cells were then washed and further incubated with 10 % Giemsa stain (#G2042, Ranbaxy, Gurugram, India) for 30 min followed by washing and mounting of cells and observed under Zeiss Axio Scope.A1 biology microscope (Zeiss, Oberkochen, Germany). The purple color indicated eukaryotic cells and pink color indicated prokaryotic cells.

To visualize the adhered bacteria by fluorescent microscopy we have constructed *S.* Typhimurium expressing GFP (LT2-GFP, **Table 1**). Briefly, *S.* Typhimurium LT2 strain was transformed with pFU95 (GFP containing plasmid). Further, as mentioned above, the Caco-2 cells were infected with LT2-GFP. After washing and fixation, the cells were stained with 300 nM DAPI (#D8417, Sigma, Missouri, USA) for 2-3 min and adhered bacteria were visualized under EVOS Life technologies FL fluorescent microscope (ThermoFisher, Massachusetts, USA).

For checking the effect on adhesion of *S.* Typhimurium to Caco-2 cells using deletion mutants, both LT2Δ*ompV* and SL1344Δ*ompV* were used. Cells were infected with wild type and mutants (LT2 for 1 h and SL1344 for 15min). Following incubation, cells were washed with 1 X PBS for five times. After washing, bacteria were stained with anti-O-antigen antibody for 1 h followed by 30 min incubation of Alexa Flour 488 conjugated secondary rabbit antibody.

### 2.4.16 Co-localization studies

To check the co-localization of OmpV with ECM component and integrins the following procedure was used. 5 x $10^4$ Caco-2 cells were plated per coverslip and incubated for 4 h. Following incubation, cells were treated with OmpV (10 μg/ml) or buffer for 1 h. Treated cells were fixed using 4 % PFA for 15 min. After fixation, cells were incubated with the primary antibody against OmpV and fibronectin/β1 integrin/α1 integrin at a dilution of 1:500 and 1:250 respectively in 1X PBS for 1 h. After washing, secondary antibody conjugated with Alexa 488 (for rabbit) and Alexa 568 (for mouse) was added at a dilution of 1:500 and 1:250 respectively. The cells were then mounted and visualized using Zeiss780 confocal microscope (Zeiss, Oberkochen, Germany). In each of the experiments, 10-15 randomly selected fields were acquired and all the images from different experimental conditions were obtained using identical exposure to assess fluorescence accurately. Each experiment was repeated at least three or four times. Therefore, a total of 30-45 images were acquired for each condition. Raw images were subsequently analyzed using Image J software (National Institutes of Health,

Maryland, USA). The images were processed using identical values of brightness and contrast to obtain representative images.

### 2.4.17 Enzyme-linked immunosorbent assay (ELISA)

**Buffers used:** Following buffers were prepared from HiMedia chemicals if otherwise not mentioned:

- **Coating buffer:** 0.2 M sodium phosphate buffer (pH 6.5) or 0.1 M sodium carbonate buffer (pH 9.5)
- **Blocking solution:** 3 % BSA in PBS
- **Wash buffer:** PBS with 0.05 % Tween-20
- **Substrate solution:** 1 mg/ml O-phenyldiamine (#78412, Sigma, Missouri, USA) in citric acid buffer (pH 4.5) containing 0.2 % hydrogen peroxide (#7722-841, Merck, New Jersey, USA)
- **Stop solution:** 2 N sulphuric acid (#100731, Merck, New Jersey, USA)

For cytokine estimation, the sandwich ELISA method (123,124) was used. Briefly, 96 microwell ELISA plates (#13-678-11E, Nunc, Rochester, NY, USA) were coated overnight at 4 ºC with 100 µl/well of diluted purified capture antibody against the cytokine in coating buffer. Next day, wells were washed thrice with 250 µl of wash buffer. Following washing 200 µl of blocking solution was added per well and incubated for 1 h. Wells were again washed thrice with wash buffer and 100 µl of samples/ standards were added for 2 h. Standards were prepared from recombinant protein provided with kit as per instructions. Following 2 h, wells were washed 5 times and 100 µl of detection antibody diluted in blocking buffer was added to it and incubated for 1 h. After incubation, wells were washed 5 times and 100 µl of substrate solution was added to the wells. The reaction was stopped by adding 100 µl of stop solution in each well. $O.D._{490}$ was taken using iMark microplate absorbance reader (BioRad, California, USA). The standard curve was plotted using standards and concentrations of test sample were determined.

For quantitative estimation of OmpV binding to Caco-2 cells or ECM matrix components, monolayer cultures of Caco-2 cells ($1 \times 10^5$ cells/100 µl/well) or ECM components (5 µg/100

µl/well) were coated on 96 well microtiter plate and incubated overnight (at 37 °C for the cells and at 4 °C for the ECM components). Following incubation, the blocking solution was added to each well. The cells were treated with OmpV or buffer for 1 h following blocking. Further, the cells were washed with wash buffer for 5 times. Bound OmpV was detected with the help of ELISA using anti-OmpV antibody (1:1000) and HRP- conjugated rabbit secondary antibody (1:1000). The $O.D._{490}$ was measured as mentioned above using a substrate solution.

### 2.4.18 F-actin modulation

$5 \times 10^4$ Caco-2 cells were plated per coverslip and incubated for 4 h at 37 °C. Further, the cells were treated with buffer, OmpV (10 µg/ml), OmpC (10 µg/ml), boiled OmpV (10 µg/ml) respectively. F-actin modulation was checked in treated cells using the F-actin staining kit (#ab112127, Abcam, Cambridge, UK) as per manufacturer's protocol. Similarly, F-actin modulation was analyzed in Caco-2 cells infected with wild type or Δ*ompV* or complemented strain of *S.* Typhimurium (both LT2 and SL1344) using above mentioned kit.

### 2.4.19 Quantification of nitric oxide (NO)

Nitrite, a stable product formed by degradation of NO was estimated in RAW 264.7 cells using Griess reagent (#G4410-10G, Sigma, Missouri, USA) (125). RAW 264.7 cells ($1 \times 10^6$ cells/ml) were plated using complete RPMI-1640 medium and treatments were given for dose response as well as time course studies. 10 µg/ml of polymyxin B was added for 30 min before treatments to neutralize the effect of LPS. After respective treatment time points supernatants were collected. Griess reagent was added to the supernatant in equal volumes and incubated for 15 min in dark at room temperature. Then $O.D._{540}$ was taken using microplate reader (Bio-Rad Laboratories, California, USA) and nitrite concentration was estimated using a standard curve. The standard curve was made using sodium nitrite (#914-10ML, Sigma, Missouri, USA) of known concentrations as described in **Table 9**. *E. coli* Lipopolysaccharide (LPS) (#L2880, Sigma, Missouri, USA) 1 µg/mL was used as a positive control in the experiments. Buffer volume equivalent to highest dose of protein was used as negative control.

| Sodium nitrite (Stock- 500 µM) | Water (µl) | Concentration (µM) |
|---|---|---|
| 0 µl | 1000 | 0 |
| 10 µl | 990 | 2.5 |
| 20 µl | 980 | 5.0 |
| 30 µl | 970 | 7.5 |
| 40 µl | 960 | 10.0 |
| 50 µl | 950 | 12.5 |
| 60 µl | 940 | 15.0 |
| 70 µl | 930 | 17.5 |

**Table 9:** Standard preparation for NO estimation

### 2.4.20 Quantification of cytokines using ELISA

TNFα, IL-6, IL-8, IL-10, IL-4, IFNγ and IL-12 were measured using BD OptEIA™ ELISA sets (BD Biosciences, CA, USA) mentioned in **Table 10**.

| ELISA | Capture antibody (Cat. No) | Detection antibody (Cat. No) | Company |
|---|---|---|---|
| Mouse TNFα | #551225 | #554415 | (Becton Dickinson, New Jersey, USA) |
| Mouse IL-6 | #554400 | #554402 | |
| Mouse IL-12 | BD OptEIA, #555256 | | |
| Mouse IL-10 | BD OptEIA, #555252 | | |
| Mouse IFNγ | BD OptEIA, #555138 | | |
| Mouse IL-4 | BD OptEIA, #555232 | | |
| Human TNFα | BD OptEIA, #551220 | BD OptEIA, #554511 | |
| Human IL-6 | BD OptEIA, #555220 | | |
| Human IL-8 | BD OptEIA, #555244 | | |

**Table 10:** ELISA kits used for the study

RAW 264.7, THP-1, HT29, BMDMs or BMDCs were plated at a density of 1 x $10^6$ cells/ml and OmpV treatments were given as indicated. Polymyxin B (10 µg/ml) was added for 30 min

before treatments to neutralize the effect of LPS. Supernatants were collected at respective time points and cytokine production was measured using ELISA.

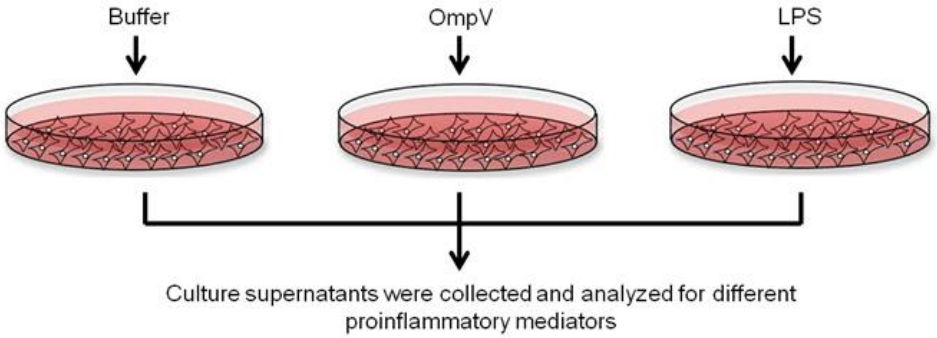


**Illustration 10:** Experimental design to determine effect of OmpV treatment

In case of *in vivo* immunizations, lymph nodes were extracted and cells obtained from these lymph nodes were plated at a density of 3 million per ml. These cells were activated using PMA (5 ng/ml) and ionomycin (500 µg/ml) for 24 h and supernatant was quantified for IL-4 and IFNγ cytokine production.

### 2.4.21 Analysis of surface expression using flow cytometry

To check the surface expression of TLRs in RAW 264.7 and THP-1 cells; and CD80 and CD86 in BMDCs, cells were plated at a density of 1 x $10^6$ cells/ml and OmpV treatments were given following 10 µg/ml polymyxin B for 30 min. After 24 h of OmpV treatment, cells were harvested and washed with 1 X PBS and FACS buffer containing 1 % FBS and 0.1 % sodium azide (#MB075, HiMedia, Mumbai, India) in 1 X PBS. For THP-1 monocytes, TLR antibodies conjugated with FITC/ allophycocyanin (APC)/ phycoerythrin (PE) were added as described in **Table 8**. On the other hand, in RAW 264.7 macrophages and BMDCs, Fc block was added and incubated for 20 min at 4 ºC before adding antibodies for TLRs, CD80 and CD86 respectively. Isotype controls were used in case of THP-1 monocytes. Following incubations with respective antibodies, cells were washed twice and resuspended in FACS buffer and were acquired by BD FACS Calibur flow cytometer (BD Biosciences, California, USA) and analysed with FLOWJO software (http://www.flowjo.com).

### 2.4.22 Neutralization of TLRs

To find the TLRs involved in OmpV recognition, RAW 264.7/THP-1/HT29 cells were plated at a density of 1 x $10^5$ cells/100 µl were plated in a 96-well plate. After pre-treatment with 5 µg/ml of anti-TLR neutralizing antibodies for 1 h (in RAW 264.7 and THP-1 cells) and 2 h (in HT29 cells), cells were treated with polymyxin B for 30 min followed by 2 µg/ml of OmpV. Supernatants were collected after 4 h for THP-1 cells and after 24 h for RAW 264.7 and HT29 cells. Further, TNFα and IL-8 were quantified using ELISA as mentioned in section 2.4.17.

To identify the α integrin subunit involved in *S.* Typhimurium infection, 2 x $10^5$ Caco-2 cells were plated in 24 well plate and incubated at 37 ºC overnight. Following incubation, the cells were pretreated with 2.5 µg/ml of neutralizing antibodies for different α subunits for 1 h followed by *S.* Typhimurium infection (MOI 100 LT2 bacteria per Caco-2 cell). Further, the adhesion was checked using cfu counting as described in section 2.4.13.

To check involvement of fibronectin in *S.* Typhimurium infection and OmpV binding, Caco-2 cells were pretreated with 5 µg/ml neutralizing antibodies for fibronectin for 1 h and infected with *S.* Typhimurium (MOI 100 LT2 bacteria per Caco-2 cell) and *E. coli*-OmpV (MOI 100 bacteria per Caco-2 cell). Further, the adhesion was checked using cfu counting as described in section 2.4.13.

The neutralizing antibodies used are described in **Table 8**.

### 2.4.23 Inhibitor studies

To check the involvement of various signaling mediators, pharmacological inhibitors (**Table 11**) were used. For this, 1 x $10^6$ cells/ml were plated and pre-treated for 1 h with different pharmacological inhibitors. Following incubation, cells were then treated with 2 µg/ml of OmpV for 24 h for RAW 264.7 cells and HT29 cells and 4 h for THP-1 cells. Following incubations, supernatants and analysed for TNFα, IL-6 and IL-8 by ELISA as mentioned in section 2.4.17.

To check the involvement of focal adhesion kinases in *S.* Typhimurium infection, Caco-2 cells were pre-treated with FAK inhibitor for 1 h and infected with bacteria *S.* Typhimurium (MOI 100 LT2 bacteria per Caco-2 cell). Further, the adhesion was checked using cfu counting as described in section 2.4.13.

| Inhibitor | Cat. no | Company | Concentration used |
|---|---|---|---|
| FAK-14 | #SML0837 | Sigma, Missouri, USA | 2.5 µM – 7.5 µM |
| IRAK 1/4 | #I5409 | Sigma, Missouri, USA | 0.5 µM – 4 µM |
| SP600125 | #57067 | | 15 nM – 50 nM |
| MLN4924 | #I502 | R&D, Minneapolis, USA | 0.5 µM – 2 µM |
| XVI | #sc-364745 | Santa Cruz Biotechnology, Texas, USA | 20 nM -100 nM |
| VX745 | #sc-361401 | | 100 nM – 200 nM |

**Table 11:** Inhibitors used in the study

### 2.4.24 Semi- Quantitative PCR

#### 2.4.24.1 RNA isolation and purification

To isolate RNA, the treated cells were rinsed with PBS and lysed by adding 1 ml of Trizol reagent (#15596-018, Invitrogen, California, USA) and passing through a syringe for 5-10 times. Then 200 µl of chloroform was added to it and vortexing was done for 15 s. Further samples were incubated at room temperature for 2 min and centrifuged at 12000 x g for 15 min at 4 ºC. The upper layer was collected in a fresh microcentrifuge tube and RNA was precipitated by adding 500 µl of isopropanol (#I9030, Sigma, Missouri, USA) followed by10 min incubation at room temperature. After incubation, samples were centrifuged at 12000 x g for 10 min at 4 ºC and the pellet was washed twice with 75 % ethanol (#1.00983, Merck, New Jersey, USA). The pellet obtained was further dried and dissolved in RNase free sigma water (#W4502, Sigma, Missouri, USA). The concentration of RNA was then measured using nanodrop (Jenway, Staffordshire, UK).

### 2.4.24.2 cDNA synthesis

cDNA was synthesized from purified RNA using Verso cDNA kit (#AB-1453/A, Thermo Scientific, Massachusetts, USA). PCR cycle included a single cycle of 42 ºC for 30 min and 95 ºC for 2 min using MyCycler thermocycler (BioRad, California, USA). PCR reaction was set as follows:

| | |
|---|---|
| **5X cDNA synthesis buffer** | 4 µl |
| **dNTP mix** | 2 µl |
| **RNA primer** | 1 µl |
| **RT enhancer** | 1 µl |
| **Verso enzyme mix** | 1 µl |
| **Template RNA** | 1 µg |
| **Nuclease-free water** | make to 20 µl |
| **Total volume** | 20 µl |

### 2.4.24.3 q-PCR program

Gene expression was studied using Maxima SYBR Green/ROX qPCR Master Mix (#KO221, Thermo Scientific, Massachusetts, USA). 10 µl of reaction mix was prepared by adding 5 µl SYBR mix (2X), 1 µl each of forward and reverse primer, cDNA and water. Reactions were set for housekeeping genes as well as gene of interest. PCR cycle included a single cycle of 95 °C (10 min) followed by 40 cycles of 95 °C (15 s) and 60 °C (60 s) in Realplex$^4$ thermocycler (Eppendorf, Hamburg, Germany). Gene expression was calculated using ΔCt method of Livak and Schmittgen (126,127). Following primers were used for RT-PCR studies

**Human α1 integrin:** **Forward:** GGATCAACTTTAGTCACCAA
**Reverse:** TGTGAATAATGAGCACTGAA

**Human TLR1:** **Forward:** CCACGTTCCTAAAGACCTATC
**Reverse:** CCAAGTGCTTGAGGTTCACAG

**Human TLR2:** **Forward:** CCTCTCGGTGTCGGAATGTC
**Reverse:** TCCCGCTCACTGTAAGAAACA

**Human TLR6:** **Forward:** TGAATGCAAAAACCCTTCACC
**Reverse:** CCAAGTCGTTTCTATGTGGTT

**Human HPRT:** **Forward:** CCTGGCGTCGTGATTAGTGAT
**Reverse:** AGACGTTCAGTCCTGTCCATAA

**Human GAPDH:** **Forward:** AAGGTGAAGGTCGGAGTCAAC
**Reverse:** GGGGTCATTGATGGCAACAATA

**Human RPL13:** **Forward:** GCCATCGTGGCTAAACAGGTA
**Reverse:** GTTGGTGTTCATCCGCTTGC

### 2.4.25 siRNA knock-down

In RAW 264.7 cells, 2.5 x $10^5$ cells were plated in a 24-well plate and TLRs were knocked down by transfection with ONTARGET plus siRNA against mouse TLR1 or mouse TLR6 (Dharmacon GE, Colorado, USA) using FuGENE HD (#E2311, Promega, Wisconsin, USA) at a ratio of 1:5 (RNA: FuGENE) for 24 h. ONTARGET plus non-targeted siRNA pool (Dharmacon GE, Colorado, USA) was used as control. After incubation, knock-down was analyzed by FACS Calibur (as mentioned in section 2.4.21) and cells were treated with 2 µg/ml of OmpV for 12 h. Supernatants were then collected and cytokine was quantified using ELISA (as mentioned in section 2.4.17).

Similarly, β1 integrin was knocked down in Caco-2 using ONTARGET plus siRNA against human β1 integrin using lipofectamine (#L3000-015, Invitrogen, Carlsbad, CA, USA). Briefly, siRNA transfection mixture was prepared by adding Mix 1 (47.325 µl of optiMEM containing 100 nM siRNA and 2 µl of P3000) into Mix 2 (49 µl of optiMEM containing 1 µl of lipofectamine) and incubated at room temperature for 15 min. This mixture was subsequently added to the cells in a dropwise fashion. Following incubation for 48 h in presence of the transfection mixture, cells were lysed and expression of β1 integrin was checked using western blot (as mentioned in section 2.4.7). The adherence of bacteria (both *S.* Typhimurium and *E.*

*coli*-OmpV) to Caco-2 cells was monitored following knock-down of β1 integrin (as mentioned in section 2.4.13).

### 2.4.26 Short hairpin RNA (shRNA) knock-down

To knock-down α1 integrin in Caco-2 cells and TLR1, TLR2 and TLR6 in THP-1 and HT29 cells, shRNA constructs (**Table 12**) were cloned under H1 promoter in GFP-expressing multi promoter vector LRV1 as described by Sharma *et al* (128). GFP-expressing multi-promoter vector LRV1 used for making a shRNA construct was a kind gift from Dr. Samarjit Bhattacharyya (IISER Mohali, Punjab, India)**.** Top and bottom strands were phosphorylated separately using protein kinase (PNK) enzyme (#M0201S, New England Biolabs, Massachusetts, USA). The 20 µl reaction was set as follows and incubated at 37 ºC for 1 h

**Oligonucleotides (100 µM stock):** 4 µl (20 µM)
**Ligase buffer (10X):** 2 µl
**PNK enzyme:** 1 µl
**Water:** 13 µl

An equal amount of top and bottom strands were annealed by boiling for 5 min followed by overnight cooling. On the other hand, LRV1 was digested using XhoI (R0146S, New England Biolabs, Massachusetts, USA) and XbaI (#R0145S New England Biolabs, Massachusetts, USA) at 37 ºC for 3 h. Then enzymes were deactivated at 65 ºC for 20 min and vector was dephosphorylated using calf intestinal alkaline phosphatase (CIP) (#M0290S, New England Biolabs, Massachusetts, USA). Vector was then ligated to phosphorylated oligonucleotides using T4 ligase. The cloned plasmid was later transformed into *E. coli* Top10 and colonies were selected using ampicillin resistance. The positive colonies were checked by PCR using H1 and U6 primers.

**H1:** CAGTGTCACTAGGCGGGAACA
**U6:** ATGTCCTTCTGCTGATACTGG

The plasmids containing shRNA and scrambled sequence were then isolated from *E. coli* Top10 using miniprep kit and further transfected into Caco-2 cells using Polyethylenimine (PEI) (#408727, Sigma, Missouri, USA) (1:3 ratio of DNA: PEI). The mixture was prepared by mixing 100 µl of optiMEM containing 1 µg DNA and 100 µl of optiMEM containing 3 µl

of PEI (1 mg/ml stock) and incubated at room temperature for 15 min. This mixture was subsequently added to the cells. The scrambled sequence of α1 integrin and TLR cloned in vector separately was used as a control. After 24 h, knock-down was checked by RT-PCR in case of Caco-2 and HT29 (as mentioned in section 2.4.24). In case of THP-1, knock-down was verified by western blotting (as mentioned in section 2.4.7). Adherence of bacteria (both *S.* Typhimurium and *E. coli*-OmpV) to cells was checked in the case of Caco-2 (as mentioned in section 2.4.13). In the case of TLR knock-down, cells were treated with 2 µg/ml of OmpV for 4 h (THP-1) and 24 h (HT29). Supernatants were then collected and TNFα and IL-8 were quantified using ELISA (as mentioned in section 2.4.17).

| **Human α1 integrin** | |
|---|---|
| **Top strand** | TCGAGAAATGAGCCTGGAACCTATTTCAAGAGAATAGGTTCCAGGCTCATTTTTTT |
| **Bottom strand** | CTAGAAAAAAATGAGCCTGGAACCTATTCTCTTGAAATAGGTTCCAGGCTCATTTC |
| **Human α1 integrin scramble** | |
| **Top strand** | TCGAGGAATTCGCACTGCAAGTAATTCAAGAGATTACTTGCAGTGCGAATTCTTTT |
| **Bottom strand** | CTAGAAAAGAATTCGCACTGCAAGTAATCTCTTGAATTACTTGCAGTGCGAATTCC |
| **Human TLR1** | |
| **Top strand** | TCGAGACAAATGTTCTTACTTCCTTTCAAGAGAAGGAAGTAAGAACATTTGTTTTT |
| **Bottom strand** | CTAGAAAAACAAATGTTCTTACTTCCTTCTCTTGAAAGGAAGTAAGAACATTTGTC |
| **Human TLR2** | |
| **Top strand** | TCGAGAGAGTTAAAAGAATCACAGTTCAAGAGACTGTGATTCTTTTAACTCTTTTT |
| **Bottom strand** | CTAGAAAAAGAGTTAAAAGAATCACAGTCTCTTGAACTGTGATTCTTTTAACTCTC |
| **Human TLR6** | |

| | |
|---|---|
| **Top strand** | TCGAGAGACAAAGAACCTATTGTTTTCAAGAGAAACAATAG GTTCTTTGTCTTTTT |
| **Bottom strand** | CTAGAAAAAGACAAAGAACCTATTGTTTCTCTTGAAAACAAT AGGTTCTTTGTCTC |
| **Human TLR scramble** | |
| **Top strand** | TCGAGGGAAGAACGATAAACTATATTCAAGAGATATAGTTTA TCGTTCTTCCTTTT |
| **Bottom strand** | CTAGAAAAGGAAGAACGATAAACTATATCTCTTGAATATAGT TTATCGTTCTTCCC |

**Table 12:** shRNA constructs used in the study

### 2.4.27 Polyclonal antisera generation

Using purified His-tagged OmpV as an antigen, polyclonal antiserum was generated in New Zealand White rabbit by antibody production service of Bangalore Genei, Bengaluru, India.

## 2.5 ***In vivo* experiments**

### 2.5.1 Survival assay and competitive index

The $LD_{50}$ dose for *S.* Typhimurium SL1344 and SL1344Δ*ompV* was calculated using female Balb/c mice. Mice were challenged orally with different doses ($1 \times 10^2$ to $1 \times 10^7$ per mouse) of SL1344 or SL1344Δ*ompV* mutant and were monitored up to 28 days. Based on the survival rate the $LD_{50}$ doses were calculated. Further, we compared the survival rate of SL1344 and SL1344Δ*ompV* infected mice by challenging mice orally with $LD_{50}$ dose ($7.5 \times 10^3$ per mouse) similar to SL1344 wild type and survival was monitored until 21 days. Kaplan-Meier plot of cumulative mortality was prepared to compare the survival rate. To analyze the number of bacteria in stools of SL1344 or SL1344Δ*ompV* or SL1344-comp (similar doses of bacteria, $5 \times 10^4$ per mouse) was orally administered to mice and stools were collected at day 4 post-infection. These stools were then weighed and dissolved in 1 X PBS. Further, different dilutions were plated on LA plates and bacteria were enumerated using CFU counting. Also, we have checked the competitive index (CI) of bacteria in different organs using CFU counting.

Towards this, mice were orally given streptomycin (7.5 mg/mouse) following fasting for 4-5 h. After 24 h of streptomycin administration, mice were kept in fasting again for 4-5 h, followed by oral challenge with equal ratio (1:1) of SL1344 and SL1344Δ*ompV* (total 5 x $10^4$ bacteria of equal ratio per mouse). Then colonization of both bacteria were checked in different organs at 2, 4 and 6 days post-infection and CI was calculated.

### 2.5.2 Mice immunization and antibody titre

Mice (n=12 per group) were immunized with four doses of OmpV (25 µg/dose) for intraperitoneal immunization and OmpV- proteoliposome (25 µg) for oral immunization at an interval of 7 days. Buffer in case of intra-peritoneal immunization and liposome in case of oral immunization were used for control mice. Following 14 days after the last dose, mice were challenged with *S.* Typhimurium SL1344 either intraperitoneally (1 x $10^3$ bacteria per mouse) or orally (7.5 x $10^3$ bacteria per mouse) and survival was monitored until 21 days. Kaplan-Meier plot of cumulative mortality was prepared to compare the survival rate.

Blood and stool were collected from the immunized (intraperitoneally and orally) mice (n=3 per group) and checked for the antibody titre. To check IgG titre, blood was taken from the retro-orbital route of immunized mice with the help of capillary. The serum was isolated by centrifuging the blood at 1000 x g for 10 min. The collected serum was then serially diluted for detection of OmpV using ELISA (as mentioned in section 2.4.17) and estimating antibody titre. Similarly, to check IgA titre, stools were collected from immunized and dissolved in 1 ml PBS containing 0.01 % sodium azide and 1 % protease inhibitor per 100 mg sample. Further the dissolved stool sample was centrifuged at 16000 x g for 10 min at 4 ºC. Serial dilutions of the supernatant were used to detect OmpV using ELISA to calculate antibody titre.

### 2.5.3 Isolation of lymph nodes

Mice were immunized with four doses of OmpV (25 µg/dose) intraperitoneally or OmpV-proteoliposome (25 µg/dose) orally at an interval of 7 days. Buffer and liposome were used respectively for the control mouse. Following 14 days of the last dose, mice were sacrificed and inguinal, mesenteric, popliteal lymph nodes (for intraperitoneal immunization) and mesenteric lymph node (for oral immunization) were extracted. These lymph nodes were squashed and filtered through a 0.45 µm filter to collect single-cell suspension. These cells were further stimulated with with PMA (5 ng/ml) (#151864, MP Biomedical, California, USA)

and ionomycin (500 µg/ml) (#I0643, Sigma, Missouri, USA) for 24 h and the presence of cytokines were detected in the supernatant using ELISA (as mentioned in section 2.4.17).

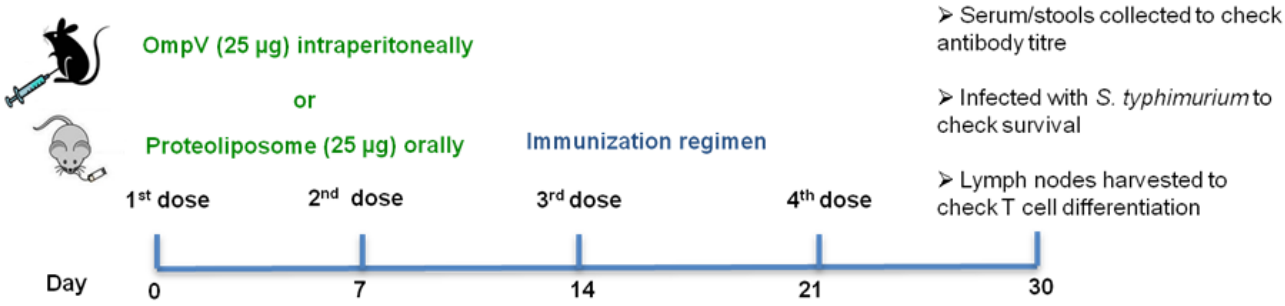


**Illustration 11:** Immunization regimen used for OmpV immunization

## 2.6 Ethical statement

This study was carried out in strict accordance with the guidelines issued by Committee for the Purpose of Control and Supervision of Experiments on Animals (CPCSEA) (Reg. No.: 1842/GO/ReBiBt/S/15/CPCSEA). All protocols involving mice experiments were approved by the Institutional Animal Ethics Committee (IAEC) (IISERM/SAFE/PRT/2016-2018/005, 010, 015).

## 2.7 Statistical analysis

Statistical significance was analyzed by the Student t-test/One way ANOVA/Two way ANOVA using GraphPad QuickCalcs software. The results were considered to be significant at *$p<0.05$, **$p<0.01$, ***$p<0.001$ and ns when $p>0.05$.

# III.
# Results

**Aim 1:** Does OmpV have a role in the pathogenesis of *S.* Typhimurium

**Chapter 1: Specific aim 1:** Whether OmpV play any role in adhesion and invasion of *S.* Typhimurium in intestinal epithelial cells

**Chapter 2: Specific aim 2:** Whether OmpV binds and activate any integrin receptors on the surface of intestinal epithelial cells

# Chapter 1

**Specific aim 1:** Whether OmpV play any role in adhesion and invasion of *S.* Typhimurium in intestinal epithelial cells

### 3.1 Adhesion and invasion is crucial to *S.* Typhimurium pathogenesis

*S.* Typhimurium enters the human body through contaminated food and water. On reaching the intestinal lumen, *S.* Typhimurium moves to intestinal epithelial cells (IECs) with the help of flagella. IECs are polarized into the apical side with brush border membrane facing the intestinal lumen and the basolateral side (129). At the luminal side intestinal epithelial layer remains covered with mucus. The mucus layer and the tight junctions between the epithelial cells keep the basolateral side almost entirely inaccessible to an invading pathogen. However, the M cells present in the intestinal epithelial layer helps *S.* Typhimurium to get access to the basolateral side (130,131). M cells are a subset of highly specialized follicle-associated epithelium (FAE) and are capable of transcytosing microorganisms from the gut lumen to the underlying Peyer's patches (132). In 2012, Tahoun *et al.* reported that *Salmonella* could transform follicle-associated epithelial cells into M cells to enhance bacterial translocation across the intestinal barrier (133). After getting transcytosed through the M cells, *S.* Typhimurium gets exposed to the basolateral side of the intestinal epithelial cells (**Illustration 12**).

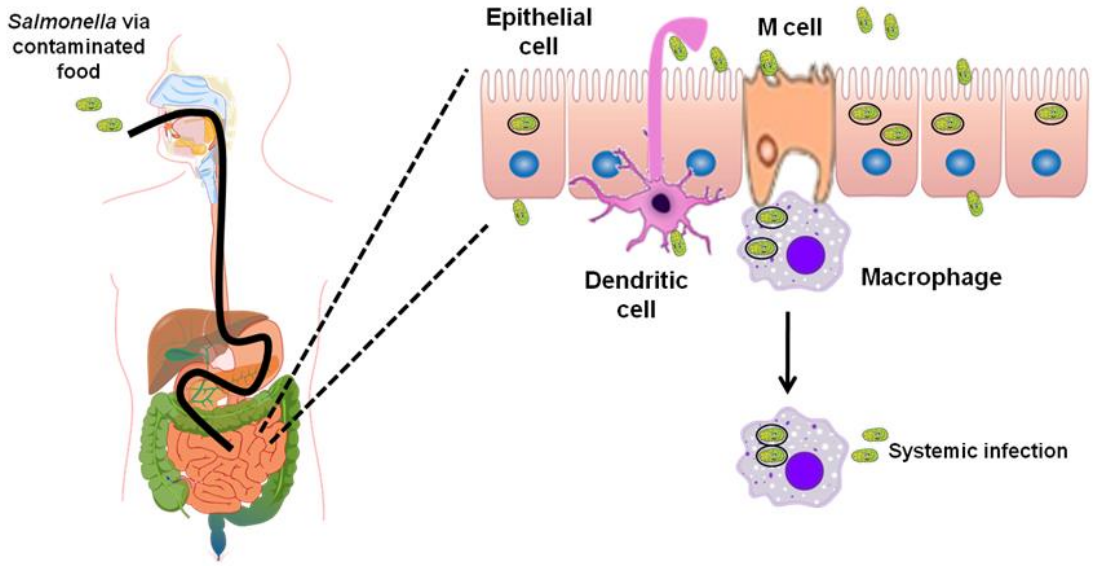


**Illustration 12:** Pathogenesis model of *Salmonella enterica*

### 3.1.1 Role of adhesins in the pathogenesis of *Salmonella*

Adhesins are required for adhering to the mucosal layer at the luminal side of the intestine, and then adhere to the basolateral side of the intestinal epithelial cells. The fimbrial adhesins participate in the initial adhesion of *S.* Typhimurium to the mucus layer, and they mostly bind to the glycoproteins and probably help in crossing the mucosal barrier (88). Some of the fimbrial proteins bind to the ECM components; for example, Type 1 fimbriae bind to laminin, and curli fimbriae bind to fibronectin (134,135). Generally, ECM is not present at the apical surface, and fimbrial adhesins do not take part in the binding at the basolateral side. Therefore, fimbrial adhesin probably binds to the ECM expressed at the apical side by adenosine produced due to inflammation (93). Non- fimbrial adhesins, including MisL, ShdA and BapA (35,93,94,136) can bind to other extracellular matrix components like fibronectin present on the basolateral side and thus help in adhesion from the basolateral side.

### 3.1.2 Invasion strategies of *Salmonella*

Adhesion is followed by invasion. *S.* Typhimurium can invade intestinal epithelial cells through both trigger and zipper mechanisms (**Illustration 13)**. The apical invasion through a trigger mechanism induced by T3SS-1 (Type 3 secretion system-1) is a long-known phenomenon (137,138); however, the basolateral invasion through the zipper mechanism has been identified recently to be used by Rck protein (139).

#### 3.1.2.1 SPI-1 mediates trigger mechanism of invasion

T3SS-1 involved in apical invasion is a needle-like apparatus that allows translocation of bacterial effector proteins (SipA, SopA, SopB, SopD, and SopE2) into host cytoplasm across intestinal epithelial cells (140-142). These effector proteins trigger actin modulation leading to ruffle formation and engulfment of bacteria by host cells (143). The proteins that help in invasion are mostly encoded by *Salmonella* pathogenicity island-1 (SPI-1). The trigger mechanism allows *Salmonella* to invade intestinal epithelial cells from the apical side (21).

### 3.1.2.2 Adhesins mediate zipper mechanism of invasion

Rck and PagN known to mediate adhesion and invasion by interacting with proteoglycan (144). It was reported that even in the absence of T3SS-1, Rck and PagN, *Salmonella* can still invade the cells, indicating the presence of other factors or modes for invasion (145). The most common receptors known to be involved in the zipper mechanism are integrins that bind to bacterial proteins either directly or through ECM components. After getting activated, integrin leads to phosphorylation of actin filaments, which further results in actin modulation (146). The modulation of actin filaments helps the bacteria to invade intestinal epithelial cells from the basolateral side (147).

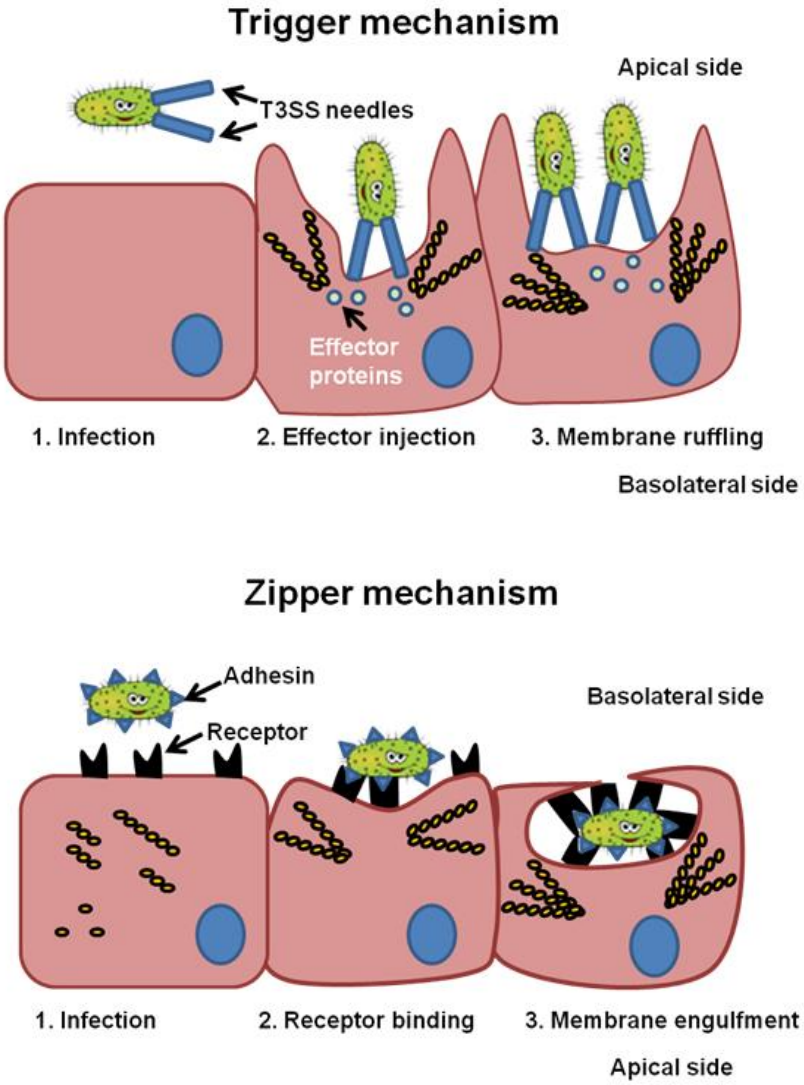


**Illustration 13:** Zipper and Trigger mechanism

## 3.2 Objective

As adhesion and invasion are the prerequisite for the pathogenesis of *S.* Typhimurium, we formulated the following objectives to check the role of OmpV in the pathogenesis of the bacterium:

1. To clone, purify and characterize OmpV protein
2. To make OmpV deletion and complement strain of *S.* Typhimurium and OmpV over-expression strain of *E. coli* (*E. coli*-OmpV)
3. To probe the role of OmpV in adhesion and invasion of *S.* Typhimurium to intestinal epithelial cells
4. To probe whether there is any effect in the pathogenesis of *S.* Typhimurium *in vivo* in the absence of OmpV.

## 3.3 Results

**3.3.1 Objective 1:** To clone, purify and characterize OmpV protein

#### 3.3.1.1 Expression and purification of recombinant protein from *E. coli*

OmpV (27.3 kDa), one of the uncharacterized outer-membrane proteins of *S.* Typhimurium belongs to the mipA family. To characterize OmpV, we first wanted to purify the protein in a large amount. Towards that, we wanted to make recombinant OmpV protein. To express this protein in *E. coli*, we have cloned the *ompV* gene in pET14b vector without the signal peptide to block the integration of protein in the outer membrane of *E. coli*. After induction with IPTG, the majority of protein (25.7 kDa) was found to be expressed in an insoluble inclusion body formed by aggregation of the protein. These aggregates were further dissolved in 8 M urea (**Fig. 1**).

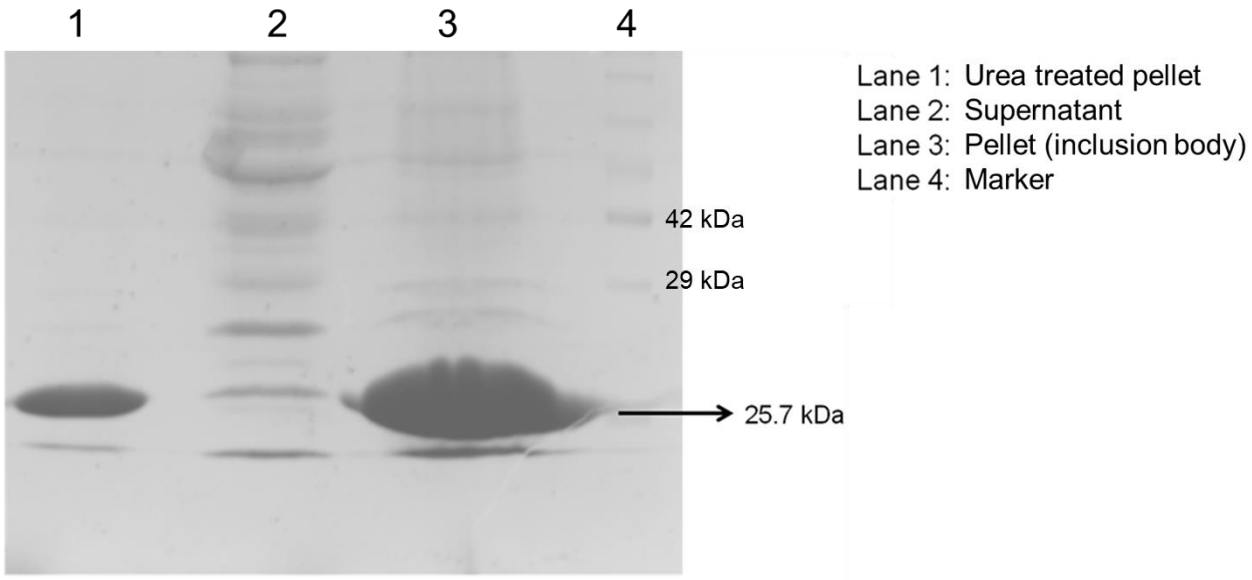


**Figure 1. Profile of overexpressed and denatured OmpV**

SDS-PAGE showing over-expression of OmpV in pellet in form of inclusion body after induction (Lane 2) as compared to supernatant (Lane 3). The pellet was dissolved in 8M urea and denatured protein is shown (Lane 4).

After solubilizing this inclusion body using 8 M urea, His-tagged OmpV (denatured) protein was purified from other proteins using nickel – NTA affinity chromatography (**Fig. 2**).

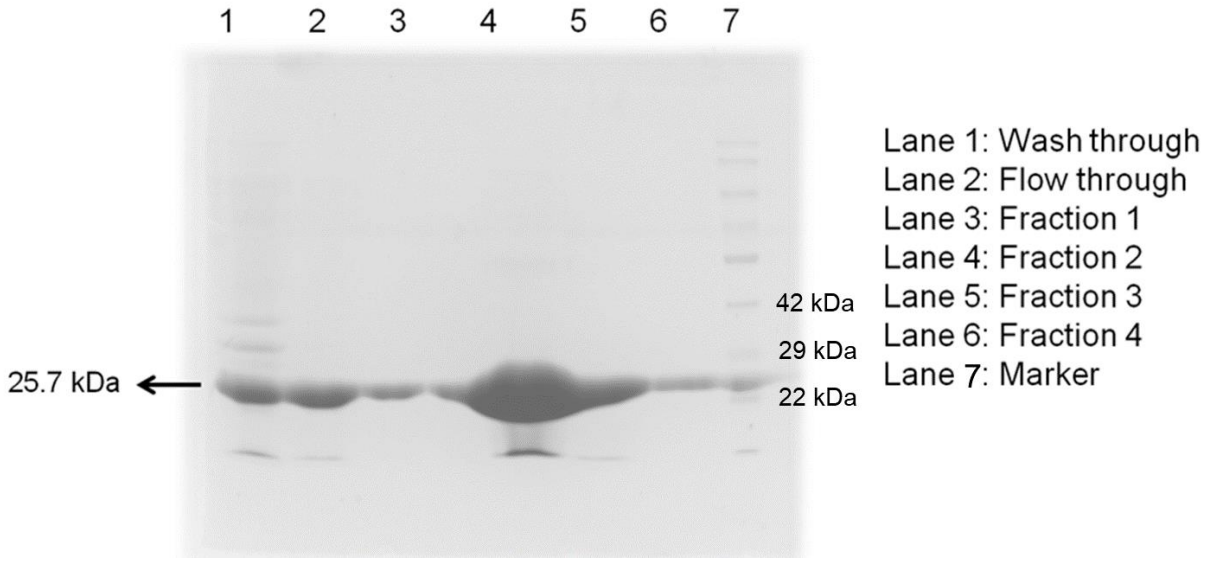


**Figure 2. Profile of purified OmpV from different fractions of nickel chromatography**

SDS-PAGE showing different fractions collected during nickel chromatography. Lane 1 and 2 represent wash through and flow through. Lane 3-6 represents fraction 1-4 of nickel chromatography.

This denatured protein was then refolded using the dilution method in a buffer containing detergents. We have observed that the maximum refolding of protein was observed using PBS containing 0.5 % LDAO and 0.01 % Triton X-100. After refolding the protein overnight at 4 ºC, the misfolded protein was removed by centrifugation at 18,500 x g for 15 min at 4 ºC. The protein was then subjected to size exclusion chromatography for buffer exchange. The concentration of this purified protein was then estimated and used for experiments.

### 3.3.1.2 Circular dichroism and protein modeling of OmpV indicates the beta-sheet structure

To confirm that the refolding of the above-purified protein is appropriate, we have analyzed the structure of OmpV using protein modeling studies. Using an amino acid sequence of OmpV in swiss modeling software (https://swissmodel.expasy.org/interactive), we observed beta-sheets structures in most of the models that were generated (**Fig. 3**).

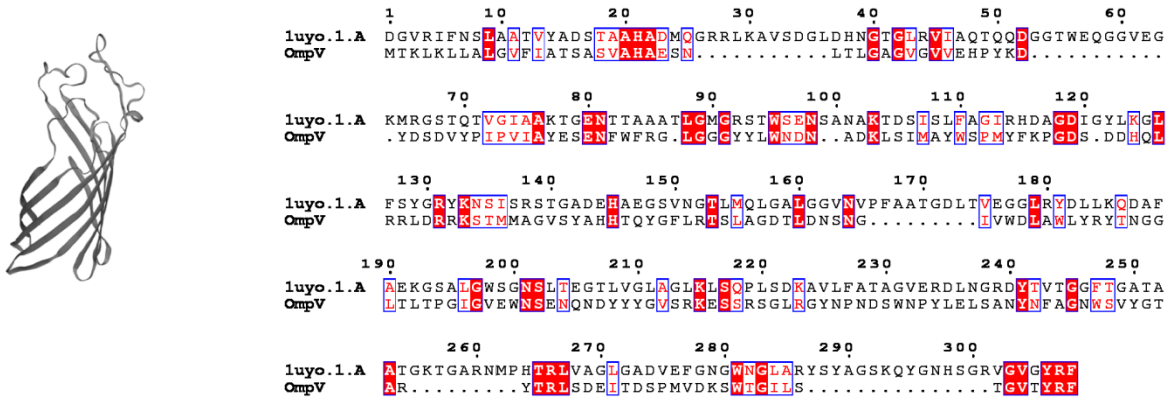


**Figure 3. Protein modelling of OmpV indicates presence of β-sheets**

Protein modeling of OmpV using structure of outer membrane protein of *Neisseria meningitidis* (1uyo) using Swiss model software (left) and sequence alignment of OmpV based on homology with outer membrane protein of *Neisseria meningitidis* (1uyo) (right).

This result is in accordance with the far-UV CD spectra of the refolded protein that shows negative ellipticity minima at 218 nm, which also indicates beta-sheet rich structures (**Fig. 4**). These beta-sheet rich structures suggest that the protein is correctly refolded.

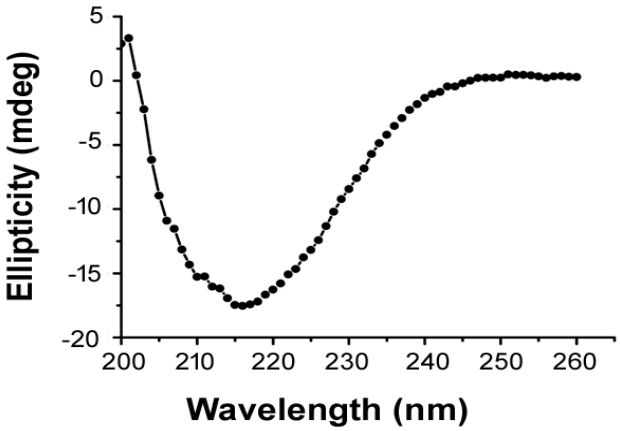


**Figure 4. Far-UV circular dichroism (CD) spectra of OmpV shows β-sheet rich structure**

Far UV CD-spectra of recombinantly purified protein showing a β-sheet rich structure with an ellipticity minimum at 218 nm.

Further, a decrease in tryptophan fluorescence and red shift in urea-denatured OmpV (**Fig. 5A**) as well as with an increase in temperature (**Fig. 5B**) suggest proper refolding of the recombinant OmpV protein. A decrease in ANS binding in urea-denatured OmpV (**Fig. 5C**) as well as with an increase in temperature (**Fig. 5D**) suggest denaturation of a properly refolded OmpV protein.

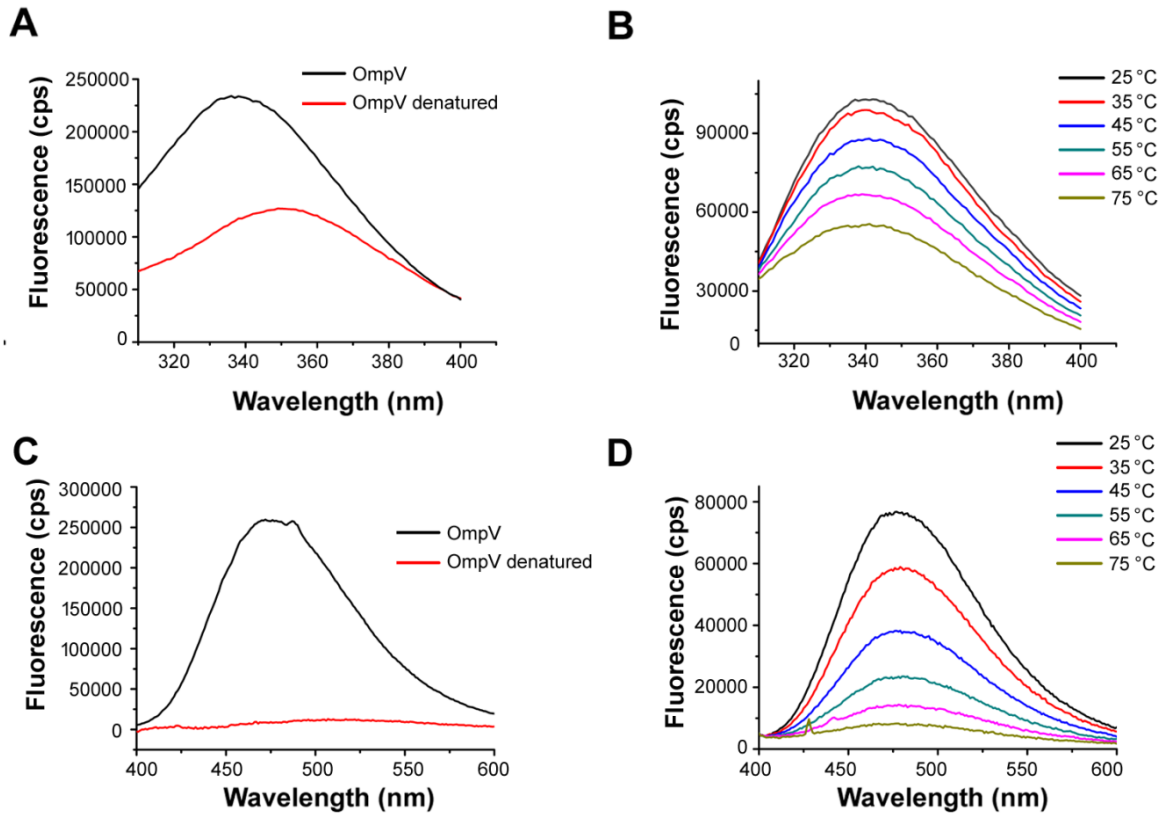


**Figure 5. Structural characterization of recombinant OmpV protein**

A) Refolded protein showed tryptophan fluorescence emission maximum at around 340 nm, whereas the urea denatured protein showed redshifted emission maximum at around 350 nm. These data suggested proper refolding of recombinant OmpV and its denaturation upon urea treatment. (B) A gradual decrease in tryptophan fluorescence and a red shift in fluorescence wavelength maxima with increase in temperature suggesting proper refolding of the recombinant OmpV protein and its thermal denaturation upon increase in temperature. (C) A decrease in ANS binding in urea-denatured OmpV as compared with refolded OmpV confirms proper refolding of recombinant OmpV protein and its denaturation upon urea treatment. (D) Decrease in ANS binding with increase in temperature, suggesting thermal denaturation of a properly refolded OmpV protein.

We have also confirmed the absence of soluble aggregates in purified OmpV by size exclusion chromatography (**Fig. 6**). Blue dextran was used as the control for void volume. Other controls, i.e., carbonic anhydrase (29 kDa) and bovine serum albumin (BSA) (66.5 kDa), indicated that OmpV is forming a trimer and eluting at approximately 70 kDa.

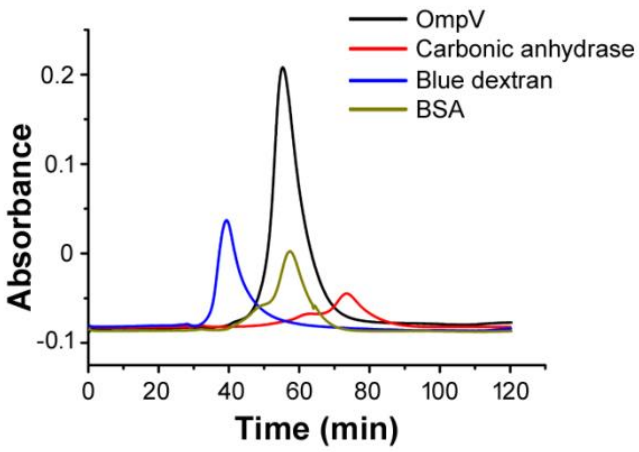


**Figure 6. Size exclusion chromatogram of recombinant OmpV protein with standards**

Size exclusion chromatography profile indicating the absence of any soluble aggregates in the OmpV preparation and elution of OmpV trimer at an elution volume corresponding to molecular weight of ~70 kDa. Blue dextran was used as control for void volume. Other molecular weight markers used are carbonic anhydrase (29 kDa) and bovine serum albumin (BSA; 66.5 kDa)

### 3.3.1.3. Liposome swelling assay suggests that OmpV is not a porin

As demonstrated by far-UV CD spectra of the refolded protein, OmpV is majorly composed of a beta-sheet rich structure, which is a structural characteristic of most porins. However, CD spectra cannot describe the functional properties of a protein. Thus, to examine whether OmpV can act as a porin functionally, a liposome swelling assay was done. This assay is used to describe the pore-forming activity of a protein by checking the rate of diffusion of different solutes through it. For liposome swelling assay, proteoliposome was prepared by the integration of recombinant OmpV into a liposome. Here we observed that OmpV-proteoliposome doesn't allow free diffusion of molecules (different saccharides) through it. Diffusion profiles for saccharides having different molecular weights were checked, but there was no swelling of liposomes due to diffusion through the lipid bilayer, as indicated by constant $O.D._{400}$. These results suggests that OmpV doesn’t disrupt lipid bilayer, hence it may not act as a porin. During the liposome swelling assay, we have included OmpU of *Vibrio cholerae* as a positive control as it is earlier reported to act as porin (**Fig. 7**).

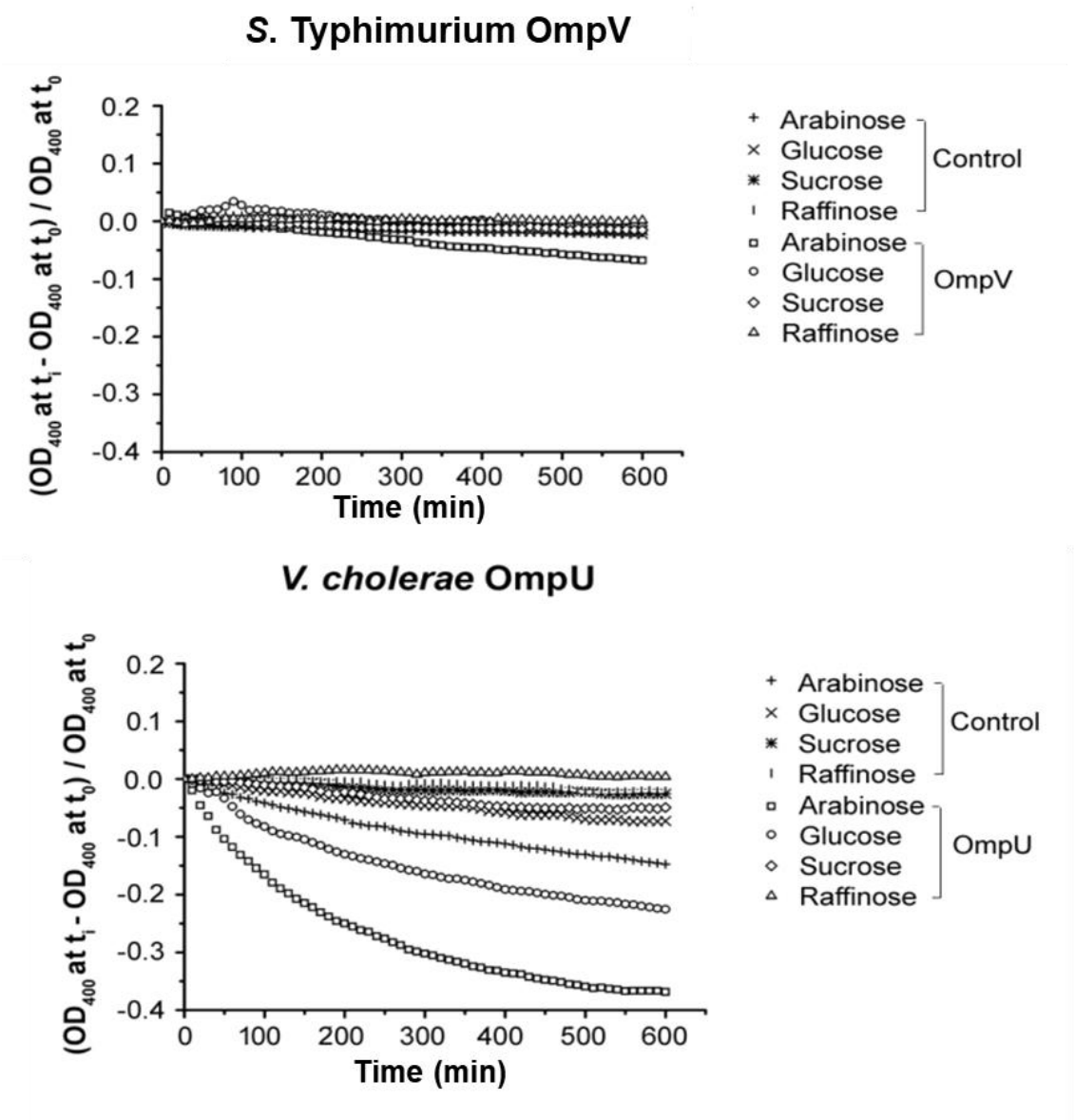


**Figure 7. Liposome swelling assay indicates OmpV is not a porin**

A constant O.D.$_{400}$ indicates absence of liposome swelling and hence no diffusion of sugars in case of OmpV-proteoliposome. OmpV-proteoliposome was prepared by adding 20 µg/ml diluted OmpV in 5 mM Tris–HCl buffer. 40 µl of this liposome/ proteoliposome was mixed with 1.2 ml of 30 mM of different sugars and OD$_{400}$ was then monitored at an interval of 10 s for 10 min. *V. cholerae* OmpU is taken as a positive control.

**3.3.2 Objective 2:** To make OmpV deletion and complement strains of *S.* Typhimurium and *S.* Typhimurium OmpV expressing strain of *E. coli* (*E. coli*-OmpV)

### 3.3.2.1. Preparation of OmpV deletion and complement strain of *S.* Typhimurium

OmpV was deleted from the chromosome of *S.* Typhimurium LT2 and *S.* Typhimurium SL1344 by lambda Red recombinase system using pKD46 plasmid. To make LT2Δ*ompV* construct, the chloramphenicol resistance cassette having 50 upstream bases of *ompV* was amplified from pKD3 using PCR, and similarly, kanamycin resistance cassette with 50 upstream bases of *ompV* was amplified from pKD13 to make SL1344Δ*ompV* construct. The amplified resistance cassette was then added to electrocompetent *S.* Typhimurium containing pKD46 using electroporator and colonies were screened for presence of *ompV* using PCR (**Fig. 8**).

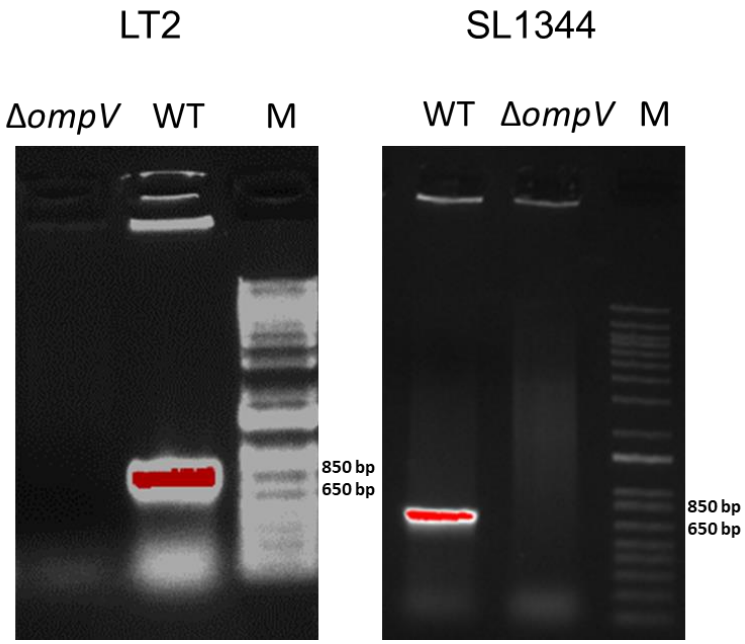


**Figure 8. PCR analysis confirms OmpV deletion in *S.* Typhimurium**

Colony PCR analysis of Δ*ompV* strain of *S.* Typhimurium LT2 and *S.* Typhimurium SL1344 using OmpV primers mentioned in Table 5 to check for the presence of OmpV. Wild type (WT) strain was taken as a positive control.

Further, complement strain LT2-comp and SL1344-comp were obtained by transforming pACYC177-*ompV* plasmid into the mutant strain LT2Δ*ompV* and SL1344Δ*ompV*. The lysates of wild type, deletion mutant and complement strain were then prepared, and the presence of OmpV was detected at the protein level using western blot (**Fig. 9**).

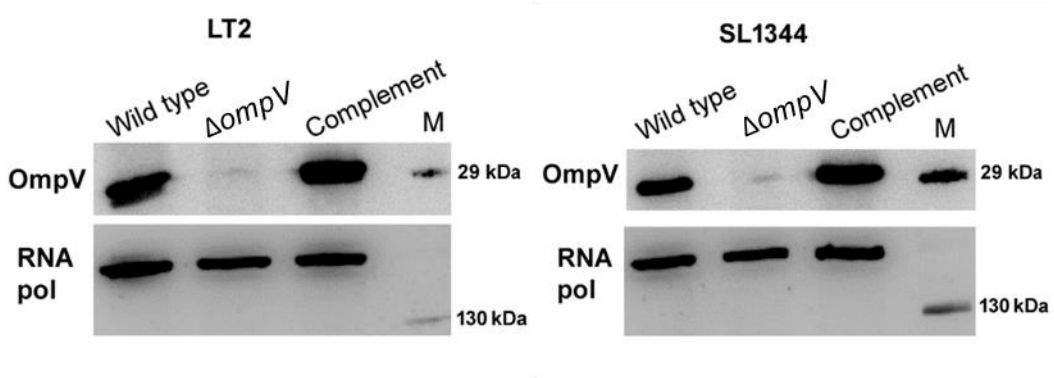


**Figure 9. Western blot analysis to check presence of OmpV in wild type, deletion mutant and complementation strain of *S.* Typhimurium**

Western blot analysis of wild type, Δ*ompV* and complemented strain of *S.* Typhimurium LT2 and *S.* Typhimurium SL1344 strains to check for the presence of OmpV. RNA polymerase (RNA pol) was used as a loading control.

### 3.3.2.2. Preparation of *E. coli*-OmpV strain

To prepare *E.* coli-OmpV strain, OmpV was cloned along with signal peptide into pET 14b and then transformed into *E. coli* BL21 (DE3). The OmpV protein was thus expressed in the outer membrane of this *E. coli* BL21 (DE3). To confirm the presence of OmpV in the outer membrane, we further isolated the outer membrane from *E. coli*-OmpV, *S.* Typhimurium as well as *S.* Typhimurium Δ*ompV* and checked for the presence of OmpV using western blot (**Fig. 10**).

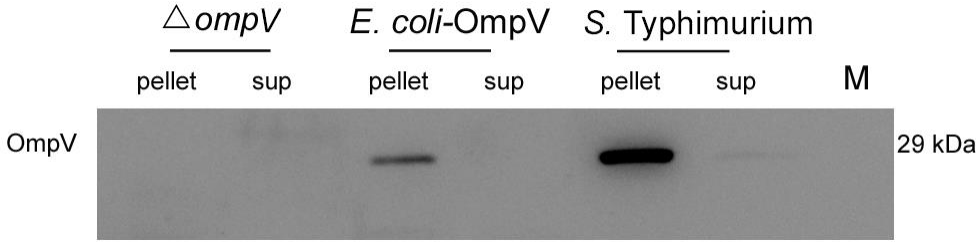


**Figure 10. Western blot analysis to check presence of OmpV in outer membrane of *E. coli*-OmpV**

Western blot of *E. coli*-OmpV outer membrane (pellet) and cytosolic fraction (sup) showing presence of OmpV protein in the outer membrane of *E. coli* only. Outer membrane of wild type *S.* Typhimurium and Δ*ompV* were used as positive and negative control respectively.

Moreover, we have also compared the level of expression of OmpV in the outer membrane of *E. coli*-OmpV strain to the wild type *S.* Typhimurium using flow cytometry (**Fig. 11**).

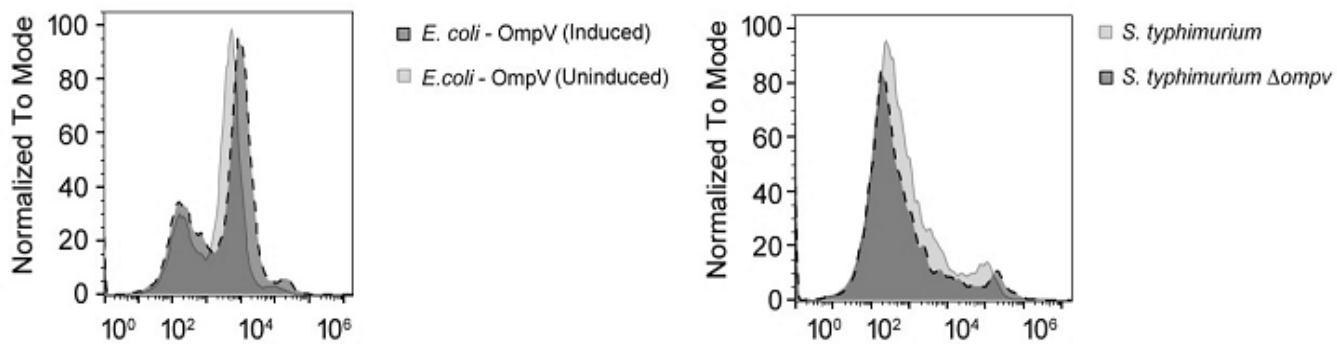


**Figure 11. Flow cytometry indicates comparable level of OmpV in outer membrane of *E. coli*-OmpV strain and *S.* Typhimurium**

Flow cytometry data indicates almost similar level of OmpV expression in the outer membrane of *E. coli*-OmpV (induced) and *S.* Typhimurium. Uninduced *E. coli*-OmpV and Δ*ompV* were taken as negative controls.

**3.3.3 Objective 3:** To probe the role of OmpV in adhesion and invasion of *S.* Typhimurium to intestinal epithelial cells

### 3.3.3.1 Deletion of the *ompV* gene decreases adhesion and invasion of *S.* Typhimurium to the intestinal epithelial cells (IECs)

Using deletion mutant and complement strain, we further examined whether, there is any change in the infection pattern of *S.* Typhimurium under the *in vitro* condition in the absence of OmpV, using the intestinal epithelial cell line Caco-2. Towards this, we infected Caco-2 cells with the wildtype, Δ*ompV* and comp strains of *S.* Typhimurium, and checked the invasion of bacteria using the gentamicin protection assay, which kills all the extracellular bacteria. We observed a significant decrease in the number of *S.* Typhimurium inside the epithelial cells upon the deletion of *ompV*, as compared to those with the wild type and the complemented strains (**Fig. 12A**).

As the adhesion step precedes invasion, we examined whether *ompV*-deletion affected the invasion or the adhesion process. For this, we infected the Caco-2 cells with wildtype, Δ*ompV* and the comp strain, and incubated for the lesser time, as compared to the invasion assay, described above. We observed significantly less number of adhered bacteria upon *ompV*-

deletion, as compared to those found with the wildtype and the complemented control (**Fig. 12B**).

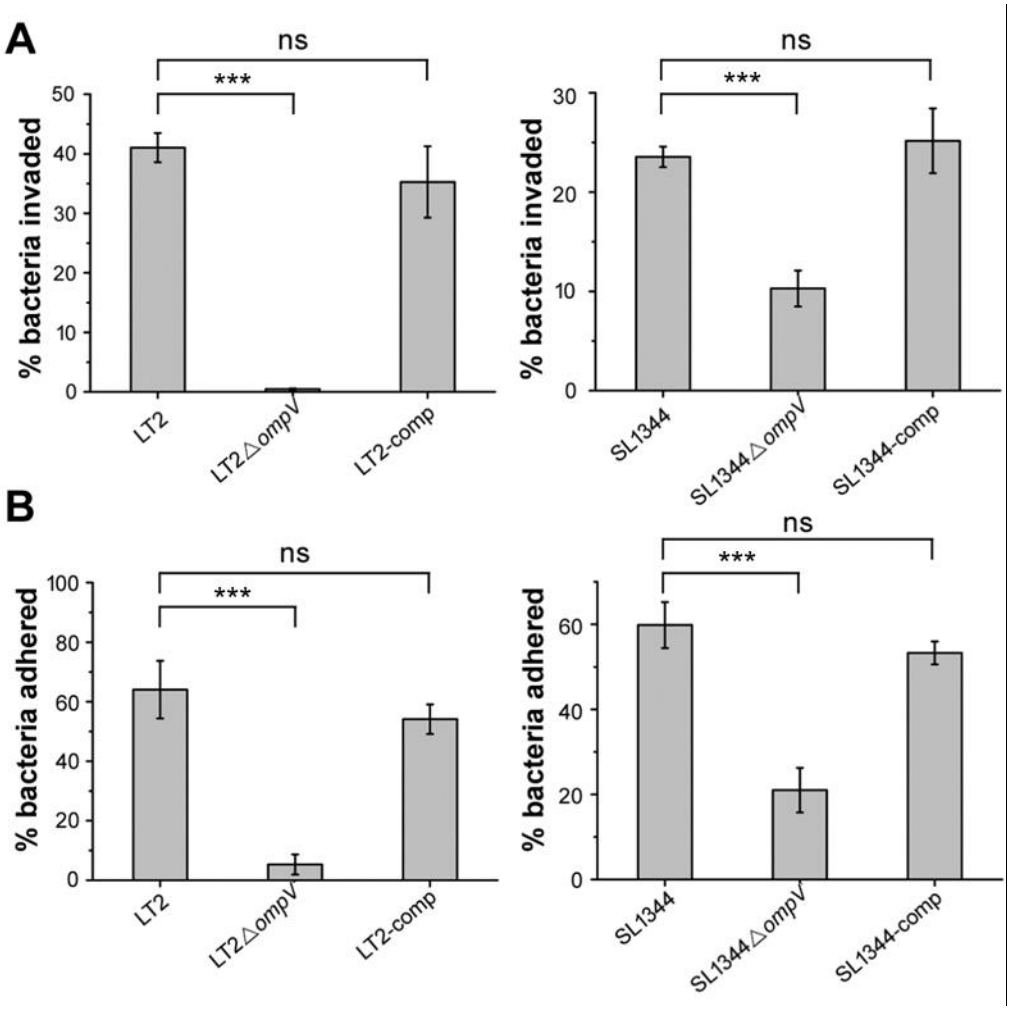


**Figure 12. Deletion of OmpV decreases invasion and adhesion of *S.* Typhimurium to IECs**

A significant decrease in the number of *S.* Typhimurium invading (A) and adhering (B) the Caco-2 cells was observed when cells were infected with LT2Δ*ompV* or SL1344Δ*ompV* as compared to the wild type bacteria. Cells were infected with LT2 (MOI 100:1; 60 min) or SL1344 (MOI 20:1; 15 min) for adhesion and LT2 (MOI 100:1; 90 min) or SL1344 (MOI 20:1; 30 min) for invasion. Following incubation, cells were washed and adhered bacteria were enumerated for adhesion assay. For invasion assay, gentamycin protection assay was performed and bacteria were enumerated using cfu counting. Cells Bar graphs are expressed as mean± SEM from three independent experiments (*$p<0.05$, **$p<0.01$, ***$p<0.001$ and ns $p>0.05$ versus bacteria adhered in wild type).

Similar results were obtained in the microscopy-based experiment, where adhesion of *S.* Typhimurium was visualized employing antibody labeling of O- antigen (**Fig. 13**)

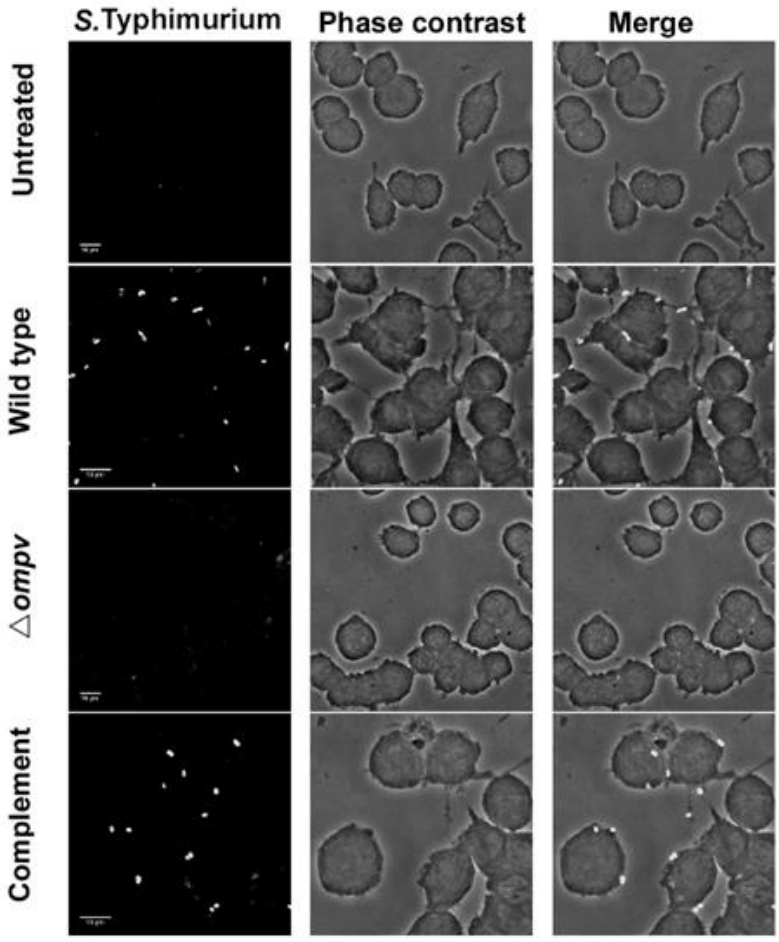


**Figure 13. Microscopic analysis determines role of OmpV in adhesion of *S.* Typhimurium**

A significant decrease in the number of Δ*ompV* bacteria adhering to Caco-2 cells was observed as compared to the wild type bacteria by microscopy analysis. Cells were infected with wild type and mutants (MOI 100:1; 60 min). Following incubation, cells were washed with 1 X PBS for five times. After washing, bacteria were stained with anti-O-antigen antibody for 1 h followed by 30 min incubation of Alexa Flour 488 conjugated secondary rabbit antibody. Untreated cells were used as control. Scale bar represents 10 μm.

To confirm further that the defect in the infection process upon *ompV*-deletion was due to compromised adhesion, and not due to compromised invasion, we employed a Δ*spi1* mutant of *S.* Typhimurium. SPI-1 is known to be involved in invasion and not in the adhesion step. Further, we made a Δ*ompV* mutant on the Δ*spi1 background* (Δ*spi1*Δ*ompV* double mutant). To confirm the role of OmpV in the adhesion or invasion, we infected the Caco-2 cells with the wildtype bacteria, Δ*spi1*, Δ*spi1*Δ*ompV*, Δ*ompV*, or the *ompV*-complemented strain. As expected, significantly reduced invasion was observed with the Δ*spi1* and Δ*ompV* mutant, as compared to the wild type bacteria and *ompV*-complemented bacteria, while Δ*spi1* showed no defect in the adhesion process (**Fig. 14A and B**). However, with the Δ*spi1*Δ*ompV* double

mutant, we observed less adhesion, as compared to the Δ*spi1* mutant, confirming that OmpV is required for adhesion (**Fig. 14B**).

These observations lead us to propose that OmpV is crucial for *S.* Typhimurium adhesion to the intestinal epithelial cells.

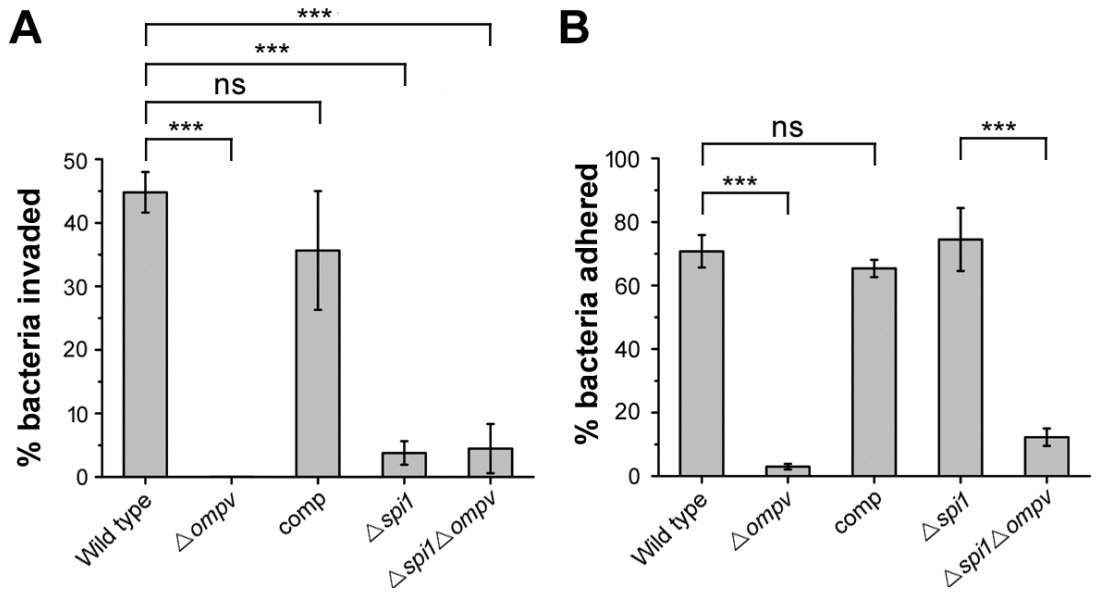


**Figure 14. Double mutant Δ*spi1*Δ*ompV* confirms the role of OmpV as a crucial adhesin**

A significant decrease in the number of Δ*ompV,* Δ*spi1* and double mutant Δ*spi1*Δ*ompV* bacteria invading the Caco-2 cells were observed compared to the wild type and *ompV*-complemented (comp) strain. Cells were infected and bacteria invading the cells were enumerated using gentamycin protection assay. Δ*spi1* was used as a positive control as it is known to be involved in the invasion (A). A significant decrease in the number of Δ*ompV* and double mutant Δ*spi1*Δ*ompV* bacteria adhering to the Caco-2 cells was observed as compared to wild type, *ompV*-complemented (comp) and Δ*spi1*infected cells. Cells were washed and no. of bacteria adhering to cells were enumerated using cfu counting (B). Bar graphs are expressed as mean± SEM from three independent experiments (*p<0.05, **p<0.01, ***p<0.001, ns p>0.05 versus bacteria adhered in wild type or Δ*spi1* infected Caco-2 cells).

### 3.3.3.2 OmpV binds to the IECs

Using the purified protein, we first examined whether OmpV can bind to the IECs. For this, Caco-2 cells were incubated with different doses of purified OmpV for an hour. After the incubation, unbound proteins were removed, and the bound protein was detected by an Enzyme-linked immunosorbent assay (ELISA)-based method. We observed a dose-dependent increase in the binding of OmpV to the Caco-2 cells (**Fig. 15**).

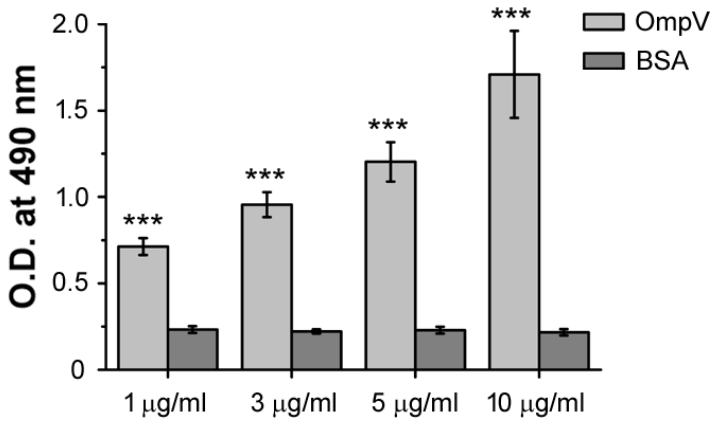


**Figure 15. OmpV binds to intestinal epithelial cells**

An increase in the binding of OmpV to Caco-2 cells was observed in a dose-dependent manner. Caco-2 cells were incubated with different concentrations of OmpV. Following incubation, unbound protein was washed, and bound protein was measured using enzyme-linked immunosorbent assay with the help of anti-OmpV antibody. BSA was taken as negative control. Bar graphs are expressed as mean± SEM from three independent experiments (*p<0.05, **p<0.01, ***p<0.001, ns p>0.05 versus BSA).

### 3.3.3.3 Purified OmpV can inhibit adhesion and invasion of *S.* Typhimurium by neutralizing the receptor on the IEC surface

If OmpV is essential for the adhesion of *S.* Typhimurium to the IEC surface, it must bind to a receptor. Accordingly, such a receptor can be neutralized by pre-treating the IECs with purified OmpV before *S.* Typhimurium infection. Therefore, to examine such a notion, we pre-treated the Caco-2 cells with a purified form of OmpV, followed by infection with *S.* Typhimurium for an hour. Cells pre-treated with *E. coli* outer membrane protein OmpC were used as a negative control. Following the infection, the cells were washed, fixed and stained with the Giemsa stain. We observed that the numbers of bacteria binding to the Caco-2 cells pre-treated with OmpV were significantly reduced, as compared to the bacteria binding to the cells pre-treated with buffer as well as OmpC (**Fig. 16A**). We obtained similar results when OmpV-pretreated Caco-2 cells were infected with GFP-expressing *S.* Typhimurium (LT2-GFP) (**Fig. 16B**).

Further, with an increase in the pre-treatment doses of OmpV, we observed a step-wise decrease in the binding of *S.* Typhimurium in a dose-dependent manner (**Fig. 16C**). Furthermore, we confirmed that the reduction in the binding of *S.* Typhimurium with the target cells was not due to deterioration in cell health (**Fig. 16D**).

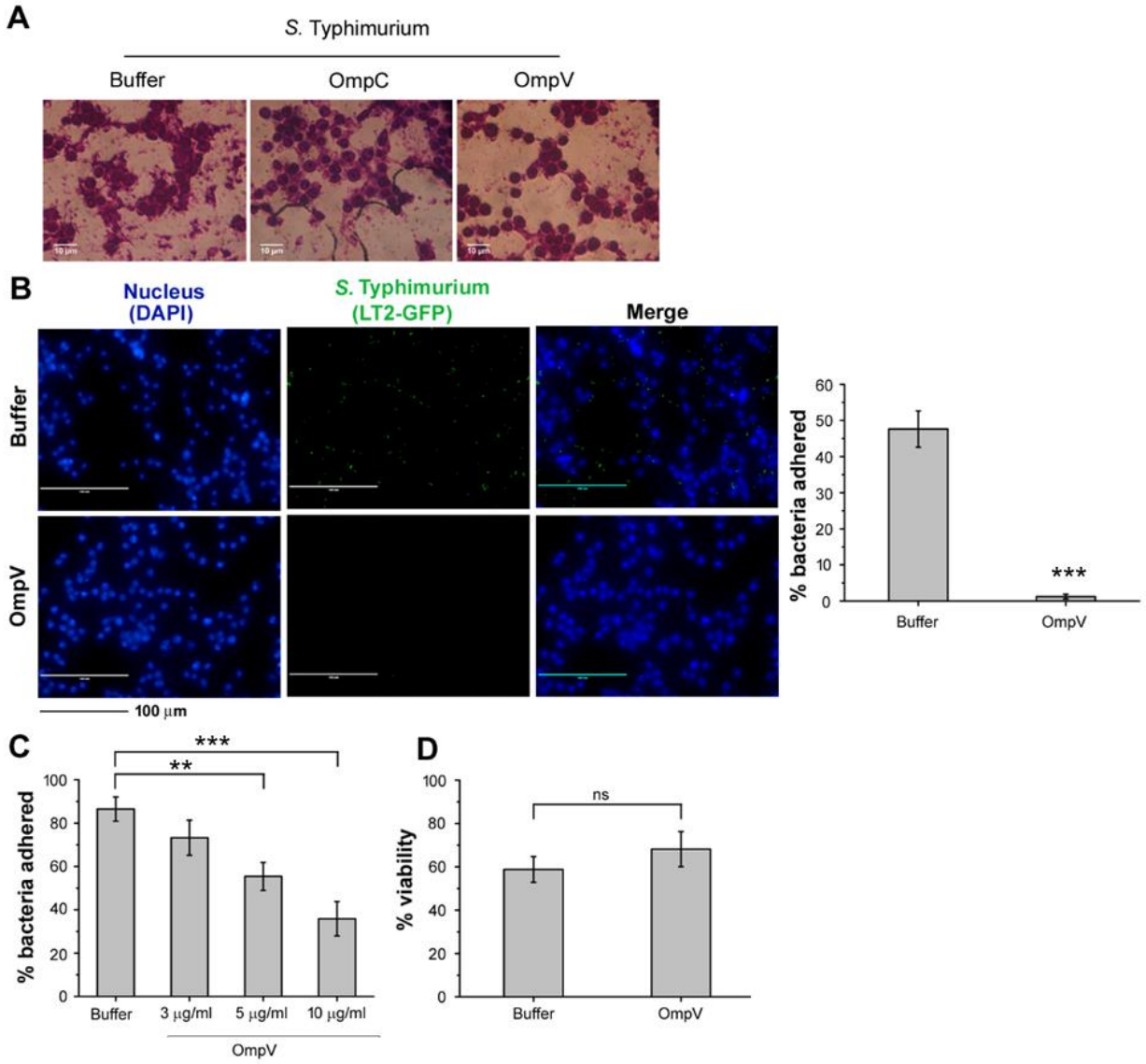


**Figure 16. Pre-treatment of OmpV competitively inhibits binding of *S.* Typhimurium**

Giemsa staining shows a decrease in the number of bacteria adhering to OmpV-pretreated Caco-2 cells as compared to buffer-pretreated cells. *E. coli* outer-membrane protein OmpC was taken as control to check the presence of any non-specific binding. Purple colour indicates eukaryotic cells whereas pink colour indicates prokaryotic cells. Scale bar represents 10 µm (A). A decrease in adherence of *S.* Typhimurium expressing GFP (LT2-GFP) to Caco-2 cells was observed when cells were pretreated with OmpV as compared to the buffer-pretreated cells. Scale bar represents 100 µm. Number of GFP-bacteria bound was quantified by making a standard curve using different MOI for infections (B). A decrease in the number of bacteria bound to Caco-2 cells was observed in a dose-dependent manner with an increase in pre-treatment doses of protein. (C). No significant difference in the viability of Caco-2 cells when pre-treated with buffer or OmpV and infected with *S.* Typhimurium (D). Bar graphs are expressed as mean± SEM from three independent experiments (*p<0.05, **p<0.01, ***p<0.001, ns p>0.05 versus controls).

### 3.3.3.4 *E. coli* expressing *S.* Typhimurium OmpV in the outer membrane shows binding to the IECs

Our observations so far confirmed that OmpV plays a role in the adhesion of *S.* Typhimurium with the IECs. Further, we wanted to examine whether OmpV alone was sufficient for the adhesion process. To explore this notion, we expressed *S.* Typhimurium OmpV in the outer membrane of *E. coli (E. coli*-OmpV*).* It is known that *E. coli* doesn't generally bind to the IECs. We examined whether *E. coli*-OmpV could bind to the IECs. A significant level of binding was observed for *E. coli*-OmpV, as compared to the control bacteria (**Fig. 17**). This data suggested that OmpV protein alone can act as an adhesin for the bacteria.

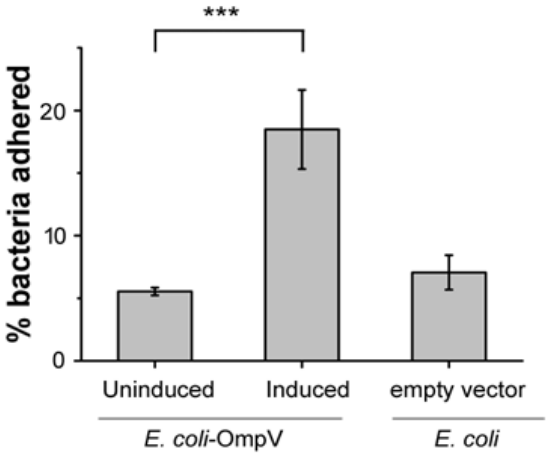


**Figure 17. *E. coli*-OmpV shows increased adhesion to IECs compared to *E. coli***

*E. coli* expressing *S.* Typhimurium OmpV in the outer membrane (*E. coli*-OmpV induced) shows a significant increase in binding to Caco-2 cells as compared to the controls. Caco-2 cells were infected with induced or uninduced*E. coli*-OmpV or *E. coli* containing empty vector. Uninduced *E. coli*-OmpV and *E. coli* containing empty vector were taken as negative controls. Bar graphs are expressed as mean± SEM from three independent experiments (*p<0.05, **p<0.01, ***p<0.001, ns p>0.05 versus cells infected with uninduced *E. coli*-OmpV).

**3.3.4 Objective 4:** To probe whether there is any effect in pathogenesis of *S.* Typhimurium in vivo in absence of OmpV.

### 3.3.4.1 OmpV-deletion reduces pathogenicity of *S.* Typhimurium

Adhesion is the first step in the virulence process of *S.* Typhimurium. Adhesion follows invasion, and establishment of the infection. Therefore, we examined the effect of deletion of OmpV on the pathogenicity of *S.* Typhimurium. To this end, we infected Balb/c mice orally with the wildtype, Δ*ompV* mutant, or the *ompV*-complemented strain. A 7-fold increase in the

$LD_{50}$ dose (median lethal dose) was observed in Δ*ompV* infected mice when compared to the wild type control (**Fig. 18A**). We observed 100% survival of Δ*ompV* infected mice when mice were orally challenged with $LD_{50}$ dose calculated for wild type infected mice (**Fig. 18B**). Further, lesser numbers of bacteria were observed in the stools of Δ*ompV*-infected mice, as compared to the mice infected with wild type and complemented bacteria (**Fig. 18C**). Furthermore, the competitive index (CI) between the Δ*ompV* mutant and wild type bacteria was determined by counting the bacteria recovered from different organs over different time points following oral administration of 1:1 ratio of the wild type and Δ*ompV* bacteria to Balb/c mice. After recovering Δ*ompV* and wild type bacteria from the different organs of mice, i.e. spleen, liver and intestine, we observed that the calculated CI, i.e. the ratio of recovered Δ*ompV* and wild type bacteria, was less than 1 in all the time points (**Fig. 18D-F**). All these results indicated that pathogenicity of Δ*ompV* is far less than the wild type bacteria.

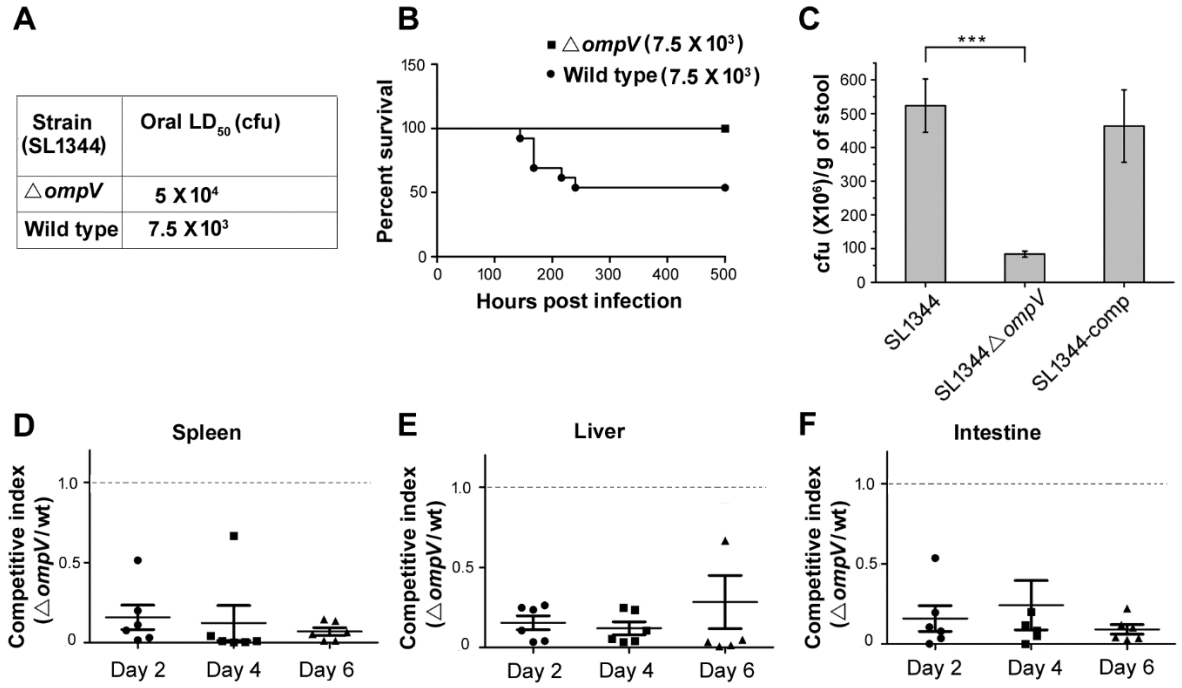


**Figure 18. OmpV affects the pathogenesis of *S.* Typhimurium**

$LD_{50}$ of wild type and Δ*ompV* mutant in orally challenged BALB/c mice (A). Kaplan-Meier plot of cumulative mortality of mice (n=12 per group) orally challenged with Δ*ompV* and wild type with $LD_{50}$ dose similar to wild type *S.* Typhimurium SL1344 ($7.5X10^3$ wild type and Δ*ompV*) (B). A significant decrease in the number of bacteria present in the stool samples was observed following oral administration of BALB/c mice with Δ*ompV* as compared to mice infected with wild type and complemented strain. Bar graphs are expressed as mean± SEM from three independent experiments (*p<0.05, **p<0.01, ***p<0.001, ns p>0.05 versus wild type infected mice) (C). Competitive index (CI) analysis shows less colonization of Δ*ompV* in different organs of mice infected with a mixture of equal numbers of wild type and Δ*ompV*. Solid lines represent the median CI for each organ. The dotted line represents the expected CI if neither strain has a competitive advantage (D-F).

### 3.4 Conclusion:

To characterize outer membrane protein OmpV, we purified recombinantly generated protein expressed in heterologous host *E. coli*. We expressed it as inclusion body, which further denatured and passed through Ni-NTA column (**Fig. 1, 2**) followed by refolding and buffer exchange. Further, to determine whether the protein was properly refolded, we did CD spectroscopy and obtained a β-sheet rich structure. This is in accordance with protein model of OmpV which revealed a β-sheet rich structure (predicted by swiss modeling software) (**Fig. 3,4**). Further, tryptophan fluorescence assay and ANS binding also confirmed the proper refolding of the protein (**Fig. 5**). We also performed size exclusion chromatography to check if there were any aggregates and no soluble aggregates were observed in the protein preparation (**Fig. 6**). Further, as OmpV is an outer-membrane protein and porins are the major class of outer-membrane protein, we wanted to check whether, OmpV is porin in nature. To find if OmpV can act as a porin, we performed a liposome swelling assay which indicated that OmpV doesn't form channels and may not act as porin (**Fig. 7**). While performing liposome swelling assay, *V. cholerae* OmpU was taken as a positive control as it is a porin.

Further, to check the role of OmpV in the pathogenesis of *S.* Typhimurium, we made deletion mutant and complemented strain of OmpV protein (**Fig. 8, 9**). Apart from this, we also made an *E. coli*-OmpV strain by introducing OmpV in the outer membrane of *E. coli* (**Fig. 10, 11**). Upon infection of intestinal epithelial cells, we observed a decrease in invasion as well as adhesion in OmpV-deleted strain compared to the wild type and complemented strain (**Fig. 12, 13**). Further, using SPI-1 deletion mutant and double mutant (OmpV and SPI-1) we confirmed that OmpV plays a significant role in the adherence of *S.* Typhimurium to intestinal epithelial cells (**Fig. 14**).

Furthermore, we observed that purified recombinant OmpV can bind to IECs (**Fig. 15**) and purified OmpV can decrease adhesion of wild type *S.* Typhimurium by acting as a competitive inhibitor. Further, we showed that *E. coli*-OmpV strain showed increased binding to IECs compared to *E. coli* not expressing *S.* Typhimurium OmpV (**Fig. 17**). In conclusion, this data suggested that OmpV protein acts as an important adhesion factor for *S.* Typhimurium.

As our study revealed that OmpV plays a crucial role in adhesion of *Salmonella*, we further investigated its role in the pathogenesis of bacteria. We observed a higher $LD_{50}$ in case of

OmpV-deletion mutant as compared to the wild type strain, as well as a lesser number of bacteria in stools of mice infected with deletion mutant. Further, we observed higher colonization of wild type bacteria in different organs of infected mice compared to the OmpV-deletion mutant (competitive index studies) (**Fig. 18**).

# Chapter 2

**Specific aim 2:** Whether OmpV binds and activates any integrin receptors on the surface of intestinal epithelial cells

### 4.1 Different cell adhesion molecules (CAMs) present on the intestinal epithelial cells

CAMs play an essential role in cell-cell interactions, embryogenesis, immunity, development and cancer metastasis. Typically, CAMs help in the interaction of cells with each other to form tissues or organs. They are generally composed of the intracellular domain, transmembrane domain, and extracellular domain. CAMs may bind to a similar receptor (homophilic interactions) or a different class of receptors or ECM (heterophilic interactions) (148). They also bind to other ligands. These cell adhesion molecules mainly divided into five families:

#### 4.1.1 Cadherins

The name cadherin is derived from "calcium-dependent adherent proteins" (149). These are glycoproteins that help in adherens junctions to bind cells to tissue. They depend on calcium and are responsible for migration. Cadherins mostly bind to other cadherins present on adjacent cells by homophilic interactions in zipper conformation (150).

The cadherin family is subdivided into type I classical cadherins, type II classical cadherins, proto-cadherins, desmosomal cadherins, seven transmembrane cadherins and FAT and dachsous group cadherins (151). All these families of cadherins are composed of mostly three components: a) extracellular cadherin domain; b) cytoplasmic domain that connects cell surface and the cytoskeleton; c) single-pass transmembrane domain (except for seven transmembrane cadherins) (152).

Classical cadherins form adherens junctions and classified based on tissue in which they were initially identified. E (epithelial)-cadherin and N (neural)-cadherin are most thoroughly studied in the literature. Other cadherins such as desmocollin and desmoglein form desmosomes (153). Apart from cell adhesion, cadherins are known to play a role in histogenesis and morphogenesis. N-cadherins are reported to play a role in building neuronal structures as well

as neurulation and neuronal migration (154). Recent studies also shown the involvement of cadherins in the development of sensory neurons, including visual and olfactory systems (155).

### 4.1.2 Selectins

Selectins (CD62) are single transmembrane polypeptides that derived their name due to their ability to bind to sugar moieties through their N-terminal C-type lectin domain. They are thus responsible for heterophilic cell-mediated interaction in a calcium-dependent manner (156). In addition to the N-terminal domain, selectins are composed of an epidermal growth factor (EGF) like domain, variable repeat domains, the transmembrane domain and a cytoplasmic tail.

L-selectin, E-selectin, and P-selectin are members of the selectin family (**Illustration 14**). They mediate adhesion between endothelial cells (E-selectin), platelets (P-selectin), and leucocytes (L-selectin) as well as play a role in leukocyte rolling and thus play a role in the migration of lymphocytes to peripheral lymph nodes (157). The lectin domain of these selectins has more than 60 % identity, due to which they can bind selectively to their ligands. The expression profile of selectins varies from minutes (P-selectin) to hours (E-selectin). L-selectin has the property to form catch bonds (that strengthen under force) with its ligands, which is rarely present in other selectins (157,158). The function of selectins depends on carbohydrate moieties, in the absence of which there is a disruption in leukocyte adhesion.

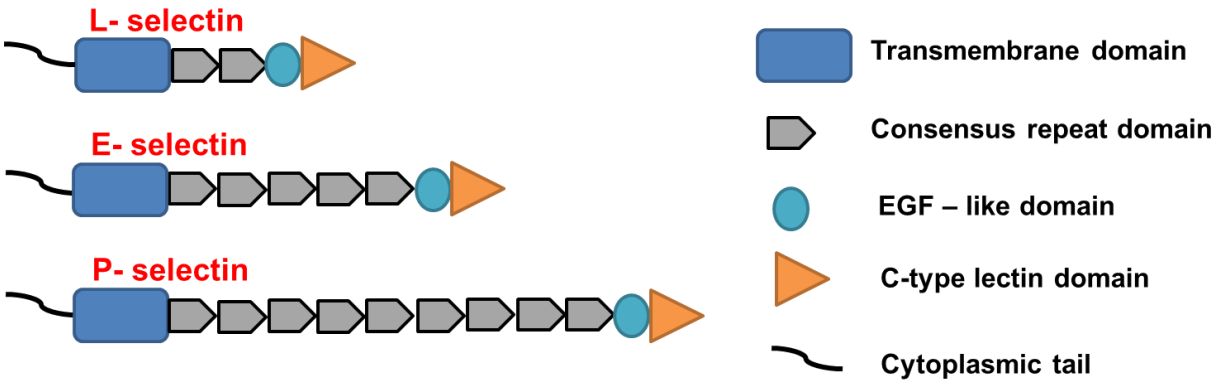


**Illustration 14:** Structure of selectins

### 4.1.3 Immunoglobulin superfamily (IgSF)

IgSF is one of the most diverse families (159) of a single pass, transmembrane proteins that can show both homophilic and heterophilic interactions. This family of receptors includes major histocompatibility complex (MHC) molecules, vascular cell adhesion molecules (VCAM), neural cell adhesion molecules (NCAM), intercellular adhesion molecules (ICAM), nectin and nectin-like (Necl) family as well as activated leukocyte cell adhesion molecule (ALCAM) (160-162). Another family of molecules i.e., MAdCAMs, contains both Ig and mucin domain and thus belongs to both IgSFs and mucin family (160). Most family members have a transmembrane domain, cytoplasmic tail, and an extracellular domain containing an Ig-like domain.

The nectin family (Necl) plays a role in cell-cell adhesion in different tissues, including endothelium, epithelium, and neural tissue (163). Like other IgSF members, they can form both hemophilic and heterophilic bond with nectins or other ligands. They are known to form adherens junctions along with cadherins (163,164). Apart from this, they help to regulate effector cell function and the generation of anti-tumor responses (165). Moreover, the expression of nectins is reported to increase during various tumors (163).

### 4.1.4 Mucins

These are family of serine and threonine rich glycoproteins that act as molecular barriers and play a part in signal transduction. Mucin also mediates cell adhesion in cancer cells (166). CD34 and GlyCAM-1 are two mucin-like molecules present on endothelial cells of lymph nodes and bind to leukocytes through L- selectins (167). Another such molecule, i.e., PSGL-1, is present on neutrophils. It can bind with selectins present on vascular endothelium (168).

### 4.1.5 Integrins

Integrins are type I transmembrane glycoproteins that act as sites for cell adhesion called focal adhesion sites (169). It exists as non-covalently bound α and β subunits forming heterodimers. There are 8 β and 18 α subunits known that form 24 integrin heterodimers having an affinity for different ligands (170,171). The intracellular domain of integrins is linked to the actin

cytoskeleton. Integrins can directly bind to other integrins or it can bind through extracellular matrix components (ECM). Out of 24 heterodimers, α8β1, α1β1, α2β1, α5β1, α3β1, αvβ6, and α3β1 are present on epithelial cells. Integrins are known to play a role in cell adhesion, migration, proliferation, cell differentiation, and apoptosis (172).

#### 4.1.5.1 Integrin signaling:

There are two mechanisms of integrin signaling (173) reported (**Illustration 15**):

1. **Inside out signaling**: In this process, cells induce straightening of bent extracellular domains. Due to change in conformation, ligand-binding site of integrins is exposed to other proteins for binding.
2. **Outside in signaling**: In this process, the signal is transmitted from ECM to integrins. The signal transduction further effects vital processes like cellular growth, differentiation, and apoptosis.

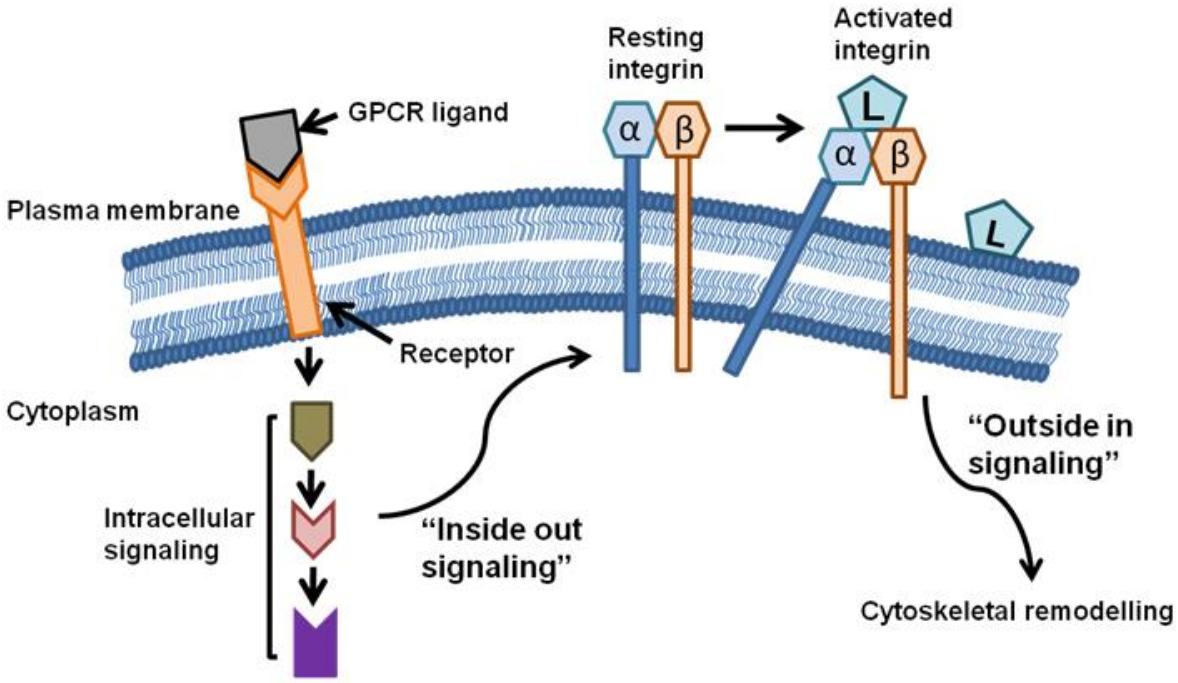


**Illustration 15:** Integrin "Inside out" and "Outside in" signaling

#### 4.1.5.2 Extracellular matrix (ECM) components

The extracellular matrix is a non-cellular, three-dimensional complex meshwork composed of collagen, proteoglycans, laminin, fibronectin, and other glycoproteins (174). Out of these, collagen is the major component of ECM, which upon modification with carbohydrates, form collagen fibrils. These fibrils are interconnected with the help of other proteoglycans. The components of ECM thus form a network around the cells present in tissues by binding to each other and receptors present on the cell surface (175).

The network formed by ECM components is dynamic and modulated by different ligands during normal and pathological conditions. Cell surface receptors get activated by modulation in ECM components and thus transduce signals into cells to regulate various cellular functions such as migration, growth, and cytoskeletal rearrangements (176). The major receptors present on the surface of cells for these ECM components are integrins. On the inner side, the integrins are linked to the cytoskeleton. Thus, activation of integrins can lead to the remodelling of the cytoskeleton (177).

The genetic abnormalities in ECM components can lead to various syndromes, thus indicating ECM's importance in cell homeostasis (178).

#### 4.1.5.3 Integrins and ECM components

Integrins are transmembrane proteins that act as linkers between ECM components and cytoskeleton (170,179,180). Upon activation of integrins by its ligand in the matrix, integrin binds to anchor proteins such as talin, α-actinin, and filamin through its cytoplasmic tail (181). These anchor proteins can further bind to actin filaments either directly or through other anchor proteins.

There are four families of integrins based on binding to different ECM components:

1. RGD-binding integrins: RGD motif is present in fibronectin as well as vinculin. α5β1, α1β1, αVβ1, α8β1, αVβ3, αVβ5, αVβ6, and αIIbβ3 are known to bind to RGD motif.

2. Collagen integrins: The collagen-binding integrins include α1β1, α2β1, α10β1, and α11β1.
3. Laminin-binding integrins: α3β1, α6β1, α7β1, and α6β4 integrins are reported to bind laminin
4. Leukocyte integrins: Apart from ECM components, some integrins can also bind to leukocytes and help in leukocyte migration. α9β1, α4β3, αEβ3, α4β1, αLβ2, αxβ2, αDβ2 and αMβ2 are leukocyte integrins.

## 4.2 Objective

Our earlier results suggested that OmpV plays a critical role in the adhesion of *S.* Typhimurium to intestinal epithelial cells (IECs). Further, we wanted to explore what receptor on intestinal epithelial cells OmpV could bind to help in the adhesion process. Based on the above background, we worked on the following objectives:

1. To probe whether OmpV can bind to any ECM components.
2. To probe whether the receptor could be an integrin
3. If OmpV binds to an integrin to probe whether it can activate the receptor-mediated signaling

## 4.3 Results

**4.3.1 Objective 1:** To probe whether OmpV can bind to any ECM components.

#### 4.3.1.1 OmpV binds to IECs through fibronectin, an ECM component

Initially, during the adhesion experiment, we observed that, *S.* Typhimurium appears to bind to the ECM component (**Fig. 16A**). Further, to explore whether OmpV binds to its receptor through ECM, we first checked the binding of OmpV with different ECM components such as fibronectin, RGD motif, laminin, and collagen. Using western blot, dot blot, and ELISA, we observed that OmpV mainly binds to fibronectin (**Fig. 19A-D**). Further, we found that OmpV co-immunoprecipitated with fibronectin in OmpV-treated cell lysate (**Fig. 19E**). A similar result was observed with the GST-pull down assay, where fibronectin co-immunoprecipitated

with GST-tagged OmpV (**Fig. 19F**). Further, by confocal microscopy, we found the co-localization of fibronectin with OmpV in the OmpV-treated IEC, thus confirming the association of OmpV with fibronectin (**Fig. 19G**).

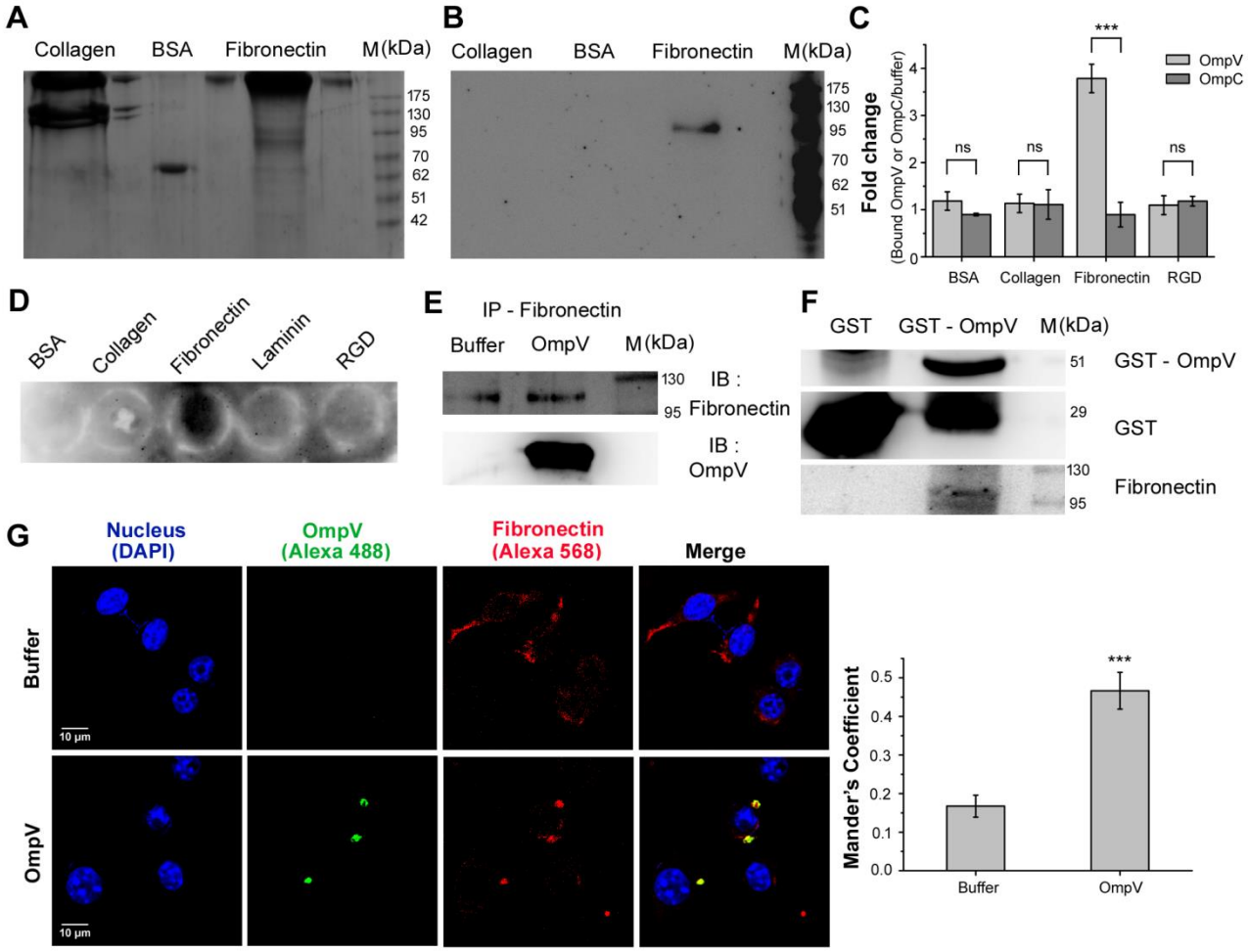


**Figure 19. OmpV binds to IECs through ECM component fibronectin**

Coomassie-stained SDS-PAGE gel showed ECM components fibronectin and collagen (A). Western blot analysis shows binding of OmpV to fibronectin (B). ELISA shows a significant increase in binding of OmpV with fibronectin compared to other ECM components (C). Bar graphs are expressed as mean± SEM from three independent experiments (*p<0.05, **p<0.01, ***p<0.001, ns p>0.05 versus OmpC). Dot blot showed binding of OmpV only with fibronectin (D). OmpV co-immunoprecipitated with fibronectin (E). Fibronectin co-immunoprecipitated with GST-OmpV (F). OmpV co-localized with fibronectin as observed by fluorescence microscopy (G). Bar graphs are expressed as mean± SEM from three independent experiments (*p<0.05, **p<0.01, ***p<0.001, ns p>0.05 versus buffer-treated cells).

Previously reported that fibronectin is crucial for adherence of *S.* Typhimurium (182). In our study as well, we observed decreased adhesion of *S.* Typhimurium in fibronectin-neutralized conditions. (**Fig. 20A**). To determine whether the crucial dependence of *S.* Typhimurium on fibronectin for adherence is mainly due to OmpV, we first checked whether OmpV present in

the outer membrane of *E. coli* drives the whole bacteria to bind to the fibronectin. We observed that *E. coli*-OmpV binds to fibronectin (**Fig. 20B**), and binding was abrogated when fibronectin neutralizing antibody was used (**Fig. 20C**). In addition to this, we observed a significant decrease in fibronectin-binding by Δ*ompV* mutant of *S.* Typhimurium, as compared to the control bacteria (**Fig. 20D**).

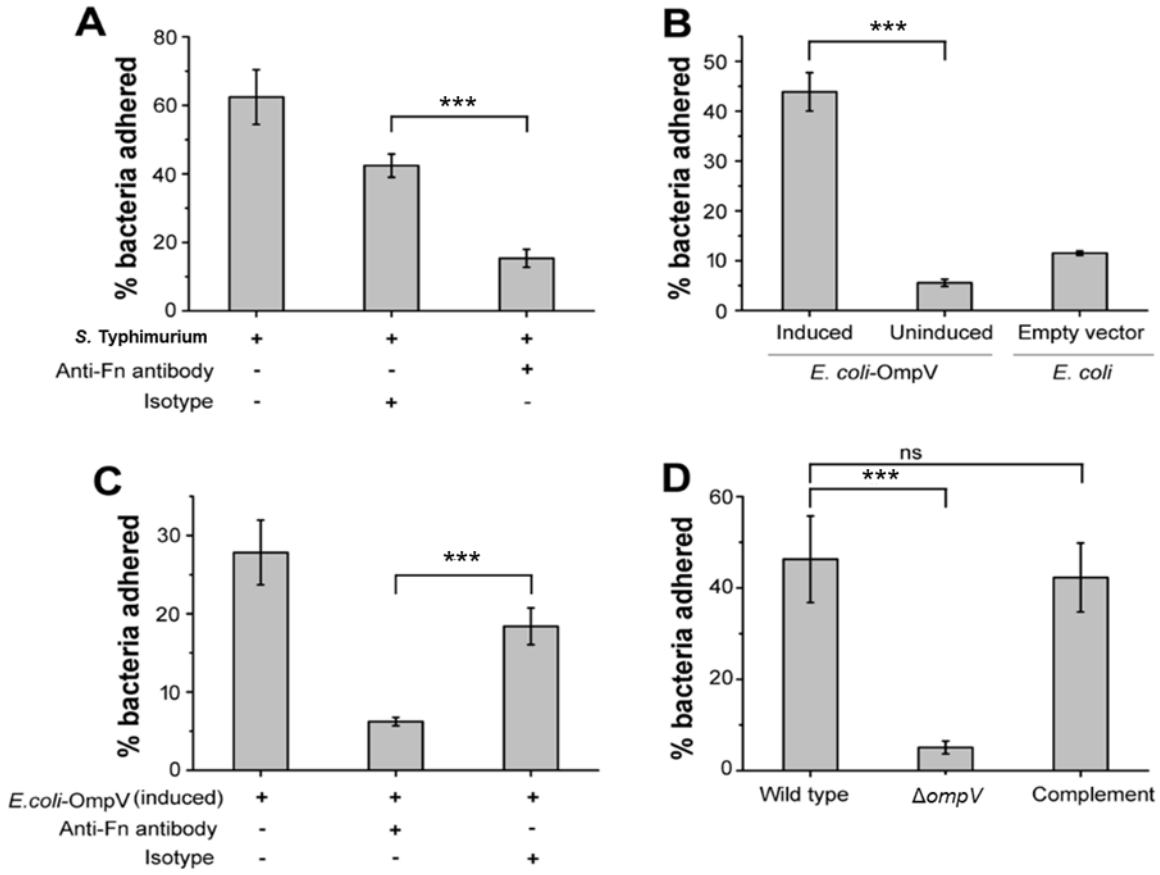


**Figure 20. Neutralization of fibronectin decreases adhesion of *S.* Typhimurium**

A significant decrease was observed in the binding of *S.* Typhimurium (A) and *E. coli*-OmpV (C) to Caco-2 cells on neutralization of fibronectin with neutralizing antibody. Caco-2 cells were pretreated with fibronectin neutralising antibody for 1 h and then infected with *S.* Typhimurium or *E. coli*. Adhered bacteria were then enumerated using cfu plating. A significant increase in binding of *E. coli*-OmpV (induced) to fibronectin was observed. Fibronectin-coated wells were incubated with induced *E. coli*-OmpV or uninduced *E. coli* or *E. coli* containing empty vector. Uninduced *E. coli* and *E. coli* containing empty vector were taken as negative controls (B). A decrease in binding of Δ*ompV* to fibronectin was observed as compared to wild type and complemented strain (D). Fibronectin-coated wells were treated with bacteria for 1 h, and adhering bacteria was then enumerated using cfu plating. Bar graphs are expressed as mean± SEM from three independent experiments (*p<0.05, **p<0.01, ***p<0.001, ns p>0.05 versus isotype control or uninduced *E. coli*-OmpV or wild type).

Further, we have pretreated the fibronectin-coated wells with OmpV protein of *S.* Typhimurium or OmpC protein of *E. coli* or buffer and then incubated with *S.* Typhimurium

or *Vibrio vulnificus* or *E. coli*. Here, *V. vulnificus* was taken as a positive control for fibronectin-binding (183) and *E. coli* was used as a negative control. *E. coli* OmpC protein was taken as non-specific protein control. We observed a significant decrease in binding of *S.* Typhimurium in only OmpV-pretreated fibronectin coated-wells compared to the controls, confirming that OmpV in the outer membrane of *S.* Typhimurium helps in binding of bacteria with the ECM component fibronectin (**Fig. 21**).

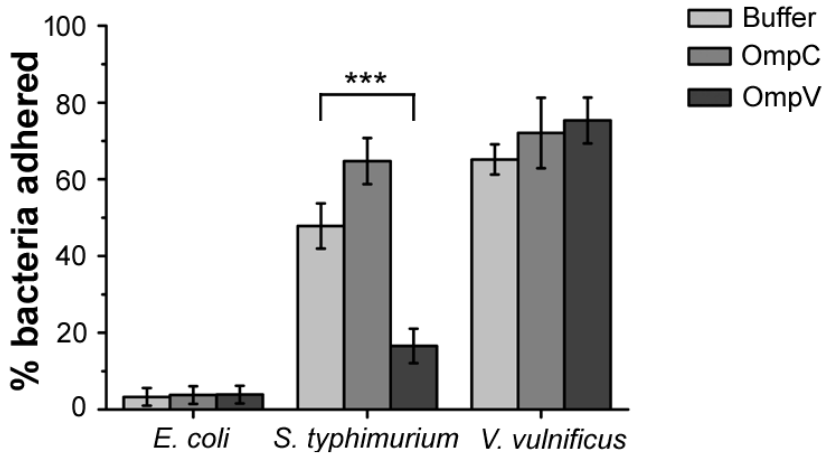


**Figure 21. OmpV-pretreatment specifically decreases binding of *S.* Typhimurium to IECs**

A decrease in the number of *S.* Typhimurium binding to fibronectin was observed on pretreatment with OmpV protein in fibronectin-coated wells. Fibronectin coated wells were treated with buffer or OmpV or OmpC respectively and then incubated with *E. coli or V. vulnificus* or *S.* Typhimurium. *E. coli* and OmpC are taken as negative controls whereas *V. vulnificus* is taken as a positive control for fibronectin binding. Bar graphs are expressed as mean± SEM from three independent experiments (*p<0.05, **p<0.01, ***p<0.001, ns p>0.05 versus buffer pretreated *S.* Typhimurium).

**4.3.2 Objective 2:** To probe whether the receptor could be an integrin

#### 4.3.2.1 OmpV binds to α1β1 integrin through fibronectin

Receptors present on IECs, in general, belong to the selectin, cadherin, integrin, and IgCAM families. Among these, integrins are known to bind mostly through the ECM components. Therefore, in case of OmpV, integrin(s) would be expected to be the most probable candidate. There are 24 receptors in the integrin family (184). Each of these integrin family members is known to form hetero-dimer with different combinations of α and β subunits. Among these, 8 are known to interact with the ligand through fibronectin. The most common integrin present

on the IECs known to bind fibronectin is β1 integrin (185). In the GST-pull down assay with the GST-OmpV-treated whole cell lysate of Caco-2 cells, we observed that β1 integrin co-immunoprecipitated with OmpV (**Fig. 22A**). Similarly, with the reverse pull down with anti-β1 integrin antibody, we found that OmpV was co-immunoprecipitated with β1 integrin (**Fig. 22B**). Above results suggested that OmpV and β1 integrin interacts with each other. Further, β1 integrin was knocked-down using small interfering RNA **(**siRNA) to confirm its role in OmpV recognition. Expression of β1 integrin was then checked using western blot (**Fig. 22C**). A decrease in binding to the Caco-2 cells by *S.* Typhimurium, as well as *E. coli*-OmpV was observed, when β1 integrin was knocked-down using siRNA (**Fig. 22D**). All this data confirms that OmpV binds with β1 integrin.

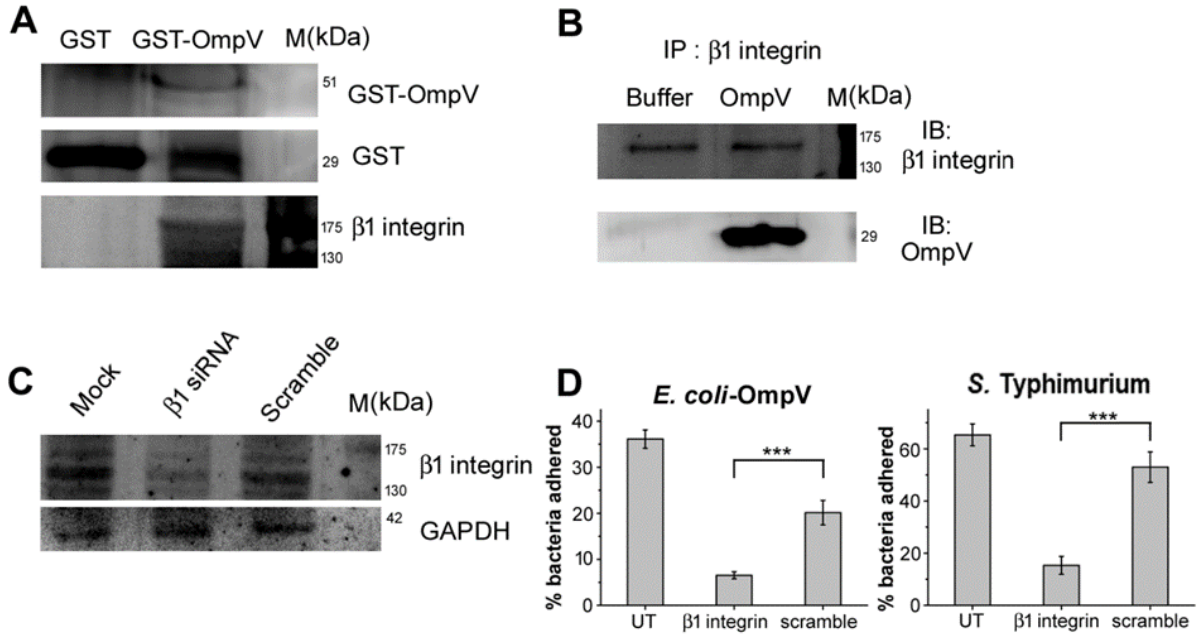


**Figure 22. β1 integrin is involved in recognition of OmpV**

β1 integrin co-immunoprecipitated with GST- OmpV (A). OmpV co-immunoprecipitated with β1 integrin (B). Western blot showed knock-down in β1 integrin expression in Caco-2 cells on transfection with siRNA. GAPDH is taken as a loading control (C). A significant decrease in *S.* Typhimurium and *E. coli*-OmpV binding was observed upon knock-down of β1 integrin in Caco-2 cells. Non targeted (scrambled) siRNA wasused as a negative control (D). Bar graphs are expressed as mean± SEM from three independent experiments (*p<0.05, **p<0.01, ***p<0.001, ns p>0.05 versus scrambled siRNA).

As β1 integrin always pairs up with α subunit, to find out which α integrin subunit is involved in recognition of OmpV, we neutralized each α subunit separately and infected the neutralized Caco-2 cells with *S.* Typhimurium. Neutralization experiment of α subunit revealed that there was a significant decrease in *S.* Typhimurium binding when α1 subunit was neutralized (**Fig. 23A**). Knock-down of α1 integrin was done using short hairpin RNA (shRNA) and confirmed

using RT-PCR (**Fig. 23B**). We observed a similar result by shRNA mediated knock-down of α1 subunit (**Fig. 23C**). Therefore, neutralization and knock-down experiments revealed that α1 integrin is crucial for *S.* Typhimurium infection. Further, to understand the involvement of α1 integrin in OmpV recognition, we performed GST pull-down assay and observed that α1 co-immunoprecipitated with OmpV (**Fig. 23D**). Further, a decrease in binding to the Caco-2 cells of *E. coli*-OmpV was observed when α1 integrin was knocked-down using shRNA (**Fig. 23E**).

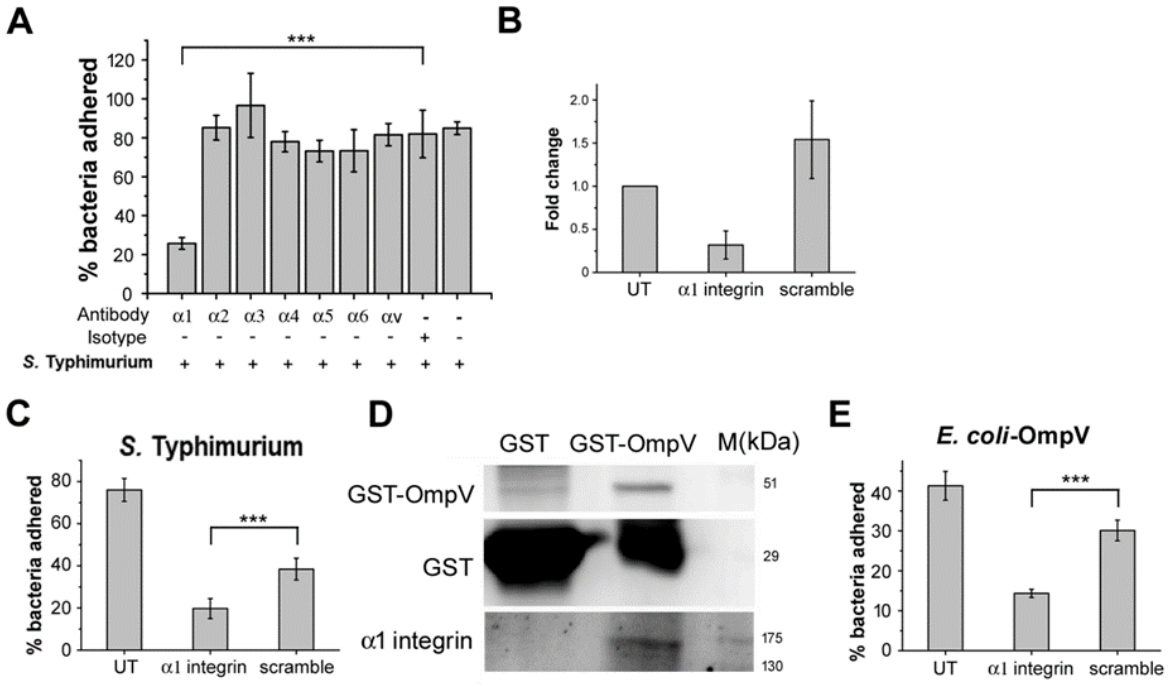


**Figure 23. β1 integrin heterodimerizes with α1 integrin for recognition of OmpV**

Neutralization of different α integrin subunits using neutralizing antibodies showed the involvement of α1 integrin in recognition of OmpV (A). The decrease in gene level expression of α1 integrin was observed in Caco-2 cells on transfection with shRNA (B). A significant decrease in *S.* Typhimurium (C) and *E. coli* (E) binding was observed upon knock-down of α1 integrin in Caco-2 cells using shRNA. Non targeted (scrambled) shRNA was used as negative control. α1 integrin co-immunoprecipitated with OmpV in GST pull-down assay (D). Bar graphs are expressed as mean± SEM from three independent experiments (*p<0.05, **p<0.01, ***p<0.001, ns p>0.05 versus isotype control or non-targeted shRNA).

Furthermore, the co-localization experiment confirmed that OmpV is interacting with both α1 and β1 integrin (**Fig. 24A and B**). Thus, our results demonstrated that α1β1 integrin is crucial for *S.* Typhimurium infection, mostly due to OmpV, which interacts with α1β1 integrin.

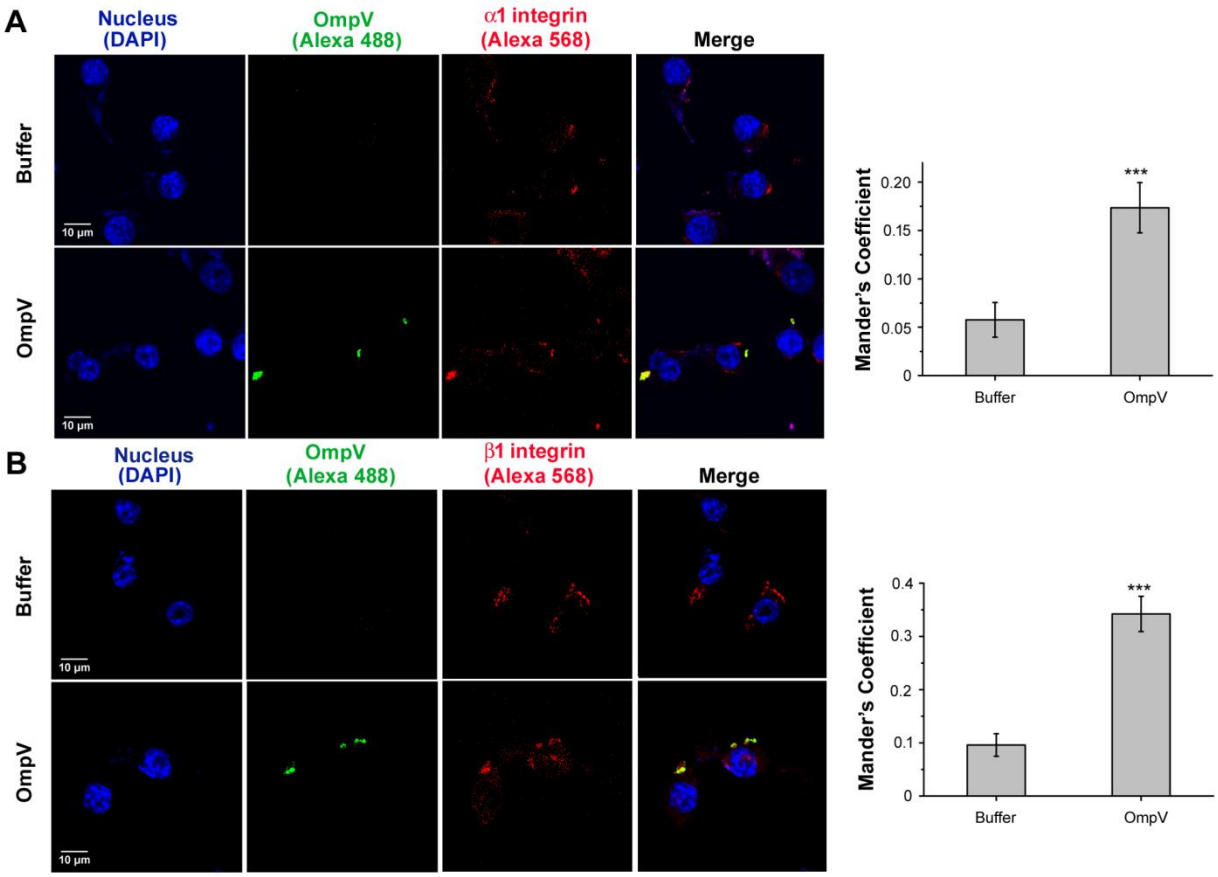


**Figure 24. α1 and β1 integrins co-localizes with OmpV**

A significant co-localization between OmpV and both α1and β1 integrin was observed by calculating Mander's coefficient. Bar graphs are expressed as mean± SEM from three independent experiments (*p<0.05, **p<0.01, ***p<0.001, ns p>0.05 versus buffer-pretreated cells).

Further, we wanted to examine whether there is any direct interaction between OmpV and the α1β1 integrin receptor, or the interaction is mediated only via fibronectin. To explore this issue, we performed dot blot assay, which showed that there was no direct binding between OmpV and β1 integrin (**Fig. 25**), thus confirming that the interaction between the receptor and OmpV is mediated via fibronectin.

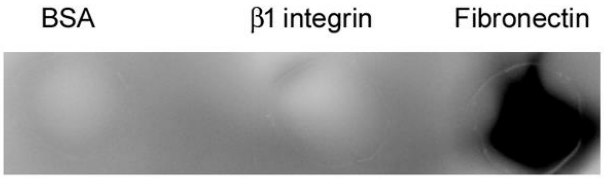


**Figure 25. OmpV binds to integrins through fibronectin**

Dot blot showed no direct interaction between OmpV and β1 integrin. Fibronectin, BSA, and β1 integrin were immobilised on nitrocellulose membrane and incubated with OmpV. Following washing, bound protein was detected using anti-OmpV antibody. Fibronectin is used as a positive control and BSA is used as the negative control.

**4.3.3 Objective 3:** To probe whether it can activate the receptor-mediated signaling

### 4.3.3.1 OmpV does not act as receptor for Type III secretion needle

Some adhesins such as CagL of *Helicobacter pylori* can act as receptor for secretion needle after binding to integrins and thus help in translocation of effector proteins (186,187). So, we further checked whether translocation of effector proteins get blocked in cells infected with *ompV* deletion mutant. For this, we transformed SifA-HA plasmid in both SL1344 and SL1344Δ*ompV* strain and infected Caco-2 cells with these strains. SifA or Salmonella induced filament A is a type II effector protein. Un-infected cells were kept as control. After 1 h of infection, we killed extracellular bacteria using gentamicin and checked cell lysates for presence of SifA-HA using anti-HA antibody (**Fig. 26**). We found SifA-HA is present both in wildtype and Δ*ompV* infected cells which suggests that OmpV is not acting as receptor for type III secretion system and thus probably does not have any role in translocation of effector proteins.

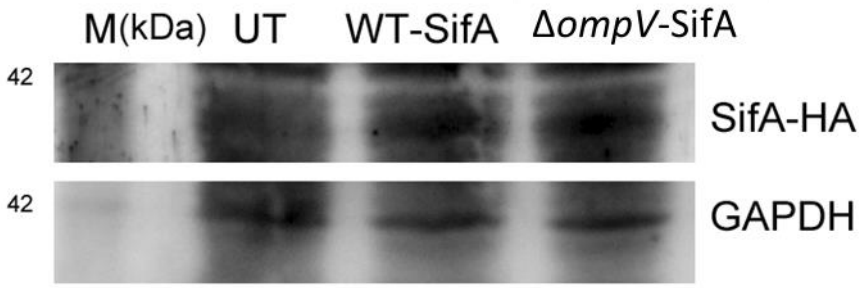


**Figure 26. OmpV is not involved in translocation of effector proteins**

Western blot indicates that there is no difference in translocation of effector proteins. Caco-2 cells were infected with SL1344 and SL1344Δ*ompV* transformed with SifA-HA plasmid. Following 1 h incubation, extracellular bacteria were killed with gentamicin and cell lysates were checked for presence of SifA-HA using HA antibody.

### 4.3.3.2 Activation of α1β1 integrin leads to phosphorylation of focal adhesion kinases (FAK) and actin modulation

We observed a decrease in invasion of *S.* Typhimurium to the Caco-2 cells upon treatment with the FAK inhibitor (**Fig. 27**).

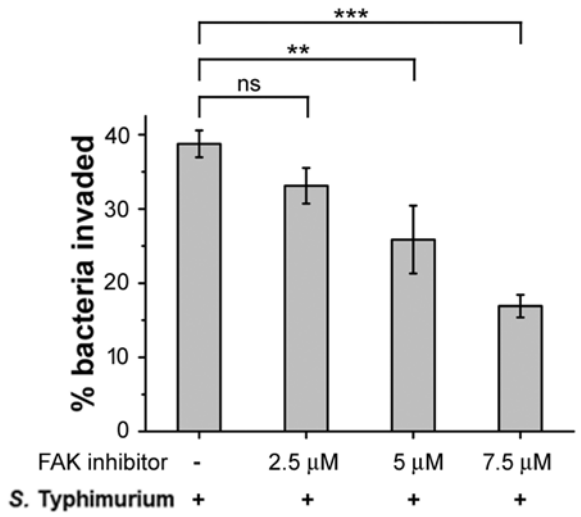


**Figure 27. FAK phosphorylation is involved in invasion of *S.* Typhimurium**

Inhibition of FAK phosphorylation decreases invasion of *S.* Typhimurium into Caco-2 cells. Caco-2 cells were pretreated with different concentrations of FAK inhibitor and infected with *S.* Typhimurium. Bar graphs are expressed as mean± SEM from three independent experiments (*p<0.05, **p<0.01, ***p<0.001, ns p>0.05 versus buffer-pretreated infected cells).

Activation of α1β1 integrin, in general, leads to the activation of FAK. To test whether OmpV can activate FAK, we probed the phosphorylation status of FAK (p-FAK) in the OmpV-treated Caco-2 cells and observed an increase in p-FAK in response to OmpV (**Fig. 28**), suggesting that OmpV can activate FAK.

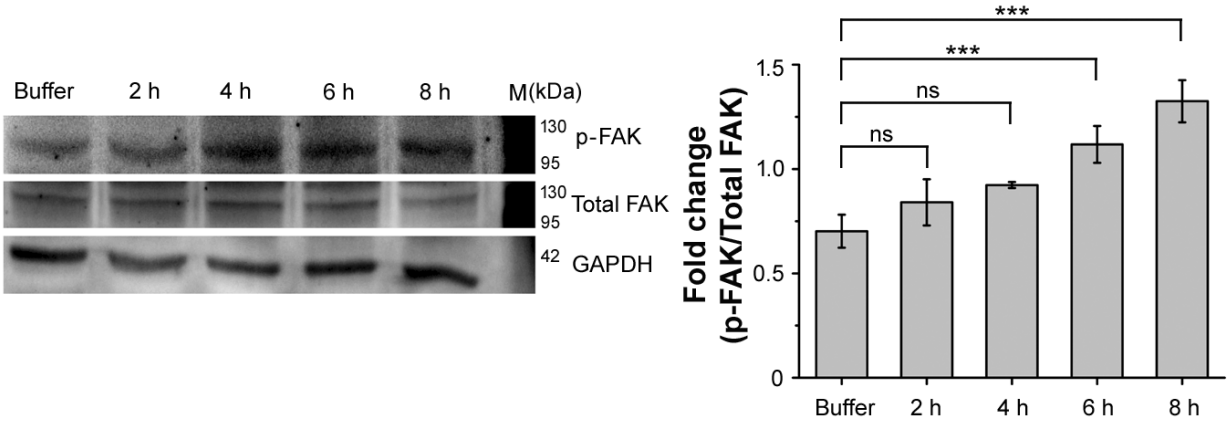


**Figure 28. OmpV induces FAK phosphorylation**

OmpV induces FAK phosphorylation in Caco-2 cells. Caco-2 cells were treated with OmpV for different time points. Whole lysates were prepared from OmpV-treated Caco-2 cells and analysed for phosphorylation of FAK by western blotting. The densitometric analysis shows the level of p-FAK over total FAK. Bar graphs are expressed as mean± SEM from three independent experiments (*p<0.05, **p<0.01, ***p<0.001, ns p>0.05 versus buffer-treated cells).

In general, FAK activation ultimately leads to the modulation of the actin filaments that help in the invasion of bacteria into the host cells (188). As OmpV-activated FAK, we further checked whether OmpV-mediated activation of the receptor could lead to the actin modulation. Towards this, we observed actin modulation in terms of surface expansion and elongation of the cells in response to OmpV treatment, as similar to the cells infected with the wildtype bacteria; whereas, cells infected with Δ*ompV* mutant showed actin modulation almost similar to buffer treatment, suggesting that OmpV leads to the actin modulation prior to *Salmonella* infection, presumably by activating α1β1 integrin (**Fig. 29**).

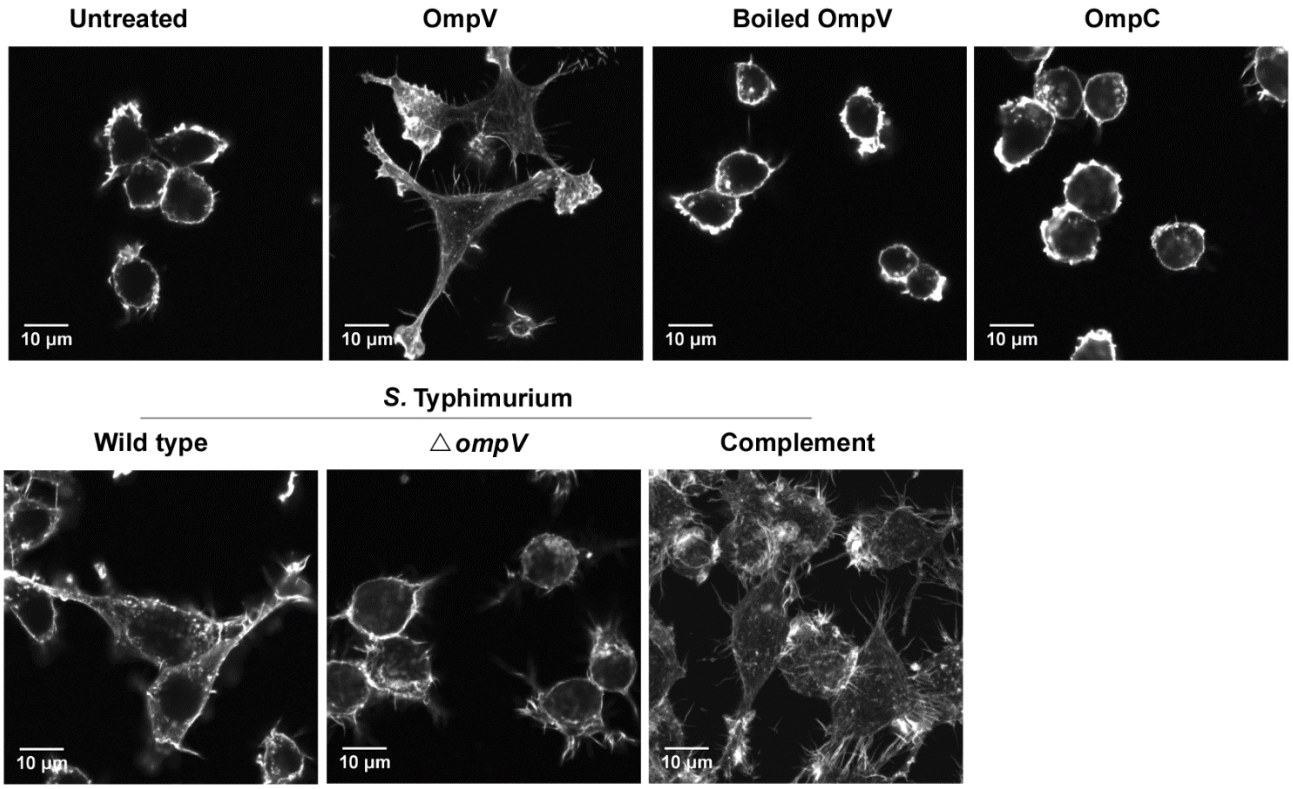


**Figure 29. OmpV induces modulation of actin filaments**

OmpV modulates actin filaments in Caco-2 cells. Caco-2 cells were treated or infected with OmpV, boiled OmpV and OmpC proteins, *S.* Typhimurium, Δ*ompV* and complemented strain. OmpC and boiled OmpV are taken as negative controls. OmpV deletion strain (Δ*ompV*) also showed lesser actin modulation than wild type and complemented strain.

## 4.4 Conclusion:

Out of various cell adhesion molecules present on cells, integrins are mostly involved in recognizing bacterial adhesins. Integrins are known to bind to the ligand through ECM components as well. From earlier observations, as it seemed that *S.* Typhimurium is binding to ECM components (**Fig. 16A**) we first probed whether OmpV can bind to any ECM components with OmpV. We observed that OmpV binds to the ECM component fibronectin (**Fig. 19**). OmpV-deletion mutant of *S.* Typhimurium showed lesser binding to fibronectin (**Fig. 20**). Further, we observed that OmpV explicitly inhibits binding of *S.* Typhimurium to fibronectin, suggesting OmpV mainly helps in the binding of the bacteria to ECM component fibronectin (**Fig. 21**). Furthermore, we observed that OmpV binds to α1β1 integrins (**Fig. 22- 24**) through fibronectin (**Fig. 25**). However, our initial studies gave us a hint that it doesn't act as a receptor for the type III secretion system (**Fig. 26)**.

Integrins, after getting activated, phosphorylate focal adhesion kinases which ultimately result in actin modulation. We observed that OmpV could activate focal adhesion kinases (**Fig. 27, 28**) leading to actin modulation (**Fig. 29**).

Thus, the overall results indicated that OmpV acts as an important adhesin for *S.* Typhimurium and helps the bacteria bind to and activate α1β1 integrins resulting in actin modulation and ruffle formation, an important prerequisite for bacterial invasion.

**Aim 2:** Whether OmpV has a potential to act as vaccine candidate

**Chapter 3: Specific aim 1:** Whether OmpV can modulate adaptive immune responses to induce protection against *Salmonella* Typhimurium infection

**Chapter 4: Specific aim 2:** How OmpV modulates innate immune responses

# Chapter 3

**Specific aim 1:** Whether OmpV can modulate adaptive immune responses to induce protection against *Salmonella* Typhimurium infection

### 5.1 Dendritic cells – a bridge between innate and adaptive immunity

In 1978, dendritic cells were first reported to be critical for the generation of immune responses (189). However, many years later in 2011, the Nobel Prize was awarded for the discovery of DCs and their role in regulating innate and adaptive immunity. Dendritic cells are professional antigen-presenting cells (APCs) that connect innate and adaptive immune system. Immature dendritic cells have pattern recognition receptors (PRRs) on their surface which help in the recognition of PAMPs and DAMPs (190). This encounter with self or non-self-antigens leads to maturation of dendritic cells, which involves changes in phagocytic capacity, migration, and phenotype. Also, there is an increased surface expression of co-stimulatory molecules such as CD80 and CD86 on the maturation of DCs (191). Mature dendritic cells then process and present antigens to adaptive immune cells such as T cells and B cells. Antigen presentation is a prerequisite for T cell activation. The activated T cell further exerts and modulate cell-mediated and humoral immunity. Dendritic cells generally present antigen through MHC II to CD4+ helper T cells, which induce both cell-mediated and humoral immunity. Via cross-presentation, dendritic cell presents exogenous antigen through MHC I to CD8+ cytotoxic T cells and induces cell-mediated immunity (192).

#### 5.1.1 Activation of CD4+ T cells by dendritic cells

APCs such as dendritic cells, macrophages, and B cells generally present antigens to CD4+ helper T cells through MHC II. T cells are generated in the thymus, and from there, they patrol the body to identify and engage with specific antigenic peptides presented by APCs. The interaction between DCs and naïve T cells occurs majorly in lymphoid organs. Co-receptor molecules expressed on T cells determine the recognition of a different class of MHC. Thus the T cell antigen receptor complex is stabilized by this tripartite interaction between MHC, antigen, and TCR (**Illustration 16**). This interaction acts as Signal 1 for the activation of T cells. In addition to signal 1, T cell activation requires a second signal by co-stimulatory molecules. In the case of CD4+ helper T cells, this Signal 2 is provided by CD28, which

recognizes CD80 and CD86 present on the surface of APCs. These two signals lead to the proliferation of T-cells (193,194). The interaction between CD80/86 and CD28 induces expression of inhibitory molecules like CTLA-4 to control the activation and proliferation of T cells (195). Other receptors such as ICOS, 4-1BB, and OX-40 present on T cells and their ligands present on APCs are only expressed following pathogen recognition (196). The absence of Signal 2 by co-stimulatory molecule leads to T-cell anergy (197). Also, the interaction between Fas ligand present on the T cell and its receptor on APCs can cause apoptosis of T cells (198). Although the above two signals can activate T cells, Signal 3 provided by cytokines is required to determine its fate. Apart from APCs, other cells in milieu can also release cytokines that can participate in T cell proliferation and differentiation. The nature of cytokines released by DCs depends on the type of antigen. The cytokines secreted by DCs act on T cells and further lead to the secretion of various effector cytokines.

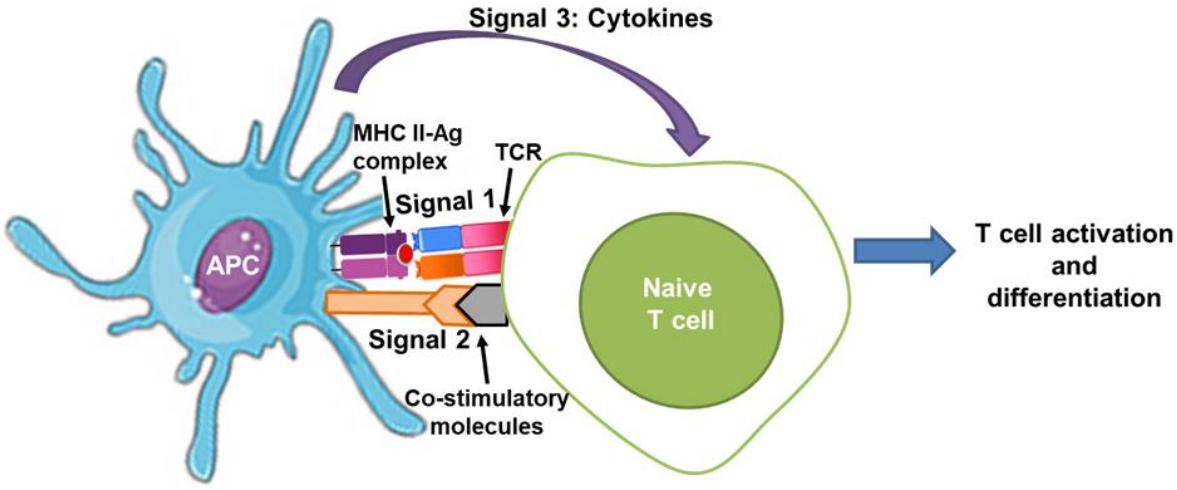


**Illustration 16:** Antigen presentation: APC and T-cell interaction

These cytokines help in the differentiation of T cells into various subsets. Earlier, Th1 and Th2 were the only subsets known, but later more subsets were recognized. Currently, there are seven subsets of T cells known (**Illustration 17**). It is also reported that the development of one subset inhibits the development of another subset. The seven subsets of T cells are described below:

**5.1.1.1 Th1 cells:** Microenvironment containing IL-12 and IFNγ are involved in the development of Th1 subset (199,200). DCs secrete IL-12 on recognition of PAMPs, and then generally activated NK cells produce IFNγ. T-box transcription factor (T-bet) is the principal transcription factor that induces differentiation of the Th1 subset. Th1 subset enhances the

production of IFNγ significantly and plays a role in suppressing the differentiation towards Th2 and Th17 subsets. IFNγ and IL-2 secreted by Th1 cells further enhance the phagocytic capacity of macrophages and proliferation of CD8+ T cells. Macrophages and CD8+ T cells then help in the clearance of intracellular pathogens. Th1 cells also enhance IgG2 production by B cells (201). They also play a role in anti-tumor responses (202).

**5.1.1.2 Th2 cells:** IL-4 and IL-2 are involved in the development of Th2 subset. IL-4 is generally secreted by the activated NKT cells, but once Th2 cells are produced, they enhance the production of IL-4. The transcription factor GATA-binding protein (GATA3) is majorly involved in the differentiation of the Th2 subset. Th2 cells produce IL-4, IL-5, IL-9, IL-13, IL-25, and amphiregulin and are majorly involved in evoking immune response against extracellular parasites (203). It also plays a role in the induction of asthma and other allergic diseases and leads to IgG1, IgE and IgA class switching of B cells (204). Th2 cells also can suppress Th1 differentiation.

**5.1.1.3 Tfh cells:** Generally, IL-6 and IL-21 are involved in the development of Tfh subset. The transcription factor STAT3 is majorly responsible for its differentiation. Tfh cells express C-X-C motif receptor-5 (CXCR $5^{+}$) and are located in follicular areas of lymphoid tissue, where they play a role in developing antibody responses and memory B cell generation (205).

**5.1.1.4 Th17 cells:** IL-6, IL-21, IL-23, and TGFβ cytokines and receptor gamma-T (RORγt) transcription factor are involved in the differentiation of Th17 subset. Th17 differs from Tfh by the requirement of TGFβ. IL-21, along with TGFβ leads to Th17 cells development. Th17 cells release IL-17A, IL-17F, IL-21, and IL-22 cytokines. Out of this, IL-17 leads to the release of proinflammatory chemokines and thus recruits immune cells to the site of inflammation (206). IL-21 activates T cells, NK cells, and differentiate B cells into memory cells. Il-22 plays a role in cell proliferation and acute inflammation (207).

**5.1.1.5 Treg cells:** TGFβ is the critical cytokine, and Forkhead transcription factor (FOXP3) is the major transcription factor involved in Treg differentiation. They play a major role in tolerance to self and foreign antigen and secretion of cytokines such as IL-10, TGFβ and IL-35. IL-10 is an inhibitory cytokine that suppresses inflammation and limits tissue damage. Treg cells also inhibit IgE production and thus attenuate allergic responses (208,209).

**5.1.1.6 Th22 cells:** TNFα and IL-6 are responsible for differentiation into Th22 cells. These cells majorly secrete IL-22 that protects organs such as skin and lungs and repair inflamed and injured tissue (210,211).

**5.1.1.7 Th9 cells:** These cells were initially characterized as a subset of Th2 cells. The combination of TGFβ and IL-4 along with IRF4 transcription factor leads to differentiation of Th9 cells. They produce IL-9 and IL-10 cytokines and regulate allergic inflammation, autoimmune inflammation, and anti-tumor immunity (212).

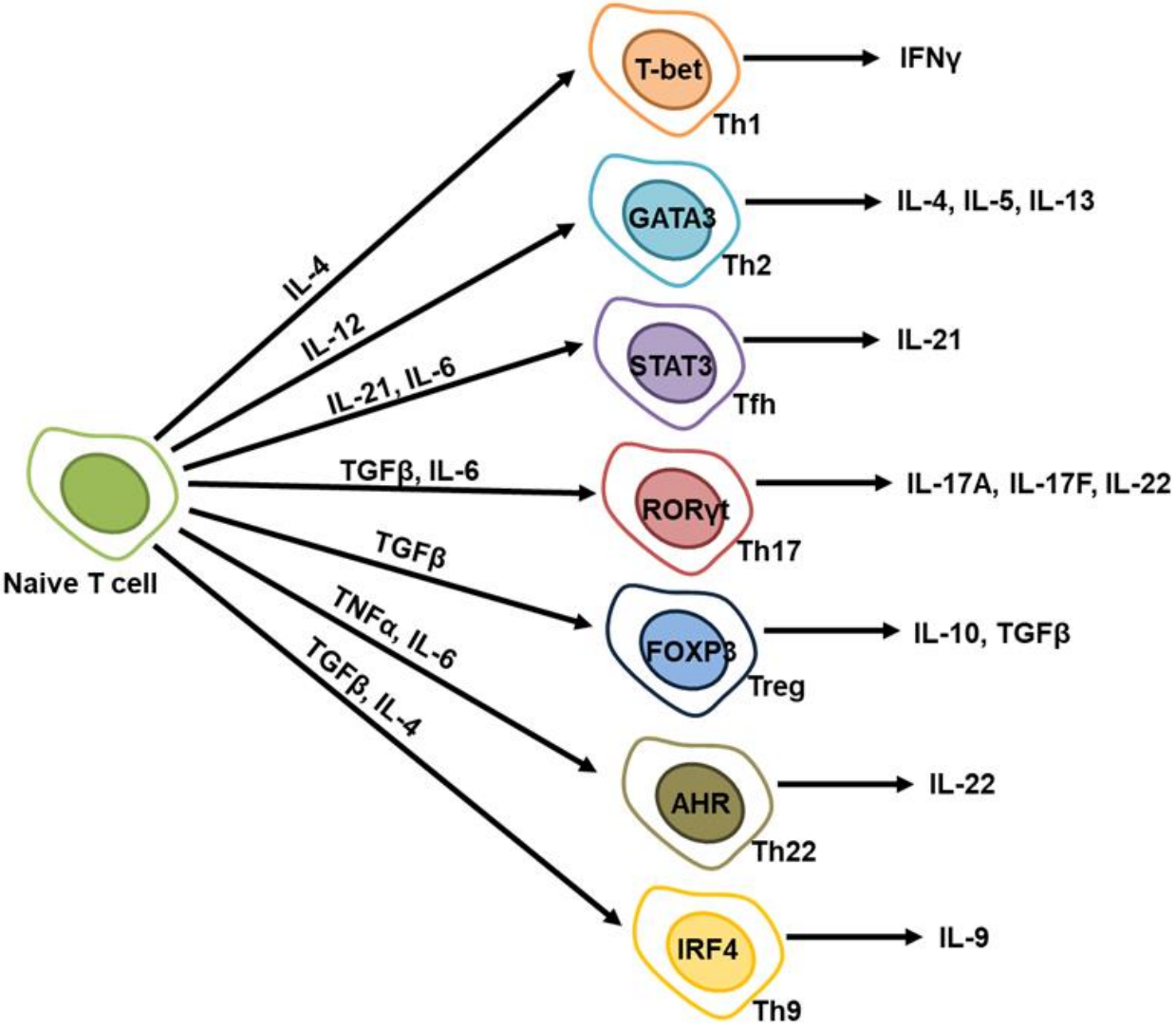


**Illustration 17:** Differentiation of T cell into various subsets

### 5.1.2 Activation of B cells

Mature B cells express IgD along with IgM on their surface and can move out of bone marrow. About 90 % of B cells are cleared in bone marrow by negative selection. B cell undergoes activation when B cell receptor (BCR) binds to a soluble or insoluble antigen (213). After activation, B cells can undergo class switching. The switching of isotype depends on the cytokines released by T cells and other cells in the milieu. B cell activation can either occur in T cell-dependent manner or T cell-independent manner (214,215).

During T cell-dependent immune response, B cell activated by an antigen, shows increased MHC II and B7 expression. The peptide-antigen displayed on the surface of B cells is then recognized by CD4+ T cells, and the co-stimulatory molecule B7 interacts with CD28 present on T cells (216). These interactions induce expression of CD40L on T cells, which then bind to CD40 on B cells (217). All these interactions lead to B cell activation and proliferation. B cell also expresses receptors for cytokines released by T cells, further helping in B cell activation.

## 5.2 Objective

Our previous results indicated that OmpV could play a role in the adhesion of *S.* Typhimurium to IECs. Further, we wanted to probe the potential of OmpV to act as a vaccine. As the primary function of the vaccine is to evoke an immune response, here we examined whether OmpV can modulate adaptive immune responses. Towards this, we worked on the following objectives:

1. To probe whether immunization with OmpV can exert protection against *S.* Typhimurium infection in the mouse model.
2. To study whether OmpV immunization can induce antibody generation.
3. To probe whether OmpV can induce dendritic cell activation and Th differentiation.

## 5.3 Results

**5.3.1 Objective 1:** To probe whether immunization with OmpV can exert protection against *S.* Typhimurium infection in mouse model

#### 5.3.1.1 OmpV induces protective immunity against *S.* Typhimurium infection

We wanted to probe whether immunization with OmpV, a crucial adhesin factor of *S.* Typhimurium, can generate protection against *S.* Typhimurium infection in mice. Towards this, we immunized mice by intraperitoneal administration of four doses of OmpV (25 µg/dose/mouse) at an interval of 7 days each. Two weeks following completion of immunization schedule, the mice were challenged with virulent *S.* Typhimurium through intraperitoneal route/oral route. In case of intraperitoneal infection with *S.* Typhimurium, we observed 100 % survival (**Fig. 30A**), but no protection was obtained in case of oral challenge (**Fig. 30B**).

To probe whether oral immunization can induce protection against oral challenge with virulent bacteria, 4 doses of purified OmpV protein (25 µg/dose/mouse) were orally administered a week apart. Following the oral immunization schedule, we checked for protection against oral challenge with the virulent bacteria. However, there was no protection against oral challenge following oral immunization. We thought that the acidic pH of the stomach and proteolytic enzymes in the gut might degrade the protein. Therefore, to avoid the protein from degradation during oral immunization, we prepared proteoliposome by incorporating OmpV into the liposome. In addition to protection, the liposome can also act as an adjuvant (218). Following immunization with proteoliposome (25 µg/dose/mouse) for four doses at an interval of 7 days, we observed 100 % survival of the immunized mice against oral challenge with *S.* Typhimurium (**Fig. 30C**). Furthermore, when we measured the intestinal length 5 days following oral infection, we observed a significant shrinkage in intestinal length in liposome-immunized mice (control) indicating higher level of infection whereas, the proteoliposome-immunized mice showed similar intestinal length as the un-infected mice (**Fig. 30D**).

The above data suggested that immunization of mice with OmpV protection against systemic and oral challenge.

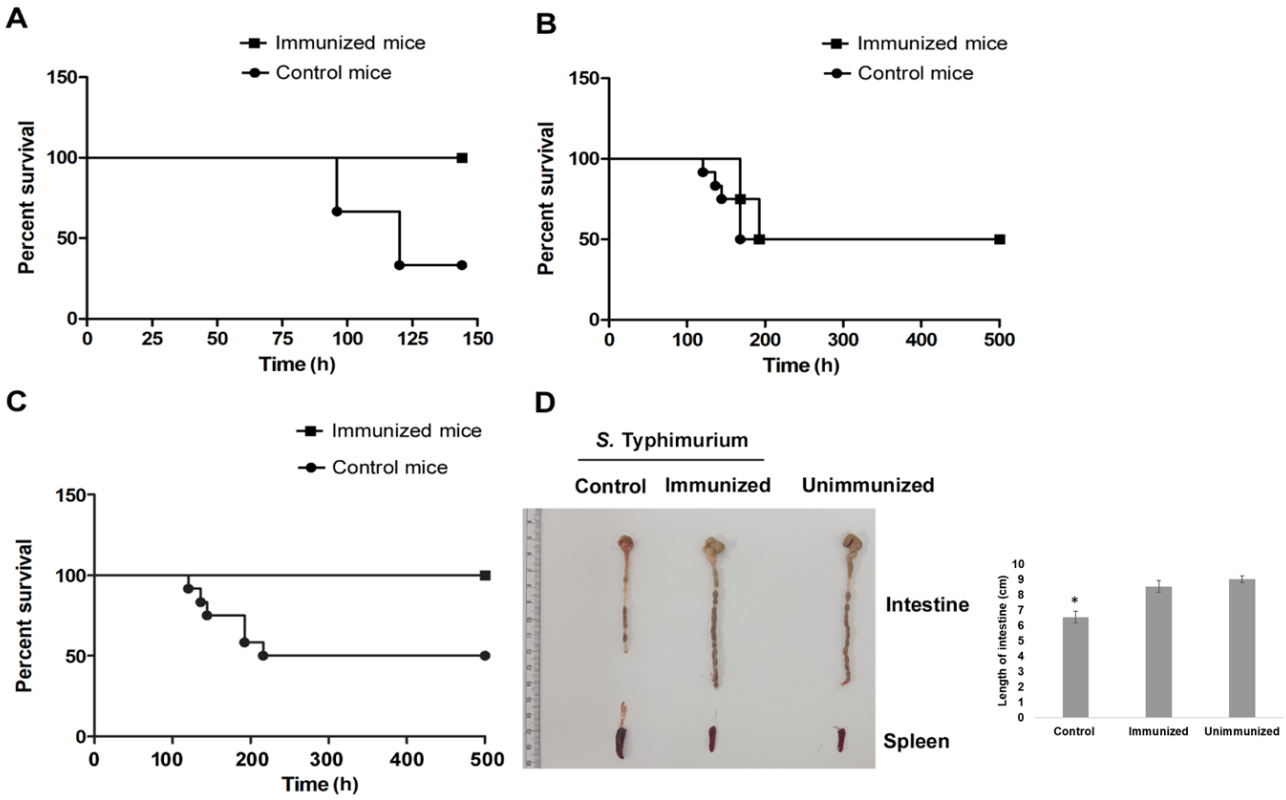


**Figure 30. OmpV induces protective immunity against *S.* Typhimurium infection**

Intraperitoneal immunization of mice with OmpV protects against systemic infection but no gastro-intestinal infection of *S.* Typhimurium as shown by Kaplan Meier plot. n=12 mice/group (4 mice per group per experiment were taken and 3 biological replicates were done) (A, B). Oral immunization of mice with OmpV-proteoliposome protects against gastro-intestinal infection of *S.* Typhimurium as shown by Kaplan Meier plot. n=12 mice/group (4 mice per group per experiment were taken and 3 biological replicates were done). (C). Lesser disease development (indicated by length of intestine) was observed in mice immunized with OmpV-proteoliposome as compared to control mice immunized with liposome upon gastro-intestinal infection (D). Bar graphs are expressed as mean ± SEM from three independent experiments (*p<0.05, **p<0.01, ***p<0.001, ns p>0.05 vs. buffer-treated cells).

**5.3.2 Objective 2:** To probe whether OmpV immunization can induce antibody generation

Antibody production plays a major role in the generation of protective immunity. Among the protective antibody, IgG and IgA are particularly important. IgG is mainly present in blood serum and protects from systemic infection (219). IgA is found primarily in secretions and help to protect the mucosal layer by blocking the initial establishment of bacteria and thus play a crucial role for protection during the gastro-intestinal infection (220). Therefore, we further checked IgG and IgA production following OmpV immunization. Following intraperitoneal immunization with OmpV (25 µg/dose/mouse/week for four weeks as mentioned above) before challenging with *S.* Typhimurium we assessed the IgG in serum and IgA in the stools of

immunized mice. We detected high IgG titre (**Fig. 31A**) but could not detect any IgA (**Fig. 31B**). As mucosal immunizations are reported to produce more IgA, we further assessed the stools for IgA production following oral immunization with OmpV (25 µg/dose/mouse/week for four weeks) but we could not detect the presence of any IgA. Furthermore, following oral immunization with OmpV-incorporated liposome, we could notice high IgA titre in the stools (**Fig. 31C**). Therefore, following systemic or intraperitoneal immunization we got only systemic protection because only IgG was generated. However, we did not get any protection against gastro-intestinal infection in this case, as there was no IgA production. Even following oral immunization with purified OmpV, no protection was observed as there was no IgA or IgG production in this case. However, as oral immunization with OmpV-incorporated liposome could induce IgA production, we observed protection against gastro-intestinal infection as well.

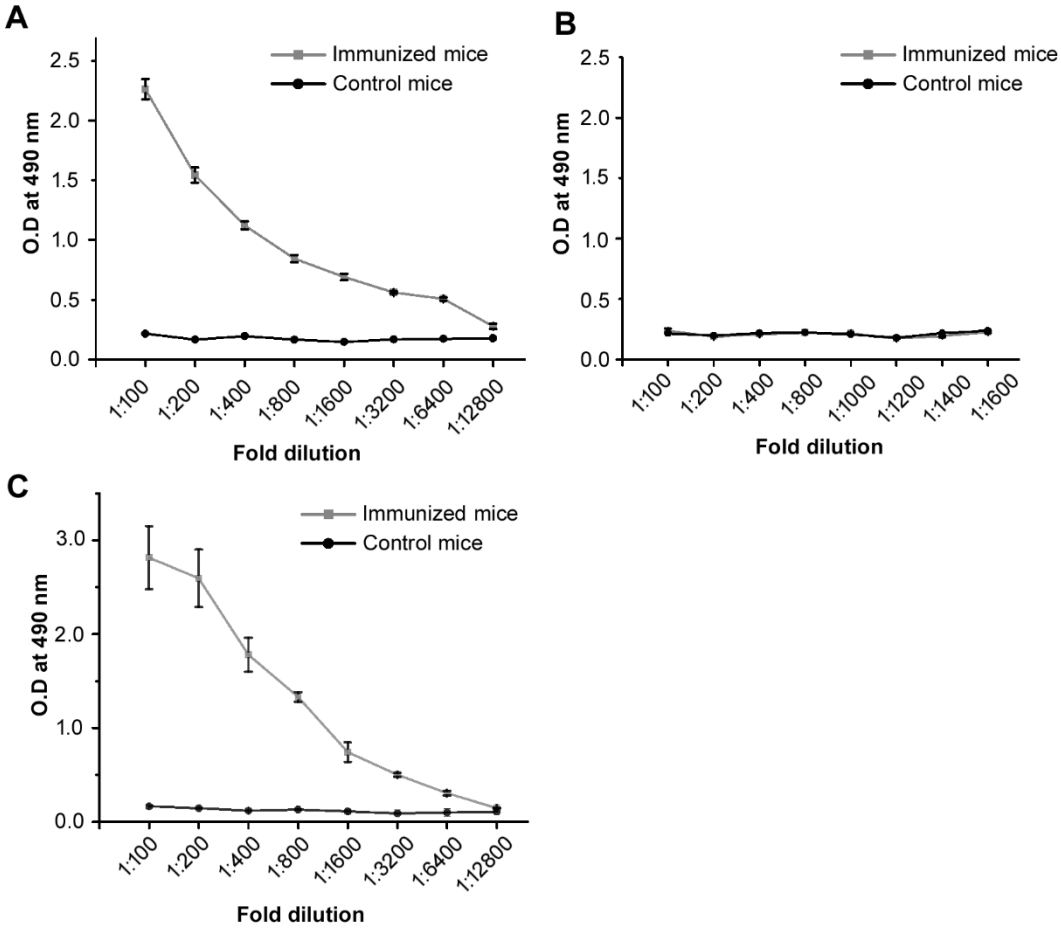


**Figure 31. OmpV immunization leads to antibody generation**

A high titre of IgG was observed in serum of mice immunized intraperitoneally with OmpV (A) but no IgA was produced in this case (B). Serum from mice immunized with buffer was taken as control (A, B). A high titre of IgA was observed in stools of mice immunized orally with OmpV-proteoliposome. Stools from liposome-immunized mice were taken as control (C).

**5.3.3 Objective 3:** To probe whether OmpV can induce dendritic cell activation and Th differentiation

### 5.3.3.1 OmpV induces dendritic cell maturation and Th1 differentiation

CD4+ T cells or T helper (Th1 and Th2) cells are instrumental to high affinity antibody production and class switching (221). Dendritic cells (DCs) act as the professional antigen-presenting cell for T cell activation and Th polarization. For T cell activation and differentiation, DC mainly provides three signals. Out of these, **Signal 1** is provided by interaction of peptide-MHC and T cell receptor and **Signal 2** is provided by the interaction of co-stimulatory molecules (CD80, CD86) with CD28 on T cell. The **Signal 3** is provided by the cytokines produced by the activated DCs or cytokines present in the milieu secreted by other immune cells in the micro-environment (222). With activation via its innate receptor, DC undergoes maturation and becomes efficient in terms of antigen presentation. One of the markers for DC maturation is an increase in the expression of co-stimulatory molecules. To assess, whether OmpV can induce DC maturation, we have treated BMDCs with OmpV and checked for surface expression of CD80 and CD86. We observed an increase in the expression of CD86 on the surface of OmpV-treated BMDCs (**Fig. 32A**), but no increase was observed in case of CD80, probably due to high basal level expression of CD80 on surface of BMDCs (**Fig. 32B**).

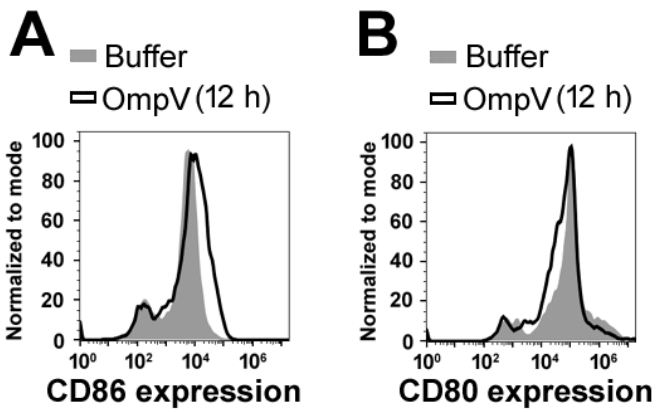


**Figure 32. OmpV induces maturation of dendritic cells**

An increase in surface expression of co-stimulatory molecule CD86 (A) was observed in response to OmpV using flow cytometry. There was no shift observed in case of CD80 (B) which can be due to high basal level of CD80. BMDCs were pre-treated with polymyxin B (PmB) followed by treatment with OmpV. Following incubations, the surface expression of co-stimulatory molecules CD86 and CD80 were analysed using flow cytometry.

Further, we wanted to check whether OmpV primed DCs can lead to proliferation of T cells. Towards this, we performed T cell proliferation assay using CFSE-labelled CD4+ T cells co-cultured with OmpV-activated splenic DCs. We observed dilution in CFSE fluorescence indicating proliferation of T cells (**Fig. 33**).

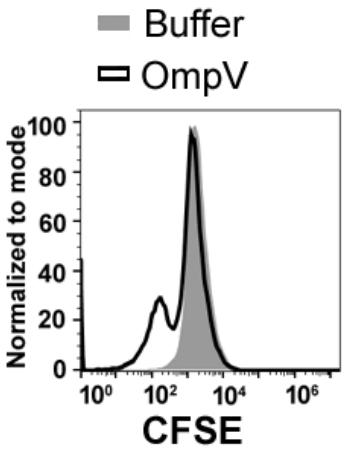


**Figure 33. OmpV induces proliferation of T cells**

A decrease in CFSE fluorescence indicates the proliferation of T cells. CFSE-labeled T cells were co-cultured with splenic DCs treated with OmpV such that DC: T cell ratio was 1:80. On Day 3, CFSE fluorescence was detected using BD FACS Accuri c6. CFSE-labelled T cells treated with buffer were taken as control.

As previously mentioned, T cell differentiation depends on cytokines secreted by the antigen-presenting cells or the presence of cytokines in the micro-environment (223). Towards this, we wanted to check whether OmpV-activated DCs can produce IL-12 or IL-10, which will impact Th1 or Th2 or Treg differentiation. Towards this, we observed that OmpV-primed DCs secrete high IL-12 compared to IL-10 (IL-12/IL-10 ratio around 20:1), indicating differentiation of T helper cells might happen towards Th1 phenotype (**Fig. 34**).

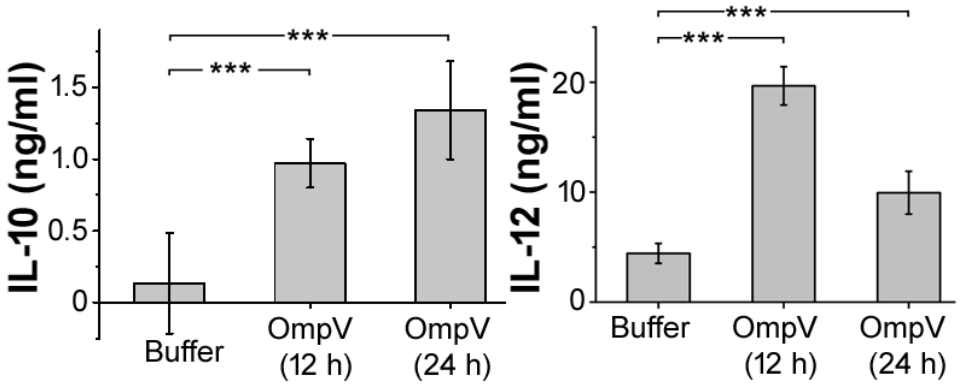


**Figure 34. OmpV leads to high IL-12/IL-10 cytokine production**

Significant production of IL-10 and Il-12 cytokines was observed in BMDCs in response to OmpV. BMDCs were treated with PmB followed by OmpV. Following incubations, the supernatants were collected and estimated for IL-10 and IL-12 cytokines using ELISA. Bar graphs are expressed as mean± SEM from three independent experiments (*p<0.05, **p<0.01, ***p<0.001, ns p>0.05 versus the buffer treated cells).

To further confirm, whether OmpV-induces polarization of T helper cells towards Th1 phenotype, we analysed cytokines released by T cells co-cultured with OmpV-activated DCs. We observed a significant production of IFN-γ in the supernatant confirming polarization of activated T cells towards Th1 (**Fig. 35**).

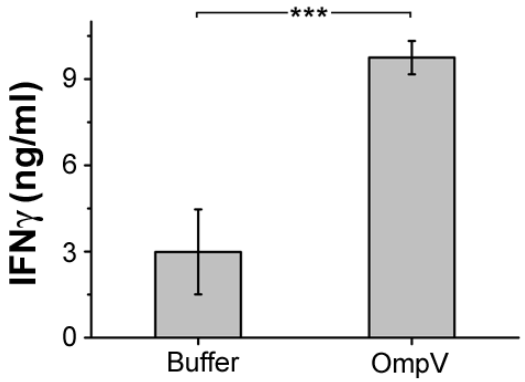


**Figure 35. OmpV induces Th1 subset proliferation during *in vitro* studies**

Significant production of IFNγ was observed by splenic T cells co-cultured with splenic DCs treated with OmpV (2 µg/ml) such that DC: T cell ratio was 1:80 for 3 days. Bar graphs are expressed as mean± SEM from three independent experiments (*p<0.05, **p<0.01, ***p<0.001, ns p>0.05 versus the buffer treated cells).

As in *in vivo* condition, other cell types also contribute to the cytokines in the milieu, we wanted to check whether in *in vivo* condition OmpV induces Th polarization towards Th1 as well.

Towards this, we administered four doses of purified OmpV in mice intraperitoneally (25 µg/dose/mouse) at an interval of 7 days. Following immunization, T cells were isolated from inguinal, popliteal and mesenteric lymph nodes and stimulated using PMA and ionomycin. We observed a high production of IFN-γ compared to negligible IL-4 confirming polarization of Th cells majorly towards Th1 phenotype (**Fig. 36**).

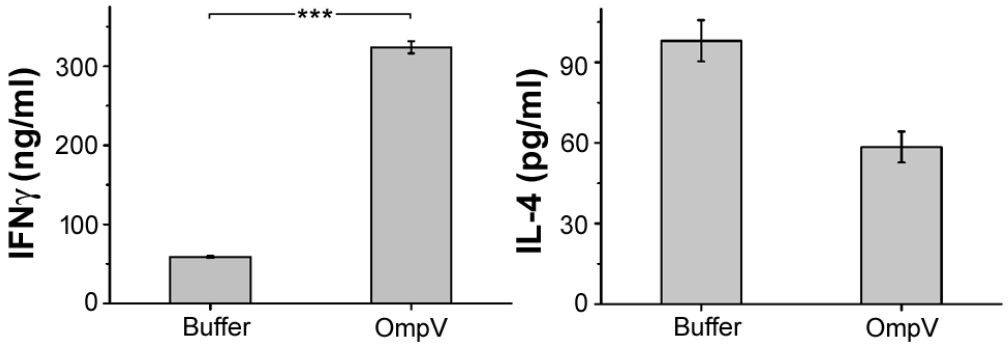


**Figure 36. OmpV induces Th1 subset proliferation during *in vivo* intraperitoneal immunization**

A significant IFNγ production was observed by T cells isolated from lymph nodes of mice prior to *in vivo* intraperitoneal immunization with OmpV. Mice immunized with buffer were taken as controls. Bar graphs are expressed as mean± SEM from three independent experiments (*p<0.05, **p<0.01, ***p<0.001, ns p>0.05 versus the mice immunized with buffer).

Further, after oral administration of OmpV-proteoliposome, T cells were isolated from mesenteric lymph node and assessed for production IFN-γ and IL-4 upon activation with PMA and ionomycin. We observed, production of more IFN-γ and less IL-4 suggesting both Th1 and Th2 phenotype with more Th1 bias (**Fig. 37**).

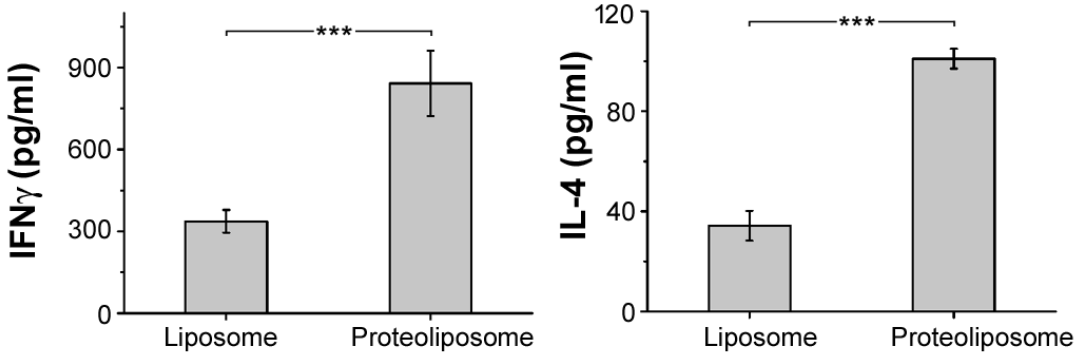


**Figure 37. OmpV induces both Th1 and Th2 subset proliferation during *in vivo* oral immunization**

A significant IFNγ and IL-4 production was observed by T cells isolated from lymph nodes of mice prior to *in vivo* oral immunization with OmpV-proteoliposome. Mice immunized with liposome were taken as control. Bar graphs are expressed as mean± SEM from three independent experiments (*p<0.05, **p<0.01, ***p<0.001, ns p>0.05 versus the mice immunized with liposome).

## 5.4 Conclusion

In the last two chapters, we observed that OmpV helps in adhesion of *S.* Typhimurium to IECs. Further, to probe the role of OmpV in protection against *S.* Typhimurium infection, we observed that systemic immunization (intraperitoneal immunization) of mice with purified OmpV protein gave protection against systemic infection but not gastro-intestinal infection (**Fig. 30**). In systemic immunization a high IgG titre was observed but no IgA was found (**Fig. 31)**. Even in oral immunization with purified OmpV we did not observe any IgA production (**Fig. 32**) as well as protection. However, when we used OmpV-proteoliposome for oral immunization of mice, we observed a high IgA titer as well as protection against gastro-intestinal infection (**Fig. 30, 31)**. Further, lesser infection in case of mice immunized with OmpV-incorporated proteoliposome was evident in terms of the intestinal length following infection (**Fig. 30**). As efficient antibody production and class switching by B cells require T cells, we further probed for DC maturation and T cell activation in response to OmpV treatment. We found that OmpV can effectively lead to the maturation of DCs as represented by increased surface expression of co-stimulatory molecules (**Fig. 32**). Also, OmpV-treated DCs when co-cultured with naive T cells, it can lead to the proliferation of these T cells shown by dilution of CFSE during proliferation assay (**Fig. 33**). Further, it was seen that the OmpV-activated DCs produce more IL-12 production as compared to IL-10, suggesting differentiation of T cells could be towards Th1 phenotype (**Fig. 34**). We further observed IFNγ production by OmpV-activated T cells in both in vitro and in vivo (**Fig. 35, 36**). However, oral immunization with OmpV-incorporated proteoliposome induces both IFNγ and IL-4, suggesting both Th1 and Th2 polarization (**Fig. 37**) and this is also reflected by both IgG and IgA antibody production by oral immunization of OmpV-incorporated proteoliposome. So, here we concluded that OmpV can activate adaptive immune responses and induces T cell differentiation and B cell activation in terms of IgA and IgG production, leading to protective immunity against *S.* Typhimurium infection.

# Chapter 4

## **Specific aim 2:** How OmpV modulates innate immune responses

### 6.1 Inflammation: host defence response against injury or infection

Innate immune system is evolutionary evolved immune defence mechanism that present in all multicellular organisms. It is present in individuals since birth and is considered as the first line of defence. The innate immunity gets activated on recognition of pathogens, damaged cells or harmful stimuli to induce inflammation. Inflammation is one of the defence mechanisms of body that helps in removing the pathogen and healing of the body (224). Four hallmarks of inflammation as described by Romans more than 2000 years ago include tumor (swelling), rubor (redness), calor (heat) and dolar (pain). One more hallmark functio laesa (loss of function) was added subsequently to these by Galen (214,215). The inflammatory process majorly starts when a pathogen infects our body. Pathogen associated molecular patterns (PAMPs) present on the surface of these pathogens are recognized by pattern recognition receptors (PRRs) present in immune cells. In addition to the pathogen, the damaged tissue in the body can release damage-associated molecular patterns (DAMPs) and trigger inflammation.

In response to inflammatory stimuli, the tissue-resident immune cells, such as macrophages, dendritic cells, and mast cells, initiate the process of inflammation. On recognition of PAMPs and DAMPs, these tissue-resident cells get activated and start release of proinflammatory mediators. The process of inflammation majorly involves four stages (**Illustration 18**):

**a)** Enlargement of the blood vessels due to vasodilation which increases blood flow to the site of infection with decreased velocity. This causes redness and heat.

**b)** Increase in the permeability of blood vessels resulting in accumulation of fluid and plasma proteins in the tissue. This causes swelling.

**c)** Margination i.e., adherence of WBCs to vascular endothelium, occurs due to a decrease in circulation (225,226). Further, migration and recruitment of neutrophils followed by other WBCs from blood lumen (extravasation) to the inflamed site.

**d)** Adjustment of metabolic pathways of the body causing fever, fatigue or loss of appetite.

Further, there is a 10,000-fold increase in acute phase proteins (such as, C reactive protein) during acute phase of inflammation (227). Inflammation is followed by repair and wound healing. Generally, inflammations are of two types chronic inflammation and acute inflammation. Usually, the process of acute inflammation is useful in minimizing the infection. However, if the source of inflammation could not be eliminated, prolonged inflammatory responses can lead to chronic inflammation. In the case of acute inflammation, neutrophils are the most abundant cells present at the site of infection for 24 h. However, lymphocytes, macrophages and plasma cells are accumulated in case of chronic inflammation (228).

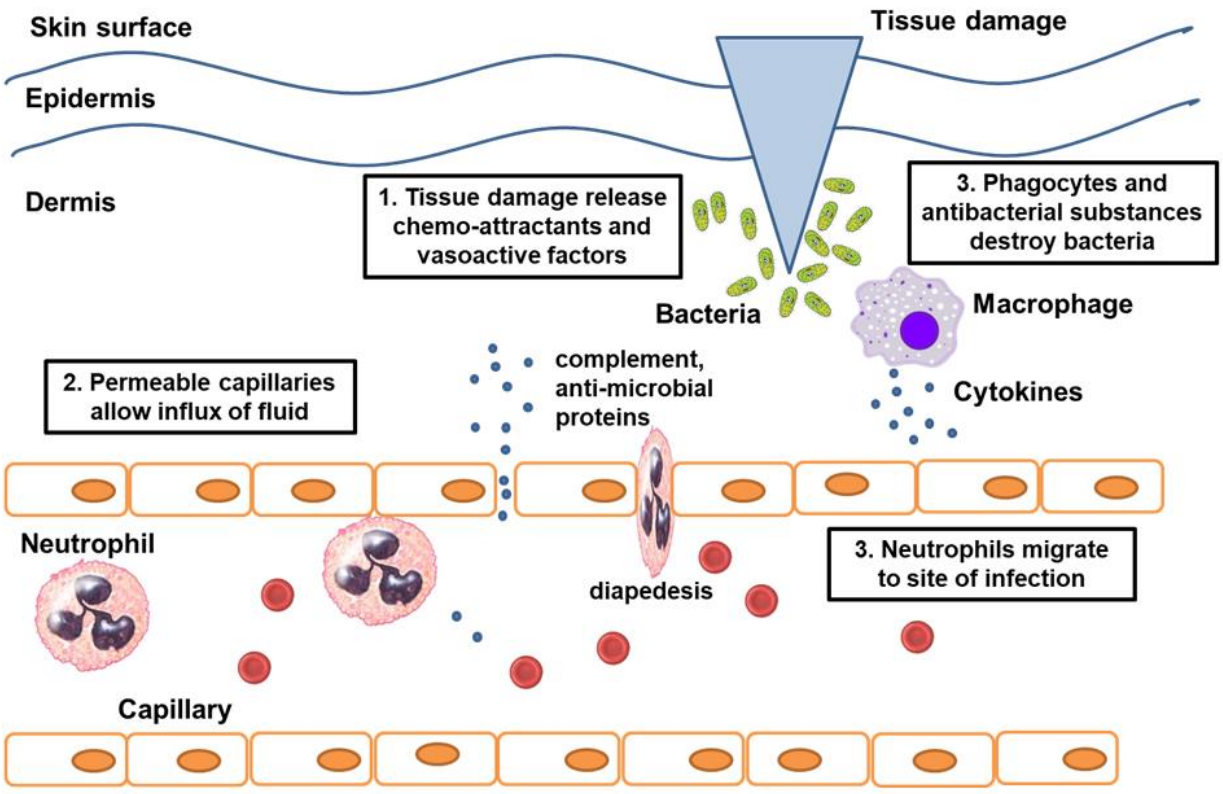


**Illustration 18:** Process of inflammation

### 6.1.1 Inflammation and intestinal epithelial cells

As the intestine is a major site for pathogen encounter, it has a tightly regulated immune system to protect against pathogens without evoking unnecessary immune activity. There is a group of lymphoid tissues present collectively known as gut-associated lymphoid tissue (GALT). It

consists of Peyer's patches, mesenteric lymph nodes, isolated lymphoid follicles, DCs and lymphocytes in lamina propria and intestinal epithelium (229).

The complex relation of the intestinal immune system and gut microbiota is crucial for intestinal cells as it helps to differentiate between pathogenic and non-pathogenic bacteria. The intestinal epithelial cells have pattern recognition receptors like TLRs present on its surface, due to which it can recognize PAMPs and thus initiate innate immune responses. The intestinal immune cells can secrete chemokines like IL-8, thus attracting adjacent immune cells such as macrophages, neutrophils, and other granulocytes to the site of infection (230).

### 6.1.2 Monocytes and macrophages are crucial players of the innate immune system

Macrophages play major roles during the process of inflammation: a) phagocytosis; b) antigen presentation; c) production of immune-modulatory cytokines. Tissue-resident macrophages such as microglia (in the nervous system), kupffer cells (in the liver), and osteoclasts (in the bone) help in phagocytosis of pathogens. The macrophages are differentiated from the precursor cells known as monocytes. As part of WBCs, monocytes are generally present in blood circulation but are recruited to the site of inflammation by getting signals from resident macrophages (226). During this process, monocytes differentiate into macrophages. Monocytes are short-lived cells having lesser phagocytic capacity as compared to macrophages. However, monocytes also have PRRs that can recognize PAMP and secrete proinflammatory cytokines similar to macrophages (231). Macrophages and monocytes together play a critical role in initiation and resolution of inflammatory responses (232).

### 6.1.3 Activation of inflammatory pathways

Activation signal via PAMP -PRR interaction triggers various inflammatory pathways by innate immune cells (233). There are four families of PRR that include TLR (Toll-like receptor), CLR (C-type lectin receptor), NLR (Nod-like receptor), and RLR (RIG-I-like receptor). Out of these, NLRs and RLRs are intracellular receptors, whereas CLRs are present on the cell surface. TLRs can be either endosomal or present on the cell surface (234-236). Based on the literature, TLRs are the most studied class of surface receptors for recognition of bacterial ligands. The signal transduction mechanism through TLRs is well studied. Following TLR activation, adaptor molecules including MyD88 or TRIF are recruited at the cytoplasmic

tail of the receptor. Depending on the recruitment of these adaptor molecules, TLR signaling can be divided into MyD88 dependent or MyD88 independent pathways. TLR4 is known to activate both MyD88 dependent and independent pathways as it can recruit both MyD88 and TRIF adaptor proteins (237,238). TLR3 signals through TRIF hence activate the MyD88 independent pathway (239). All other TLRs are known to activate the MyD88 dependent signaling pathway.

#### 6.1.3.1 MyD88-dependent signaling pathway

At the C terminal, MyD88 has the TIR domain associating TIR domain of TLRs upon stimulation. At the N terminal, there is a death domain, which helps the recruitment of IL-1 receptor-associated kinase (IRAK) to TLRs (240). Further, IRAK upon phosphorylation gets activated and then associates with TRAF6, leading to the activation of two distinct signaling pathways, one of the siganalling pathways leading to the activation of transcription factor NF-κB and another involving MAPkinases (MAPKs), finally activating transcription factors NF-κB and AP-1 both. A schematic representation of MyD88 dependent signal pathway is shown in **Illustration 19**.

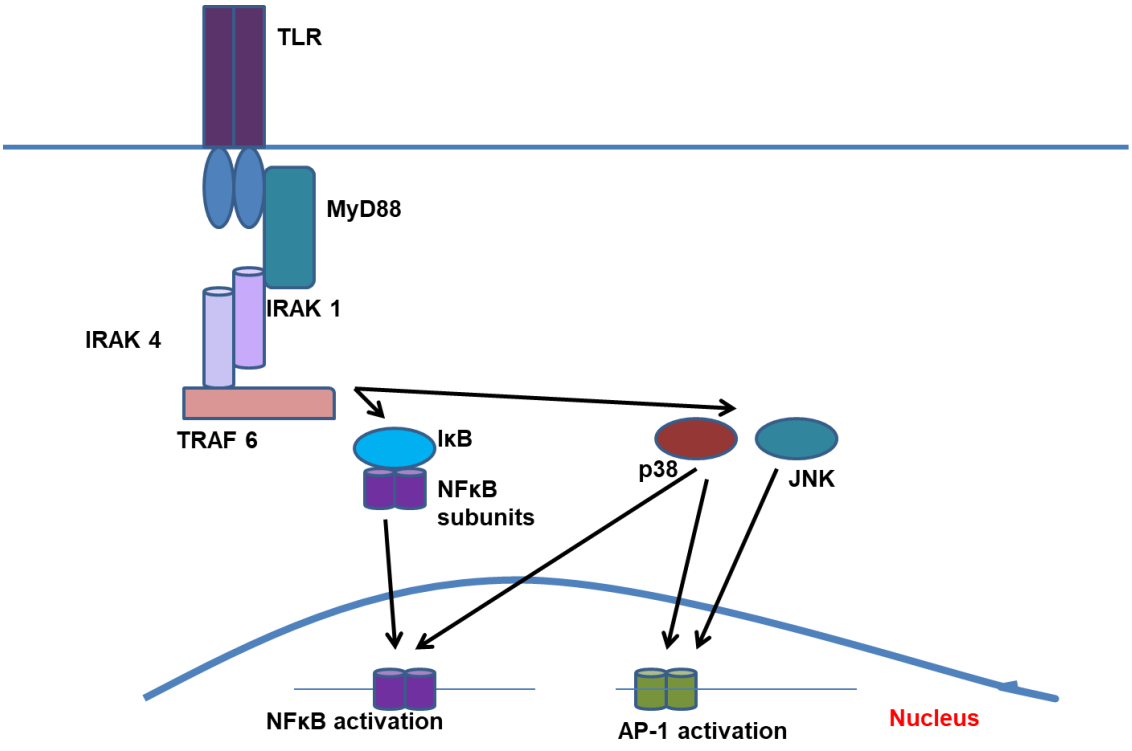


**Illustration 19:** MyD88-dependent inflammatory pathways

#### 6.1.3.1.1 MAPkinase signaling pathway

MAPKs are a serine/ threonine family of protein kinases that get activated by heat shock, osmotic stress, and inflammation. MAPK signaling is initiated by MAPKKK (MAPK kinase kinase) which phosphorylate and activate MAPKK (MAPK kinase) which further phosphorylate and activate MAPKs. MAPKs such as JNK and p38 are majorly activated by inflammatory responses. Another MAPK i.e., ERK1/2, was earlier thought to be involved in differentiation, but later its role in inflammation was also reported (233).

#### 6.1.3.1.2 NF-κB transcription factor

NF-κB plays an important role in inflammation, survival, and apoptosis. The family of NF-κB transcription factor is composed of five subunits: p52, p50, RelA (p65), RelB, and c-Rel as shown in **Illustration 20**. Under normal circumstances, these subunits are inhibited in cytoplasm by IκB. On recognition of pathogen, PRRs activate IκB kinases, which leads to phosphorylation of IκB. The phosphorylated IκB thus gets degraded and NF-κB subunits move to nucleus leading to proinflammatory cytokine production (241).

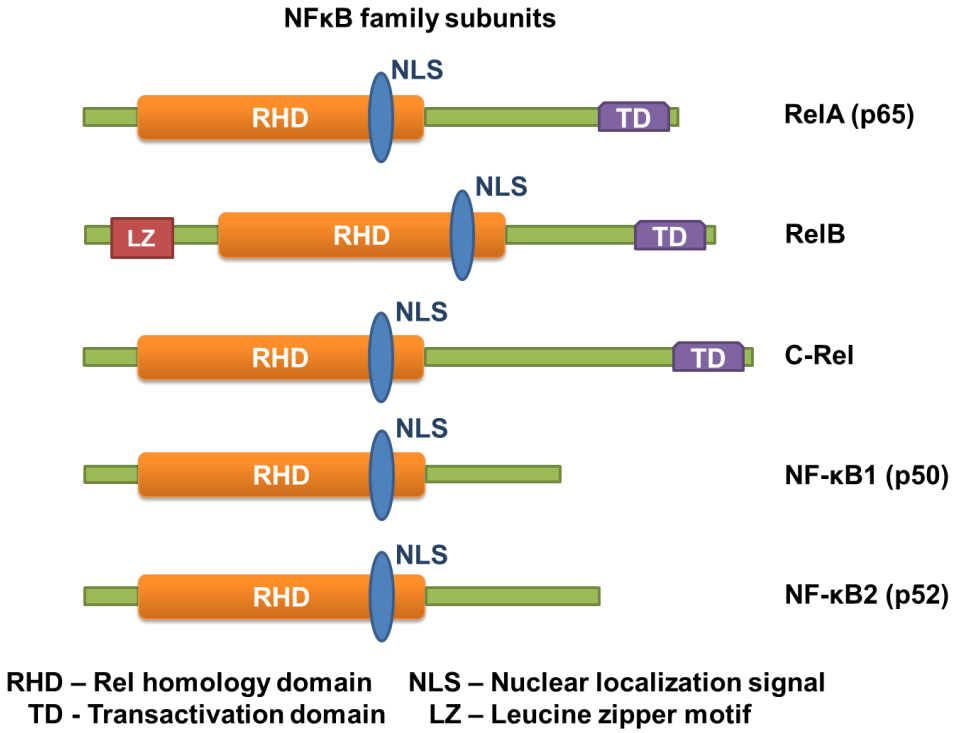


**Illustration 20:** Schematic diagram of NF-κB family subunits

#### 6.1.3.1.3 AP-1 transcription factor

AP-1 is known to be involved in a wide range of cellular processes, including differentiation, cell growth, and apoptosis. AP-1 is a dimeric complex composed of members from Jun, Fos, ATF or MAF families. Out of these Jun and ATF proteins can form homodimers as well as heterodimers whereas Fos family members can only form heterodimers with Jun family. These Jun-Fos heterodimers are known to be strong activators of pro-inflammation (242). The schematic representation of members of Jun and Fos family are shown in **Illustration 21**. MAPKs regulate the phosphorylation and differential expression of these AP-1 subunits.

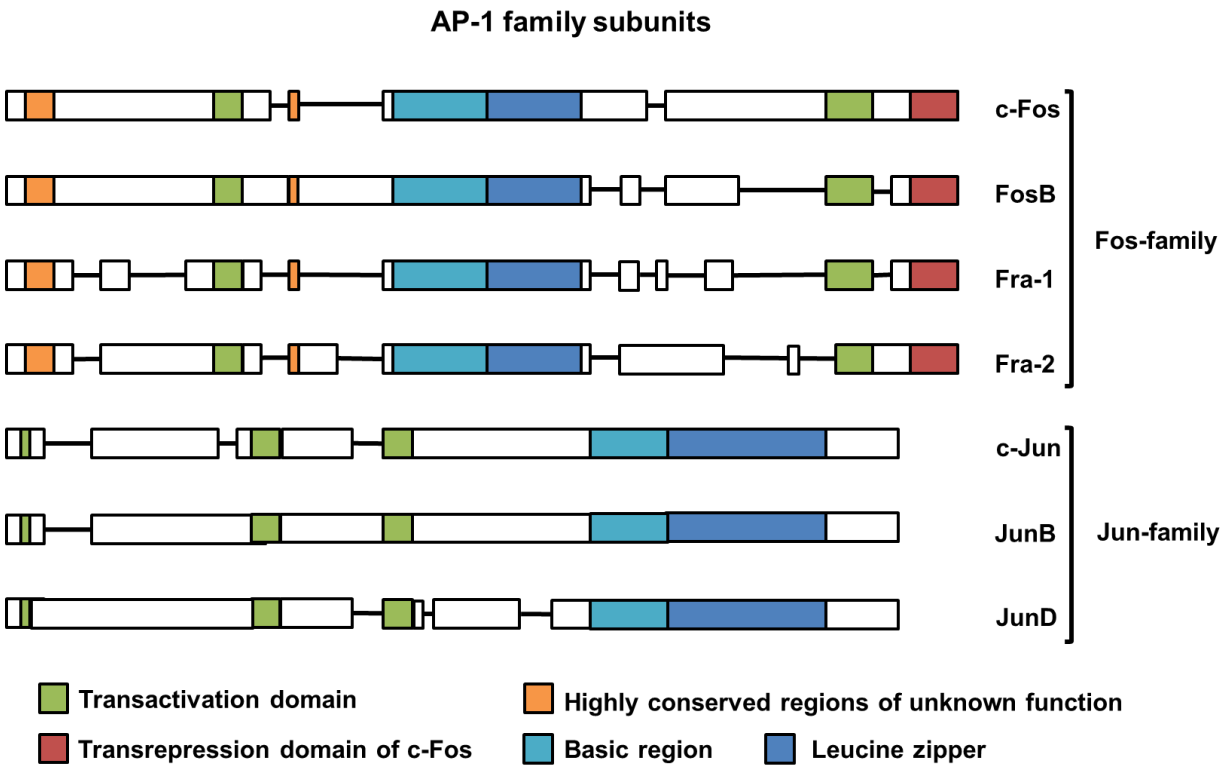


**Illustration 21:** Schematic diagram of AP-1 family subunits

### 6.2 Objective

It was previously studied that OmpV can modulate adaptive immune responses. As the innate immune system is crucial for activation of the adaptive immune system, so further to probe the role of OmpV in the modulation of innate immune responses, we formulated the following objectives:

1. To probe whether OmpV can induce pro-inflammatory responses
2. To find out the pattern recognition receptor of OmpV
3. To find out the signaling mediators involved in OmpV-mediated proinflammatory signaling

## 6.3 Results

### 6.3.1 Objective 1: To probe whether OmpV can induce proinflammatory responses

#### 6.3.1.1 OmpV can activate innate immune cells leading to the production of pro-inflammatory mediators

As innate immune responses are crucial in shaping up of adaptive immunity, we further investigated the innate immune responses involved in OmpV signaling. Towards this, we at first treated RAW 264.7 (murine macrophages), THP-1 (human monocytes), HT29 and T84 (human intestinal epithelial cells) in response to different doses of OmpV and incubated for 24 h. We observed significant production of various pro-inflammatory cytokines and chemokines in response to different doses of OmpV (**Fig. 38A-G**). In both RAW 264.7 macrophages (**Fig. 38A, B**) and THP-1 monocytes (**Fig. 38C, D**), a considerable production of TNFα and IL-6 were observed in response to 2 µg/ml of OmpV and a plateau was observed in pro-inflammatory cytokine release in macrophages with an increase in OmpV doses beyond 2 µg/ml (**Fig. 38A, B**). Further, we observed that IL-8 was significantly produced by HT29 (**Fig. 38E**) and T84 intestinal epithelial cells (**Fig. 38F**) in response to different doses of OmpV and there was significant release of IL-8 at 2 µg/ml beyond which there was either a decrease (**Fig. 38E**) or a plateau (**Fig. 38F**) in IL-8 production. Apart from cytokines, another major sign of inflammatory responses by macrophages is nitric oxide (NO) production (243). NO is unstable and thus converted to nitrite at room temperature that can thus be measured with the help of Griess reagent. By using that method, we checked NO production in response to different doses of OmpV. Maximum NO production was observed at 2 µg/ml concentration of OmpV (**Fig. 38G**). Further, we assessed cell viability by MTT assay with different doses of OmpV following incubation for 24 h (Fig. **38H-K**). We observed a dose dependent decrease in cell

viability in RAW 264.7 (**Fig. 38H**). As significant production of pro-inflammatory responses with no significant decrease in viability was observed in any cell type in response to 2 µg/ml OmpV, therefore, we further used this concentration for time-course studies.

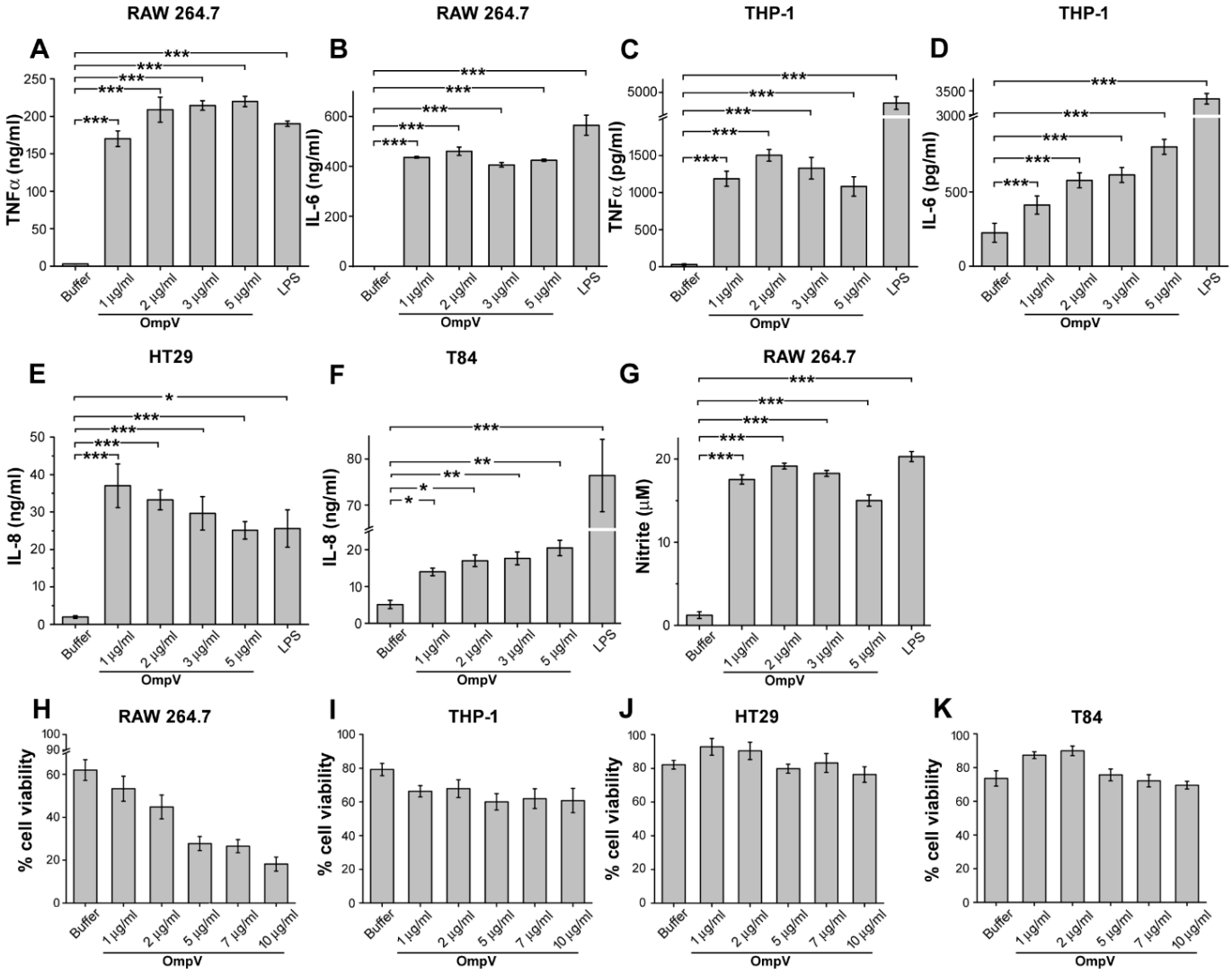


**Figure 38. OmpV induces production of proinflammatory mediators in RAW 264.7 macrophages, THP-1 monocytes and intestinal epithelial cells (IECs)**

A significant production of TNFα and IL-6 was observed in RAW 264.7 macrophages (A, B) and THP-1 monocytes (C, D) on treatment with OmpV. A significant production of IL-8 was observed in IECs on treatment with OmpV (E, F). A significant production of NO was observed in RAW 264.7 macrophages on treatment with OmpV (G). 1 µg/ml LPS is used as positive control. Bar graphs are expressed as mean± SEM from three independent experiments (*p<0.05, **p<0.01, ***p<0.001, ns p>0.05 versus the buffer treated cells). Cell viability assay indicated that 2 µg/ml OmpV minimally effects the cell health in case of macrophages, monocytes and IECs (H-K).

For time course studies, we treated RAW 264.7 macrophages, THP-1 monocytes**,** T84 and HT29 IECs with 2 µg/ml of OmpV and incubated for different time periods. After respective

incubations, the supernatant was collected and analyzed for the presence of pro-inflammatory mediators (**Fig 39A-G**). We assessed TNFα and IL-6 production by RAW 264.7 macrophages and THP-1 monocytes and observed a time dependent increase of both TNFα and IL-6 till 24 h in RAW 264.7 macrophages (**Fig. 39A-B**), whereas, in THP-1 monocytes maximum release of TNFα was observed at 4 h (**Fig. 39C**) and IL-6 was maximally produced at 24 h (**Fig. 39D**). Further, nitrite production in RAW 264.7 macrophages was assessed at different time points and maximum generation was seen at 24 h (**Fig. 39E**). Further, we assessed IL-8 production in both HT29 and T84 cells in response to OmpV at different time points and maximum release was observed at 24 h (**Fig. 39F, G**). LPS (1 µg/ml) was taken as positive control for these experiments.

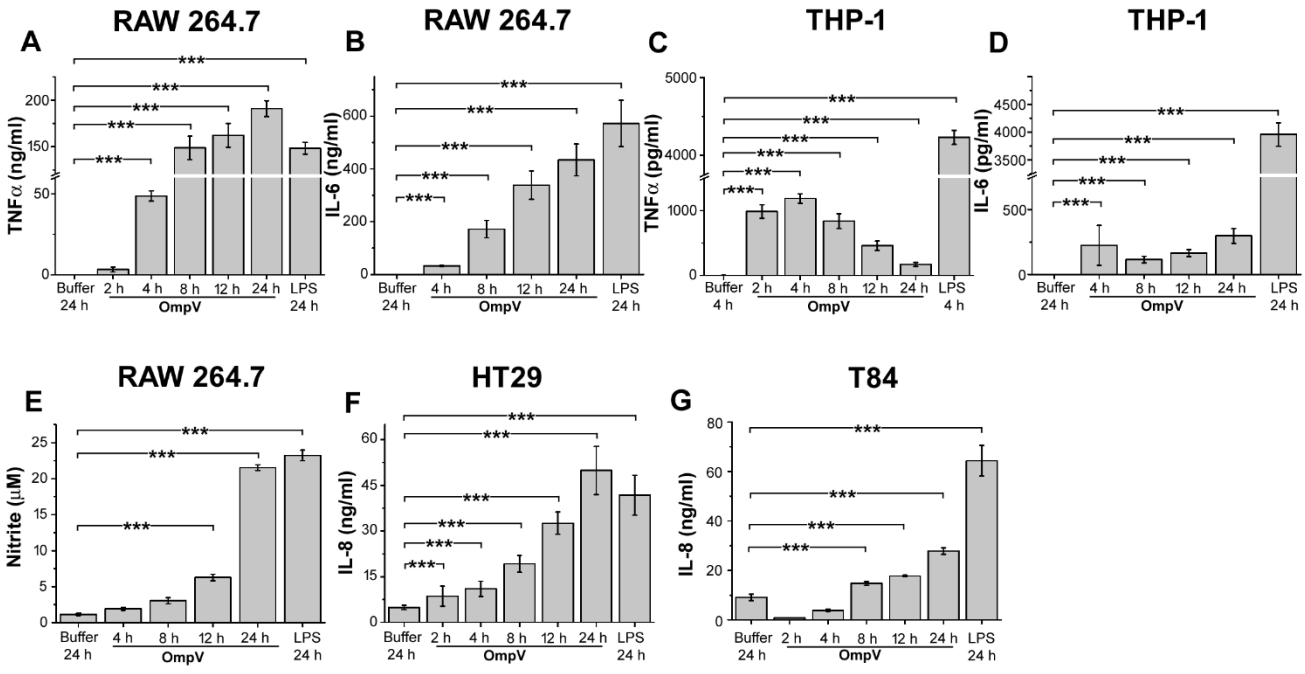


**Figure 39. Time course analysis for production of proinflammatory mediators in RAW 264.7 macrophages, THP-1 monocytes and IECs**

Maximum production of TNFα and IL-6 was observed at 24 h in RAW 264.7 macrophages (A, B) whereas in case of THP-1 monocytes TNFα was maximally produced at 4 h and IL-6 at 24 h (C, D). Maximum production of NO was observed at 24 h in RAW 264.7 macrophages (E). Maximum production of IL-8 was observed at 24 h in HT29 and T84 (F-G). Bar graphs are expressed as mean± SEM from three independent experiments (*p<0.05, **p<0.01, ***p<0.001, ns p>0.05 versus the buffer treated cells).

Further, with proteoliposome as well, we observed similar levels TNFα production as compared to OmpV-treated cells in both RAW 264.7 macrophages and THP-1 monocytes (**Fig. 40A-D**).

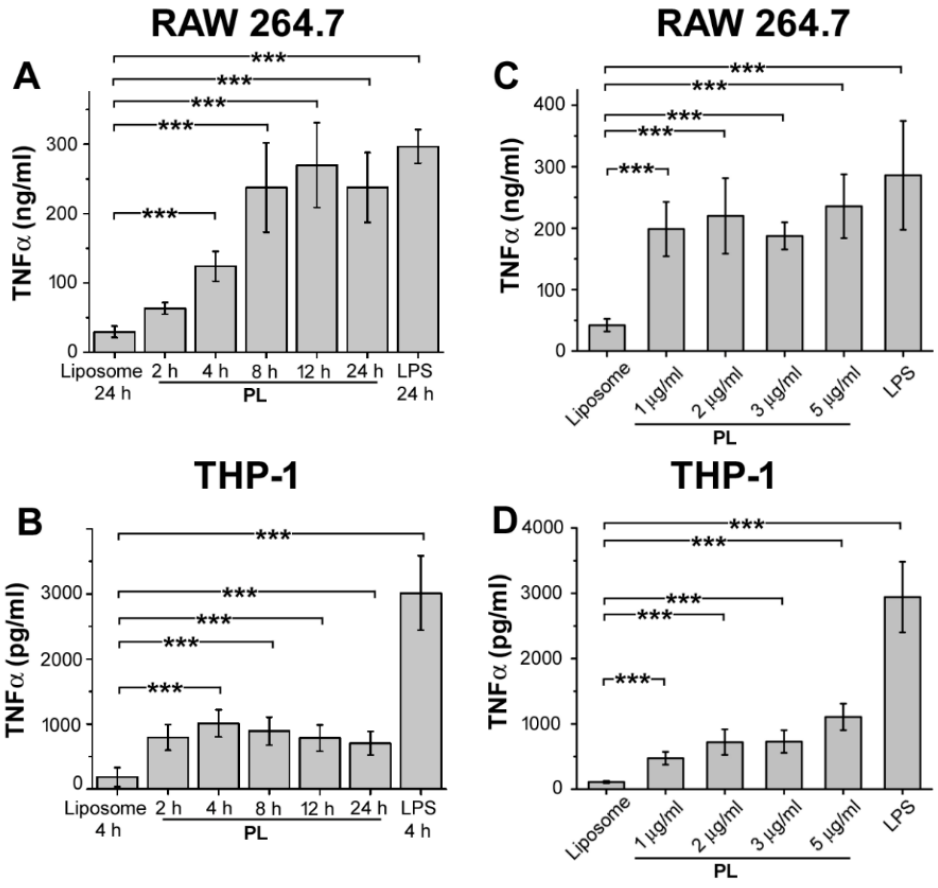


**Figure 40. Proteoliposome induces similar proinflammatory responses as OmpV**

Similar time course and dose dependent production of TNFα was observed in RAW 264.7 macrophages (A-B) and THP-1 monocytes (C-D) on treatment with OmpV-proteoliposome as compared to OmpV treatment. 1 µg/ml LPS was used as positive control. Bar graphs are expressed as mean± SEM from three independent experiments (*p<0.05, **p<0.01, ***p<0.001, ns p>0.05 versus the liposome treated cells).

**6.3.2 Objective 2:** To find out the pattern recognition receptor (PRR) of OmpV

### 6.3.2.1 OmpV induces activation of innate immune cells via TLR2

Generally, for the production of pro-inflammatory mediators PAMPs are recognized by PRRs present on the immune cells. As OmpV induces pro-inflammatory cytokine production then

certainly it acted as a PAMP and recognized by PRR. Therefore, we wanted to check which PRR is involved in recognition of OmpV. Being an outer membrane protein, OmpV will probably come in contact with surface PRRs at first. The majority of surface PRRs includes TLR out of which, TLR1, TLR2, TLR4 and TLR6 are mostly known to recognize bacterial ligands (244). Therefore, towards it, we first checked whether there was any increase in surface expression of these TLRs in response to OmpV treatment. We observed an increase in surface expression of TLR1, TLR2 and TLR6 in OmpV-activated RAW 264.7 macrophages (**Fig. 41A**) whereas in OmpV-activated THP-1 monocytes, we observed an increase in surface expression of only TLR1 and TLR2 (**Fig. 41B**). Our observations indicated the involvement of TLR1, TLR2 and TLR6 in RAW 264.7 macrophages and only TLR1 and TLR2 in THP-1 monocytes in recognition of OmpV**.**

Further, we observed that in RAW 264.7 macrophages OmpV co-immunoprecipitated with TLR2, TLR1 and TLR6 (**Fig. 41C-E**), whereas, in OmpV-activated THP-1 monocytes OmpV co-immunoprecipitated only with TLR2 and TLR1 but not with TLR6 (**Fig. 41F-H**). Similar to the surface expression data, the co-immunoprecipitation strongly suggested that TLR2 might be involved in OmpV recognition by innate immune cells. Moreover, as it was known that TLR2 generally hetero-dimerizes either with TLR1 or TLR6, in response to OmpV, TLR2 probably hetero dimerizes with both TLR1 and TLR6 in macrophages but only with TLR1 in monocytes.

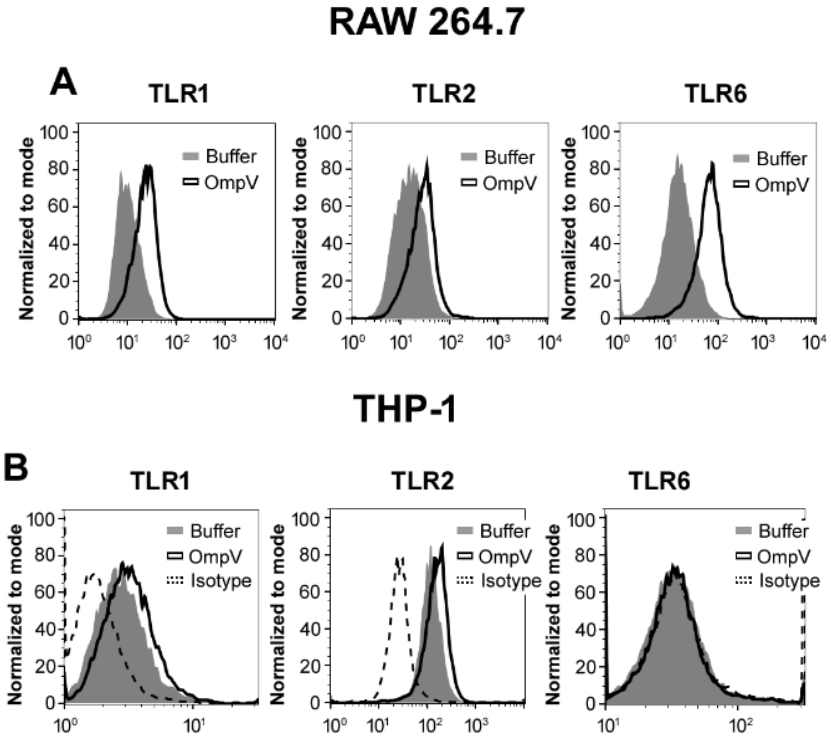

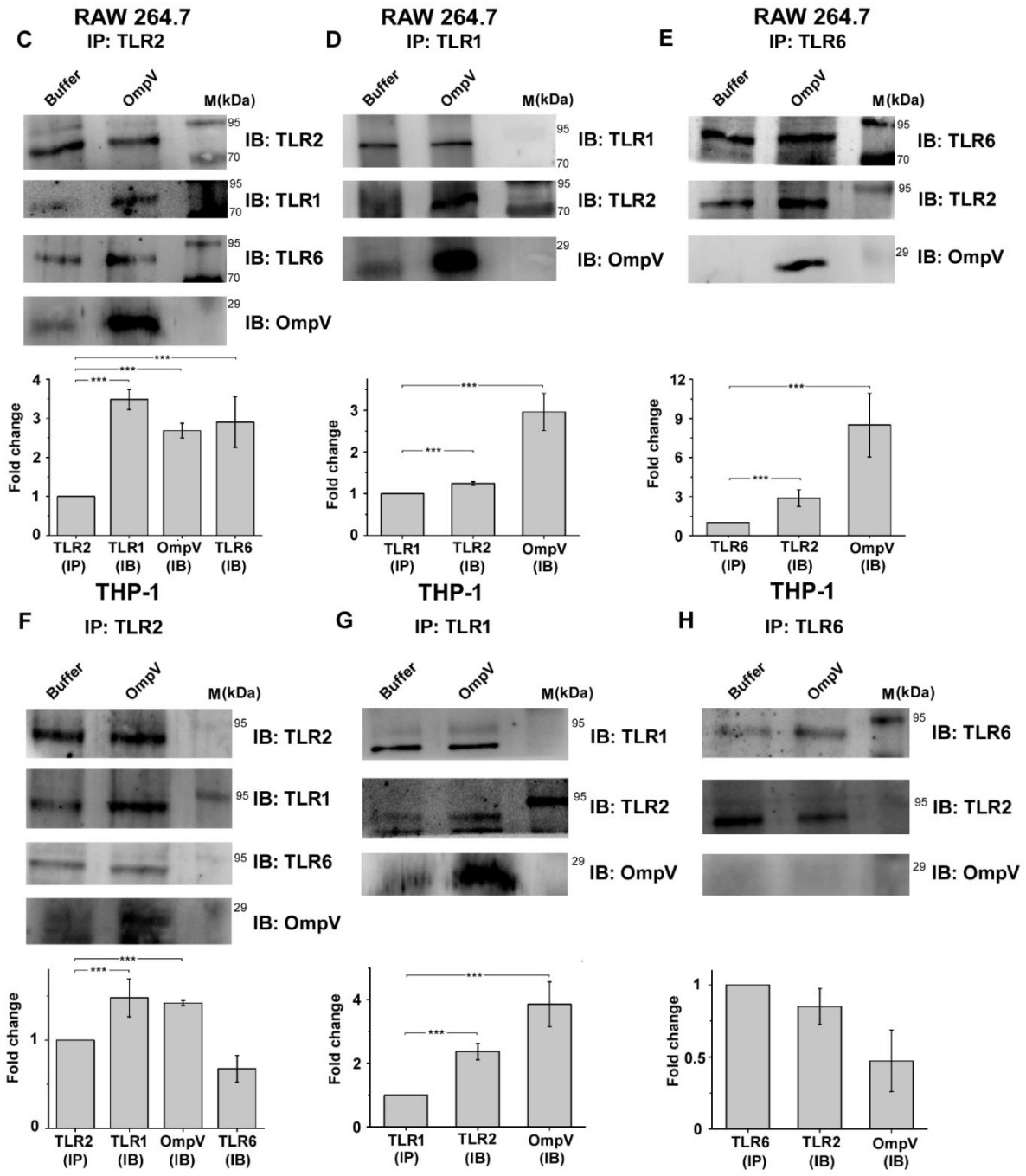


**Figure 41. OmpV is recognized by TLR1/TLR2 and TLR2/TLR6 heterodimer in RAW 264.7 macrophages and TLR1/TLR2 heterodimer in THP-1 monocytes**

OmpV induces increased surface expression of TLR1, TLR2 and TLR6 on RAW 264.7 macrophages (A) while TLR1 and TLR2 on THP-1 monocytes (B). OmpV, TLR1 and TLR6 co-immunoprecipitated with TLR2 in RAW 264.7 macrophages (C). OmpV and TLR2 co-immunoprecipitated with TLR1 in RAW 264.7 macrophages (D). OmpV and TLR2 co-immunoprecipitated with TLR6 in RAW 264.7 macrophages (E). OmpV, TLR1 and not TLR6 co-immunoprecipitated with TLR2 in THP-1 monocytes (F). OmpV and TLR2 co-immunoprecipitated with TLR1 in THP-1 monocytes (G). TLR2 and TLR6 doesn't form heterodimer for recognition of OmpV in THP-1 monocytes (H). Buffer treated cells were taken as control for co-immunoprecipitaion experiments. Bar graphs represent the densitometric analysis of western blots. Bar graphs are expressed as mean± SEM from three independent experiments (*p<0.05, **p<0.01, ***p<0.001 versus IP controls).

For further confirmation of the role of TLR2 in macrophages, we used neutralizing antibody against TLR2 in RAW 264.7 as well as we used bone marrow differentiated macrophages (BMDM) from TLR2$^{-/-}$ mice. In both the cases we observed a significant decrease in cytokine production (**Fig. 42A, B**) confirming involvement of TLR2 in OmpV recognition in macrophages. Further, to confirm the dimerizing partners of TLR2 in recognition of OmpV in macrophages, we knocked down TLR1 and TLR6 with siRNA in RAW 264.7 and activated with OmpV. Following activation, we observed a significant decrease in the pro-inflammatory signal in both TLR1 as well as TLR6 knock down cells as compared to the control confirming involvement of both TLR1 and TLR6 in recognition of OmpV along with TLR2 in macrophages (**Fig. 42C**). Knock-down of TLR2 and TLR6 was confirmed by checking surface expression using flow cytometry (**Fig. 42D**). These data suggested that both TLR1/TLR2 and TLR2/TLR6 hetero-dimer are involved in recognition of OmpV in macrophages.

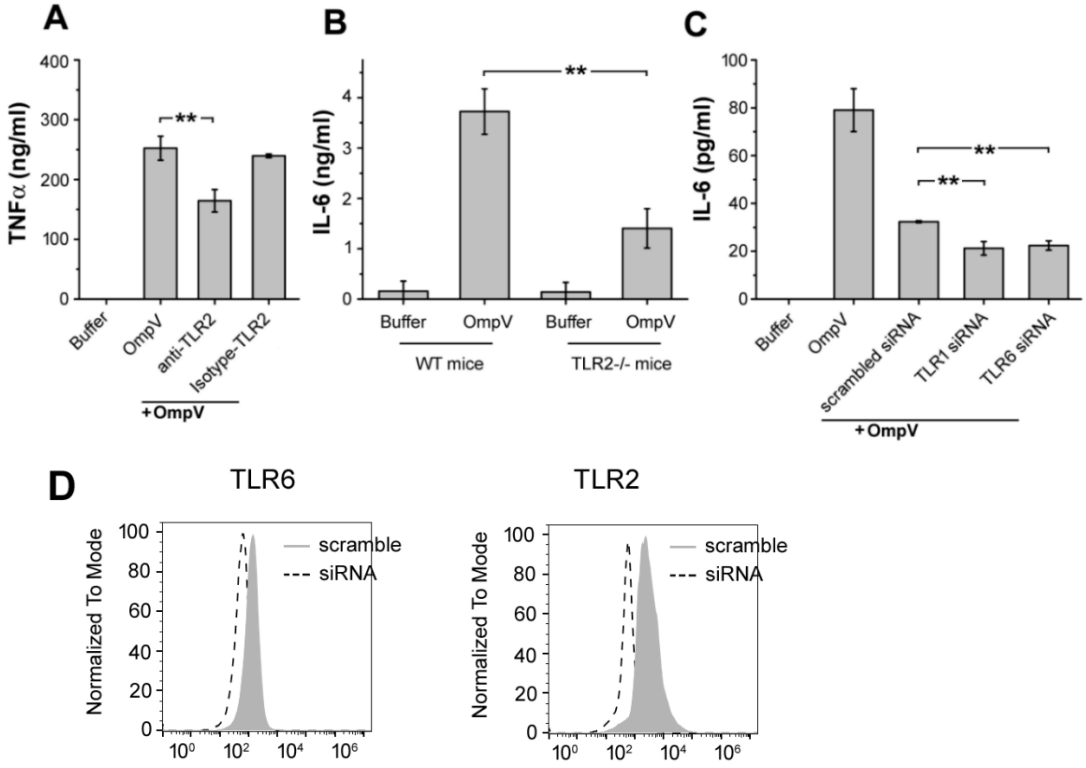


**Figure 42. TLR2/TLR1 and TLR2/TLR6 is involved in recognition of OmpV in RAW 264.7 macrophages**

Neutralization of TLR2 indicates its involvement in recognition of OmpV in RAW 264.7 macrophages (A). BMDMs from TLR2 -/- mice shows significant decrease in IL-6 production as compared to wild type mice treated with OmpV (B). A significant decrease in production of IL-6 was observed upon knock-down of TLR1 and TLR6 in RAW 264.7 macrophages. Non targeted (scrambled) siRNA was used as a negative control. Bar graphs are expressed as mean± SEM from three independent experiments (*p<0.05, **p<0.01, ***p<0.001, ns p>0.05 versus OmpV treated cells or wild type mice or scrambled siRNA). Knock-down mediated by siRNA was observed using flow cytometry (D).

Similarly, using neutralizing antibodies against TLR1, TLR2 and TLR6 in THP-1 monocytes we have observed that only TLR1 is involved along with TLR2 in recognition of OmpV, whereas, TLR6 is not involved (**Fig. 43A**). These data along with surface expression (**Fig. 41B**) and co-immunoprecipitation data (**Fig. 41F-H**) indicated that in monocytes, OmpV is recognized probably by TLR1/TLR2 heterodimer and there is no involvement of TLR2/TLR6 heterodimer. Further confirmation was achieved using shRNA-mediated knock down of TLR1, TLR2 and TLR6 (**Fig. 43B**). Knock down of TLRs was observed and quantified using western blotting and densitometry (**Fig. 43C-E**).

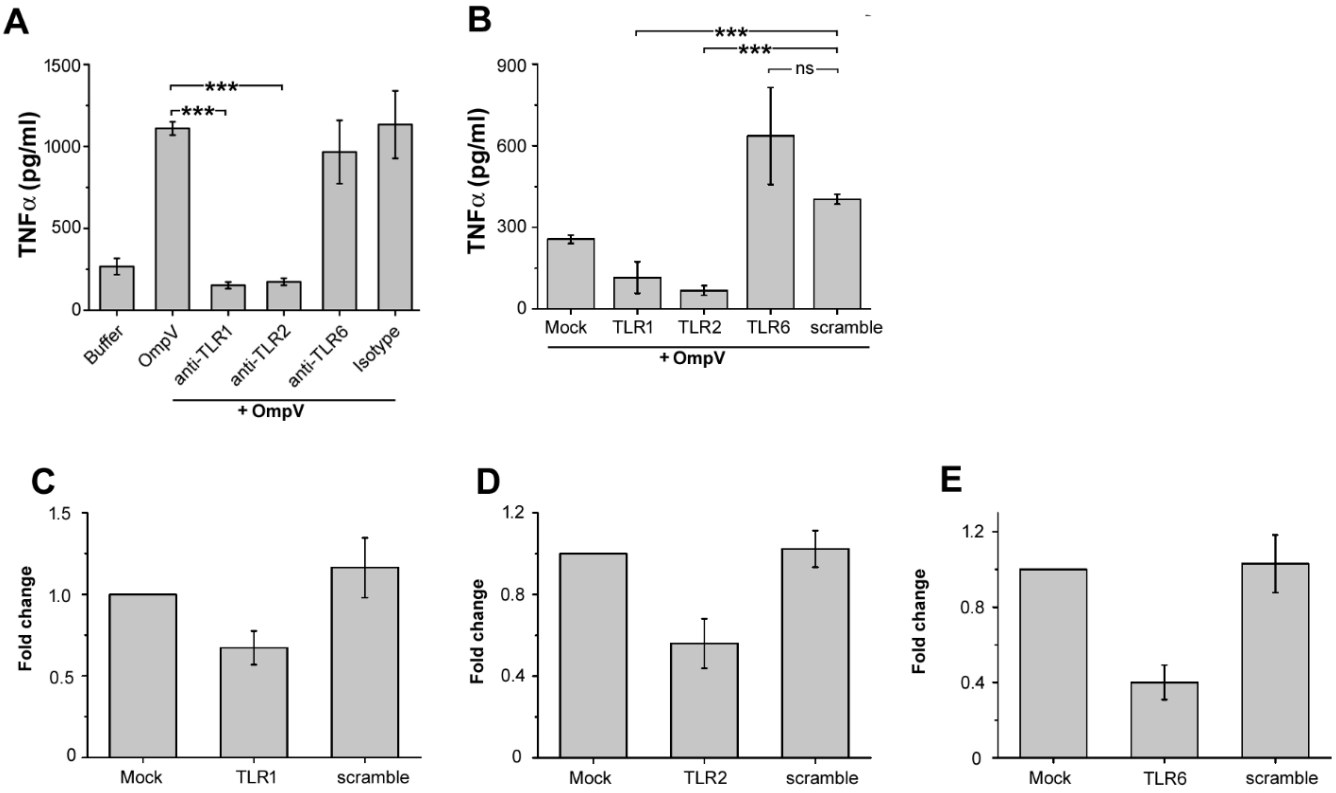


**Figure 43. TLR2/TLR1 is involved in recognition of OmpV in THP-1 monocytes**

Neutralization of TLR1 and TLR2 indicates their involvement in recognition of OmpV in THP-1 monocytes (A). Bar graphs are expressed as mean± SEM from three independent experiments. A significant decrease in production of TNFα was observed upon knock-down of TLR1 and TLR2 in THP-1 monocytes. Non targeted (scrambled) shRNA was used as a negative control. No decrease was observed in case of TLR6 knock-down (B). Bar graphs are expressed as mean± SEM from three independent experiments (*$p<0.05$, **$p<0.01$, ***$p<0.001$, ns $p>0.05$ versus OmpV treated cells or scrambled shRNA). Knock-down mediated by shRNA was observed using western blotting and quantified using densitometric analysis (C-E)

In intestinal epithelial cells neutralization experiment, shRNA-mediated knockdown experiment and co-immunoprecipitation experiment confirmed involvement of TLR2 in recognition of OmpV (**Fig. 44A-B; 44D-F**). Knock-down of TLRs was quantified using RT-PCR (**Fig. 44C**). Further, co-immunoprecipitation studies suggested that similar to macrophages in intestinal epithelial cell as well TLR2 probably makes hetero-dimer with both TLR1 and TLR6.

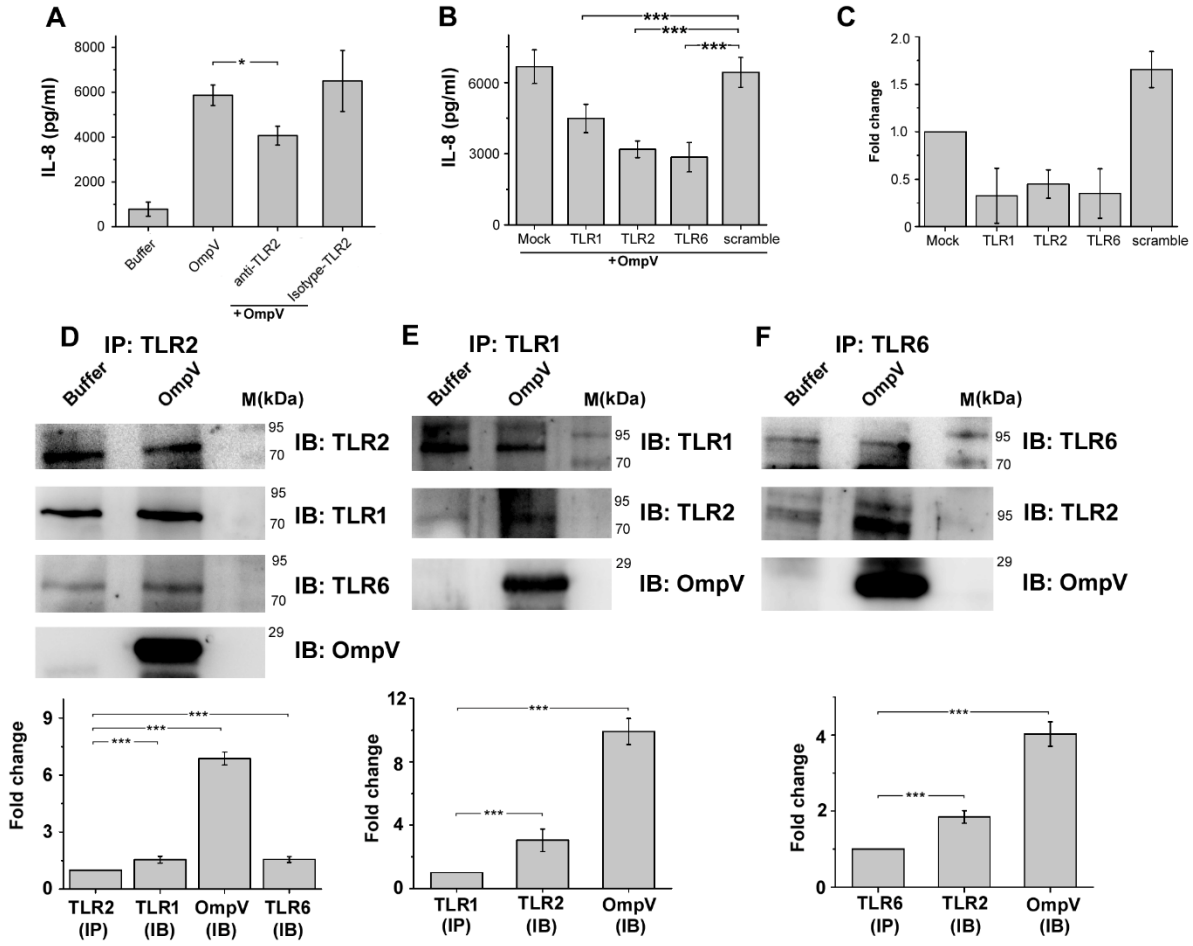


**Figure 44. TLR2/TLR1 and TLR2/TLR6 is involved in recognition of OmpV in IECs**

Neutralization of TLR2 indicates its involvement in recognition of OmpV in HT29 cells (A). A significant decrease in production of IL-8 was observed upon knock-down of TLR1, TLR2 and TLR6 in HT29 cells (B). Non-targeted (scrambled) shRNA was used as a negative control (B). Bar graphs are expressed as mean± SEM from three independent experiments (*p<0.05, **p<0.01, ***p<0.001, ns p>0.05 versus OmpV treated cells or scrambled shRNA). Knock-down mediated by shRNA was observed using RT-PCR (C). OmpV, TLR1 and TLR6 co-immunoprecipitated with TLR2 in HT29 cells (D). OmpV and TLR2 co-immunoprecipitated with TLR1 in HT29 cells (E). OmpV and TLR2 co-immunoprecipitated with TLR6 in HT29 cells (F). Buffer treated cells were taken as control for co-immunoprecipitaion experiments. Bar graphs represent the densitometric analysis of western blots. Bar graphs are expressed as mean± SEM from three independent experiments (*p<0.05, **p<0.01, ***p<0.001 versus IP controls).

Above observations with macrophages, monocytes and intestinal epithelial cells confirmed that TLR2 is mainly responsible for activation of innate immunity against OmpV.

**6.3.3 Objective 3:** To find out the signaling mediators involved in OmpV-mediated proinflammatory signaling

### 6.3.3.1 Downstream signaling of TLR activation by OmpV in innate immune cells involve MyD88 and IRAK-1

MyD88 is one of the major adaptor molecules recruited in the cytoplasmic tail of TLR2 (245). However, TLR2 could induce its signaling via MyD88-independent pathway as well (246,247), therefore, we checked whether MyD88 is involved in OmpV-mediated signaling. We observed that MyD88 co-immunoprecipitated with TLR2 in both OmpV-activated macrophages and monocytes (**Fig. 45A, B**). Further, the involvement of MyD88 was confirmed using BMDMs from MyD88$^{-/-}$ mice (**Fig. 45C**). For further signaling, MyD88 recruits IRAK-1/4 complex and activated IRAK-1 carry forward downstream signaling (248). Therefore, to investigate the involvement of IRAK-1 we used IRAK-1 inhibitor and observed a significant decrease in TNFα and IL-6 production following OmpV activation in cells pre-treated with the IRAK-1 inhibitor in both macrophages and monocytes (**Fig. 45D-G**) compared to the control. Furthermore, in intestinal epithelial cell HT29, we observed a significant decrease in IL-8 production with prior inhibition of IRAK-1 compared to the control cells (**Fig. 45H**). These results confirmed the involvement of both MyD88 and IRAK-1 in OmpV-mediated induction of innate immune responses. We observed a similar pattern upon proteoliposome treatment (**Fig. 45I-J**).

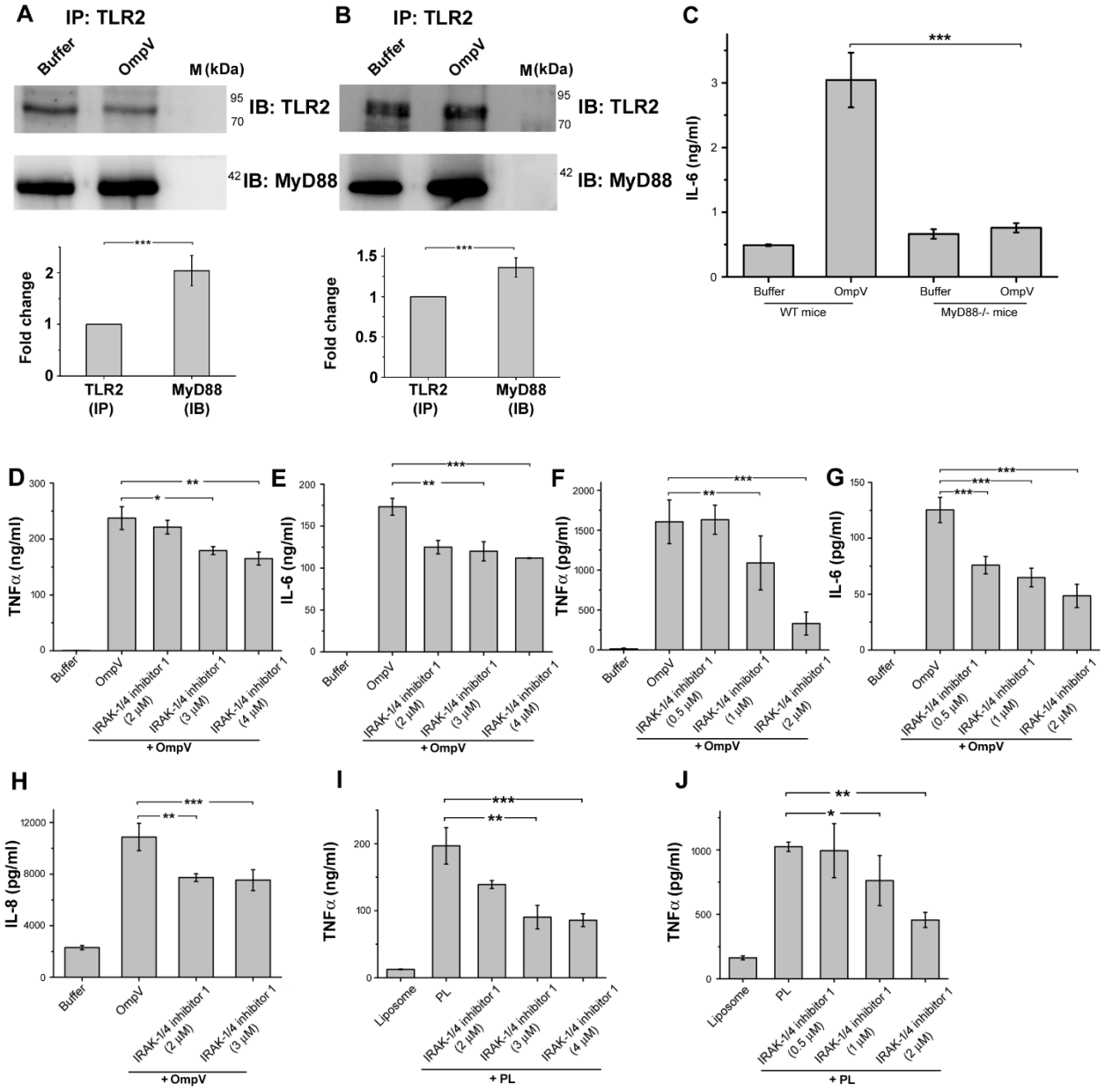


**Figure 45. MyD88 and IRAK is involved OmpV-mediated signaling in RAW 264.7 macrophages, THP-1 monocytes and IECs**

MyD88 is co-immunoprecipitated with TLR2 in RAW 264.7 macrophages (A) and THP-1 monocytes (B). Bar graphs represent the densitometric analysis of western blots. Bar graphs are expressed as mean± SEM from three independent experiments (*p<0.05, **p<0.01, ***p<0.001 versus IP controls). Buffer treated cells were taken as control. A significant decrease in IL-6 production was observed in case of BMDMs from MyD88 -/- mice as compared to wild type mice treated with OmpV (C). A significant decrease in TNFα and IL-6 was observed on pretreatment of IRAK inhibitor in RAW 264.7 (D, E) and THP-1 cells (F, G). A significant decrease in IL-8 was observed on pretreatment of IRAK inhibitor in HT29 cells (H). IRAK is involved in proteoliposome mediated signaling in RAW 264.7 (I) and THP-1 cells (J). Bar graphs are expressed as mean± SEM from three independent experiments (*p<0.05, **p<0.01, ***p<0.001, ns p>0.05 versus wild type mice or OmpV treated cells or PL treated cells).

### 6.3.3.2 Both NF-κB and AP-1 transcription factors are involved in OmpV-mediated activation of innate immune responses

Downstream signaling of PAMP-PRR interaction culminates in the activation of transcription factors. Majorly NF-κB and AP-1 transcription factors are involved in triggering of inflammatory responses (249). Therefore, we checked whether these transcription factors are involved in OmpV-mediated activation of innate immune responses. Using chemical inhibitors against NF-κB, we observed a significant decrease in production TNFα and IL-6 in both macrophages and monocytes (**Fig. 46A-D**) and IL-8 production by intestinal epithelial cells (**Fig. 46E**). These results indicated the involvement of NF-κB in OmpV-mediated pro-inflammatory signaling. Further, with proteoliposome treatment we observed similar response as the purified OmpV. Downstream signaling in proteoliposome-activated innate immune cells also involves NF-κB **(Fig. 46F, G).**

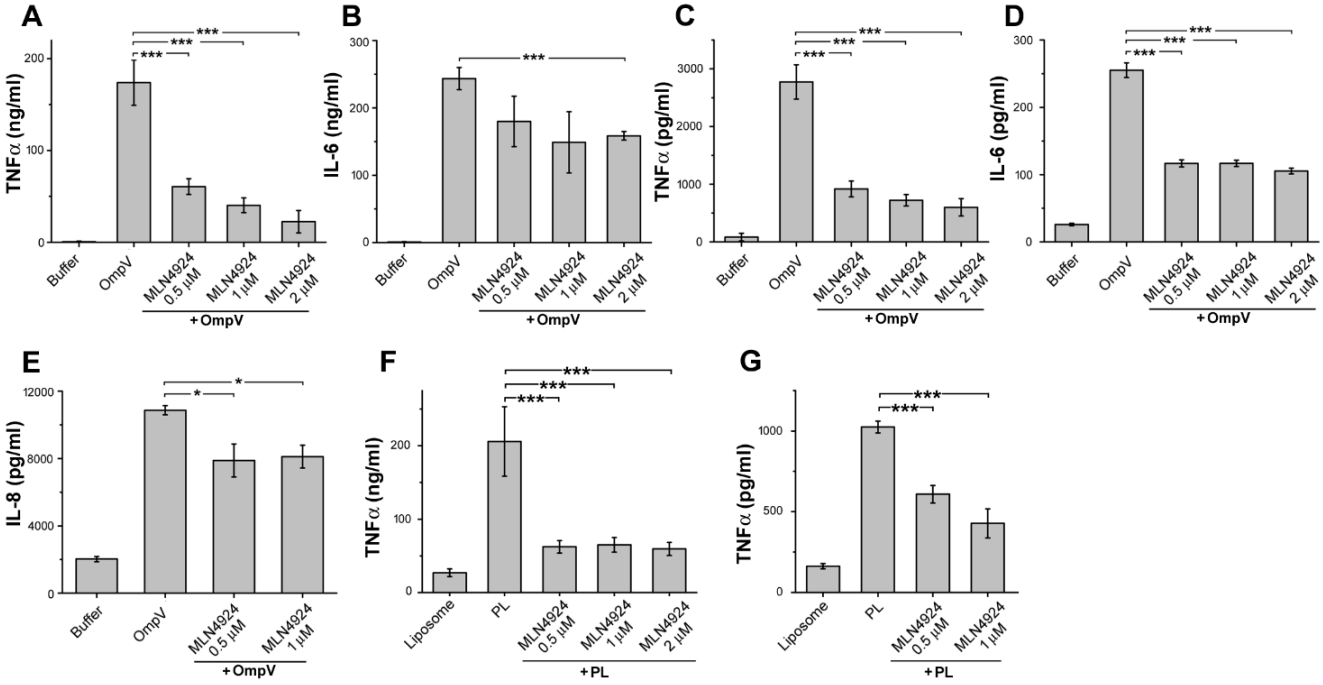


**Figure 46. NF-κB is involved OmpV-mediated signaling in RAW 264.7 macrophages, THP-1 monocytes and IECs**

A significant decrease in TNFα and IL-6 was observed on pretreatment of NF-κB inhibitor in RAW 264.7 (A, B) and THP-1 cells (C, D) and IL-8 in HT29 cells (E). NF-κB is also involved in proteoliposome mediated signaling in RAW 264.7 and THP-1 cells (F, G). Bar graphs are expressed as mean± SEM from three independent experiments (*p<0.05, **p<0.01, ***p<0.001, ns p>0.05 versus OmpV or PL treated cells).

It is known that NF-κB remains present in cytosol in inactivated state bound to inhibitor IκB. When IκB gets phosphorylated and degraded, NF-κB moves to the nucleus and leads to transcriptional upregulation of cytokine genes (250). Therefore, to further confirm the involvement of NF-κB in response to OmpV, we checked phosphorylation as well as degradation of IκB using western blots. We observed an increased phosphorylation (p-IκB) as well as degradation of IκB in both OmpV-activated RAW264.7 macrophages and THP-1 monocytes (**Fig. 47A**). Further, it was known that among 5 NF-κB family members p65 (REL-A), Rel-B or cRel are mainly involved in pro-inflammatory responses (251). Therefore, we checked the translocation of p65 and cRel subunits to the nucleus using western blots and we observed an increase in translocation of both p65 and cRel subunits in nuclear lysates with a corresponding decrease in the cytoplasmic lysate of both OmpV-activated RAW 264.7 macrophages and THP-1 monocytes (**Fig. 47B**).

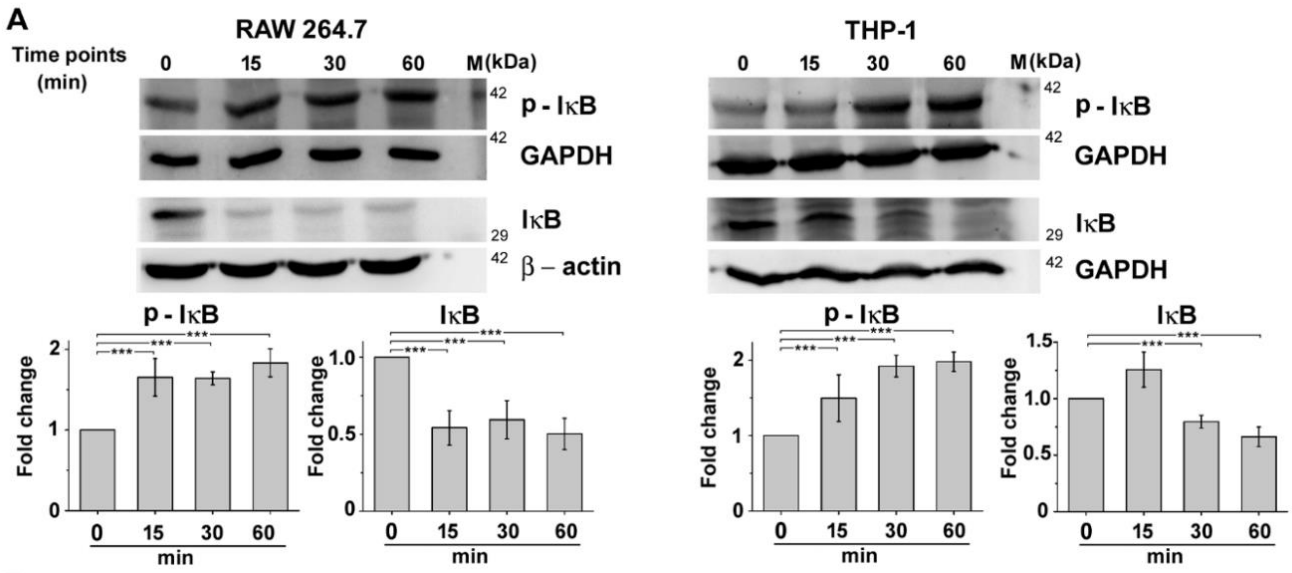

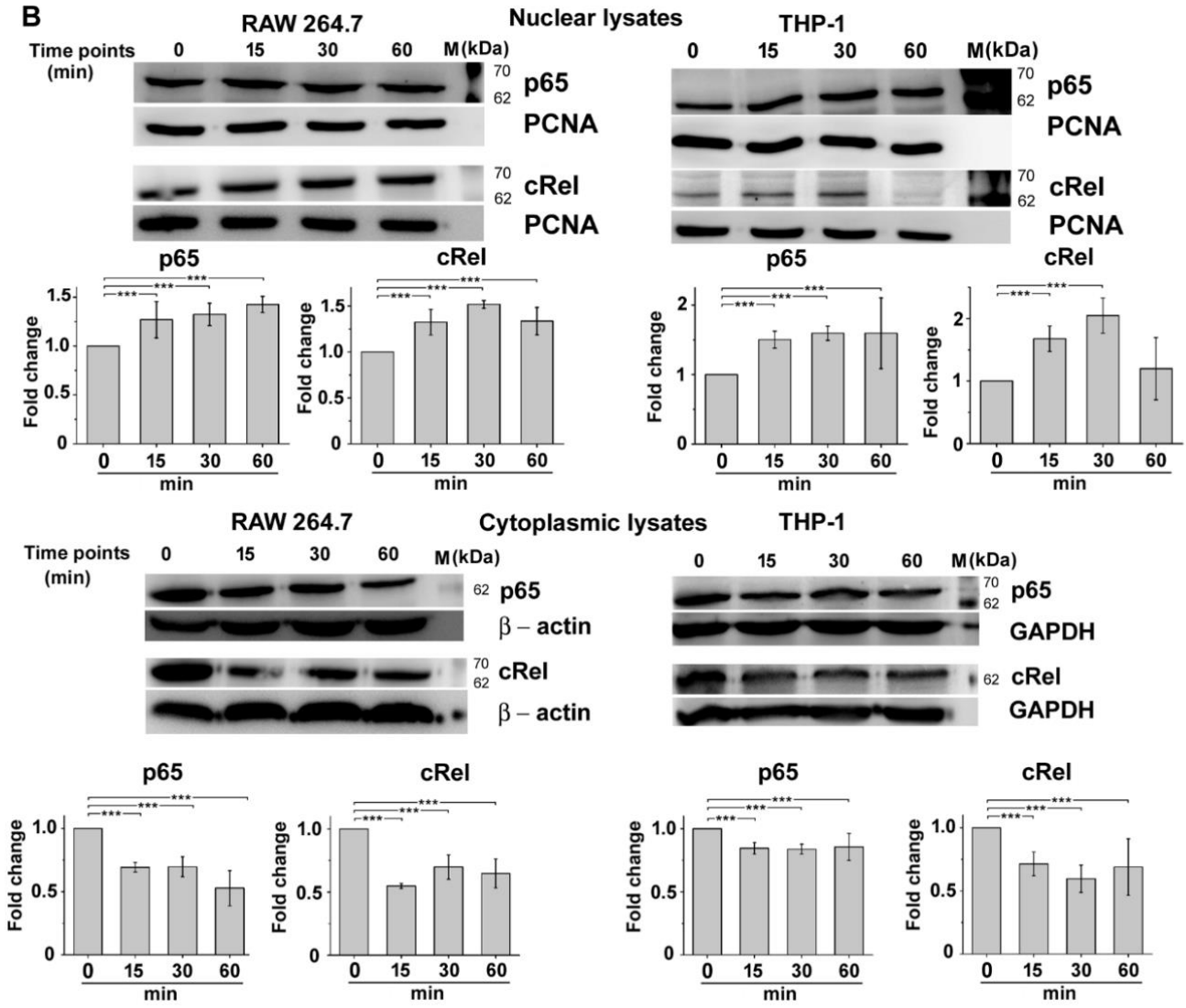


**Figure 47. OmpV treatment leads to NF-κB activation**

OmpV leads to phosphorylation and degradation of IκB in both RAW 264.7 and THP-1 cells (A). OmpV treatment leads to translocation of p65 and cRel subunits to nucleus from cytoplasm (B). GAPDH, β-actin and PCNA were taken as loading control. Bar graphs represent the densitometric analysis of western blots. Bar graphs are expressed as mean± SEM from three independent experiments (*p<0.05, **p<0.01, ***p<0.001 versus control).

Similar to NF-κB, with chemical inhibitor of AP-1 we observed that OmpV-mediated innate immune responses could involve AP-1 activation as well (**Fig. 48A-E**). Further, AP-1 is also composed of different family members. Out of these Jun and Fos family members mainly form heterodimers and are involved in transcriptional up-regulation of pro-inflammatory cytokine genes. We checked the presence of these family members into the nucleus of OmpV-activated macrophages and monocytes. We observed the presence of c-Fos, c-Jun and JunD subunits in

the nuclear lysate of OmpV-activated RAW 264.7 macrophages and c-Fos and c-Jun in case of THP-1 monocytes (**Fig. 48H**).

All these above results suggested the involvement of NF-κB and AP-1 in OmpV-mediated pro-inflammatory responses.

Further, with proteoliposome treatment we observed similar response as the purified OmpV. Downstream signaling in proteoliposome-activated innate immune cells also involves AP-1 (Fig. **48F, G**)

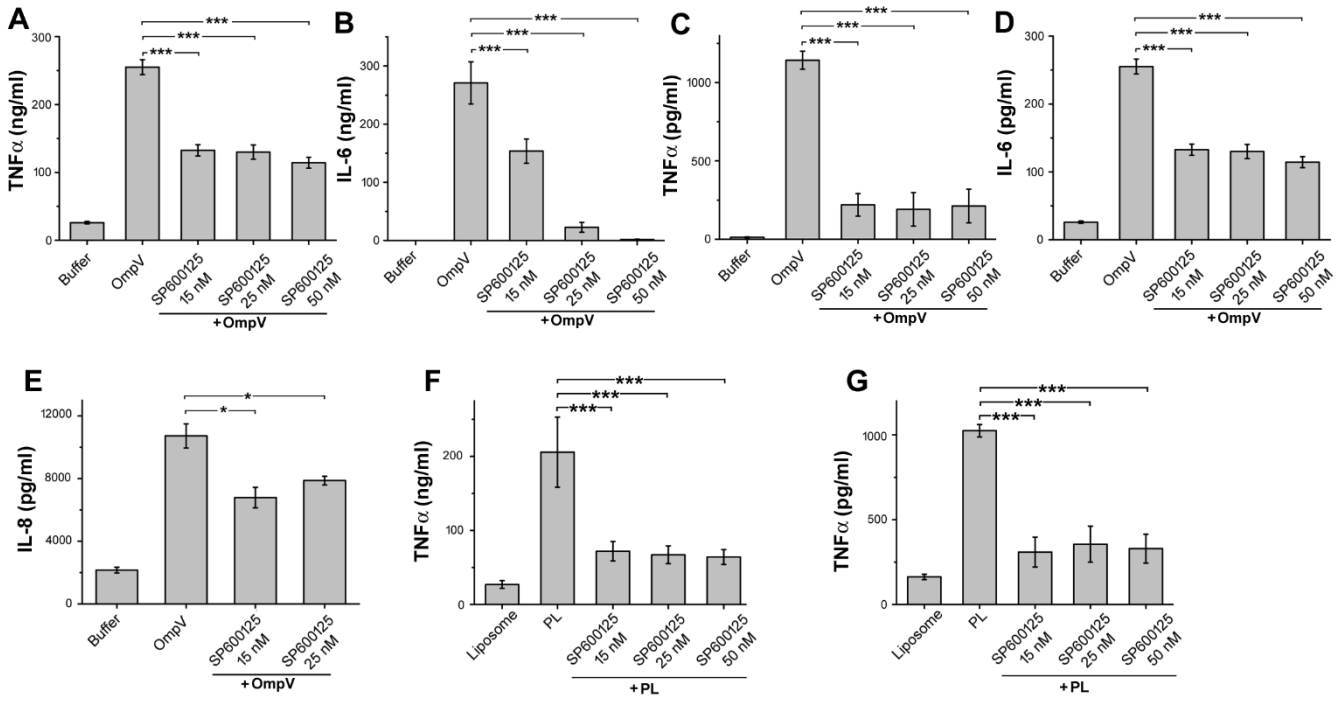

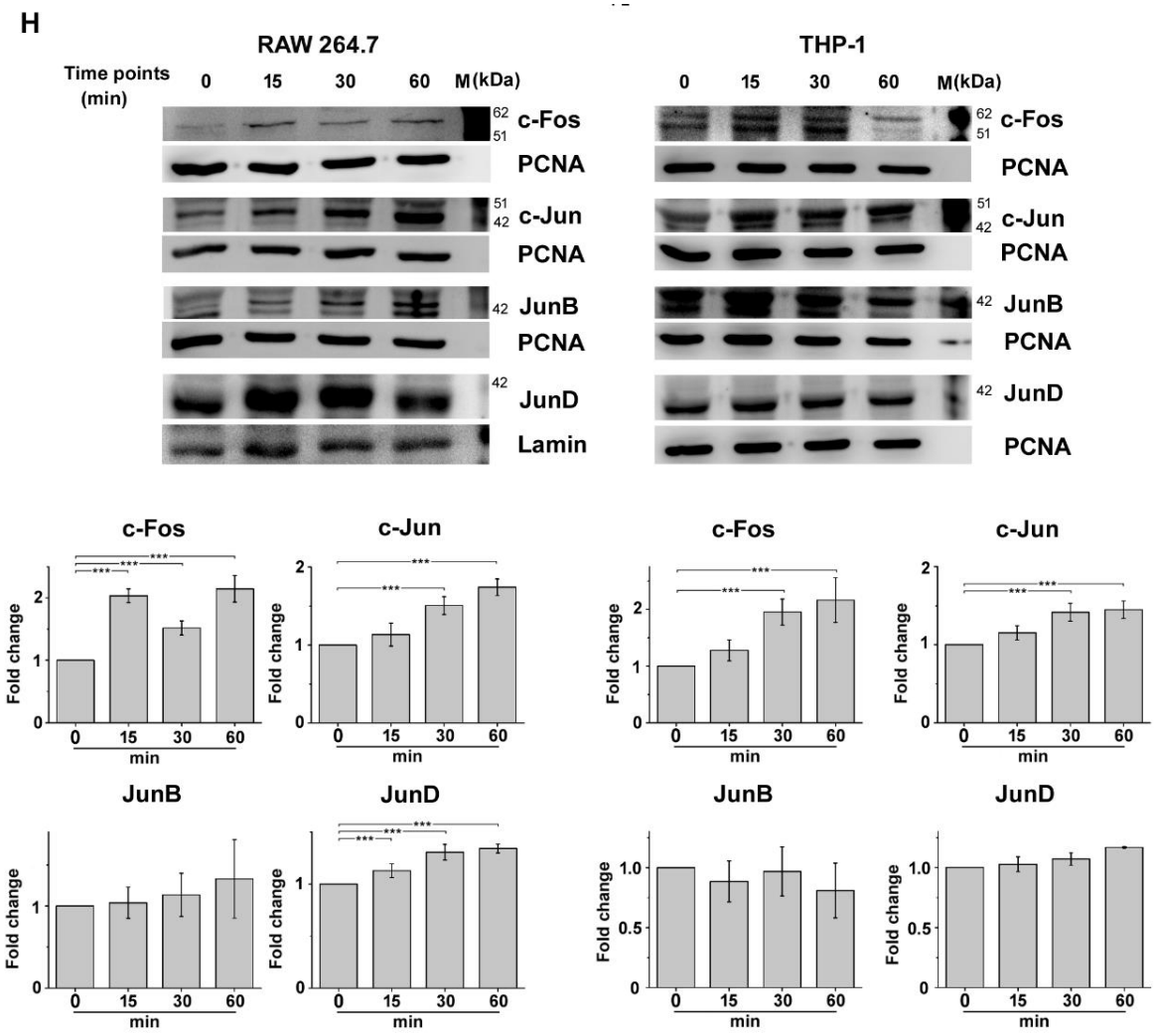


**Figure 48. AP-1 is involved OmpV-mediated signaling in RAW 264.7 macrophages, THP-1 monocytes and IECs**

A significant decrease in TNFα and IL-6 was observed on pretreatment of AP-1 inhibitor in RAW 264.7 (A, B) and THP-1 cells (C, D) and IL-8 in HT29 cells (E). AP-1 is also involved in proteoliposome-mediated signaling in RAW 264.7 (F) and THP-1 cells (G). Bar graphs are expressed as mean± SEM from three independent experiments (*p<0.05, **p<0.01, ***p<0.001, ns p>0.05 versus OmpV or proteoliposome treated cells). OmpV treatment leads to translocation of AP-1 subunits to nucleus (H). PCNA and lamin was taken as loading control for nuclear lysates. Bar graphs represent the densitometric analysis of western blots. Bar graphs are expressed as mean± SEM from three independent experiments (*p<0.05, **p<0.01, ***p<0.001 versus control).

### 6.3.3.3 Involvement of p38 and JNK in OmpV-mediated signaling

Activation of AP-1 transcription factor happens through the activation of upstream MAP-kinases (252). Therefore, OmpV-mediated activation of AP-1 suggested that OmpV can activate MAP-kinase cascades in innate immune cells. Towards this we have used

pharmacological inhibitors against p38 and JNK MAPKs. We have observed a significant decrease in TNFα and IL-6 production in both macrophages (**Fig. 49A, B, F, H, I, M**) and monocytes (**Fig. 49C, D, G, J, K, N**) and IL-8 production by HT29 (**Fig. 49E, L**) in presence of both JNK and p38 inhibitor upon activation with both purified OmpV and proteoliposome, suggesting their involvement in OmpV-activated innate immune cells.

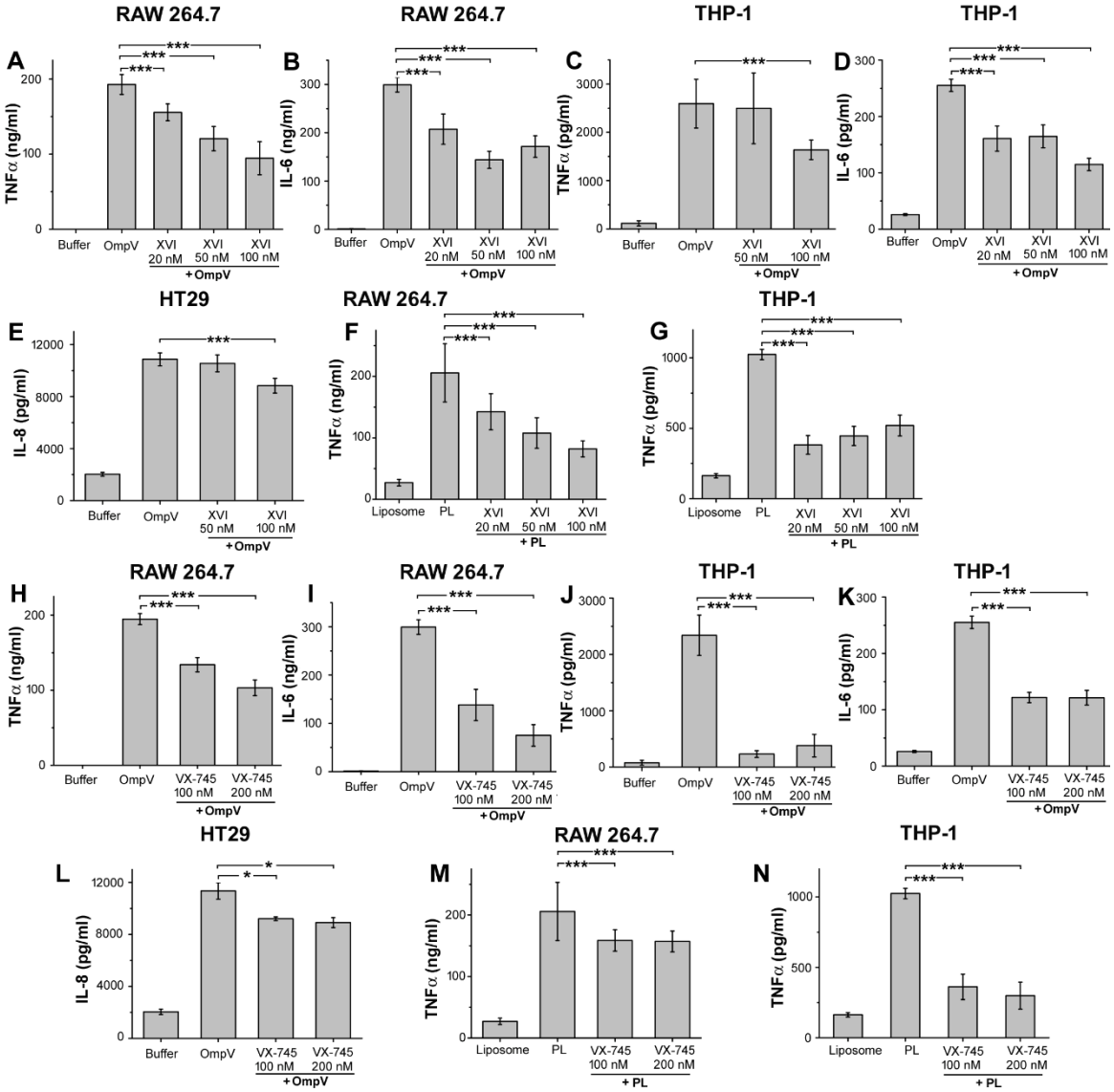


**Figure 49. p38 and JNK are involved OmpV-mediated signaling in RAW 264.7 macrophages, THP-1 monocytes and IECs**

A significant decrease in TNFα and IL-6 was observed on pretreatment of JNK inhibitor in RAW 264.7 (A, B) and THP-1 cells (C, D) and IL-8 in HT29 cells (E). JNK is involved in proteoliposome mediated signaling in RAW 264.7 (F) and THP-1 cells (G). A significant decrease in TNFα and IL-6 was observed on pretreatment of p38 inhibitor in RAW 264.7 (H, I) and THP-1 cells (J, K) and IL-8 in HT29 cells (L). p38 is involved in proteoliposome mediated signaling in RAW 264.7 (M) and THP-1 cells (N). Bar graphs are expressed as mean± SEM from three independent experiments (*p<0.05, **p<0.01, ***p<0.001, ns p>0.05 versus OmpV or proteoliposome treated cells).

Further, we have checked phosphorylated status which is indicative of activation status of p38 and JNK MAPKs. We have observed an increase in phosphorylation of both JNK and p38 (**Fig. 50A, B**) upon OmpV treatment.

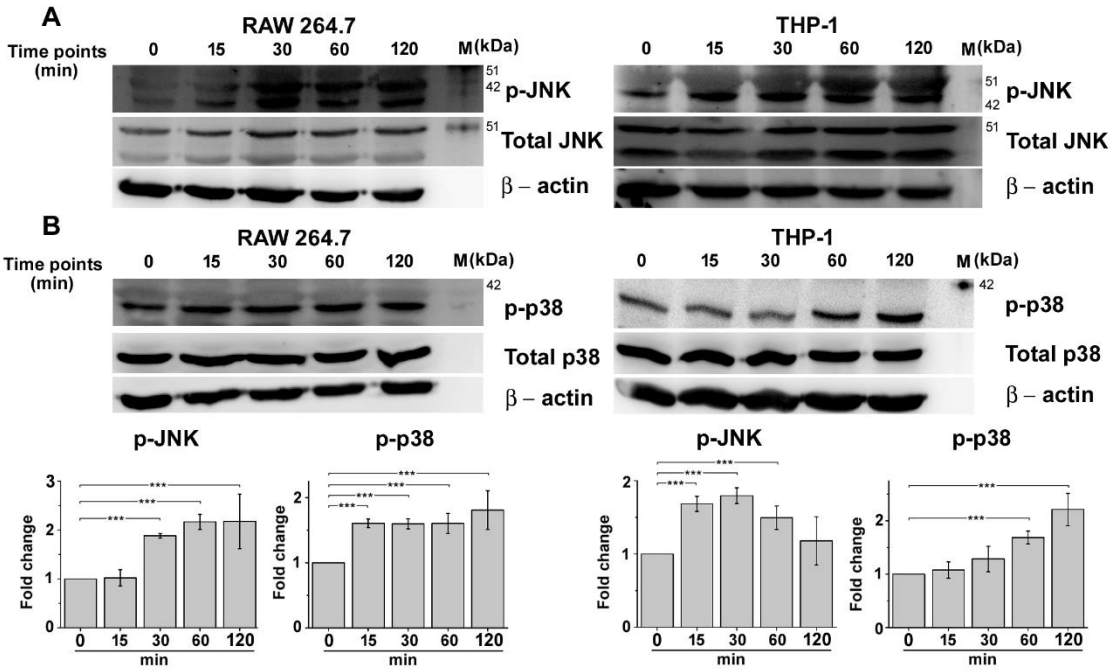


**Figure 50. OmpV induces phosphorylation of JNK and p38 in RAW 264.7 macrophages, THP-1 monocytes and IECs**

OmpV treatment leads to phosphorylation of JNK (A) and p38 (B). β-actin was used as loading control. Bar graphs represent the densitometric analysis of western blots. Bar graphs are expressed as mean± SEM from three independent experiments (*p<0.05, **p<0.01, ***p<0.001 versus control).

Above results suggested that induction of OmpV-mediated innate immune responses involves MAP-kinase activation.

## 6.4 Conclusion

In the previous chapter, OmpV was observed to activate adaptive immune responses. As innate immune responses are the first line of defense and is a prerequisite to activate adaptive immune responses, we further checked the modulation of innate immune responses by OmpV. To proceed with this, we used macrophages, monocytes, and intestinal epithelial cells. Upon treatment of these cells with recombinant OmpV, we observed significant production of proinflammatory cytokines. Also, we found that OmpV doesn't cause significant cell death up to 2 µg/ml (**Fig. 38**). Therefore, we used this 2 µg/ml concentration for further experiments. During time course studies, we found a time-dependent increase in the production of proinflammatory mediators in response to OmpV except for TNFα production in THP-1 monocytes where it was maximally produced at 4 h (**Fig. 39**). In addition to recombinant OmpV, we also checked production of proinflammatory mediators in response to OmpV-incorporated proteoliposome (OmpV-proteoliposome). Here, we found that OmpV-proteoliposome induces similar pro-inflammatory responses compared to recombinant OmpV (**Fig. 40**). Towards finding out the receptor involved in recognition of OmpV, we observed that OmpV is recognized by both TLR1/2 and TLR2/6 heterodimers in macrophages and intestinal epithelial cells whereas in monocytes, only by TLR1/2 heterodimer (**Fig. 41- 44**). As the TLR-dependent pathway can either be MyD88 dependent or independent, we further observed that OmpV-mediated signaling is MyD88-dependent (**Fig. 45**). Further, downstream signaling involves MAPKs and NF-κB and AP-1 transcription factors (**Fig. 46-50**).

# IV.
# Discussion

## 7.1 Discussion

*S.* Typhimurium is one of the major causes of salmonellosis across the globe. There is no vaccine available against *S.* Typhimurium yet, and antibiotics are the only mode of treatment. But due to increase in the prevalence of antibiotic-resistant strains of *S.* Typhimurium, treatment has become complicated (253,254). The unavailability of any appropriate treatment thus emphasizes the need to study the pathogenesis of *S.* Typhimurium in detail to find out new vaccine candidates.

*S.* Typhimurium enters the human body through contaminated food and water. On reaching the intestine, it adheres to intestinal epithelial cells from the apical side. In addition, it crosses the epithelial layer through microfold cells, i.e., M cells (255). After crossing the intestinal epithelial layer, *Salmonella* adheres to the basolateral side of intestinal epithelial cells. Extracellular matrix (ECM) components such as collagen, fibronectin and laminin present at the basolateral side are majorly responsible for mediating adhesion from the basolateral side. Adhesins of bacteria are known to bind to integrins present on the basolateral side through these ECM components. These extracellular matrix components thus play a prime role in the colonization of bacteria in the gut region.

After adhering to intestinal epithelial cells, the next step in the pathogenesis of bacteria is invasion. *Salmonella* can invade intestinal epithelial cells through both trigger and zipper mechanisms. The apical invasion through a trigger mechanism induced by T3SS-1 is long known phenomenon; however, the basolateral invasion through the zipper mechanism has been identified recently to be used by Rck protein (139). PagN is also known to mediate adhesion and invasion by interacting with proteoglycan (144). Apart from this, even in the absence of T3SS-1, Rck and PagN, *Salmonella* can still invade the cells indicating the involvement of other factors (145). The most common receptors known to be involved in the zipper mechanism are integrins that bind to bacterial proteins either directly or through ECM components.

Being a gram-negative bacterium, *S.* Typhimurium has an additional outer membrane, which is majorly composed of lipopolysaccharides (LPS) and outer membrane proteins. These outer membrane proteins play a major role in the pathogenesis of bacteria as they are the first ones to come in contact with the host.

In this study, we characterized one such outer membrane protein OmpV of *S.* Typhimurium. Towards this, we recombinantly expressed OmpV protein in *E. coli,* and then purified from inclusion body (**Fig. 1**) using Ni-NTA chromatography (**Fig. 2**). As the protein structure is not solved earlier, we further performed homology modeling of this protein, which revealed presence of β-sheets (**Fig. 3**). Further circular dichroism (CD) spectra of recombinant protein also showed β-sheets, which hints towards proper refolding of the protein (**Fig. 4**). The proper refolding was further confirmed using tryptophan fluorescence assay and ANS binding assay of the protein (**Fig. 5**). Further, to check the presence of aggregates in refolded protein, we additionally performed size exclusion chromatography. The absence of any peak in void volume confirms the absence of aggregates in refolded protein (**Fig. 6**). Further, we did a liposome swelling assay to check whether OmpV is porin in nature. The results indicated that OmpV is not a porin (**Fig. 7**).

Towards characterizing the role of OmpV in the pathogenesis of *S.* Typhimurium, we constructed *ompV* deletion mutant as well as complemented strain. The deletion of *ompV* was checked at the gene level using PCR (**Fig. 8**) as well as at the protein level using western blot (**Fig. 9**). Moreover, we expressed *S.* Typhimurium OmpV in the outer membrane of *E. coli* using the signal peptide. To check the protein expression, the outer membrane was isolated, and OmpV was probed using western blot (**Fig. 10**). Moreover, flow cytometry analysis also indicated an equal amount of OmpV in the outer membrane of *E. coli* compared to *S.* Typhimurium (**Fig. 11**).

As discussed earlier, both adhesion and invasion are crucial steps for establishing bacteria in host cells. Adhesion, the first step in the pathogenesis of bacteria, is majorly mediated by the adhesins. Using OmpV deletion mutant (Δ*ompV*) we observed a significant decrease in the invasion and adherence of *S.* Typhimurium to the IECs compared to the wild type bacteria (**Fig. 12**). Also, microscopy data further confirmed the decreased adhesion of Δ*ompV* mutant to IECs (**Fig. 13**). To further establish the role of OmpV in adhesion, we have used Δ*spi1* mutant of *S.* Typhimurium, as SPI-1 is known to play a role in the invasion but not in adhesion. When IECs were infected with Δ*spi1*, a decrease in invasion was observed while there was no difference in adhesion compared to the wild type bacteria (**Fig. 14**). But, in a double mutant Δ*spi1*Δ*ompV*, where *ompV* was deleted in Δ*spi1* background, we observed a significant decrease in adhesion as compared to only Δ*spi1* mutant and wild type control, confirming the notion that OmpV is

a major factor that helps in adhering *S.* Typhimurium to the intestinal epithelial cells (**Fig. 14**). Moreover, to study the potential of purified OmpV to bind IECs, we further checked the binding of purified OmpV with IECs. Here we found that purified OmpV can bind to IECs in a dose-dependent manner (**Fig. 15**). Pretreatment of purified OmpV leads to neutralization of OmpV receptors, resulting in competitive inhibition in the binding of *S.* Typhimurium to these IECs (**Fig. 16**). Furthermore, *S.* Typhimurium OmpV was expressed in the outer membrane of a non-pathogenic strain of *E. coli* (*E. coli*-OmpV) which otherwise does not adhere to intestinal epithelial cells. We used *E. coli*-OmpV to check whether OmpV can drive whole bacteria to bind to IECs. Here, we found out that *E. coli*-OmpV can bind to IECs, interpreting that OmpV alone can act as an adhesion (**Fig. 17**).

So far, we observed that OmpV plays a crucial role in adhesion during *in vitro* experiments. To check the potential of OmpV in *in vivo* conditions, we further infected mice with wild type and *ompV* deletion strain of *S.* Typhimurium. Here we observed about seven fold higher $LD_{50}$ dose of the Δ*ompV* strain than wild type strain. Further, using competitive index assay we observed lesser colonization of Δ*ompV* strain in different organs such as spleen, liver and intestine compared to the wild type strain in infected mice suggesting the critical role of OmpV in the disease development (**Fig. 18**).

Our studies in both *in vivo* and *in vitro* conditions established the role of OmpV in pathogenesis of *S.* Typhimurium. OmpV plays a crucial role in adhesion of bacteria to IECs. Further, we aimed to probe the receptor of OmpV present on the surface of IECs. Earlier in adhesion experiment with Giemsa staining, we observed that *S.* Typhimurium seems to bind to the extracellular matrix (ECM) (**Fig. 16**). Therefore, we checked whether OmpV can bind to any component of ECM. Using purified OmpV and ECM proteins, we found that OmpV binds to the ECM component fibronectin (**Fig. 19**). This binding was also confirmed using co-immunoprecipitation assay and colocalization study (**Fig. 19**). The decrease in binding Δ*ompV* to fibronectin compared to wild type bacteria also supports the notion that OmpV binds to fibronectin (**Fig. 20**). We further found that *E. coli* expressing *S.* Typhimurium OmpV also can bind to fibronectin (**Fig. 20**). Upon neutralization of IECs with fibronectin, binding of both *S.* Typhimurium and *E. coli*-OmpV was decreased. This result indicated that OmpV binds IECs in a fibronectin-dependent manner and acts as one of the major adhesins of *S.* Typhimurium (**Fig. 20**). To rule out the assumption, that protein treatment might be non-specifically decreasing the binding of *S.* Typhimurium to fibronectin and thus IECs, we also used controls

like OmpC protein (outer membrane protein of non-pathogenic *E. coli*) for negative control and *Vibrio vulnificus* bacteria that is reported to bind to fibronectin as positive control (183). Here we observed that OmpC could not decrease the binding of *S.* Typhimurium or *V. vulnificus* to fibronectin. OmpV specifically reduces binding of *S.* Typhimurium and not *V. vulnificus* (**Fig. 21)**. Thus, our study strongly suggests that OmpV helps in adhesion of *S.* Typhimurium to IECs through fibronectin.

Out of receptors present on the surface of IECs, integrins mostly bind through ECM components. As OmpV is binding to fibronectin, it makes integrin the most probable candidate to act as its receptor. After probing for different integrin subunits, we found that OmpV binds to α1β1 integrin (**Fig. 22-24**). This binding was confirmed using GST pull down (**Fig. 22-23**), colocalization studies (**Fig. 24**) as well as knockdown studies using siRNA and shRNA (**Fig. 22-23**). Adhesins of gram-negative bacteria are known to bind to integrins either directly or through ECM components. For example, *Yersinia* is known to express two outer membrane adhesins, invasin and YadA. Out of these, invasin binds to β1 integrin directly whereas, YadA binds through extracellular matrix (ECM) components (256). Similarly, in *Campylobacter jejuni*, CadF and FlpA bind to integrins through fibronectin (257). Also, in case of *Bartonella*, *Bhe* interacts with integrin β1 in a fibronectin dependent manner (258). Moreover, in the case of *Staphylococcus aureus* that is a gram-positive bacterium, ClfA adhesin binds to integrins through fibronectin (259). So, we further investigated whether OmpV can bind to integrins directly or through fibronectin. The dot blot results revealed that the binding of OmpV and α1β1 integrin is dependent on fibronectin (**Fig. 25**). It was known for some time that fibronectin is crucial for adherence of *S.* Typhimurium (182,260). Our study indicated that probably one of the critical need of fibronectin in *S.* Typhimurium infection is due to OmpV, which is one of the major adhesins of *S.* Typhimurium that help bacteria in binding to integrins present on basolateral surface through fibronectin.

Many other adhesins, including 13 fimbrial and 7 nonfimbrial adhesins are already known to play a role *S.* Typhimurium infection (87). So, the question is why the bacteria need so many adhesins. IECs are polarized into the apical side with brush border membrane facing the intestinal lumen, and the basolateral side. At the luminal side intestinal epithelial layer remains covered with mucus. The mucus layer and the tight junctions between the epithelial cells keep the basolateral side almost entirely inaccessible to an invading pathogen. However, the M cells present in the intestinal epithelial layer helps *Salmonella* to get access to the basolateral side

(132). *Salmonella,* upon entry through the oral route, adhere to the mucus layer, transcytose through the M cells, and then get exposed to the basolateral side of the intestinal epithelial cells and adhere to it. Adhesion is followed by invasion and ultimately disruption of the intestinal epithelial layer destroying the mechanical barrier and exposing the body tissue for further infection.

As adhesion is the first step of the pathogenesis, the complexity of the invasion process suggests that the adhesins are necessary for adhesion in the multiple steps of infection. First, adhesins are needed to adhere to the mucosal layer at the luminal side of the intestine and then adhere to the basolateral side of the intestinal epithelial cells. The fimbrial adhesins bind to the glycoproteins and mediates initial adhesion of *S.* Typhimurium to the mucus layer. Some fimbrial adhesins can also bind to ECM expressed at the apical side by adenosine produced due to inflammation. OmpV is a non-fimbrial adhesin. Other non-fimbrial adhesins such as BapA, SadA, SiiE, Rck, PagN, MisL and ShdA are known to mediate adhesion from basolateral side through ECM components. Among these, MisL and ShdA are reported to bind to fibronectin, but they are only expressed when the bacterium is present in the caecum region (93,94) . Therefore, they are probably required for binding to fibronectin in the caecum region.

The presence of different adhesins for colonization at every step indicates their importance in the virulence of *Salmonella*. However, the dependence of these adhesins on each other is not well studied. Whatsoever, the difference in the spatio-temporal expression and function indicates that each of the adhesins has a specialized role in the virulence mechanism of the bacteria.

Apart from adhesion, the adhesins can also mediate translocation of effectors into the host cells by acting as a receptor for secretion needle. One such example is CagL of *Helicobacter pylori* that binds to β1 integrin followed by injection of CagA effector protein (186) . So, we further studied whether OmpV can also act as a receptor for the type III secretion needle. Here we couldn't observe any difference in translocation of effector proteins in the absence of OmpV (**Fig. 26)**. This result gives a hint that OmpV is not acting as receptor for type III secretion needle and the decrease in invasion observed in OmpV-deficient strain might be a result of decreased adhesion of bacteria.

Apart from this, CagL was also observed to activate FAK and Src, thus leading to F-actin modulation (187,261). Our study indicated that OmpV can activate α1β1 integrin leading to intracellular FAK phosphorylation (**Fig. 27, 28**) and F-actin modulation (**Fig. 29**). Thus, our study indicated that apart from acting as an adhesin, OmpV also plays a role in F-actin modulation and ruffle formation which is the prerequisite for *S.* Typhimurium invasion to the epithelial cells. Due to its adhesion and invasion role, OmpV thus plays an essential role in the pathogenicity of *S.* Typhimurium in mice (**Illustration 22)**.

Our study demonstrated for the first time that a MipA family protein can act as an adhesin. Only one previous report has suggested that the antibody against MipA protein can block adhesion of the enterohaemorrhagic *E. coli* (262) . Also, our results for the first time showed that an outer membrane protein can activate α1β1 integrin through fibronectin. In most of the studies, collagen and laminin are involved in recognition by α1β1 integrin, and fibronectin is involved mostly in the recognition by α5β1, α8β1, αvβ1, αvβ3 and αvβ6 integrin receptors (179). Fabbri *et al.* in 1996 published a report showing that fibronectin can bind to α1β1 integrin (263), but no ligand has been reported to date that can lead to such modulation.

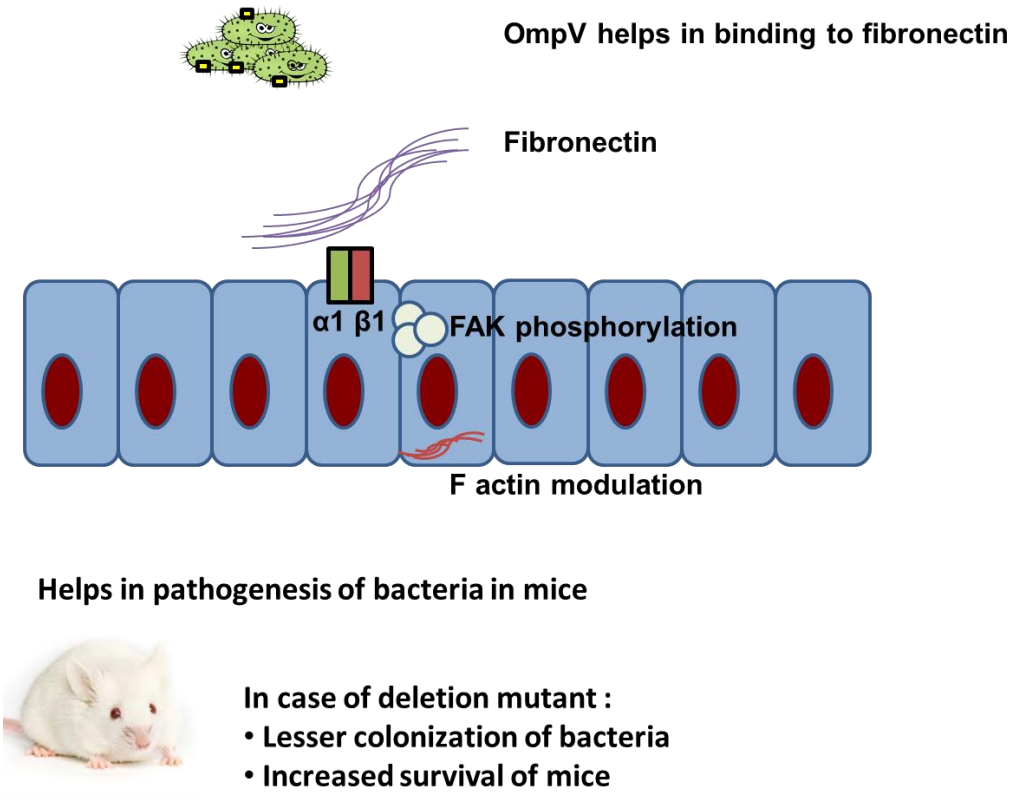


**Illustration 22**: Summary showing the role of OmpV in adhesion of *S.* Typhimurium to IECs

As OmpV plays a vital role in the pathogenesis of *S.* Typhimurium, we further probed whether OmpV can act as a vaccine candidate against *S.* Typhimurium infection. Activation of the immune system, antibody production and protection against disease are major roles of an ideal vaccine candidate (112). Therefore, we first probed whether OmpV immunization can evoke immune system and give protection against *S.* Typhimurium infection in mice. As *S.* Typhimurium causes gastro-intestinal infection, salmonellosis in humans and typhoid-like systemic disease in mice, we evaluated the protection both in case of gastro-intestinal and systemic infection of *S.* Typhimurium. Here, we observed that intraperitoneal immunization could provide protection against systemic infection but not gastro-intestinal infection of *S.* Typhimurium (**Fig. 30).** Further, protection against gastro-intestinal infection of *S.* Typhimurium was observed when mice were immunized orally with OmpV-proteoliposome (**Fig. 30).** B cells play a major role in evoking protective immune response as they lead to antibody production. Therefore, we further investigated whether OmpV immunization can induce antibody production. We found a significant IgG production in response to intraperitoneal immunization of mice with OmpV, whereas no IgA was observed in this case (**Fig. 31)**. In literature, IgG is reported to protect against systemic infection as it is present in serum, whereas IgA protect against gastro-intestinal infection as it can cross the intestinal epithelial layer and moves to the lumen to block the initial establishment of bacteria. During intraperitoneal immunization of OmpV, no IgA was found, which could be the reason behind the absence of any protection against gastro-intestinal infection in this case (**Fig. 30**). As IgA is produced more during mucosal immunization, we further immunized mice orally with OmpV-proteoliposome. In this case, we observed high IgA production (**Fig. 31),** which might be the reason for protection against gastro-intestinal infection (**Fig. 30**).

So far, we observed IgG and IgA production, which indicated that OmpV can activate B cells (**Fig. 31**). However, antibody production by B cells require T helper cells (Th1 or Th2), which in turn are activated by antigen-presenting cells, such as dendritic cells (DCs). Therefore, we checked the modulation of dendritic cell activation and T cell activation and polarization in responses to OmpV. Towards that, we observed maturation of OmpV-activated DCs in terms of increased surface expression of co-stimulatory molecules (**Fig. 32**)**.** In addition to that, we detected T cell proliferation (**Fig. 33**) and Th1 polarization *in vitro* induced by OmpV-activated DCs (**Fig. 34, 35**). However, we observed both Th1 and Th2 polarization in *in vivo* with more Th1 bias in response to purified OmpV compared to OmpV incorporated proteoliposome (**Fig. 36, 37**). Th2 polarization observed during oral immunization with OmpV incorporated

proteoliposome supported the IgA production as Th2 biased T cells reportedly induce more IgA production (264). Thus both *in vivo* and *in vitro* studies suggest that OmpV immunization can activate the adaptive immune system leading to antibody production which further provide protection against systemic as well as gastro-intestinal infection of *S.* Typhimurium.

Furthermore, as adaptive responses are shaped by the innate immune system, we next studied the immunomodulatory effect of OmpV on innate immune cells such as monocytes and macrophages. Being an enteric pathogen, *S.* Typhimurium first comes in contact with intestinal epithelial cells (IECs), which also have characteristics of innate immune cells. Therefore, we have also included IECs for immunomodulatory study. We found significant production of pro-inflammatory mediators following activation with OmpV (**Fig. 38, 39**). OmpV was found to elicit pro-inflammatory responses majorly via TLR2 (**Fig. 41-44**). Further, we have observed that in monocytes, OmpV signals through TLR2/6 heterodimer but interestingly in macrophages and IECs, both TLR1/2 and TLR2/6 heterodimer was found to be involved (**Fig. 41-44**). Fascinatingly, it has been reported in the literature that mice deficient in TLR2 and TLR4 are more susceptible to *S.* Typhimurium infection (265). Our observations underlined the necessity of TLR2 in OmpV recognition. Further, the downstream signaling involved MyD88, IRAK-1, MAPkinases and transcription factors NF-κB and AP-1 in OmpV-activated monocytes, macrophages and IECs (**Fig. 45-50**).

To conclude the study, our results established that OmpV acts as a very crucial adhesin in S. Typhimurium pathogenesis. Further, our study strongly suggested that OmpV can activate innate (**Illustration 23**) and adaptive immune responses leading to IgG and IgA antibody production and protection, against *S.* Typhimurium infection revealing the efficacy of OmpV as a vaccine candidate.

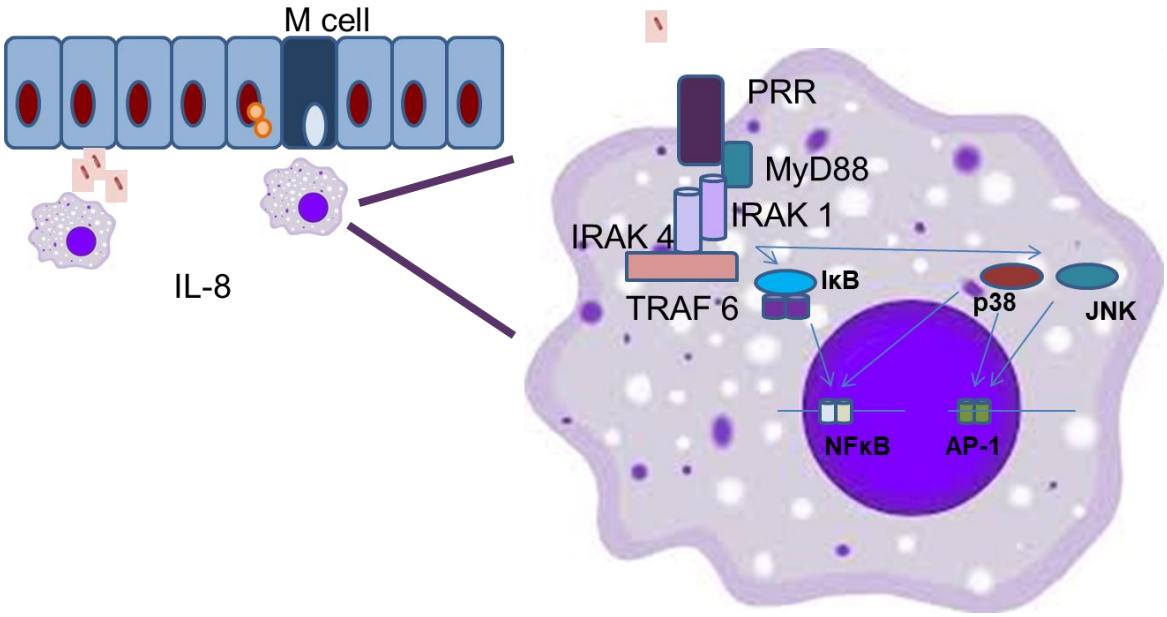


**Illustration 23:** Summary of OmpV-induced responses in inflammation

Further, as OmpV shows a high potential to activate innate and adaptive immune system; thus apart from acting as a vaccine candidate, OmpV can also qualify as a suitable adjuvant in vaccine formulations as adjuvants are desired to evoke good innate immune responses to increase the potential of antigen.

Further, the fact that there is an outer-membrane protein in *S.* Typhi with a 100 % homologous sequence of OmpV opens up the possibility that OmpV could play an important role in protection against typhoid.

# V.
# References

1. Alberts, B. (2008) *Molecular biology of the cell. [Hauptbd.]. [Hauptbd.]*, Garland Science Taylor & Francis, New York, NY [u.a.]
2. Hornef, M. W., Wick, M. J., Rhen, M., and Normark, S. (2002) Bacterial strategies for overcoming host innate and adaptive immune responses. *Nature immunology* **3**, 1033-1040
3. Hassard, F., Gwyther, C. L., Farkas, K., Andrews, A., Jones, V., Cox, B., Brett, H., Jones, D. L., McDonald, J. E., and Malham, S. K. (2016) Abundance and Distribution of Enteric Bacteria and Viruses in Coastal and Estuarine Sediments-a Review. *Frontiers in microbiology* **7**, 1692
4. Cabral, J. P. (2010) Water microbiology. Bacterial pathogens and water. *International journal of environmental research and public health* **7**, 3657-3703
5. George, A. M. (1996) Multidrug resistance in enteric and other gram-negative bacteria. *FEMS microbiology letters* **139**, 1-10
6. Donnenberg, M. S. (2000) Pathogenic strategies of enteric bacteria. *Nature* **406**, 768-774
7. Field, M. (1979) Modes of Action of Enterotoxins from Vibrio cholerae and Escherichia coli [with Discussion]. *Reviews of Infectious Diseases* **1**, 918-926
8. Formal, S. B., Gemski, P., Jr., Giannella, R. A., and Takeuchi, A. (1976) Studies on the pathogenesis of enteric infections caused by invasive bacteria. *Ciba Foundation symposium*, 27-43
9. Baron, S. (2001) Medical microbiology.
10. Brenner, F. W., Villar, R. G., Angulo, F. J., Tauxe, R., and Swaminathan, B. (2000) Salmonella nomenclature. *Journal of clinical microbiology* **38**, 2465-2467
11. Kauffmann, F., and Kauffmann, F. (1966) The bacteriology of enterobacteriaceae collected studies. Williams & Wilkins, Baltimore
12. Crosa, J. H., Brenner, D. J., Ewing, W. H., and Falkow, S. (1973) Molecular relationships among the Salmonelleae. *Journal of bacteriology* **115**, 307-315
13. Le Minor, L., and Popoff, M. Y. (1987) Designation of Salmonella enterica sp. nov., nom. rev., as the Type and Only Species of the Genus Salmonella: Request for an Opinion. *International Journal of Systematic and Evolutionary Microbiology* **37**, 465-468
14. Matthews, T. D., Schmieder, R., Silva, G. G., Busch, J., Cassman, N., Dutilh, B. E., Green, D., Matlock, B., Heffernan, B., Olsen, G. J., Farris Hanna, L., Schifferli, D. M., Maloy, S., Dinsdale, E. A., and Edwards, R. A. (2015) Genomic Comparison of

the Closely-Related Salmonella enterica Serovars Enteritidis, Dublin and Gallinarum. *PloS one* **10**, e0126883

15. Hurley, D., McCusker, M. P., Fanning, S., and Martins, M. (2014) Salmonella-host interactions - modulation of the host innate immune system. *Frontiers in immunology* **5**, 481
16. Pui, C. F., Wong, W. C., Chai, L. C., Lee, H. Y., Noorlis, A., Zainazor, T. C., Tang, J. Y., Ghazali, F. M., Cheah, Y. K., Nakaguchi, Y., Nishibuchi, M., and Radu, S. (2011) Multiplex PCR for the concurrent detection and differentiation of Salmonella spp., Salmonella Typhi and Salmonella Typhimurium. *Tropical medicine and health* **39**, 9-15
17. Grassl, G. A., and Finlay, B. B. (2008) Pathogenesis of enteric Salmonella infections. *Current opinion in gastroenterology* **24**, 22-26
18. Gillespie, I. A., O'Brien, S. J., Adak, G. K., Ward, L. R., and Smith, H. R. (2005) Foodborne general outbreaks of Salmonella Enteritidis phage type 4 infection, England and Wales, 1992-2002: where are the risks? *Epidemiology and infection* **133**, 795-801
19. Foster, J. W., and Hall, H. K. (1991) Inducible pH homeostasis and the acid tolerance response of Salmonella typhimurium. *Journal of bacteriology* **173**, 5129-5135
20. Lund, P., Tramonti, A., and De Biase, D. (2014) Coping with low pH: molecular strategies in neutralophilic bacteria. *FEMS microbiology reviews* **38**, 1091-1125
21. Boumart, Z., Velge, P., and Wiedemann, A. (2014) Multiple invasion mechanisms and different intracellular Behaviors: a new vision of Salmonella-host cell interaction. *FEMS microbiology letters* **361**, 1-7
22. Kraehenbuhl, J. P., and Neutra, M. R. (2000) Epithelial M cells: differentiation and function. *Annual review of cell and developmental biology* **16**, 301-332
23. Neutra, M. R., Frey, A., and Kraehenbuhl, J. P. (1996) Epithelial M cells: gateways for mucosal infection and immunization. *Cell* **86**, 345-348
24. Neutra, M. R., Mantis, N. J., and Kraehenbuhl, J. P. (2001) Collaboration of epithelial cells with organized mucosal lymphoid tissues. *Nature immunology* **2**, 1004-1009
25. Neutra, M. R., Pringault, E., and Kraehenbuhl, J. P. (1996) Antigen sampling across epithelial barriers and induction of mucosal immune responses. *Annual review of immunology* **14**, 275-300

26. Sakhon, O. S., Ross, B., Gusti, V., Pham, A. J., Vu, K., and Lo, D. D. (2015) M cell-derived vesicles suggest a unique pathway for trans-epithelial antigen delivery. *Tissue barriers* **3**, e1004975
27. Ochman, H., Soncini, F. C., Solomon, F., and Groisman, E. A. (1996) Identification of a pathogenicity island required for Salmonella survival in host cells. *Proceedings of the National Academy of Sciences of the United States of America* **93**, 7800-7804
28. Groisman, E. A. (2001) The pleiotropic two-component regulatory system PhoP-PhoQ. *Journal of bacteriology* **183**, 1835-1842
29. Cirillo, D. M., Valdivia, R. H., Monack, D. M., and Falkow, S. (1998) Macrophage-dependent induction of the Salmonella pathogenicity island 2 type III secretion system and its role in intracellular survival. *Molecular microbiology* **30**, 175-188
30. Thompson, J. A., Liu, M., Helaine, S., and Holden, D. W. (2011) Contribution of the PhoP/Q regulon to survival and replication of Salmonella enterica serovar Typhimurium in macrophages. *Microbiology* **157**, 2084-2093
31. Riquelme, S., Varas, M., Valenzuela, C., Velozo, P., Chahin, N., Aguilera, P., Sabag, A., Labra, B., Alvarez, S. A., Chavez, F. P., and Santiviago, C. A. (2016) Relevant Genes Linked to Virulence Are Required for Salmonella Typhimurium to Survive Intracellularly in the Social Amoeba Dictyostelium discoideum. *Frontiers in microbiology* **7**, 1305
32. Steele-Mortimer, O. (2008) The Salmonella-containing vacuole: moving with the times. *Current opinion in microbiology* **11**, 38-45
33. Salcedo, S. P., and Holden, D. W. (2003) SseG, a virulence protein that targets Salmonella to the Golgi network. *The EMBO journal* **22**, 5003-5014
34. Knuff, K., and Finlay, B. B. (2017) What the SIF Is Happening-The Role of Intracellular Salmonella-Induced Filaments. *Frontiers in cellular and infection microbiology* **7**, 335
35. Fabrega, A., and Vila, J. (2013) Salmonella enterica serovar Typhimurium skills to succeed in the host: virulence and regulation. *Clinical microbiology reviews* **26**, 308-341
36. Groisman, E. A., and Ochman, H. (1997) How Salmonella became a pathogen. *Trends in microbiology* **5**, 343-349
37. Nieto, P. A., Pardo-Roa, C., Salazar-Echegarai, F. J., Tobar, H. E., Coronado-Arrazola, I., Riedel, C. A., Kalergis, A. M., and Bueno, S. M. (2016) New insights

about excisable pathogenicity islands in Salmonella and their contribution to virulence. *Microbes and infection* **18**, 302-309

38. Hueck, C. J. (1998) Type III protein secretion systems in bacterial pathogens of animals and plants. *Microbiology and molecular biology reviews : MMBR* **62**, 379-433
39. McGhie, E. J., Brawn, L. C., Hume, P. J., Humphreys, D., and Koronakis, V. (2009) Salmonella takes control: effector-driven manipulation of the host. *Current opinion in microbiology* **12**, 117-124
40. Thomas, M., and Holden, D. W. (2009) Ubiquitination - a bacterial effector's ticket to ride. *Cell host & microbe* **5**, 309-311
41. Lapaque, N., Hutchinson, J. L., Jones, D. C., Meresse, S., Holden, D. W., Trowsdale, J., and Kelly, A. P. (2009) Salmonella regulates polyubiquitination and surface expression of MHC class II antigens. *Proceedings of the National Academy of Sciences of the United States of America* **106**, 14052-14057
42. Niemann, G. S., Brown, R. N., Gustin, J. K., Stufkens, A., Shaikh-Kidwai, A. S., Li, J., McDermott, J. E., Brewer, H. M., Schepmoes, A., Smith, R. D., Adkins, J. N., and Heffron, F. (2011) Discovery of novel secreted virulence factors from Salmonella enterica serovar Typhimurium by proteomic analysis of culture supernatants. *Infection and immunity* **79**, 33-43
43. Srinivasan, A., Nanton, M., Griffin, A., and McSorley, S. J. (2009) Culling of activated CD4 T cells during typhoid is driven by Salmonella virulence genes. *Journal of immunology* **182**, 7838-7845
44. Lostroh, C. P., and Lee, C. A. (2001) The Salmonella pathogenicity island-1 type III secretion system. *Microbes and infection* **3**, 1281-1291
45. Waterman, S. R., and Holden, D. W. (2003) Functions and effectors of the Salmonella pathogenicity island 2 type III secretion system. *Cellular microbiology* **5**, 501-511
46. McClelland, M., Sanderson, K. E., Spieth, J., Clifton, S. W., Latreille, P., Courtney, L., Porwollik, S., Ali, J., Dante, M., Du, F., Hou, S., Layman, D., Leonard, S., Nguyen, C., Scott, K., Holmes, A., Grewal, N., Mulvaney, E., Ryan, E., Sun, H., Florea, L., Miller, W., Stoneking, T., Nhan, M., Waterston, R., and Wilson, R. K. (2001) Complete genome sequence of Salmonella enterica serovar Typhimurium LT2. *Nature* **413**, 852-856
47. Raffatellu, M., Chessa, D., Wilson, R. P., Dusold, R., Rubino, S., and Baumler, A. J. (2005) The Vi capsular antigen of Salmonella enterica serotype Typhi reduces Toll-

like receptor-dependent interleukin-8 expression in the intestinal mucosa. *Infection and immunity* **73**, 3367-3374

48. Sharma, A., and Qadri, A. (2004) Vi polysaccharide of Salmonella typhi targets the prohibitin family of molecules in intestinal epithelial cells and suppresses early inflammatory responses. *Proceedings of the National Academy of Sciences of the United States of America* **101**, 17492-17497
49. Wilson, R. P., Raffatellu, M., Chessa, D., Winter, S. E., Tukel, C., and Baumler, A. J. (2008) The Vi-capsule prevents Toll-like receptor 4 recognition of Salmonella. *Cellular microbiology* **10**, 876-890
50. Robbins, J. D., and Robbins, J. B. (1984) Reexamination of the protective role of the capsular polysaccharide (Vi antigen) of Salmonella typhi. *The Journal of infectious diseases* **150**, 436-449
51. Hone, D. M., Attridge, S. R., Forrest, B., Morona, R., Daniels, D., LaBrooy, J. T., Bartholomeusz, R. C., Shearman, D. J., and Hackett, J. (1988) A galE via (Vi antigen-negative) mutant of Salmonella typhi Ty2 retains virulence in humans. *Infection and immunity* **56**, 1326-1333
52. Zhang, X. L., Jeza, V. T., and Pan, Q. (2008) Salmonella typhi: from a human pathogen to a vaccine vector. *Cellular & molecular immunology* **5**, 91-97
53. McClelland, M., Sanderson, K. E., Clifton, S. W., Latreille, P., Porwollik, S., Sabo, A., Meyer, R., Bieri, T., Ozersky, P., McLellan, M., Harkins, C. R., Wang, C., Nguyen, C., Berghoff, A., Elliott, G., Kohlberg, S., Strong, C., Du, F., Carter, J., Kremizki, C., Layman, D., Leonard, S., Sun, H., Fulton, L., Nash, W., Miner, T., Minx, P., Delehaunty, K., Fronick, C., Magrini, V., Nhan, M., Warren, W., Florea, L., Spieth, J., and Wilson, R. K. (2004) Comparison of genome degradation in Paratyphi A and Typhi, human-restricted serovars of Salmonella enterica that cause typhoid. *Nature genetics* **36**, 1268-1274
54. Sabbagh, S. C., Forest, C. G., Lepage, C., Leclerc, J. M., and Daigle, F. (2010) So similar, yet so different: uncovering distinctive features in the genomes of Salmonella enterica serovars Typhimurium and Typhi. *FEMS microbiology letters* **305**, 1-13
55. Nuccio, S. P., and Baumler, A. J. (2014) Comparative analysis of Salmonella genomes identifies a metabolic network for escalating growth in the inflamed gut. *mBio* **5**, e00929-00914
56. Stecher, B., Robbiani, R., Walker, A. W., Westendorf, A. M., Barthel, M., Kremer, M., Chaffron, S., Macpherson, A. J., Buer, J., Parkhill, J., Dougan, G., von Mering,

C., and Hardt, W. D. (2007) Salmonella enterica serovar typhimurium exploits inflammation to compete with the intestinal microbiota. *PLoS biology* **5**, 2177-2189

57. Thiennimitr, P., Winter, S. E., Winter, M. G., Xavier, M. N., Tolstikov, V., Huseby, D. L., Sterzenbach, T., Tsolis, R. M., Roth, J. R., and Baumler, A. J. (2011) Intestinal inflammation allows Salmonella to use ethanolamine to compete with the microbiota. *Proceedings of the National Academy of Sciences of the United States of America* **108**, 17480-17485
58. Marineli, F., Tsoucalas, G., Karamanou, M., and Androutsos, G. (2013) Mary Mallon (1869-1938) and the history of typhoid fever. *Annals of gastroenterology* **26**, 132-134
59. Kobayashi, T., Kutsuna, S., Hayakawa, K., Kato, Y., Ohmagari, N., Uryu, H., Yamada, R., Kashiwa, N., Nei, T., Ehara, A., Takei, R., Mori, N., Yamada, Y., Hayasaka, T., Kagawa, N., Sugawara, M., Suzaki, A., Takahashi, Y., Nishiyama, H., Morita, M., Izumiya, H., and Ohnishi, M. (2016) Case Report: An Outbreak of Food-Borne Typhoid Fever Due to Salmonella enterica Serotype Typhi in Japan Reported for the First Time in 16 Years. *The American journal of tropical medicine and hygiene* **94**, 289-291
60. Bullis, K. L. (1977) The history of avian medicine in the U.S. III. Salmonellosis. *Avian diseases* **21**, 430-435
61. Baumler, A. J., Hargis, B. M., and Tsolis, R. M. (2000) Tracing the origins of Salmonella outbreaks. *Science* **287**, 50-52
62. Qi, X., Li, P., Xu, X., Yuan, Y., Bu, S., and Lin, D. (2019) Epidemiological and Molecular Investigations on Salmonella Responsible for Gastrointestinal Infections in the Southwest of Shanghai From 1998 to 2017. *Frontiers in microbiology* **10**, 2025
63. Ford, L., Moffatt, C. R. M., Fearnley, E., Miller, M., Gregory, J., Sloan-Gardner, T. S., Polkinghorne, B. G., Bell, R., Franklin, N., Williamson, D. A., Glass, K., and Kirk, M. D. (2018) The Epidemiology of Salmonella enterica Outbreaks in Australia, 2001–2016. *Frontiers in Sustainable Food Systems* **2**
64. MacLennan, C. A., Martin, L. B., and Micoli, F. (2014) Vaccines against invasive Salmonella disease: current status and future directions. *Human vaccines & immunotherapeutics* **10**, 1478-1493
65. Devi Nelluri, K. D., and Thota, N. S. (2018) Chapter 9 - Challenges in Emerging Food-Borne Diseases. in *Food Safety and Preservation* (Grumezescu, A. M., and Holban, A. M. eds.), Academic Press. pp 231-268

66. Sparham, S. J., Kwong, J. C., Valcanis, M., Easton, M., Trott, D. J., Seemann, T., Stinear, T. P., and Howden, B. P. (2017) Emergence of multidrug resistance in locally-acquired human infections with Salmonella Typhimurium in Australia owing to a new clade harbouring blaCTX-M-9. *International journal of antimicrobial agents* **50**, 101-105
67. Collaborators, G. B. D. C. o. D. (2018) Global, regional, and national age-sex-specific mortality for 282 causes of death in 195 countries and territories, 1980-2017: a systematic analysis for the Global Burden of Disease Study 2017. *Lancet* **392**, 1736-1788
68. Disease, G. B. D., Injury, I., and Prevalence, C. (2018) Global, regional, and national incidence, prevalence, and years lived with disability for 354 diseases and injuries for 195 countries and territories, 1990-2017: a systematic analysis for the Global Burden of Disease Study 2017. *Lancet* **392**, 1789-1858
69. Majowicz, S. E., Musto, J., Scallan, E., Angulo, F. J., Kirk, M., O'Brien, S. J., Jones, T. F., Fazil, A., Hoekstra, R. M., and International Collaboration on Enteric Disease 'Burden of Illness, S. (2010) The global burden of nontyphoidal Salmonella gastroenteritis. *Clinical infectious diseases : an official publication of the Infectious Diseases Society of America* **50**, 882-889
70. Marathe, S. A., Kumar, R., Ajitkumar, P., Nagaraja, V., and Chakravortty, D. (2013) Curcumin reduces the antimicrobial activity of ciprofloxacin against Salmonella typhimurium and Salmonella typhi. *The Journal of antimicrobial chemotherapy* **68**, 139-152
71. Hawkey, J., Edwards, D. J., Dimovski, K., Hiley, L., Billman-Jacobe, H., Hogg, G., and Holt, K. E. (2013) Evidence of microevolution of Salmonella Typhimurium during a series of egg-associated outbreaks linked to a single chicken farm. *BMC genomics* **14**, 800
72. Wilmes-Riesenberg, M. R., Foster, J. W., and Curtiss, R., 3rd. (1997) An altered rpoS allele contributes to the avirulence of Salmonella typhimurium LT2. *Infection and immunity* **65**, 203-210
73. Jarvik, T., Smillie, C., Groisman, E. A., and Ochman, H. (2010) Short-term signatures of evolutionary change in the Salmonella enterica serovar typhimurium 14028 genome. *Journal of bacteriology* **192**, 560-567
74. Kroger, C., Dillon, S. C., Cameron, A. D., Papenfort, K., Sivasankaran, S. K., Hokamp, K., Chao, Y., Sittka, A., Hebrard, M., Handler, K., Colgan, A.,

Leekitcharoenphon, P., Langridge, G. C., Lohan, A. J., Loftus, B., Lucchini, S., Ussery, D. W., Dorman, C. J., Thomson, N. R., Vogel, J., and Hinton, J. C. (2012) The transcriptional landscape and small RNAs of Salmonella enterica serovar Typhimurium. *Proceedings of the National Academy of Sciences of the United States of America* **109**, E1277-1286

75. Savage, P. B. (2001) Multidrug-resistant bacteria: overcoming antibiotic permeability barriers of gram-negative bacteria. *Annals of medicine* **33**, 167-171
76. Raetz, C. R., and Whitfield, C. (2002) Lipopolysaccharide endotoxins. *Annual review of biochemistry* **71**, 635-700
77. Nikaido, H. (2003) Molecular basis of bacterial outer membrane permeability revisited. *Microbiology and molecular biology reviews : MMBR* **67**, 593-656
78. Vaara, M. (1992) The outer membrane as the penetration barrier against mupirocin in gram-negative enteric bacteria. *The Journal of antimicrobial chemotherapy* **29**, 221-222
79. Erridge, C., Bennett-Guerrero, E., and Poxton, I. R. (2002) Structure and function of lipopolysaccharides. *Microbes and infection* **4**, 837-851
80. Silhavy, T. J., Kahne, D., and Walker, S. (2010) The bacterial cell envelope. *Cold Spring Harbor perspectives in biology* **2**, a000414
81. Koebnik, R., Locher, K. P., and Van Gelder, P. (2000) Structure and function of bacterial outer membrane proteins: barrels in a nutshell. *Molecular microbiology* **37**, 239-253
82. Dudek, B., Krzyzewska, E., Kapczynska, K., Rybka, J., Pawlak, A., Korzekwa, K., Klausa, E., and Bugla-Ploskonska, G. (2016) Proteomic Analysis of Outer Membrane Proteins from Salmonella Enteritidis Strains with Different Sensitivity to Human Serum. *PloS one* **11**, e0164069
83. Chooneea, D., Karlsson, R., Encheva, V., Arnold, C., Appleton, H., and Shah, H. (2010) Elucidation of the outer membrane proteome of Salmonella enterica serovar Typhimurium utilising a lipid-based protein immobilization technique. *BMC microbiology* **10**, 44
84. Singh, R., Shasany, A. K., Aggarwal, A., Sinha, S., Sisodia, B. S., Khanuja, S. P., and Misra, R. (2007) Low molecular weight proteins of outer membrane of Salmonella typhimurium are immunogenic in Salmonella induced reactive arthritis revealed by proteomics. *Clinical and experimental immunology* **148**, 486-493

85. Vollmer, W., von Rechenberg, M., and Holtje, J. V. (1999) Demonstration of molecular interactions between the murein polymerase PBP1B, the lytic transglycosylase MltA, and the scaffolding protein MipA of Escherichia coli. *The Journal of biological chemistry* **274**, 6726-6734
86. Yang, T. C., Ma, X. C., Liu, F., Lin, L. R., Liu, L. L., Liu, G. L., Tong, M. L., Fu, Z. G., and Zhou, L. (2012) Screening of the Salmonella paratyphi A CMCC 50973 strain outer membrane proteins for the identification of potential vaccine targets. *Molecular medicine reports* **5**, 78-83
87. Hansmeier, N., Miskiewicz, K., Elpers, L., Liss, V., Hensel, M., and Sterzenbach, T. (2017) Functional expression of the entire adhesiome of Salmonella enterica serotype Typhimurium. *Scientific reports* **7**, 10326
88. Chessa, D., Winter, M. G., Jakomin, M., and Baumler, A. J. (2009) Salmonella enterica serotype Typhimurium Std fimbriae bind terminal alpha(1,2)fucose residues in the cecal mucosa. *Molecular microbiology* **71**, 864-875
89. Latasa, C., Roux, A., Toledo-Arana, A., Ghigo, J. M., Gamazo, C., Penades, J. R., and Lasa, I. (2005) BapA, a large secreted protein required for biofilm formation and host colonization of Salmonella enterica serovar Enteritidis. *Molecular microbiology* **58**, 1322-1339
90. Raghunathan, D., Wells, T. J., Morris, F. C., Shaw, R. K., Bobat, S., Peters, S. E., Paterson, G. K., Jensen, K. T., Leyton, D. L., Blair, J. M., Browning, D. F., Pravin, J., Flores-Langarica, A., Hitchcock, J. R., Moraes, C. T., Piazza, R. M., Maskell, D. J., Webber, M. A., May, R. C., MacLennan, C. A., Piddock, L. J., Cunningham, A. F., and Henderson, I. R. (2011) SadA, a trimeric autotransporter from Salmonella enterica serovar Typhimurium, can promote biofilm formation and provides limited protection against infection. *Infection and immunity* **79**, 4342-4352
91. Morgan, E., Bowen, A. J., Carnell, S. C., Wallis, T. S., and Stevens, M. P. (2007) SiiE is secreted by the Salmonella enterica serovar Typhimurium pathogenicity island 4-encoded secretion system and contributes to intestinal colonization in cattle. *Infection and immunity* **75**, 1524-1533
92. Rosselin, M., Virlogeux-Payant, I., Roy, C., Bottreau, E., Sizaret, P. Y., Mijouin, L., Germon, P., Caron, E., Velge, P., and Wiedemann, A. (2010) Rck of Salmonella enterica, subspecies enterica serovar enteritidis, mediates zipper-like internalization. *Cell research* **20**, 647-664

93. Dorsey, C. W., Laarakker, M. C., Humphries, A. D., Weening, E. H., and Baumler, A. J. (2005) Salmonella enterica serotype Typhimurium MisL is an intestinal colonization factor that binds fibronectin. *Molecular microbiology* **57**, 196-211
94. Kingsley, R. A., Santos, R. L., Keestra, A. M., Adams, L. G., and Baumler, A. J. (2002) Salmonella enterica serotype Typhimurium ShdA is an outer membrane fibronectin-binding protein that is expressed in the intestine. *Molecular microbiology* **43**, 895-905
95. Cooke, F. J., and Wain, J. (2004) The emergence of antibiotic resistance in typhoid fever. *Travel medicine and infectious disease* **2**, 67-74
96. Simon, R., Tennant, S. M., Wang, J. Y., Schmidlein, P. J., Lees, A., Ernst, R. K., Pasetti, M. F., Galen, J. E., and Levine, M. M. (2011) Salmonella enterica serovar enteritidis core O polysaccharide conjugated to H:g,m flagellin as a candidate vaccine for protection against invasive infection with S. enteritidis. *Infection and immunity* **79**, 4240-4249
97. Simon, R., Wang, J. Y., Boyd, M. A., Tulapurkar, M. E., Ramachandran, G., Tennant, S. M., Pasetti, M., Galen, J. E., and Levine, M. M. (2013) Sustained protection in mice immunized with fractional doses of Salmonella Enteritidis core and O polysaccharide-flagellin glycoconjugates. *PloS one* **8**, e64680
98. Watson, D. C., Robbins, J. B., and Szu, S. C. (1992) Protection of mice against Salmonella typhimurium with an O-specific polysaccharide-protein conjugate vaccine. *Infection and immunity* **60**, 4679-4686
99. Svenson, S. B., Nurminen, M., and Lindberg, A. A. (1979) Artificial Salmonella vaccines: O-antigenic oligosaccharide-protein conjugates induce protection against infection with Salmonella typhimurium. *Infection and immunity* **25**, 863-872
100. Micoli, F., Rondini, S., Gavini, M., Pisoni, I., Lanzilao, L., Colucci, A. M., Giannelli, C., Pippi, F., Sollai, L., Pinto, V., Berti, F., MacLennan, C. A., Martin, L. B., and Saul, A. (2013) A scalable method for O-antigen purification applied to various Salmonella serovars. *Analytical biochemistry* **434**, 136-145
101. Hindle, Z., Chatfield, S. N., Phillimore, J., Bentley, M., Johnson, J., Cosgrove, C. A., Ghaem-Maghami, M., Sexton, A., Khan, M., Brennan, F. R., Everest, P., Wu, T., Pickard, D., Holden, D. W., Dougan, G., Griffin, G. E., House, D., Santangelo, J. D., Khan, S. A., Shea, J. E., Feldman, R. G., and Lewis, D. J. (2002) Characterization of Salmonella enterica derivatives harboring defined aroC and Salmonella pathogenicity

island 2 type III secretion system (ssaV) mutations by immunization of healthy volunteers. *Infection and immunity* **70**, 3457-3467

102. Tennant, S. M., Wang, J. Y., Galen, J. E., Simon, R., Pasetti, M. F., Gat, O., and Levine, M. M. (2011) Engineering and preclinical evaluation of attenuated nontyphoidal Salmonella strains serving as live oral vaccines and as reagent strains. *Infection and immunity* **79**, 4175-4185
103. Choi, J., Shin, D., and Ryu, S. (2010) Salmonella enterica serovar Typhimurium ruvB mutant can confer protection against salmonellosis in mice. *Vaccine* **28**, 6436-6444
104. Allam, U. S., Krishna, M. G., Lahiri, A., Joy, O., and Chakravortty, D. (2011) Salmonella enterica serovar Typhimurium lacking hfq gene confers protective immunity against murine typhoid. *PloS one* **6**, e16667
105. Pesciaroli, M., Aloisio, F., Ammendola, S., Pistoia, C., Petrucci, P., Tarantino, M., Francia, M., Battistoni, A., and Pasquali, P. (2011) An attenuated Salmonella enterica serovar Typhimurium strain lacking the ZnuABC transporter induces protection in a mouse intestinal model of Salmonella infection. *Vaccine* **29**, 1783-1790
106. Berlanda Scorza, F., Doro, F., Rodriguez-Ortega, M. J., Stella, M., Liberatori, S., Taddei, A. R., Serino, L., Gomes Moriel, D., Nesta, B., Fontana, M. R., Spagnuolo, A., Pizza, M., Norais, N., and Grandi, G. (2008) Proteomics characterization of outer membrane vesicles from the extraintestinal pathogenic Escherichia coli DeltatolR IHE3034 mutant. *Molecular & cellular proteomics : MCP* **7**, 473-485
107. MacLennan, C. A. (2013) Vaccines for low-income countries. *Seminars in immunology* **25**, 114-123
108. Gil-Cruz, C., Bobat, S., Marshall, J. L., Kingsley, R. A., Ross, E. A., Henderson, I. R., Leyton, D. L., Coughlan, R. E., Khan, M., Jensen, K. T., Buckley, C. D., Dougan, G., MacLennan, I. C., Lopez-Macias, C., and Cunningham, A. F. (2009) The porin OmpD from nontyphoidal Salmonella is a key target for a protective B1b cell antibody response. *Proceedings of the National Academy of Sciences of the United States of America* **106**, 9803-9808
109. Yang, Y., Wan, C., Xu, H., and Wei, H. (2013) Identification and characterization of OmpL as a potential vaccine candidate for immune-protection against salmonellosis in mice. *Vaccine* **31**, 2930-2936
110. Valero-Pacheco, N., Blight, J., Aldapa-Vega, G., Kemlo, P., Perez-Toledo, M., Wong-Baeza, I., Kurioka, A., Perez-Shibayama, C., Gil-Cruz, C., Sanchez-Torres, L. E., Pastelin-Palacios, R., Isibasi, A., Reyes-Sandoval, A., Klenerman, P., and Lopez-

Macias, C. (2019) Conservation of the OmpC Porin Among Typhoidal and Non-Typhoidal Salmonella Serovars. *Frontiers in immunology* **10**, 2966

111. Lee, J. S., Jung, I. D., Lee, C. M., Park, J. W., Chun, S. H., Jeong, S. K., Ha, T. K., Shin, Y. K., Kim, D. J., and Park, Y. M. (2010) Outer membrane protein a of Salmonella enterica serovar Typhimurium activates dendritic cells and enhances Th1 polarization. *BMC microbiology* **10**, 263
112. Beverley, P. C. (2002) Immunology of vaccination. *British medical bulletin* **62**, 15-28
113. De Gregorio, E., Caproni, E., and Ulmer, J. B. (2013) Vaccine adjuvants: mode of action. *Frontiers in immunology* **4**, 214
114. Shi, S., Zhu, H., Xia, X., Liang, Z., Ma, X., and Sun, B. (2019) Vaccine adjuvants: Understanding the structure and mechanism of adjuvanticity. *Vaccine* **37**, 3167-3178
115. Augustyniak, D., Mleczko, J., and Gutowicz, J. (2010) The immunogenicity of the liposome-associated outer membrane proteins (OMPs) of Moraxella catarrhalis. *Cellular & molecular biology letters* **15**, 70-89
116. Skwarczynski, M., and Tóth, I. (2017) Micro- and nanotechnology in vaccine development. William Andrew, Amsterdam, [Netherlands]
117. Wang, N., Chen, M., and Wang, T. (2019) Liposomes used as a vaccine adjuvant-delivery system: From basics to clinical immunization. *Journal of controlled release : official journal of the Controlled Release Society* **303**, 130-150
118. Datsenko, K. A., and Wanner, B. L. (2000) One-step inactivation of chromosomal genes in Escherichia coli K-12 using PCR products. *Proceedings of the National Academy of Sciences of the United States of America* **97**, 6640-6645
119. Rai, A. K., Paul, K., and Chattopadhyay, K. (2013) Functional mapping of the lectin activity site on the beta-prism domain of vibrio cholerae cytolysin: implications for the membrane pore-formation mechanism of the toxin. *The Journal of biological chemistry* **288**, 1665-1673
120. Lata, K., and Chattopadhyay, K. (2015) Helicobacter pylori TlyA Forms Amyloid-like Aggregates with Potent Cytotoxic Activity. *Biochemistry* **54**, 3649-3659
121. Bradford, M. M. (1976) A rapid and sensitive method for the quantitation of microgram quantities of protein utilizing the principle of protein-dye binding. *Analytical biochemistry* **72**, 248-254
122. Morgan, D. M. (1998) Tetrazolium (MTT) assay for cellular viability and activity. *Methods in molecular biology* **79**, 179-183

123. Hornbeck, P., Winston, S. E., and Fuller, S. A. (2001) Enzyme-linked immunosorbent assays (ELISA). *Current protocols in molecular biology* **Chapter 11**, Unit11 12
124. Hornbeck, P. V. (2015) Enzyme-Linked Immunosorbent Assays. *Current protocols in immunology* **110**, 2 1 1-2 1 23
125. Csonka, C., Pali, T., Bencsik, P., Gorbe, A., Ferdinandy, P., and Csont, T. (2015) Measurement of NO in biological samples. *British journal of pharmacology* **172**, 1620-1632
126. Livak, K. J., and Schmittgen, T. D. (2001) Analysis of relative gene expression data using real-time quantitative PCR and the 2(-Delta Delta C(T)) Method. *Methods* **25**, 402-408
127. Raeymaekers, L. (2000) Basic principles of quantitative PCR. *Molecular biotechnology* **15**, 115-122
128. Sharma, R., Gulia, R., and Bhattacharyya, S. (2018) A Critical Role for Sorting Nexin 1 in the Trafficking of Metabotropic Glutamate Receptors. *The Journal of neuroscience : the official journal of the Society for Neuroscience* **38**, 8605-8620
129. Kong, S., Zhang, Y. H., and Zhang, W. (2018) Regulation of Intestinal Epithelial Cells Properties and Functions by Amino Acids. *BioMed research international* **2018**, 2819154
130. Criss, A. K., and Casanova, J. E. (2003) Coordinate regulation of Salmonella enterica serovar Typhimurium invasion of epithelial cells by the Arp2/3 complex and Rho GTPases. *Infection and immunity* **71**, 2885-2891
131. Dillon, A., and Lo, D. D. (2019) M Cells: Intelligent Engineering of Mucosal Immune Surveillance. *Frontiers in immunology* **10**, 1499
132. Neutra, M. R. (1998) Current concepts in mucosal immunity. V Role of M cells in transepithelial transport of antigens and pathogens to the mucosal immune system. *The American journal of physiology* **274**, G785-791
133. Tahoun, A., Mahajan, S., Paxton, E., Malterer, G., Donaldson, David S., Wang, D., Tan, A., Gillespie, Trudi L., O'Shea, M., Roe, Andrew J., Shaw, Darren J., Gally, David L., Lengeling, A., Mabbott, Neil A., Haas, J., and Mahajan, A. (2012) Salmonella Transforms Follicle-Associated Epithelial Cells into M Cells to Promote Intestinal Invasion. *Cell host & microbe* **12**, 645-656
134. Collinson, S. K., Doig, P. C., Doran, J. L., Clouthier, S., Trust, T. J., and Kay, W. W. (1993) Thin, aggregative fimbriae mediate binding of Salmonella enteritidis to fibronectin. *Journal of bacteriology* **175**, 12-18

135. Kukkonen, M., Raunio, T., Virkola, R., Lahteenmaki, K., Makela, P. H., Klemm, P., Clegg, S., and Korhonen, T. K. (1993) Basement membrane carbohydrate as a target for bacterial adhesion: binding of type I fimbriae of Salmonella enterica and Escherichia coli to laminin. *Molecular microbiology* **7**, 229-237
136. Kingsley, R. A., Abi Ghanem, D., Puebla-Osorio, N., Keestra, A. M., Berghman, L., and Baumler, A. J. (2004) Fibronectin binding to the Salmonella enterica serotype Typhimurium ShdA autotransporter protein is inhibited by a monoclonal antibody recognizing the A3 repeat. *Journal of bacteriology* **186**, 4931-4939
137. Coburn, B., Sekirov, I., and Finlay, B. B. (2007) Type III secretion systems and disease. *Clinical microbiology reviews* **20**, 535-549
138. Que, F., Wu, S., and Huang, R. (2013) Salmonella pathogenicity island 1(SPI-1) at work. *Current microbiology* **66**, 582-587
139. Velge, P., Wiedemann, A., Rosselin, M., Abed, N., Boumart, Z., Chausse, A. M., Grepinet, O., Namdari, F., Roche, S. M., Rossignol, A., and Virlogeux-Payant, I. (2012) Multiplicity of Salmonella entry mechanisms, a new paradigm for Salmonella pathogenesis. *MicrobiologyOpen* **1**, 243-258
140. Kubori, T., Matsushima, Y., Nakamura, D., Uralil, J., Lara-Tejero, M., Sukhan, A., Galan, J. E., and Aizawa, S. I. (1998) Supramolecular structure of the Salmonella typhimurium type III protein secretion system. *Science* **280**, 602-605
141. Sukhan, A., Kubori, T., Wilson, J., and Galan, J. E. (2001) Genetic analysis of assembly of the Salmonella enterica serovar Typhimurium type III secretion-associated needle complex. *Journal of bacteriology* **183**, 1159-1167
142. Lou, L., Zhang, P., Piao, R., and Wang, Y. (2019) Salmonella Pathogenicity Island 1 (SPI-1) and Its Complex Regulatory Network. *Frontiers in cellular and infection microbiology* **9**, 270
143. Zhou, D., Mooseker, M. S., and Galan, J. E. (1999) An invasion-associated Salmonella protein modulates the actin-bundling activity of plastin. *Proceedings of the National Academy of Sciences of the United States of America* **96**, 10176-10181
144. Lambert, M. A., and Smith, S. G. (2009) The PagN protein mediates invasion via interaction with proteoglycan. *FEMS microbiology letters* **297**, 209-216
145. Mambu, J., Virlogeux-Payant, I., Holbert, S., Grepinet, O., Velge, P., and Wiedemann, A. (2017) An Updated View on the Rck Invasin of Salmonella: Still Much to Discover. *Frontiers in cellular and infection microbiology* **7**, 500

146. Zamir, E., and Geiger, B. (2001) Components of cell-matrix adhesions. *J Cell Sci* **114**, 3577-3579
147. Scibelli, A., Roperto, S., Manna, L., Pavone, L. M., Tafuri, S., Della Morte, R., and Staiano, N. (2007) Engagement of integrins as a cellular route of invasion by bacterial pathogens. *Veterinary journal* **173**, 482-491
148. Lodish, H. F. (2016) *Molecular cell biology*,
149. Patel, S. D., Chen, C. P., Bahna, F., Honig, B., and Shapiro, L. (2003) Cadherin-mediated cell-cell adhesion: sticking together as a family. *Current opinion in structural biology* **13**, 690-698
150. van Roy, F. (2018) Cadherins. in *Encyclopedia of Signaling Molecules* (Choi, S. ed.), Springer International Publishing, Cham. pp 627-642
151. Harris, T. J., and Tepass, U. (2010) Adherens junctions: from molecules to morphogenesis. *Nature reviews. Molecular cell biology* **11**, 502-514
152. Yu, W., Yang, L., Li, T., and Zhang, Y. (2019) Cadherin Signaling in Cancer: Its Functions and Role as a Therapeutic Target. *Frontiers in oncology* **9**, 989
153. (2014) Desmocollin and desmoglein – different roles in desmosomes. *Journal of Cell Science* **127**, e1001
154. Wang, N. (2014) Cell Adhesion Molecules (CAMs). in *Encyclopedia of the Neurological Sciences (Second Edition)* (Aminoff, M. J., and Daroff, R. B. eds.), Academic Press, Oxford. pp 628-629
155. Suzuki, S. C., and Takeichi, M. (2008) Cadherins in neuronal morphogenesis and function. *Development, growth & differentiation* **50 Suppl 1**, S119-130
156. Bevilacqua, M., Butcher, E., Furie, B., Furie, B., Gallatin, M., Gimbrone, M., Harlan, J., Kishimoto, K., Lasky, L., McEver, R., and et al. (1991) Selectins: a family of adhesion receptors. *Cell* **67**, 233
157. McEver, R. P., and Zhu, C. (2010) Rolling cell adhesion. *Annual review of cell and developmental biology* **26**, 363-396
158. Kappelmayer, J., and Nagy, B., Jr. (2017) The Interaction of Selectins and PSGL-1 as a Key Component in Thrombus Formation and Cancer Progression. *BioMed research international* **2017**, 6138145
159. Wai Wong, C., Dye, D. E., and Coombe, D. R. (2012) The role of immunoglobulin superfamily cell adhesion molecules in cancer metastasis. *International journal of cell biology* **2012**, 340296

160. Briskin, M. J., McEvoy, L. M., and Butcher, E. C. (1993) MAdCAM-1 has homology to immunoglobulin and mucin-like adhesion receptors and to IgA1. *Nature* **363**, 461-464

161. Cayrol, R., Wosik, K., Berard, J. L., Dodelet-Devillers, A., Ifergan, I., Kebir, H., Haqqani, A. S., Kreymborg, K., Krug, S., Moumdjian, R., Bouthillier, A., Becher, B., Arbour, N., David, S., Stanimirovic, D., and Prat, A. (2008) Activated leukocyte cell adhesion molecule promotes leukocyte trafficking into the central nervous system. *Nature immunology* **9**, 137-145

162. Muller, W. A. (2013) Getting leukocytes to the site of inflammation. *Veterinary pathology* **50**, 7-22

163. Samanta, D., and Almo, S. C. (2015) Nectin family of cell-adhesion molecules: structural and molecular aspects of function and specificity. *Cellular and molecular life sciences : CMLS* **72**, 645-658

164. Tachibana, K., Nakanishi, H., Mandai, K., Ozaki, K., Ikeda, W., Yamamoto, Y., Nagafuchi, A., Tsukita, S., and Takai, Y. (2000) Two cell adhesion molecules, nectin and cadherin, interact through their cytoplasmic domain-associated proteins. *The Journal of cell biology* **150**, 1161-1176

165. Dougall, W. C., Kurtulus, S., Smyth, M. J., and Anderson, A. C. (2017) TIGIT and CD96: new checkpoint receptor targets for cancer immunotherapy. *Immunological reviews* **276**, 112-120

166. Perez-Vilar, J., and Hill, R. L. (1999) The structure and assembly of secreted mucins. *The Journal of biological chemistry* **274**, 31751-31754

167. Hernandez Mir, G., Helin, J., Skarp, K. P., Cummings, R. D., Makitie, A., Renkonen, R., and Leppanen, A. (2009) Glycoforms of human endothelial CD34 that bind L-selectin carry sulfated sialyl Lewis x capped O- and N-glycans. *Blood* **114**, 733-741

168. Stadtmann, A., Germena, G., Block, H., Boras, M., Rossaint, J., Sundd, P., Lefort, C., Fisher, C. I., Buscher, K., Gelschefarth, B., Urzainqui, A., Gerke, V., Ley, K., and Zarbock, A. (2013) The PSGL-1-L-selectin signaling complex regulates neutrophil adhesion under flow. *The Journal of experimental medicine* **210**, 2171-2180

169. Hynes, R. O., and Zhao, Q. (2000) The evolution of cell adhesion. *The Journal of cell biology* **150**, F89-96

170. Hynes, R. O. (2002) Integrins: Bidirectional, Allosteric Signaling Machines. *Cell* **110**, 673-687

171. Bokel, C., and Brown, N. H. (2002) Integrins in development: moving on, responding to, and sticking to the extracellular matrix. *Developmental cell* **3**, 311-321
172. Shin, S., Wolgamott, L., and Yoon, S. O. (2012) Integrin trafficking and tumor progression. *International journal of cell biology* **2012**, 516789
173. Harburger, D. S., and Calderwood, D. A. (2009) Integrin signalling at a glance. *J Cell Sci* **122**, 159-163
174. Theocharis, A. D., Skandalis, S. S., Gialeli, C., and Karamanos, N. K. (2016) Extracellular matrix structure. *Advanced drug delivery reviews* **97**, 4-27
175. Cooper, G., and Hausman, R. E. (2000) *The cell ; a molecular approach*, Sinauer Associates, Oxford
176. Lu, P., Takai, K., Weaver, V. M., and Werb, Z. (2011) Extracellular matrix degradation and remodeling in development and disease. *Cold Spring Harbor perspectives in biology* **3**
177. Schwartz, M. A. (2010) Integrins and extracellular matrix in mechanotransduction. *Cold Spring Harbor perspectives in biology* **2**, a005066
178. Jarvelainen, H., Sainio, A., Koulu, M., Wight, T. N., and Penttinen, R. (2009) Extracellular matrix molecules: potential targets in pharmacotherapy. *Pharmacological reviews* **61**, 198-223
179. Humphries, J. D., Byron, A., and Humphries, M. J. (2006) Integrin ligands at a glance. *J Cell Sci* **119**, 3901-3903
180. Hynes, R. O. (1987) Integrins: a family of cell surface receptors. *Cell* **48**, 549-554
181. Danen, E. H. J. (2000) *Madame Curie Bioscience Database*, Landes Bioscience., [Place of publication not identified
182. Walia, B., Castaneda, F. E., Wang, L., Kolachala, V. L., Bajaj, R., Roman, J., Merlin, D., Gewirtz, A. T., and Sitaraman, S. V. (2004) Polarized fibronectin secretion induced by adenosine regulates bacterial-epithelial interaction in human intestinal epithelial cells. *The Biochemical journal* **382**, 589-596
183. Goo, S. Y., Lee, H. J., Kim, W. H., Han, K. L., Park, D. K., Lee, H. J., Kim, S. M., Kim, K. S., Lee, K. H., and Park, S. J. (2006) Identification of OmpU of Vibrio vulnificus as a fibronectin-binding protein and its role in bacterial pathogenesis. *Infection and immunity* **74**, 5586-5594
184. Takada, Y., Ye, X., and Simon, S. (2007) The integrins. *Genome biology* **8**, 215
185. Akiyama, S. K. (1996) Integrins in cell adhesion and signaling. *Human cell* **9**, 181-186

186. Kwok, T., Zabler, D., Urman, S., Rohde, M., Hartig, R., Wessler, S., Misselwitz, R., Berger, J., Sewald, N., Konig, W., and Backert, S. (2007) Helicobacter exploits integrin for type IV secretion and kinase activation. *Nature* **449**, 862-866

187. Pachathundikandi, S. K., Tegtmeyer, N., and Backert, S. (2013) Signal transduction of Helicobacter pylori during interaction with host cell protein receptors of epithelial and immune cells. *Gut microbes* **4**, 454-474

188. Boehm, M., Krause-Gruszczynska, M., Rohde, M., Tegtmeyer, N., Takahashi, S., Oyarzabal, O. A., and Backert, S. (2011) Major host factors involved in epithelial cell invasion of Campylobacter jejuni: role of fibronectin, integrin beta1, FAK, Tiam-1, and DOCK180 in activating Rho GTPase Rac1. *Frontiers in cellular and infection microbiology* **1**, 17

189. Steinman, R. M., and Witmer, M. D. (1978) Lymphoid dendritic cells are potent stimulators of the primary mixed leukocyte reaction in mice. *Proceedings of the National Academy of Sciences of the United States of America* **75**, 5132-5136

190. Reis e Sousa, C. (2006) Dendritic cells in a mature age. *Nature reviews. Immunology* **6**, 476-483

191. Dalod, M., Chelbi, R., Malissen, B., and Lawrence, T. (2014) Dendritic cell maturation: functional specialization through signaling specificity and transcriptional programming. *The EMBO journal* **33**, 1104-1116

192. Joffre, O. P., Segura, E., Savina, A., and Amigorena, S. (2012) Cross-presentation by dendritic cells. *Nature reviews. Immunology* **12**, 557-569

193. Bretscher, P., and Cohn, M. (1970) A theory of self-nonself discrimination. *Science* **169**, 1042-1049

194. Frauwirth, K. A., and Thompson, C. B. (2002) Activation and inhibition of lymphocytes by costimulation. *The Journal of clinical investigation* **109**, 295-299

195. Chen, L., and Flies, D. B. (2013) Molecular mechanisms of T cell co-stimulation and co-inhibition. *Nature reviews. Immunology* **13**, 227-242

196. Croft, M. (2003) Costimulation of T cells by OX40, 4-1BB, and CD27. *Cytokine & Growth Factor Reviews* **14**, 265-273

197. Appleman, L. J., and Boussiotis, V. A. (2003) T cell anergy and costimulation. *Immunological reviews* **192**, 161-180

198. Coquet, J. M., Rausch, L., and Borst, J. (2015) The importance of co-stimulation in the orchestration of T helper cell differentiation. *Immunology and cell biology* **93**, 780-788

199. Murphy, K. M., Ouyang, W., Szabo, S. J., Jacobson, N. G., Guler, M. L., Gorham, J. D., Gubler, U., and Murphy, T. L. (1999) T helper differentiation proceeds through Stat1-dependent, Stat4-dependent and Stat4-independent phases. *Current topics in microbiology and immunology* **238**, 13-26
200. O'Garra, A. (1998) Cytokines induce the development of functionally heterogeneous T helper cell subsets. *Immunity* **8**, 275-283
201. Boehm, U., Klamp, T., Groot, M., and Howard, J. C. (1997) Cellular responses to interferon-gamma. *Annual review of immunology* **15**, 749-795
202. Taylor, G. A., Feng, C. G., and Sher, A. (2004) p47 GTPases: regulators of immunity to intracellular pathogens. *Nature reviews. Immunology* **4**, 100-109
203. Sokol, C. L., Chu, N. Q., Yu, S., Nish, S. A., Laufer, T. M., and Medzhitov, R. (2009) Basophils function as antigen-presenting cells for an allergen-induced T helper type 2 response. *Nature immunology* **10**, 713-720
204. Del Prete, G. (1992) Human Th1 and Th2 lymphocytes: their role in the pathophysiology of atopy. *Allergy* **47**, 450-455
205. Crotty, S. (2011) Follicular helper CD4 T cells (TFH). *Annual review of immunology* **29**, 621-663
206. Weaver, C. T., Harrington, L. E., Mangan, P. R., Gavrieli, M., and Murphy, K. M. (2006) Th17: an effector CD4 T cell lineage with regulatory T cell ties. *Immunity* **24**, 677-688
207. Annunziato, F., Cosmi, L., Santarlasci, V., Maggi, L., Liotta, F., Mazzinghi, B., Parente, E., Fili, L., Ferri, S., Frosali, F., Giudici, F., Romagnani, P., Parronchi, P., Tonelli, F., Maggi, E., and Romagnani, S. (2007) Phenotypic and functional features of human Th17 cells. *The Journal of experimental medicine* **204**, 1849-1861
208. Sakaguchi, S., Ono, M., Setoguchi, R., Yagi, H., Hori, S., Fehervari, Z., Shimizu, J., Takahashi, T., and Nomura, T. (2006) Foxp3+ CD25+ CD4+ natural regulatory T cells in dominant self-tolerance and autoimmune disease. *Immunological reviews* **212**, 8-27
209. Ouyang, W., Rutz, S., Crellin, N. K., Valdez, P. A., and Hymowitz, S. G. (2011) Regulation and functions of the IL-10 family of cytokines in inflammation and disease. *Annual review of immunology* **29**, 71-109
210. Eyerich, K., and Eyerich, S. (2015) Th22 cells in allergic disease. *Allergo journal international* **24**, 1-7

211. Jia, L., and Wu, C. (2014) The biology and functions of Th22 cells. *Advances in experimental medicine and biology* **841**, 209-230
212. Kaplan, M. H. (2013) Th9 cells: differentiation and disease. *Immunological reviews* **252**, 104-115
213. Yam-Puc, J. C., Zhang, L., Zhang, Y., and Toellner, K. M. (2018) Role of B-cell receptors for B-cell development and antigen-induced differentiation. *F1000Research* **7**, 429
214. Kindt, T. J., Osborne, B. A., and Goldsby, R. A. (2007) *Immunology*, W.H. Freeman ; Palgrave [distributor], New York; Basingstoke
215. Janeway, C. A., and Walport, M. (2001) *Immunobiology 5 : the immune system in health and disease*, Churchill Livingstone, Edinburgh
216. Harris, N. L., and Ronchese, F. (1999) The role of B7 costimulation in T-cell immunity. *Immunology and cell biology* **77**, 304-311
217. Klaus, S. J., Pinchuk, L. M., Ochs, H. D., Law, C. L., Fanslow, W. C., Armitage, R. J., and Clark, E. A. (1994) Costimulation through CD28 enhances T cell-dependent B cell activation via CD40-CD40L interaction. *The Journal of Immunology* **152**, 5643
218. Tandrup Schmidt, S., Foged, C., Korsholm, K. S., Rades, T., and Christensen, D. (2016) Liposome-Based Adjuvants for Subunit Vaccines: Formulation Strategies for Subunit Antigens and Immunostimulators. *Pharmaceutics* **8**
219. Zeng, M. Y., Cisalpino, D., Varadarajan, S., Hellman, J., Warren, H. S., Cascalho, M., Inohara, N., and Nunez, G. (2016) Gut Microbiota-Induced Immunoglobulin G Controls Systemic Infection by Symbiotic Bacteria and Pathogens. *Immunity* **44**, 647-658
220. Blutt, S. E., and Conner, M. E. (2013) The gastrointestinal frontier: IgA and viruses. *Frontiers in immunology* **4**, 402
221. Nurieva, R. I., and Chung, Y. (2010) Understanding the development and function of T follicular helper cells. *Cellular & molecular immunology* **7**, 190-197
222. Alloatti, A., Kotsias, F., Magalhaes, J. G., and Amigorena, S. (2016) Dendritic cell maturation and cross-presentation: timing matters! *Immunological reviews* **272**, 97-108
223. O'Garra, A., and Murphy, K. M. (2009) From IL-10 to IL-12: how pathogens and their products stimulate APCs to induce T(H)1 development. *Nature immunology* **10**, 929-932

224. Josef Pfeilschifter, A. H. (2004) Inflammation. in *Encyclopedic Reference of Molecular Pharmacology*, Springer Berlin Heidelberg, Berlin, Heidelberg. pp 487-491
225. Cannon, P. R. (1940) Defense Mechanisms in Infectious and Related Diseases. *Annual Review of Physiology* **2**, 387-410
226. Harris, H. (1960) Mobilization of defensive cells in inflammatory tissue. *Bacteriological reviews* **24**, 3-15
227. Sproston, N. R., and Ashworth, J. J. (2018) Role of C-Reactive Protein at Sites of Inflammation and Infection. *Frontiers in immunology* **9**, 754
228. Chen, L., Deng, H., Cui, H., Fang, J., Zuo, Z., Deng, J., Li, Y., Wang, X., and Zhao, L. (2018) Inflammatory responses and inflammation-associated diseases in organs. *Oncotarget* **9**, 7204-7218
229. Ruth, M. R., and Field, C. J. (2013) The immune modifying effects of amino acids on gut-associated lymphoid tissue. *Journal of animal science and biotechnology* **4**, 27
230. Eckmann, L., Kagnoff, M. F., and Fierer, J. (1993) Epithelial cells secrete the chemokine interleukin-8 in response to bacterial entry. *Infection and immunity* **61**, 4569-4574
231. Mogensen, T. H. (2009) Pathogen recognition and inflammatory signaling in innate immune defenses. *Clinical microbiology reviews* **22**, 240-273, Table of Contents
232. Hakansson, A., and Molin, G. (2011) Gut microbiota and inflammation. *Nutrients* **3**, 637-682
233. Kawai, T., and Akira, S. (2009) The roles of TLRs, RLRs and NLRs in pathogen recognition. *International immunology* **21**, 317-337
234. Akira, S., Uematsu, S., and Takeuchi, O. (2006) Pathogen recognition and innate immunity. *Cell* **124**, 783-801
235. Takeuchi, O., and Akira, S. (2010) Pattern recognition receptors and inflammation. *Cell* **140**, 805-820
236. Schroder, K., and Tschopp, J. (2010) The inflammasomes. *Cell* **140**, 821-832
237. Medzhitov, R., Preston-Hurlburt, P., Kopp, E., Stadlen, A., Chen, C., Ghosh, S., and Janeway, C. A., Jr. (1998) MyD88 is an adaptor protein in the hToll/IL-1 receptor family signaling pathways. *Molecular cell* **2**, 253-258
238. Yamamoto, M., Sato, S., Hemmi, H., Hoshino, K., Kaisho, T., Sanjo, H., Takeuchi, O., Sugiyama, M., Okabe, M., Takeda, K., and Akira, S. (2003) Role of adaptor TRIF in the MyD88-independent toll-like receptor signaling pathway. *Science* **301**, 640-643

239. Broad, A., Kirby, J. A., Jones, D. E., Applied, I., and Transplantation Research, G. (2007) Toll-like receptor interactions: tolerance of MyD88-dependent cytokines but enhancement of MyD88-independent interferon-beta production. *Immunology* **120**, 103-111
240. Lin, S. C., Lo, Y. C., and Wu, H. (2010) Helical assembly in the MyD88-IRAK4-IRAK2 complex in TLR/IL-1R signalling. *Nature* **465**, 885-890
241. Oeckinghaus, A., and Ghosh, S. (2009) The NF-kappaB family of transcription factors and its regulation. *Cold Spring Harbor perspectives in biology* **1**, a000034
242. Wang, A., Al-Kuhlani, M., Johnston, S. C., Ojcius, D. M., Chou, J., and Dean, D. (2013) Transcription factor complex AP-1 mediates inflammation initiated by Chlamydia pneumoniae infection. *Cellular microbiology* **15**, 779-794
243. Sharma, J. N., Al-Omran, A., and Parvathy, S. S. (2007) Role of nitric oxide in inflammatory diseases. *Inflammopharmacology* **15**, 252-259
244. Janssens, S., and Beyaert, R. (2003) Role of Toll-like receptors in pathogen recognition. *Clinical microbiology reviews* **16**, 637-646
245. Warner, N., and Nunez, G. (2013) MyD88: a critical adaptor protein in innate immunity signal transduction. *Journal of immunology* **190**, 3-4
246. Ding, A., Yu, H., Yang, J., Shi, S., and Ehrt, S. (2005) Induction of macrophage-derived SLPI by Mycobacterium tuberculosis depends on TLR2 but not MyD88. *Immunology* **116**, 381-389
247. Gao, Q., Qi, L., Wu, T., and Wang, J. (2012) Clostridium butyricum activates TLR2-mediated MyD88-independent signaling pathway in HT-29 cells. *Molecular and cellular biochemistry* **361**, 31-37
248. De Nardo, D., Balka, K. R., Cardona Gloria, Y., Rao, V. R., Latz, E., and Masters, S. L. (2018) Interleukin-1 receptor-associated kinase 4 (IRAK4) plays a dual role in myddosome formation and Toll-like receptor signaling. *The Journal of biological chemistry* **293**, 15195-15207
249. Fujioka, S., Niu, J., Schmidt, C., Sclabas, G. M., Peng, B., Uwagawa, T., Li, Z., Evans, D. B., Abbruzzese, J. L., and Chiao, P. J. (2004) NF-kappaB and AP-1 connection: mechanism of NF-kappaB-dependent regulation of AP-1 activity. *Molecular and cellular biology* **24**, 7806-7819
250. Kanarek, N., and Ben-Neriah, Y. (2012) Regulation of NF-kappaB by ubiquitination and degradation of the IkappaBs. *Immunological reviews* **246**, 77-94

251. Lawrence, T. (2009) The nuclear factor NF-kappaB pathway in inflammation. *Cold Spring Harbor perspectives in biology* **1**, a001651
252. Gazon, H., Barbeau, B., Mesnard, J. M., and Peloponese, J. M., Jr. (2017) Hijacking of the AP-1 Signaling Pathway during Development of ATL. *Frontiers in microbiology* **8**, 2686
253. Kingsley, R. A., Msefula, C. L., Thomson, N. R., Kariuki, S., Holt, K. E., Gordon, M. A., Harris, D., Clarke, L., Whitehead, S., Sangal, V., Marsh, K., Achtman, M., Molyneux, M. E., Cormican, M., Parkhill, J., MacLennan, C. A., Heyderman, R. S., and Dougan, G. (2009) Epidemic multiple drug resistant Salmonella Typhimurium causing invasive disease in sub-Saharan Africa have a distinct genotype. *Genome research* **19**, 2279-2287
254. Gordon, M. A., Graham, S. M., Walsh, A. L., Wilson, L., Phiri, A., Molyneux, E., Zijlstra, E. E., Heyderman, R. S., Hart, C. A., and Molyneux, M. E. (2008) Epidemics of invasive Salmonella enterica serovar enteritidis and S. enterica Serovar typhimurium infection associated with multidrug resistance among adults and children in Malawi. *Clinical infectious diseases : an official publication of the Infectious Diseases Society of America* **46**, 963-969
255. Mabbott, N. A., Donaldson, D. S., Ohno, H., Williams, I. R., and Mahajan, A. (2013) Microfold (M) cells: important immunosurveillance posts in the intestinal epithelium. *Mucosal immunology* **6**, 666-677
256. Hudson, K. J., Bliska, J. B., and Bouton, A. H. (2005) Distinct mechanisms of integrin binding by Yersinia pseudotuberculosis adhesins determine the phagocytic response of host macrophages. *Cellular microbiology* **7**, 1474-1489
257. T, O. C., and Backert, S. (2012) Host epithelial cell invasion by Campylobacter jejuni: trigger or zipper mechanism? *Frontiers in cellular and infection microbiology* **2**, 25
258. Truttmann, M. C., Misselwitz, B., Huser, S., Hardt, W. D., Critchley, D. R., and Dehio, C. (2011) Bartonella henselae engages inside-out and outside-in signaling by integrin beta1 and talin1 during invasome-mediated bacterial uptake. *J Cell Sci* **124**, 3591-3602
259. Josse, J., Laurent, F., and Diot, A. (2017) Staphylococcal Adhesion and Host Cell Invasion: Fibronectin-Binding and Other Mechanisms. *Frontiers in microbiology* **8**, 2433

260. Baloda, S. B., Dyal, R., Gonzalez, E. A., Blanco, J., Hajdu, L., and Mansson, I. (1991) Fibronectin binding by Salmonella strains: evaluation of a particle agglutination assay. *Journal of clinical microbiology* **29**, 2824-2830

261. Tegtmeyer, N., Hartig, R., Delahay, R. M., Rohde, M., Brandt, S., Conradi, J., Takahashi, S., Smolka, A. J., Sewald, N., and Backert, S. (2010) A small fibronectin-mimicking protein from bacteria induces cell spreading and focal adhesion formation. *The Journal of biological chemistry* **285**, 23515-23526

262. Kumar, A., Hays, M., Lim, F., Foster, L. J., Zhou, M., Zhu, G., Miesner, T., and Hardwidge, P. R. (2015) Protective Enterotoxigenic Escherichia coli Antigens in a Murine Intranasal Challenge Model. *PLoS neglected tropical diseases* **9**, e0003924

263. Fabbri, M., Castellani, P., Gotwals, P. J., Kotelianski, V., Zardi, L., and Zocchi, M. R. (1996) A functional monoclonal antibody recognizing the human alpha 1-integrin I-domain. *Tissue antigens* **48**, 47-51

264. Wu, Y., Kudsk, K. A., DeWitt, R. C., Tolley, E. A., and Li, J. (1999) Route and type of nutrition influence IgA-mediating intestinal cytokines. *Annals of surgery* **229**, 662-667; discussion 667-668

265. Arpaia, N., Godec, J., Lau, L., Sivick, K. E., McLaughlin, L. M., Jones, M. B., Dracheva, T., Peterson, S. N., Monack, D. M., and Barton, G. M. (2011) TLR signaling is required for Salmonella typhimurium virulence. *Cell* **144**, 675-688

# VI.
# Synopsis

**Synopsis**

**Title: Understanding the role of OmpV, an outer-membrane protein of *Salmonella* Typhimurium towards bacterial pathogenesis and host-immune activation**

**Deepinder Kaur**
**Indian Institute of Science Education and Research Mohali**
**Sector 81, SAS Nagar, Mohali,**
**Punjab, India-140306**

## Introduction

*Salmonella enterica* serovar Typhimurium is one of the major causes of a foodborne gastro-enteric illness known as salmonellosis (1). *S.* Typhimurium is reported to contribute 50 % cases of salmonellosis in humans (2). Salmonellosis can be self-limiting in healthy individuals, but in the case of infants, elderly people and immune-compromised individuals, the risk of infection are higher and the infection often becomes fatal. The Global Burden of Diseases, Injuries, and Risk Factors Study (GBD) 2017 reported 95.1 million cases and 50771 deaths worldwide due to salmonellosis in 2017 (3).

To date, no vaccine is available for salmonellosis and antibiotics are the only mode of treatment available, which are not widely accepted for pregnant women and infants. Moreover, the emergence of multidrug-resistant strains of *S.* Typhimurium further complicated the treatment of this disease leading to frequent outbreaks. Recently, a highly invasive strain of *S.* Typhimurium, ST313 has emerged that shows resistance to multiple antibiotics that are recommended as first-line treatment (4). Further, 90% of salmonellosis causing strains in Malawi are multi-drug resistant (5). The increasing rate of multidrug-resistant strains underscores the need to establish a vaccine against salmonellosis that requires an understanding of the pathogenesis of non-typhoidal *Salmonella* in detail. Many factors that play crucial roles in the pathogenesis of *S.* Typhimurium are well studied, but yet, some uncharacterized virulence factors limit our knowledge regarding the pathogenesis of the bacteria.

Generally, *Salmonella enterica* enters the human body through the oral route by contaminated food or water. After reaching the small intestine, *Salmonella* establishes itself and penetrates the microfold cells (M cells) and thus gets access to the basolateral side of the intestinal

epithelium (6,7). In 2012, Tahoun *et al*. (8) reported that *Salmonella* could transform follicle-associated epithelial cells into M cells to enhance bacterial translocation across the intestinal barrier. Thus *Salmonella* can invade epithelial cells from both the apical and basolateral side. Outer membrane proteins are major players in the pathogenesis of bacteria as they are the first to come in contact with the host immune system. So far, 69 outer membrane proteins of *S.* Typhimurium are known. Among these, few proteins like Lpp1, Lpp2, PagN, ShdA and OmpX are implicated in *S.* Typhimurium pathogenesis (9). In the present study, we have attempted to characterize an outer membrane protein OmpV of *S.* Typhimurium. OmpV is a member of the MltA-interacting protein (mipA) family of proteins, which are earlier reported to be involved in the septation of the murein sacculus (10). These proteins are known to form adhesion sites for transglycosylase enzymes, and one such protein has also been reported to give protection during *S.* Paratyphi infection (11).

Based on this background, we aimed to understand the following:

**Aim I:** Does OmpV has a role in the pathogenesis of *S.* Typhimurium

**Aim II:** Whether OmpV has the potential to act as a vaccine candidate

**Aim I: Does OmpV has a role in the pathogenesis of *S.* Typhimurium**

As mentioned in the introduction section, *S.* Typhimurium enters our body through contaminated food and water. Following entry, *Salmonella* adheres and invade the IECs. Adhesion process is mediated by different adhesins, and invasion of *Salmonella* is majorly mediated by by SPI1 (Salmonella pathogenicity island 1)-regulated effector proteins secreted by a needle-like complex named as Type III secretion system, or invasosome (12). Towards finding out whether OmpV plays any role in adhesion or invasion, we undertook the following objectives:

**Objective 1: Purification and characterization of recombinant OmpV**

OmpV without signal peptide was cloned in pET-14b and then expressed recombinantly in *E. coli*. The protein was then purified using Ni-NTA chromatography from the inclusion body. The secondary structure of the refolded protein was checked using CD spectroscopy. Tryptophan fluorescence and ANS binding fluorescence experiment were done to verify the correct folding of the protein. Moreover, size exclusion chromatography was done to check the presence of any soluble aggregates in purified protein. Results from the above experiments revealed proper refolding and the absence of any aggregation in refolded OmpV protein.

**Objective 2: To determine the role of OmpV in *S.* Typhimurium infection using OmpV-deletion mutant (**Δ*ompV*)

To understand the role of OmpV protein in adhesion or invasion, we deleted the *ompv* gene (Δ*ompV*), and also made OmpV-complemented strain (comp). Further, we infected intestinal epithelial cells (Caco-2 cells) with the wildtype, Δ*ompV* and comp strains of *S.* Typhimurium, and checked the invasion and adhesion of bacteria. We observed a significant decrease in the number of *S.* Typhimurium invaded and adhered to the epithelial cells upon the deletion of *ompV*, as compared to those with the wild type and the complemented strains. To determine further that the defect in the infection process upon *ompV*-deletion was due to compromised adhesion and not due to compromised invasion, we employed a SPI1 mutant (Δ*spi1*) of *S.* Typhimurium. SPI1 is known to be involved in invasion and not in the adhesion step. As expected, significantly reduced invasion was observed with both Δ*spi1* and mutant, as compared to the wild type bacteria and *ompV*-complemented bacteria. However, Δ*spi1* showed no defect in the adhesion process but Δ*ompV* showed decreased adhesion and invasion. Further,

with the Δ*spi1*Δ*ompV* double mutant, we observed a decreased adhesion, as compared to the only Δ*spi1* mutant, confirming that OmpV was required for adhesion.

Furthermore, we also observed that OmpV can bind to IECs in a dose-dependent manner and there is a decrease in *S.* Typhimurium binding in cells pretreated with purified OmpV protein suggesting the presence of a specific receptor for OmpV protein.

**Objective 3: To find out the receptor of OmpV on intestinal epithelial cells**

Receptors present on IECs, in general, belong to the selectin, cadherin, integrin and IgCAM families. Among these, integrins are known to bind mostly through the ECM components. With Giemsa staining, it seems that *Salmonella* predominantly binds to ECM (extracellular matrix) of IECs in case of infection with wild type strain but not in Δ*ompV* strain suggesting OmpV probably help Salmonella to bind to ECM complex. Further, we observed that OmpV binds to fibronectin of the ECM complex. It was previously reported that fibronectin is crucial for adherence of *S.* Typhimurium to IECs. Our study proved that the crucial dependence of *S.* Typhimurium on fibronectin for adherence is probably due to OmpV.

From the above study, it seemed that in the case of OmpV, integrin(s) are the most probable candidate. From the literature, we found out that there are 24 receptors in the integrin family (13). The integrin family members generally form heterodimers with different combinations of α and β subunits. Among these, eight hetero-dimers are known to interact with the ligand through fibronectin. The most common integrin present on the IECs known to bind fibronectin is β1 integrin (14). We observed that in GST-pull down, OmpV co-immunoprecipitated with β1 integrin. Further, we confirmed that OmpV interacts with α1β1 integrin receptor via fibronectin.

**Objective 4: To investigate whether purified OmpV can activate receptor-mediated downstream signalling**

Activation of α1β1 integrin, in general, leads to the activation of FAK. In general, FAK activation ultimately leads to the modulation of the actin filaments that help in the invasion of bacteria into the host cells (15). We observed that OmpV also could lead to the activation of FAK and actin modulation.

**Objective 5: To determine whether OmpV deletion affects *S.* Typhimurium infection *in vivo*.**

We examined the effect of the deletion of OmpV on the pathogenicity of *S.* Typhimurium. We observed a 7-fold increase in the $LD_{50}$ dose (median lethal dose) in Δ*ompV* infected mice compared to the wild type control. Furthermore, less than 1 competitive index (CI) ratio of Δ*ompV* mutant and wild type bacteria from the different organs of infected mice, i.e., spleen, liver and intestine, indicated colonization and pathogenicity of Δ*ompV* is far less than the wild type bacteria. As adhesion is the first step in the virulence process of *S.* Typhimurium; therefore, OmpV deletion severely impacted the pathogenicity of the *S.* Typhimurium.

**Aim II: Whether OmpV has the potential to act as a vaccine candidate**

The primary goal of a vaccine candidate is to evoke both innate and adaptive immune responses in the host. Innate immune cells are the first line of defense against infection. These cells play an essential role in further shaping adaptive immunity that is more specific and long-lasting. Dendritic cells (DCs) can induce T-cell proliferation and differentiation. Differentiated T-helper cells further help B cells to produce high-affinity antibodies and class switching. To understand the mechanism of immune signaling induced by OmpV and its role in the protection against *S.* Typhimurium, we have undertaken the following objectives under this aim.

**Objective 1: To investigate whether immunization with OmpV leads to protection against *S.* Typhimurium infection**

To determine the role of OmpV in protection against *S.* Typhimurium, we immunized mice with four doses of OmpV (25 µg/dose) intraperitoneally at an interval of 7 days. Following immunization, mice were infected (intraperitoneal/oral) with virulent *S.* Typhimurium SL1344 strain. We observed 100 % protection in the intraperitoneal infection of *S.* Typhimurium (systemic infection). But no protection was observed in the case of oral infection of *S.* Typhimurium (gastro-intestinal infection). Further, we detected high IgG production in immunized mice but no IgA production.

Further, oral immunization with purified OmpV protein did not generate either IgG or IgA and there was no protection against systemic and gastro-intestinal infection with *S.* Typhimurium. The reason behind this could be the degradation of protein by enzymes or the acidic environment of the stomach. Therefore, we further integrated OmpV protein as a

proteoliposome and used for oral immunization as liposome can protect the protein and act as an adjuvant. We observed a high IgA production when mice were administered orally OmpV incorporated proteoliposome and also observed 100 % survival of immunized mice against gastro-intestinal infection of *S.* Typhimurium. Further, post-infection length of the intestine in immunized seemed similar with the non-infected mice whereas, infected unimmunized mice have shortening of the intestinal length with an enlarged spleen. Hence indicated unimmunized mice had a higher level of infection compared to the immunized mice.

**Objective 2: To determine whether OmpV can activate dendritic cell responses, T cell activation and T-helper polarization**

An activation signal from T-helper (Th1 and Th2) cells is required to activate B cells, antibody production, and class switching. In turn, the T-cells get activated by antigen-presenting cells (APCs) such as dendritic cells (DCs). For the activation and differentiation of T-cells, DCs provides three signals. Out of these three signals, Signal 1 is provided by the interaction of MHC molecules with the T-cell receptor. Signal 2 involves the interaction of co-stimulatory molecules like CD80 and CD86 with CD28 present on T-cells. Signal 3 is induced by cytokines produced by DCs or other immune cells in the milieu. On recognition of ligand by innate receptor known as pattern recognition receptors (PRRs) present on the surface DCs get activated and undergo maturation. The maturation of DCs is a pre-requisite for efficient antigen presentation and is characterized by an increase in surface expression of co-stimulatory molecules. We observed that OmpV could induce an increase in surface expression of CD86. Further, to check whether OmpV-primed DCs can lead to the proliferation of T-cells we co-cultured CFSE labeled CD4+ T-cells with OmpV-activated splenic DCs of BALB/c mice. We observed CFSE dilution indicating T cell proliferation. DCs are known to secrete cytokines such as IL-10 or IL-12, which can induce T-cell differentiation towards either Th1 or Th2 or Treg phenotype. We observed that OmpV-primed DCs secrete a high IL-12/IL-10 ratio (approximately 20:1), indicating differentiation of T-helper (Th)-cells could be towards Th1 phenotype. Further, we observed significant production of IFNγ by Th-cells co-cultured with OmpV-activated splenic DCs confirming Th1 polarization.

However, as in *in vivo* conditions, other cells also contribute to the cytokine in the milieu and affect Th polarization; we immunized mice with OmpV. Following intraperitoneal immunization, T-cells were isolated from inguinal, mesenteric and popliteal lymph nodes.

Upon activation with PMA and ionomycin, these cells show massive production of IFNγ and almost no IL-4, confirming OmpV induces polarization of Th cells towards Th1 phenotype. However, when T-cells isolated from mesenteric lymph node following oral immunization of mice with OmpV-incorporated proteoliposome, we observed the production of both IFNγ and IL-4 with more IFNγ than to IL-4, indicating Th-polarization towards both Th1 and Th2 phenotype with more Th1 bias.

**Objective 3: To determine whether OmpV can modulate innate immune responses**

To study this, we used RAW 264.7 (murine macrophages), THP-1 (human monocytes), HT29 and T84 (human intestinal epithelial cells). Here, we probed the production of pro-inflammatory mediators such as, TNFα, IL-6 in monocytes, and TNFα, IL-6 and nitric oxide (NO) in macrophages, and IL-8 in IECs as these are the best signature pro-inflammatory mediators of the particular cell types. Therefore, it seems OmpV acts as a PAMP and induces pro-inflammatory responses upon recognition by some PRR, and being an outer-membrane protein, OmpV probably is recognized by PRRs present on the surface of these cells. The majority of surface PRRs include TLRs, out of which TLR1, TLR2, TLR4 and TLR6 are mostly known to recognize bacterial ligands. Surface expression, co-immunoprecipitation and knock-down studies indicated the involvement of TLR1, TLR2 and TLR6 in macrophages and IECs and whereas, only TLR1 and TLR2 in monocytes. TLR2 mostly forms a heterodimer with either TLR1 or TLR6. Therefore, it seemed that in macrophages and IECs, TLR2 makes hetero-dimer with both TLR1 and TLR6 in response to OmpV, whereas, in monocytes, TLR2 forms heterodimer with TLR1 only. As for downstream signalling, we observed the involvement of MyD88, IRAK1 and MAPkinases. Further, OmpV-mediated downstream signal leads to the activation of NF-κB and AP-1 transcription.

**Conclusions:**

Altogether, our observation indicated that OmpV by acting as adhesin helps *S.* Typhimurium in adhering to intestinal epithelial cells. It binds to α1β1 integrin receptor through ECM component fibronectin and results in FAK phosphorylation and F-actin modulation, which is important for *Salmonella* invasion. Deletion mutant of *ompV* showed lesser pathogenicity than the wild type bacteria.

During this study, we observed that OmpV could be recognized by both TLR1/2 and TLR2/6 in macrophages and intestinal epithelial cells, whereas by TLR1/2 in monocytes. Further, the OmpV-mediated TLR activation signaling cascade involves MyD88 and IRAK-1, MAPK, and transcription factors NF-κB and AP-1.

Further, we studied whether OmpV can modulate adaptive responses and the potential of OmpV to act as a vaccine candidate. We observed that intraperitoneal immunization in mice with OmpV protein leads to IgG production and protection against systemic infection of *S.* Typhimurium. Further, oral immunization with OmpV-incorporated proteoliposome induces production of IgA as well as protection against gastro-intestinal infection. In addition to protection and B cell responses in terms of antibody generation, we checked the modulation of DC and T cell responses by OmpV. Our study showed that OmpV can lead to DC maturation and T-cell activation and differentiation towards Th1, whereas towards both Th1 and Th2 with more Th1 bias in case of OmpV-incorporated proteoliposome.

Thus, our study proved that OmpV can be considered a potential subunit vaccine candidate against *S.* Typhimurium. Moreover, as OmpV can modulate both innate and adaptive immune systems and can recognized by different TLR heterodimers to amplify the inflammatory response, it makes it a suitable candidate as an adjuvant in other vaccine formulations.

**References:**


1. Antunes, P., Mourao, J., Campos, J., and Peixe, L. (2016) Salmonellosis: the role of poultry meat. *Clinical microbiology and infection : the official publication of the European Society of Clinical Microbiology and Infectious Diseases* **22**, 110-121
2. Sparham, S. J., Kwong, J. C., Valcanis, M., Easton, M., Trott, D. J., Seemann, T., Stinear, T. P., and Howden, B. P. (2017) Emergence of multidrug resistance in locally-acquired human infections with Salmonella Typhimurium in Australia owing to a new clade harbouring blaCTX-M-9. *International journal of antimicrobial agents* **50**, 101-105
3. Collaborators, G. B. D. N.-T. S. I. D. (2019) The global burden of non-typhoidal salmonella invasive disease: a systematic analysis for the Global Burden of Disease Study 2017. *The Lancet. Infectious diseases* **19**, 1312-1324

4. Kingsley, R. A., Msefula, C. L., Thomson, N. R., Kariuki, S., Holt, K. E., Gordon, M. A., Harris, D., Clarke, L., Whitehead, S., Sangal, V., Marsh, K., Achtman, M., Molyneux, M. E., Cormican, M., Parkhill, J., MacLennan, C. A., Heyderman, R. S., and Dougan, G. (2009) Epidemic multiple drug resistant Salmonella Typhimurium causing invasive disease in sub-Saharan Africa have a distinct genotype. *Genome research* **19**, 2279-2287
5. Gordon, M. A., Graham, S. M., Walsh, A. L., Wilson, L., Phiri, A., Molyneux, E., Zijlstra, E. E., Heyderman, R. S., Hart, C. A., and Molyneux, M. E. (2008) Epidemics of invasive Salmonella enterica serovar enteritidis and S. enterica Serovar typhimurium infection associated with multidrug resistance among adults and children in Malawi. *Clinical infectious diseases : an official publication of the Infectious Diseases Society of America* **46**, 963-969
6. Hohmann, A. W., Schmidt, G., and Rowley, D. (1978) Intestinal colonization and virulence of Salmonella in mice. *Infection and immunity* **22**, 763-770
7. Jones, B. D., Ghori, N., and Falkow, S. (1994) Salmonella typhimurium initiates murine infection by penetrating and destroying the specialized epithelial M cells of the Peyer's patches. *The Journal of experimental medicine* **180**, 15-23
8. Tahoun, A., Mahajan, S., Paxton, E., Malterer, G., Donaldson, D. S., Wang, D., Tan, A., Gillespie, T. L., O'Shea, M., Roe, A. J., Shaw, D. J., Gally, D. L., Lengeling, A., Mabbott, N. A., Haas, J., and Mahajan, A. (2012) Salmonella transforms follicle-associated epithelial cells into M cells to promote intestinal invasion. *Cell host & microbe* **12**, 645-656
9. Chooneea, D., Karlsson, R., Encheva, V., Arnold, C., Appleton, H., and Shah, H. (2010) Elucidation of the outer membrane proteome of Salmonella enterica serovar Typhimurium utilising a lipid-based protein immobilization technique. *BMC microbiology* **10**, 44
10. Vollmer, W., von Rechenberg, M., and Holtje, J. V. (1999) Demonstration of molecular interactions between the murein polymerase PBP1B, the lytic transglycosylase MltA, and the scaffolding protein MipA of Escherichia coli. *The Journal of biological chemistry* **274**, 6726-6734
11. Yang, T. C., Ma, X. C., Liu, F., Lin, L. R., Liu, L. L., Liu, G. L., Tong, M. L., Fu, Z. G., and Zhou, L. (2012) Screening of the Salmonella paratyphi A CMCC 50973 strain outer membrane proteins for the identification of potential vaccine targets. *Molecular medicine reports* **5**, 78-83

12. Deng, W., Marshall, N. C., Rowland, J. L., McCoy, J. M., Worrall, L. J., Santos, A. S., Strynadka, N. C. J., and Finlay, B. B. (2017) Assembly, structure, function and regulation of type III secretion systems. *Nature reviews. Microbiology* **15**, 323-337
13. Takada, Y., Ye, X., and Simon, S. (2007) The integrins. *Genome biology* **8**, 215
14. Akiyama, S. K. (1996) Integrins in cell adhesion and signaling. *Human cell* **9**, 181-186
15. Boehm, M., Krause-Gruszczynska, M., Rohde, M., Tegtmeyer, N., Takahashi, S., Oyarzabal, O. A., and Backert, S. (2011) Major host factors involved in epithelial cell invasion of Campylobacter jejuni: role of fibronectin, integrin beta1, FAK, Tiam-1, and DOCK180 in activating Rho GTPase Rac1. *Frontiers in cellular and infection microbiology* **1**, 17